NOVEL AMINOCATALYTIC AND PHOTOCHEMICAL REACTIONS

Manuel Nappi

UNIVERSITAT ROVIRA I VIRGILI
NOVEL AMINOCATALYTIC AND PHOTOCHEMICAL REACTIONS
Manuel Nappi

Manuel Nappi

Novel Aminocatalytic and Photochemical Reactions

Doctoral Thesis

Supervised by Prof. Paolo Melchiorre

ICIQ – Institut Català d'Investigació Química

UNIVERSITAT ROVIRA I VIRGILI

Tarragona

2014

Prof. Paolo Melchiorre, ICREA Research Professor & ICIQ Group Leader

I STATE that the present study, entitled “Novel Aminocatalytic and Photochemical Reactions”, presented by MANUEL NAPPI to receive the degree of Doctor, has been carried out under my supervision at the Institut Català d'Investigació Química (ICIQ).

Tarragona, October the 16th 2014

Doctoral Thesis Supervisor

Prof. Paolo Melchiorre

Acknowledgements

As usual, behind a great and priceless experience, there are many persons who strongly contributed to make it feasible. First, I would like to thank with all myself my supervisor and Professor Paolo Melchiorre, who gave me the unforgettable opportunity to spend 4 years of my life here, in Tarragona. From my interview at the ICIQ, he always believed on me. Paolo taught me the inestimable value of the time in the scientific research. He enhanced my huge passion for chemistry, allowing me to pursue my own ideas and to spend an important period of my life and carrier in the group of Professor David W. C. MacMillan. I would like to thank Dave for this unique experience at Princeton (US), either for my personal and scientific growing.

But all of this was not possible without the help and the love of a magnificent family.

Ma tutto questo non sarebbe stato possibile senza l'aiuto e l'amore di una famiglia magnifica. Vorrei ringraziare mia madre, Novella, mio padre, Antonio, e mia sorella, Clizia, per tutto il supporto che mi avete dato in questi anni, nei momenti difficili, e per la felicitá che avete condiviso con me, nei momenti di gioia. Tra i tanti e stupendi valori che mi avete trasmesso, quelli di umiltá, determinazione, coerenza e sacrificio hanno reso possibile il raggiungimento di tutti i risultati ottenuti finora.

During my PhD I was not working alone, but with many incredible and unforgettable chemists and persons. I would like to thank all the former and current members of the Melchiorre group.

Special thanks are for Dr. Yankai Liu, Mattia Silvi and Dr. John Murphy. Yankai was my master during the first year of my experience; he taught me how to efficiently work in a lab and shared with me his enormous knowledge and passion for chemistry. Mattia was my "travel companion"; we shared 3 years of difficult and happy moments. We were always present for each others, no matter why, when and where. John was John; a really funny and Irish postdoc who shared with me unforgettable moments in the lab and outside (I also thanks him for the proof reading of this thesis). All the three guys are very brilliant chemists as well as beautiful persons and friends. It was a pleasure to stay with them and to learn togheter about chemistry and life.

Of course I cannot forget to thank all the persons and friends from Italy that always supported me. Professor Paolo Venturello and Professor Cristina Prandi, who helped me during my master thesis and in the decision to come at the ICIQ. Dr. Paolo Larini, who introduced me in the world of the research and for all the chemistry and life suggestions. All my friends from Druento, per tutti i bei momenti passati insieme: Puppa, Luca, Serena, Valentina, Frank, Mariano, Alessandra, Laky, Alessio, Marta, Elisa, Marco, Isa, Ramona, Pipi, Luca, Giorgia, Ferre, Lo zio, Stefano, Marghe e Carlotta.

Finally, I would like to thank all the persons that shared with me beautiful moments in these 4 years, rendering this experience incredible and unique: especially Maria and Ester.

Support from the Institute of Chemical Research of Catalonia (ICIQ) Foundation, from MICINN (grant CTQ2010-15513) and from the European Research Council (ERC Starting grant agreement no. 278541—ORGA-NAUT) are gratefully acknowledged.

I am personally grateful to:

- ICIQ Foundation for a first year predoctoral fellowship (ref. 14/09) and
- Ministry of Education, Culture and Sport of Spain for an FPU predoctoral fellowship (ref. AP2010-1963)

List of Publications

Some of the results presented in this thesis have been published:

- "Metal-Free Photochemical Aromatic Perfluoroalkylation of α-Cyano Arylacetates" Manuel Nappi,[†] Giulia Bergonzini,[†] Paolo Melchiorre, *Angew. Chem. Int. Ed.* **2014**, *53*, 49214925.
- "Direct β-Functionalization of Cyclic Ketones with Aryl Ketones via the Merger of Photoredox and Organocatalysis"
  Filip R. etroni evi ,[†] Manuel Nappi,[†] David W. C. MacMillan, *J. Am. Chem. Soc.* **2013**, *135* (49), 18323–18326.
- "Multicatalytic Asymmetric Synthesis of Complex Tetrahydrocarbazoles via a Diels-Alder Benzoin Reaction Sequence"
  Yankai Liu, Manuel Nappi, Eduardo C. Escudero-Adán, Paolo Melchiorre, *Org. Lett.* **2012**, *14* (5), 1310–1313.
- "Asymmetric Catalysis of Diels-Alder Reactions with *in Situ* Generated Heterocyclic ortho-Quinodimethanes"
  Yankai Liu, Manuel Nappi, Elena Arceo, Silvia Vera, Paolo Melchiorre, *J. Am. Chem. Soc.* **2011**, *133* (38), 15212–15218.

[†] These authors contributed equally

UNIVERSITAT ROVIRA I VIRGILI
NOVEL AMINOCATALYTIC AND PHOTOCHEMICAL REACTIONS
Manuel Nappi

BE THE BEST OF WHATEVER YOU ARE

"If you can't be a pine on the top of a hill
Be a shrub in the valley—but be
The best little shrub on the side of the hill,
Be a bush if you can't be a tree.
If you can't be a highway just be a trail
If you can't be the sun be a star;
It isn't by size that you win or fail—
Be the best of whatever you are."

SIATE IL MEGLIO

"Se non potete essere un pino sulla vetta del monte,
siate un cespuglio nella valle,
ma siate il miglior piccolo cespuglio sulla sponda della collina.

Se non potete essere una via maestra siate un sentiero.
Se non potete essere il sole siate una stella,
non con la mole vincete o fallite.

Siate il meglio di qualunque cosa siate
Cercate ardentemente di capire a cosa siete chiamati
e poi mettetevi a farlo appassionatamente."

Martin Luther King

To my family

Table of Contents

UNIVERSITAT ROVIRA I VIRGILI
NOVEL AMINOCATALYTIC AND PHOTOCHEMICAL REACTIONS
Manuel Nappi

Chapter I Introduction

The request of high-efficiency energetic systems is prompting the scientific community toward the design and the development of new sustainable processes. A process is defined as sustainable if is *capable of being continued with minimal long-term effect on the environment*. Recently, within the general definition were also included the concepts of *societally beneficial* and *economically robust*. Regarding the organic chemistry, the design of sustainable organic reactions is one of the most challenging and important objectives that chemists are pursuing not only in the industry, but also in academic research. Many efforts have been devoted to develop new sustainable reactions, especially in the fields of methodologies and catalysis. Nowadays, two types of catalysis are particularly promising in this sense: organocatalysis and visible light photocatalysis. Though some examples appeared in the last century, these innovative methodologies are relatively new and modernly developed from the beginning of the current century. Basically, organocatalysis relies on the use of small and simple chiral organic molecules to catalyze enantioselective transformations, while photocatalysis exploits the light, particularly in the range of the *visible* region (380-750 nm), to promote organic reactions.

The advent of organocatalysis[1] brought the prospect of a complementary mode of catalysis, with the potential for savings in cost and energy, an easier experimental procedure, and reductions in potentially toxic chemical waste. These benefits arise from three factors. First, organic molecules are generally insensitive to oxygen and moisture in the atmosphere, so there is no need for special reaction vessels, storage containers and experimental techniques, or for ultra-dry reagents and solvents. Second, a wide variety of chiral organic reagents, which can serve as catalysts precursor - such as amino acids, carbohydrates and hydroxy acids - are naturally available from biological sources as single enantiomers. Chiral organocatalysts are therefore usually cheap to prepare and readily accessible in a range of quantities, suitable for small-scale reactions to industrial-scale reactions. Third, small organic molecules are typically non-toxic and environmentally friendly, increasing the safety of catalysis in both biological and chemical research across all research settings, including industry and academic institutions.

On the other hand, s*unlight* is a unique natural resource. It is an inexpensive, nonpolluting, abundant and endlessly renewable source of clean energy. Nature has found the best way to exploit this precious energy through the photosynthetic system contained in all the Earth-plants. Indeed, the photosynthesis is able to capture the light energy and convert it in chemical energy

[1] D. W. C. MacMillan. The Advent and Development of Organocatalysis. *Nature* **2008**, *455*, 304.

represented by the carbohydrates, allowing the life on the Earth. Thus, solar light can be considered as primary form of energy.

Scientists have been always fascinated by the photosynthetic system and many attempts were made to create an artificial system to directly use the light. The observation that light alone could affect unique chemical changes in organic compounds led early twentieth century photochemists to recognize that the sun might represent an inexhaustible source of clean chemical potential. One of the earliest and most remarkable articulations of this idea can be found in a lecture presented to the 8th International Congress of Applied Chemistry in 1912 by Giacomo Ciamician, an Italian chemist who is widely regarded as a pioneering figure in the development of organic photochemistry. In his work, entitled "The hotochemistry of the Future", Ciamician speculated that a new, more environmentally responsible chemical industry could replace high-energy synthetic processes with clean, cost-efficient photochemical transformations, with dramatic ecological benefits:[2]

On the arid lands there will spring up industrial colonies without smoke and without smokestacks; forests of glass tubes will extend over the plains and glass buildings will rise everywhere; inside of these will take place the photochemical processes that hitherto have been the guarded secret of the plants, but that will have been mastered by human industry which will know how to make them bear even more abundant fruit than nature, for nature is not in a hurry and mankind is. And if in a distant future the supply of coal becomes completely exhausted, civilization will not be checked by that, for life and civilization will continue as long as the sun shines!

G. Ciamician (1912)

Driven by this visionary idea, in the past decades chemists developed many reactions based on the employment of light as reactant. Since most of the organic molecules absorb only UV light in low efficiency, almost all the discovered reactions are based on the use of expensive and harmful UV lamps in harsh protocols. Precious are instead the transformations promoted by *visible light*,[3] since they occur under mild reaction conditions using inexpensive artificial lamps, and the representative natural major source is the sun.

In this introduction, some of the basic principles of organocatalysis and photocatalysis, two modern, environmentally respectful methodologies, will be discussed. Specifically, the reactivity concepts that were key to developing the chemistry discussed in the thesis are considered.

---

[2] G. Ciamician. The Photochemistry of the Future. *Science* **1912**, *36*, 385.

[3] a) T. P. Yoon, M. A. Ischay, J. Du. Visible Light Photocatalysis as a Greener Approach to Photochemical Synthesis. *Nature Chem.* **2010**, *2*, 527. b) D. M. Schultz, T. P. Yoon. Solar Synthesis: Prospects in Visible Light Photocatalysis. *Science* **2014**, *343*, 1239176.

1.1 Organocatalysis and Aminocatalysis

The first example of organocatalytic reaction can be traced back to the von Liebig's synthesis of oxamide **1** in 1859 (Scheme 1a).[4] As such, the concept behind organocatalysis is almost as old as the term "catalysis" itself.[5] In 1912, Bredig and Fiske reported the first example of asymmetric organocatalysis, where the enantio-enriched compound **3** was formed using quinine **2** to catalyze the cyanide addition to benzaldehyde (Scheme 1b).[6] In the 1970s, two industrial research groups independently demonstrated that a simple natural aminoacid, such as L-proline, could effectively catalyze an asymmetric intramolecular aldol reaction to give the highly enantioenriched chiral bicyclic product **4** (Scheme 1c).[7] This process provided the first example of asymmetric aminocatalysis,[8] where chiral secondary or primary amines serve as catalysts for the stereoselective functionalization of unmodified carbonyl compounds.

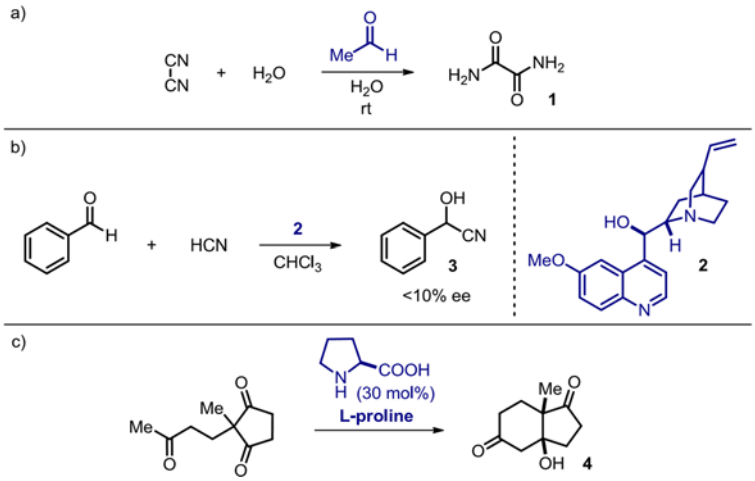

Scheme 1. First examples of organocatalysis and aminocatalysis.

After 30 years, in 2000, two seminal publications introduced the modern concept of asymmetric aminocatalysis. List, Lerner, and Barbas III reported a stereoselective intermolecular prolinecatalyzed

[4] J. von Liebig. *Liebigs Ann. Chem.* **1860**, *113*, 246.
[5] J. J. Berzelius, Annual Report on Progress in Physics and Chemistry, Stockholm, Sweden: Royal Swedish Academy of Sciences, **1835**.
[6] G. Bredig, P. S. Fiske. *Biochem. Z.* **1912**, *46*, 7.
[7] a) U. Eder, G. Sauer, R. Wiechert. New Type of Asymmetric Cyclization to Optically Active Steroid CD Partial Structures. *Angew. Chem. Int. Ed. Engl.*, **1971**, *10*, 496. b) Z. G Hajos, D. R. Parrish. Asymmetric Synthesis of Bicyclic Intermediates of Natural Product Chemistry. *J. Org. Chem.*, **1974**, *39*, 1615.
[8] P. Melchiorre, M. Marigo, A. Carlone, G. Bartoli. Asymmetric Aminocatalysis-Gold Rush in Organic Chemistry. *Angew. Chem. Int. Ed.* **2008**, *33*, 6138.

aldol reaction (Scheme 2a),[9] while MacMillan developed the first organocatalytic asymmetric Diels-Alder reaction[10] (Scheme 2b).

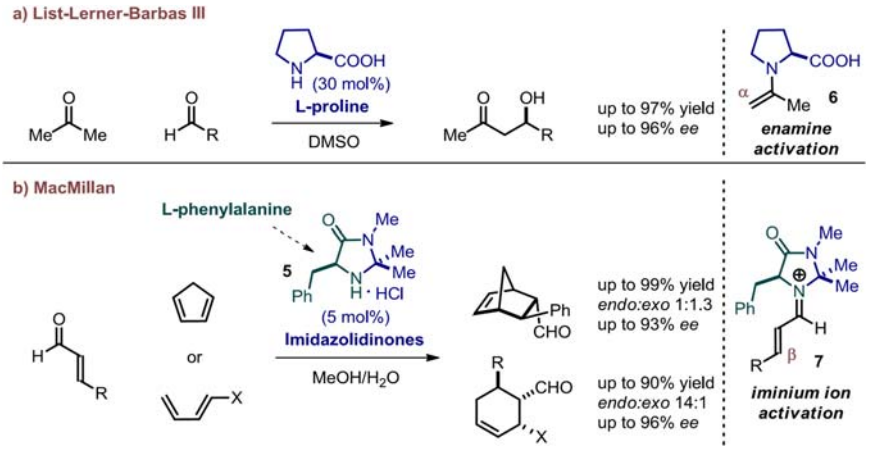

Scheme 2. Asymmetric organocatalytic aldol and Diels-Alder reactions.

Both transformations were catalyzed by natural amino acids derivatives: in the first case, Lproline was directly used as catalyst while a new class of chiral secondary amines (the imidazolidinones or MacMillan catalysts **5**), prepared from L-phenylalanine, was employed in the Diels-Alder reaction. The intermolecular aldol reaction allowed the direct asymmetric α functionalization of ketones exploiting the transient formation of the enamine **6**, while the DielsAlder reaction proceeded through the iminium ion intermediate **7**. These studies conceptualized enamine[11] and iminium ion[12] as two general activation modes in aminocatalysis. A generic activation mode describes a reactive species that can participate in many reaction types with consistently high enantioselectivity (as opposed to one or two unique transformations). Such reactive species arise from the interaction of a single chiral catalyst with a basic functional group (such as a ketone, aldehyde or imine) in a highly organized and predictable manner. In the case of aminocatalysis, the key enamine (**6**) and iminium ion (**7**) intermediates derive from the initial condensation of the chiral amine catalyst with carbonyl compounds and their α,β-unsaturated analogues (Scheme 3). After elimination of water, the iminium ion **9** is firstly generated. When a double bond is conjugated with the iminium ion moiety, a lowering of the energy of lowest unoccupied molecular orbital (LUMO), compared to the original α,β-unsaturated carbonyl compound **8**, occurs; as a result, the β position in the iminium ion intermediate **9** is highly activated toward a nucleophilic attack. This activation mode serves for the activation of α,βunsaturated carbonyl

[9] B. List, R. A. Lerner, C. F. Barbas III. Proline-Catalyzed Direct Asymmetric Aldol Reactions. *J. Am. Chem. Soc.*, **2000**, *122*, 2395.
[10] K. A. Ahrendt, C. J. Borths, D. W. C. MacMillan. New Strategies for Organic Catalysis: The First Highly Enantioselective Organocatalytic Diels−Alder Reaction. *J. Am. Chem. Soc.*, **2000**, *122*, 4243.
[11] S. Mukherjee, J. W. Yang, S. Hoffmann, B. List. Asymmetric Enamine Catalysis. *Chem. Rev.* **2007**, *107*, 5471.
[12] G. Lelais, D. W. C. MacMillan. Modern Strategies in Organic Catalysis: The Advent and Development of Iminium Activation. *Aldrichimica Acta* **2006**, *39*, 79.

compounds allowing the β-functionalization with soft nucleophiles or transformations that require an electron-poor olefin, for example normal electron-demand cycloadditions.

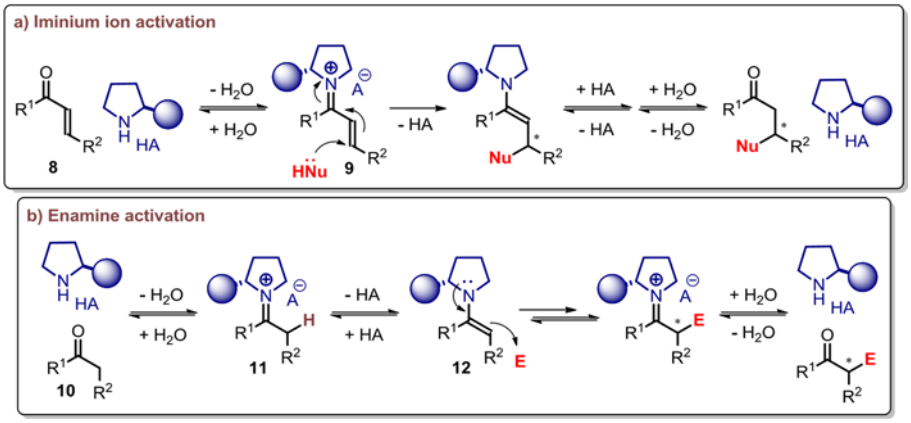

Scheme 3. Iminium ion and enamine activation modes. Nu = nuclephile; E = electrophile.

If an enolizable carbonyl substrate **10** is used instead (Scheme 3b), the proton adjacent to the iminium ion **11** become very acidic and can be easily removed under the reaction conditions. Enamine **12** is thus formed; this intermediate is electron-rich and, due to a raising of the energy of the highest occupied molecular orbital (HOMO) compared to the corresponding enol, can only react with an electrophile. Consequently, enolizable carbonyl compounds can be functionalized at the α position with electrophilic partners. One of the major benefits of aminocatalysis is that this strategy does not require the prefunctionalization of the carbonyl compounds.

1.1.1 Vinylogous Reactivity

Over the past decade, asymmetric aminocatalysis has become a reliable synthetic platform to stereoselectively forge stereogenic centers at the α and β positions of unmodified carbonyl compounds *via* enamine and iminium ion activation, respectively. Recently, the chemists' interest has shifted toward the stereocontrolled generation of stereocentres remote from the carbonyl moiety. Moving along the chain of a carbonyl substrate requires the propagation of the electronic effects inherent to enamine and iminium ion activations through the conjugated πsystem of poly-unsaturated carbonyls. Such an electronic transmission is peculiar to vinylogous reactivity, as originally defined in 1935 by Reynold C. Fuson.[13] The combination of aminocatalysis with the principle of vinylogy has brought about the development of dienamine[14] and trienamine[15] catalysis (HOMO-raising strategies), and vinylogous

[13] R. C. Fuson. The Principle of Vinylogy. *Chem. Rev.* **1935**, *16*, 1.
[14] S. Bertelsen, M. Marigo, S. Brandes, P. Diner, K. A. Jørgensen. Dienamine Catalysis: Organocatalytic Asymmetric γ-Amination of α,β-Unsaturated Aldehydes. *J. Am. Chem. Soc.* **2006**, *128*, 12973.
[15] a) Z.-J. Jia, H. Jiang, J.-L. Li, B. Gschwend, Q.-Z. Li, X. Yin, J. Grouleff, Y.-C. Chen, K. A. Jørgensen. Trienamines in Asymmetric Organocatalysis: Diels-Alder and Tandem Reactions. *J. Am. Chem. Soc.* **2011**, *133*, 5053. b) Y. Liu, M. Nappi, E. Arceo, S. Vera, P. Melchiorre. Asymmetric Catalysis of Diels-Alder Reactions with *in Situ* Generated Heterocyclic *ortho*-Quinodimethanes. *J. Am. Chem. Soc.* **2011**, *133*, 15212. [16] X. Tian, Y. Liu, P.

iminium ion[16] activation (LUMO-lowering strategy), novel approaches for the asymmetric functionalization of carbonyl compounds at their γ-, ε-, and δ-positions, respectively (Scheme 4).[16]

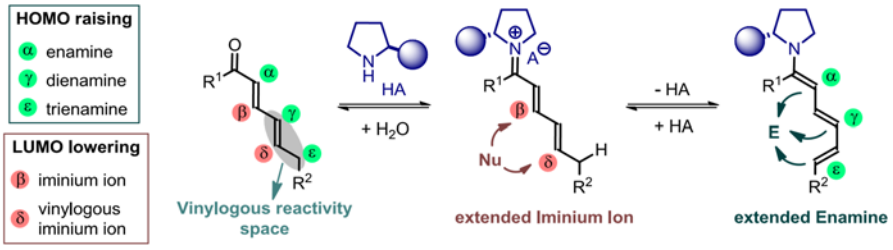

Scheme 4. Vinylogous reactivity in aminocatalysis. E = electrophile; Nu = nucleophile

1.1.2 Aminocatalysis Coupled with NHC Catalysis

One of the main features of aminocatalysis is the high tolerance of different reaction conditions, which allows the coupling with other organocatalytic activation modes. As an example, the use of chiral secondary amines and *N*-heterocyclic carbenes (NHC) served for the construction of complex molecular skeletons.

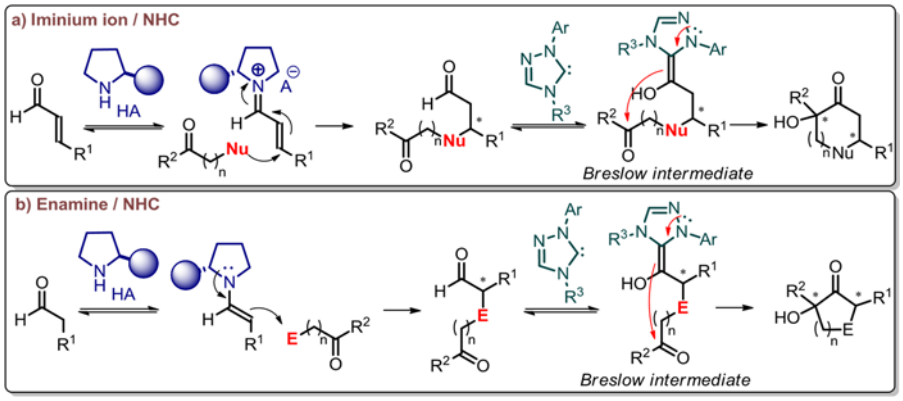

Scheme 5. Combining NHC catalysis with iminium ion and enamine activation. E = electrophile; Nu = nucleophile.

In particular, while aminocatalysis promotes the classical reactivity of carbonyl compounds, NHC catalysis induces umpolung reactivity[18] *via* formation of the well-known Breslow intermediate.[19] Both

Melchiorre. Aminocatalytic Enantioselective 1,6-Additions of Alkyl Thiols to Cyclic Dienones: Vinylogous Iminium Ion Activation. *Angew. Chem. Int. Ed.* **2012**, *51*, 6439.

[16] a) I. D. Jurberg, I. Chatterjee, R. Tannert, P. Melchiorre. When Asymmetric Aminocatalysis Meets the Vinylogy Principle. *Chem. Commun.* **2013**, *49*, 4869. b) H. Jiang, Ł. Albrechtab, K. A. Jørgensen. Aminocatalytic Remote Functionalization Strategies. *Chem. Sci.* **2013**, *4*, 2287.

enamine and iminium ion activations can be combined with NHC chemistry to design [17][18]cascade processes (Scheme 5).[19]

1.2 Merging Photoredox Catalysis with Aminocatalysis

Ruthenium polypyridyl complexes are well-established one-electron photoredox catalysts, which can absorb *visible light*. These inorganic complexes have found widespread applications in the areas of energy storage, hydrogen and oxygen evolution from water, and methane production from carbon dioxide.[20] However, until 2008, tris(2,2'-bipyridyl)dichlororuthenium(II) **15** did not find a substantial application in organic synthesis. A breakthrough study by MacMillan and Nicewicz demonstrated the potential of the ruthenium photoredox catalyst to promote previously elusive organic transformations. Specifically, the merger of the ruthenium complex photochemistry and enamine activation served to develop the first direct and highly enantioselective α-alkylation of aldehydes (Scheme 6).[21]

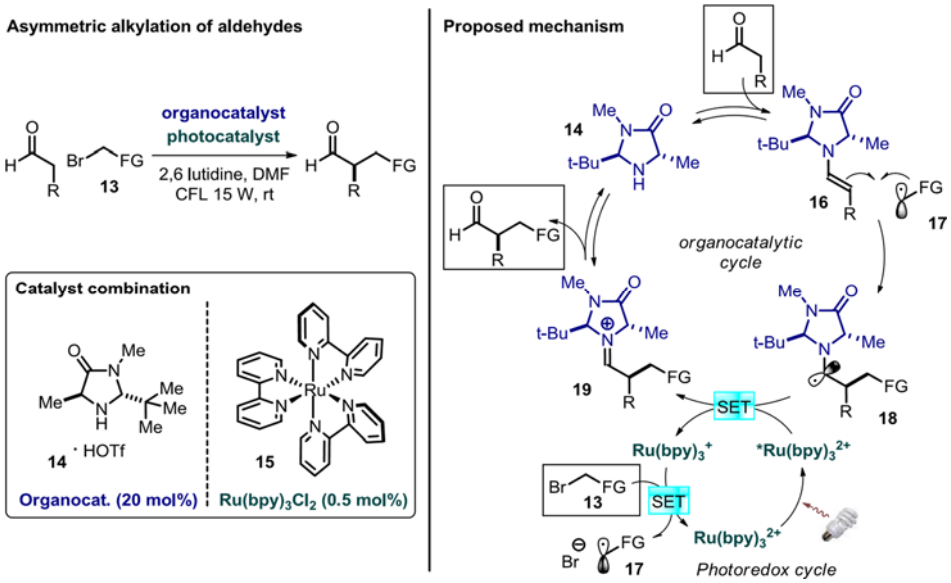

Scheme 6. Asymmetric organocatalytic photoredox alkylation of aldehydes and the proposed reaction mechanism. CFL = compact fluorescence lamp; SET = single electron transfer.

---

[17] B.-T. Gröbel, D. Seebach. Umpolung of the Reactivity of Carbonyl Compounds through SulfurContaining Reagents. *Synthesis* **1977**, 357.
[18] R. Breslow. On the Mechanism of Thiamine Action. IV. Evidence from Studies on Model Systems. *J. Am. Chem. Soc.* **1958**, *80*, 3719.
[19] K. E. Ozboya, T. Rovis. Enamine/Carbene Cascade Catalysis in the Diastereo- and Enantioselective Synthesis of Functionalized Cyclopentanones. *Chem. Sci*. **2011**, *2*, 1835.
[20] K. Kalyanasundaram. Photophysics, Photochemistry and Solar Energy Conversion with Tris(bipyridyl)ruthenium(II) and its Analogues. *Coord. Chem. Rev.* **1982**, *46*, 159.
[21] D. Nicewicz, D. W. C. MacMillan. Merging Photoredox Catalysis with Organocatalysis: The Direct Asymmetric Alkylation of Aldehydes. *Science*, **2008**, *322*, 77.

This study demonstrated that the combination of visible light photocatalysis with an aminocatalytic system can solve challenging problems connected with the synthesis of chiral molecules. According to the proposed mechanism, the imidazolidinone catalyst **14** activates the aldehyde via enamine (**16**) formation while the electro-deficient radical **17** is generated by the ruthenium (I) complex. In particular, the electron-deficient bromo-compound **13** is reduced by $Ru(bpy)_3^+$ to the corresponding radical anion (not shown), which *via* rapid fragmentation (mesolysis) of the C-Br bond releases the electrophilic radical **17** and the bromide. The combination of the chiral electron-rich enamine **16** with the radical **17** yields the α-amino radical **18,** which is prone to oxidation from the excited $Ru(bpy)_3^{2+}$. The photoredox cycle is thus closed. The hydrolysis of the iminium ion **19** provides the desired alkylated aldehyde while the imidazolidinone **14** can restart another catalytic cycle. The first photoredox cycle is supposed to start with the oxidation of a sacrificial amount of enamine **16**, which leads to the formation of the strongly reducing Ru(I) (this initiation step is not shown in Scheme 6).

After this seminal work, and other pioneering contributions from the group of Yoon,[22] many reactions were developed using the visible light-driven photoredox strategy. The combination of the classical polar reactivity with the radical reactivity has extended the number of transformations available in organic chemistry.[23]

1.3 Combining the Photochemical Activity of Electron Donor Acceptor Complexes with Aminocatalysis

Electron donor acceptor (EDA) complexes have been defined by Mulliken in the '50s of the last century as colored molecular association of two or more colorless species.[24] EDA complexes are generated from the interaction between electron donor (D) and electron acceptor (A) molecules. The resulting molecular ground state association is characterized by a new absorption band that generally lies in the visible range of the light. When the EDA complexes are irradiated with a proper light, a single electron transfer from the electron donor to the acceptor can occur, generating radicals or radical ions (Eq. 1). Despite the attractive theory of EDA complexes, this type of activation did not found many applications in organic synthesis because of the rapid and unproductive back electron transfer processes (BET) (Eq. 1). Open-shell species are high-energy intermediates and, after the first photoinduced electron transfer (PET), they can return to the initial status. The BET are generally fast compared to all other processes that could happen after the PET ($k_{BET} >> k_P$), which limits the synthetic utility of EDA activation (Eq. 1).

$$D + A \rightleftharpoons \underset{\text{ground state}}{[D,A]} \overset{h\nu}{\underset{k_{BET}}{\overset{k_{PET}}{\rightleftharpoons}}} [D^{\bullet+},A^{\bullet-}] \xrightarrow{k_P} P \qquad \text{(Eq. 1)}$$

[22] M. A. Ischay, M. E. Anzovino, J. Du, T. P. Yoon. Efficient Visible Light Photocatalysis of [2+2] Enone Cycloadditions. *J. Am. Chem. Soc.* **2008**, *130*, 12886.
[23] C. K. Prier, D. A. Rankic, D. W. C. MacMillan. Visible Light Photoredox Catalysis with Transition Metal Complexes: Applications in Organic Synthesis. *Chem. Rev.* **2013**, *113*, 5322.
[24] a) R. S. Mulliken. Molecular Compounds and their Spectra II. *J. Am. Chem. Soc.* **1952**, *74*, 811; b) R. Foster. Electron Donor–Acceptor Complexes. *J. Phys. Chem.* **1980**, *84*, 2135.

In 2013, our research group found that the photochemical activity of EDA complexes can be used to productively render radical species under very mild reaction conditions, only using visible light irradiation and without the need of any photocatalyst or radical initiators. The combination of EDA activation and aminocatalysis served to develop a stereoselective catalytic α-alkylation of aldehydes (Scheme 7).[25] The condensation of aldehydes with the chiral secondary amine **20** (a prolinol silyl ether derivative) provides the enamine **21**. This electron-rich specie **21** forms a yellow-orange colored EDA complex upon association with the electron-deficient benzyl bromide **22** in the ground state. Irradiation with visible light, using a simple CFL (compact fluorescence lamp), promotes a single electron transfer (SET) from the enamine **21** to the bromo-compound **22**, affording the two open-shell species **23** and **24**. The radical anion **23** undergoes a fast fragmentation (mesolysis) yielding the bromide and the benzyl radical **25**, which reacts in the solvent cage with the open-shell chiral intermediate **24** to give the enantioenriched α-alkylated aldehyde. Alternative pathways are feasible, where the photo-excitation of the EDA complex acts only as initiation of a radical chain mechanism, proceeding via a Kornblum-Russell $S_{RN}1$-type alkylation pathway.[27]

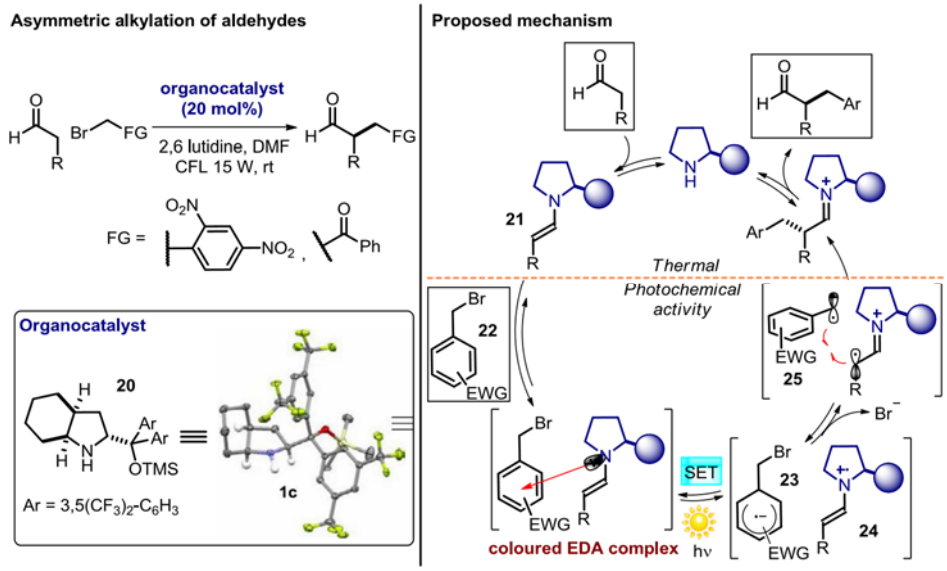

Scheme 7. Photo-organocatalytic asymmetric alkylation of aldehydes via EDA complex activation.

1.4 Objectives and Summary of the Doctoral Thesis

The following chapters detail the efforts carried out to develop new, operationally simple synthetic reactions using aminocatalysis, photochemistry, and their combination.

---

[25] E. Arceo, I. D. Jurberg, A. Alvarez-Fernandez, P. Melchiorre. Photochemical Activity of a Key Donor–Acceptor Complex Can Drive Stereoselective Catalytic α-Alkylation of Aldehydes. *Nat. Chem.* **2013**, *5*, 751. [27] G. A. Russell, & K. Wang. Electron Transfer Processes. 53. Homolytic Alkylation of Enamines by Electrophilic Radicals'. *J. Org. Chem.* **1991**, *56*, 3475.

Chapter **II** describes how aminocatalytic vinylogous reactivity served to *in situ* generate heterocyclic *ortho*-quinodimethane (*o*-QDM) intermediates **27** from indole-based unsaturated aldehydes **26** under mild conditions. In particular, we found that the aromaticity of indole can be broken in favor of *o*-QDM **27** by means of trienamine activation of **26** (Scheme 8). The intermediate **27** reacts as an activated diene in asymmetric Diels-Alder reactions with two different classes of dienophiles. Highly functionalized chiral tetrahydrocarbazoles (**28** and **29**) were synthesized in almost enantiopure form.[13b]

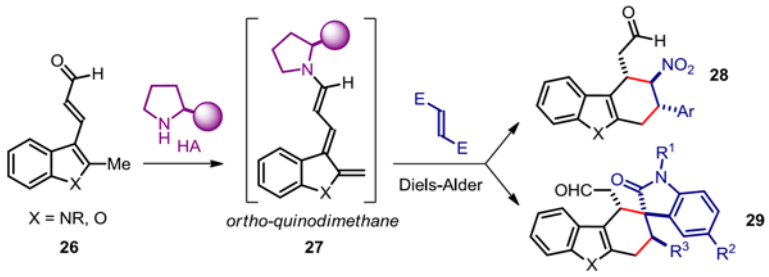

Scheme 8. Organocatalytic asymmetric Diels-Alder reaction via *in situ* generated *o*-QDMs.

This was the first project I was involved in within the Melchiorre group. I successfully optimized the asymmetric Diels-Alder reaction of *in situ* generated heterocyclic *o*QDMs, reactive diene species that have never before succumbed to a catalytic approach. The chemistry was developed in collaboration with Dr. Yankai Liu, a postdoctoral researcher. He taught me how to efficiently work in a lab either by my own or with other colleagues. He, together with Prof. Melchiorre, made me understand that the time is a priceless value for a researcher. During the project, I extended my knowledge in asymmetric organocatalysis and in pericyclic reactions.

Chapter **III** discusses the combination of organocatalytic vinylogous reactivity with Nheterocyclic carbenes (NHC) to synthesize complex polycyclic molecules **30**. Based on the previously discovered *o*-QDM activation process via trienamine formation, a Diels-Alder/cross benzoin reaction sequence was developed (Scheme 9).[26]

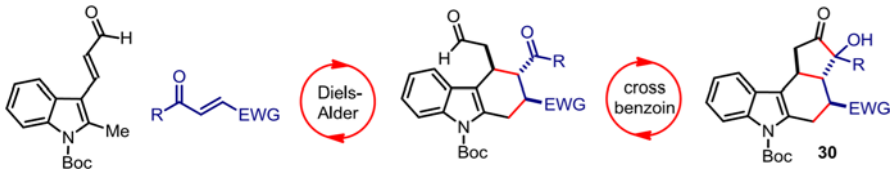

Scheme 9. Construction of polycycle structures via one-pot Diels-Alder/cross benzoin condensation.

In this project, I directly contributed to the initial idea, together with Dr. Yankai Liu. We found the appropriate dienophile to realize the new organocatalytic one-pot sequence. I increased my

[26] Y. Liu, M. Nappi, E. C. Escudero-Adán, P. Melchiorre. Multicatalytic Asymmetric Synthesis of Complex Tetrahydrocarbazoles via a Diels-Alder Benzoin Reaction Sequence. *Org. Lett.* **2012**, *14*, 1310.

knowledge of the synthetically powerfull concept of cascade reactions and the principles of NHC catalysis. Moreover, I performed NOE experiments to determine the relative configuration of the products, increasing my expertise of NMR spectroscopic techniques.

Chapter **IV** illustrates how a nitrogen atom-centered dienamine can promote an asymmetric azaMichael reaction. The dienamine formation enhances the nucleophilicity of the nitrogen in 1Hindazole-3-carboxaldehyde **31**, allowing the Michael addition to nitrostyrenes **32** to proceed in a stereoselective manner (Scheme 10).

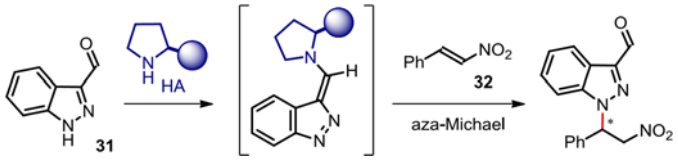

Scheme 10. Organocatalytic asymmetric aza-Michael reaction *via* an N-centered dienamine.

This was the first independent project I was involved in, where I could develop my own ideas. Supported by my supervisor, who always encouraged us to come up with our own ideas, I transformed the simple concept of N-centered dienamine, distilled out from an observation made during a precedent study, in something real. I learned how to handle a project working on my own, trying to optimize the conditions to let the new reaction work.

Chapter **V** describes the development of a direct organocatalytic photoredox β-aldol reaction. This chemistry was developed in the research laboratories of Professor MacMillan at Princeton University (USA). The merger of aminocatalysis and photoredox serves for the direct construction of γ-hydroxyketones **37** without pre-functionalization of the starting ketones (Scheme 11).[27] The reaction proceeds through a radical-radical coupling of the β-enaminyl radical specie **35** (a 5πe$^-$ intermediate generated from **33**)[30] and the diaryl or aryl-alkyl radicals **36**, generated *in situ* through a single electron reduction of the corresponding ketones **34**.

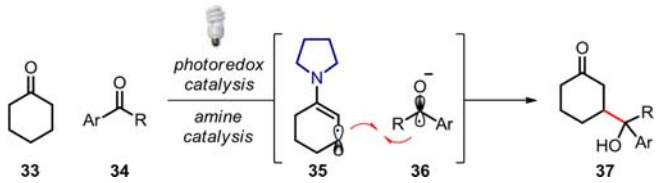

Scheme 11. Merging aminocatalysis with photoredox catalysis to promote the direct β-aldol reaction.

The period in the MacMillan group was crucial for my formation. I was exposed to a different field of catalysis, expanding my reactivity knowledge to include radical patterns and photoredox catalysis. I

---

[27] . . Petroni evic , M. Nappi, D. W. C. MacMillan. Direct β-Functionalization of Cyclic Ketones with Aryl Ketones *via* the Merger of Photoredox and Organocatalysis. *J. Am. Chem. Soc.* **2013**, *135*, 18323. [30] M. T. Pirnot, D. A. Rankic, D. B. C. Martin, D. W. C. MacMillan. Photoredox Activation for the Direct β-Arylation of Ketones and Aldehydes. *Science* **2013**, 339, 1593.

developed and optimized the direct β-aldol chemistry, capitalizing upon the βenaminyl 5πe- intermediate reactivity previously discovered by the MacMillan group.[30] The excellent scientific environment within the group and the support by Professor MacMillan has allowed me to increase my independent thinking, thus making me a better-rounded chemist.

Finally, chapter **VI** shows how the simple use of visible light, without the need of any photocatalysts or radical initiators, can promote a photochemical aromatic perfluoroalkylation and trifluromethylation of α-aryl cyanoacetates via EDA complex activation (Scheme 12).[28] A homolytic aromatic substitution (HAS) chain mechanism is proposed as the main pathway. Investigations to support this mechanistic scenario, including a quantum yield of 2.03, will be discussed.

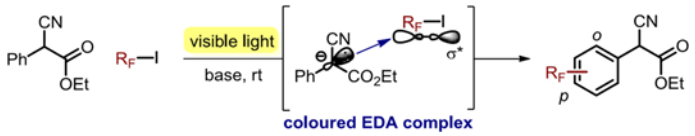

Scheme 12. Metal-free photochemical aromatic perfluoroalkylation and trifluoromethylation of α-aryl cyanoacetates via EDA complex formation.

Conceptually, this study established the possibility for enolates to work as suitable donors in EDA formation. These results corroborate the idea that the photochemistry of EDA complexes, formed upon aggregation of organic substrates, may provide a general reactivity framework for the design of unprecedented photochemical transformations. After the optimization studies and the scope of the reactivity, I mainly focused on the reaction mechanism, performing competition experiments, kinetic isotope effect (including the synthesis of deuterated substrate) and measuring the resonance Taft parameter. I also learned by myself how to perform the quantum yield of a photochemical reaction, an important parameter which allowed us to propose the reaction mechanism.

[28] M. Nappi, G. Bergonzini, P. Melchiorre. Metal-Free Photochemical Aromatic Perfluoroalkylation of αCyano Arylacetates. *Angew. Chem. Int. Ed.* **2014**, *53*, 4921.

Chapter II

Asymmetric Catalysis of Diels-Alder Reactions with in situ Generated Heterocyclic ortho-Quinodimethanes

Target

Synthesis of highly functionalized tetrahydrocarbazoles via asymmetric Diels-Alder reactions of *in situ* generated ortho-quinodimethane (o-QDM) intermediates. Formation of o-QDMs under mild conditions.

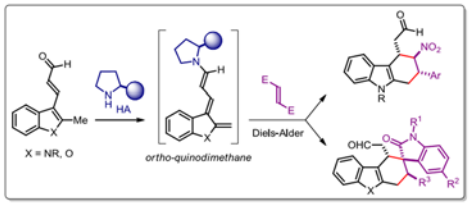

Tool

Ability of trienamine catalysis to activate unsaturated aldehydes toward vinylogous reactivity.[29]

Over the last 15 years, asymmetric aminocatalysis has become a reliable synthetic platform for forging stereogenic centres at the α and β positions of unmodified carbonyl compounds with high enantioselectivity.[2] More recently, chemists have become interested in using aminocatalysis for targeting stereocentres more remote from the catalyst's point of action.[30] The key to success is the ability of the amine catalyst to propagate the electronic effects inherent to aminocatalytic reactivity modes (*i.e.* the HOMO-raising and the LUMO-lowering activating effects) through the conjugated π-system of poly-unsaturated carbonyls while transmitting the stereochemical information at distant positions. As for the HOMO activation strategy, the combination of aminocatalysis with the principle of vinylogy[31] has brought about the development of dienamine and trienamine catalysis, novel strategies for the asymmetric functionalization of carbonyl compounds at their γ-, and ε-positions, respectively. This chapter outlines how the trienamine activation allows: i) the *in situ* formation of transient *ortho*quinodomethanes (*o*-QDMs) *via* a dearomatization process under mild reaction conditions

[29] The work discussed in this chapter has been published. see: Y. Liu, M. Nappi, E. Arceo, S. Vera, P. Melchiorre. Asymmetric Catalysis of Diels-Alder Reactions with *in situ* Generated Heterocyclic *ortho*Quinodimethanes. *J. Am. Chem. Soc.* **2011**, *133*, 15212. Experimental part developed together with Y. Liu. [2] P. Melchiorre, M. Marigo, A. Carlone, G. Bartoli. Asymmetric Aminocatalysis-Gold Rush in Organic Chemistry. *Angew. Chem. Int. Ed.* **2008**, *33*, 6138-6171.
[30] I. D. Jurberg, I. Chatterjee, R. Tannert, P. Melchiorre. When asymmetric aminocatalysis meets the vinylogy principle. *Chem. Commun.* **2013**, *49*, 4869-4883.
[31] R. C. Fuson. The Principle of Vinylogy. *Chem. Rev.* **1935**, *16*, 1.

(usually harsh settings are required to obtain *o*-QDMs) and ii) the consequent catalytic use of *o*QDMs (highly reactive dienes) in asymmetric Diels-Alder reactions .

2.1 Diels-Alder Reactions

This section provides some basic concepts of the Diels-Alder reactivity. The Diels-Alder reaction is among the most powerful synthetic tools in organic chemistry for the construction of cyclic molecules. The reaction generally occurs between a diene and a dienophile to generate a cyclohexene via a [4+2] cycloaddition process (Scheme 1). It was first described by Otto Paul Hermann Diels and Kurt Alder in 1928,[32] for which work they were awarded with the Nobel Prize in Chemistry in 1950.

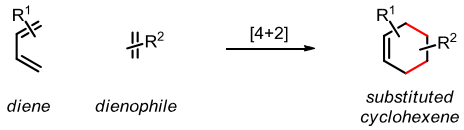

Scheme 1. The Diels-Alder cycloaddition [4+2].

The Diels-Alder reaction is a concerted pericyclic cycloaddition that occurs through a cyclic transition state. The term "concerted" intends that all the bond formations happen at the same time, defining a precise stereochemistry in the resulting cyclohexene. In 1952, Fukui proposed the modern Frontier Molecular Orbital (FMO) theory, which is based on the consideration of the highest occupied molecular orbital (HOMO) and the lowest unoccupied molecular orbital (LUMO), to explain and predict reaction mechanisms.[33] In brief; when two molecules collide, three major interactions occur:

1. The occupied orbitals of one molecule repel the occupied orbital of the other.
2. Any positive charge of one molecule attracts any negative charge of the other (and repels any positive).
3. The occupied orbitals (especially the HOMOs) of each molecule interact with the unoccupied orbitals (especially the LUMOs) of the other, causing an attraction between the molecules.[34]

Inspired by this seminal work, Roald Hoffmann and Robert Burns Woodward in 1965 published the first milestone of the later homonymous rules upon conservation of orbital symmetry,[35] which are summarized in the following statement for thermal pericyclic reactions:

---

[32] O. Diels, K. Alder. Synthesis in the Hydroaromatic Series, IV. Announcement: The rearrangement of Malein Acid Anhydride on Arylated Diene, Triene and Fulvene. *Chem. Ber.* **1929**, *62*, 2081.
[33] K. Fukui, T. Yonezawa, H. Shingu. A Molecular Orbital Theory of Reactivity in Aromatic Hydrocarbons. *J. Chem. Phys* **1952**, *20*, 722.
[34] Ian Fleming. Frontier Orbitals and Organic Chemical Reactions. **1978** London: Wiley.
[35] a) R. B. Woodward, R. Hoffmann. Stereochemistry of Electrocyclic Reactions. *J. Am. Chem. Soc.* **1965**, *87*, 395. b) R. B. Woodward, R. Hoffmann. The Conservation of Orbital Symmetry. *Angew. Chem. Int. Ed.* **1969**, *8*, 781.

"A thermal pericyclic reaction is symmetry-allowed when the total number of π electrons involved in the process obeys the rule 4n + 2; n is an integer"[9]

Employing the Woodward-Hoffmann rules with frontier molecular orbital (FMO) theory allows to predict and explain the feasibility, regioselectivity and stereochemistry of general cycloaddition reactions. The classical "*endo*-rule" observed in most of the reported [4+2] cycloadditions can be readily explained by considering the secondary orbital interactions (SOI) in the transition state of the reaction (Scheme 2). For instance, the Diels-Alder reaction between cyclopentadiene **1** (diene, HOMO) and maleic anhydride **2** (dienophile, LUMO) leads to the almost exclusive formation of the *endo* adduct over the *exo* adduct (99:1 ratio).[10] Indeed, in the *endo* transition state the internal position of the carbonyl groups provide an additional type of interactions in comparison with those that appear in the transition state of the *exo* approach.

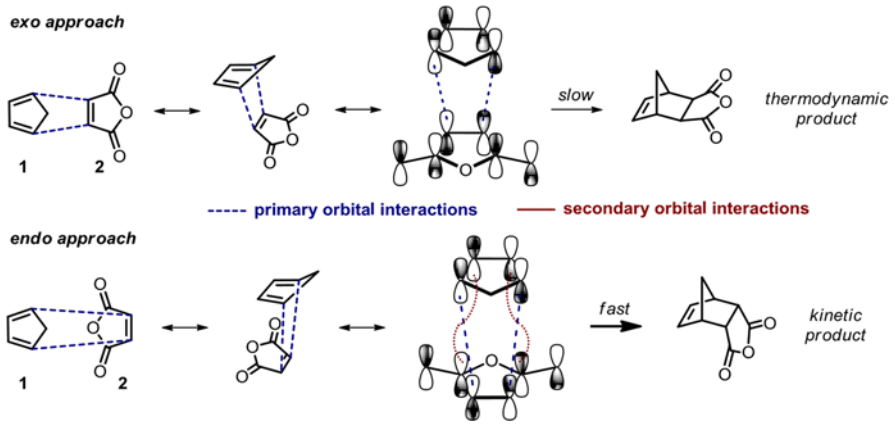

Scheme 2. *Exo* and *endo* selectivity in Diels-Alder reactions: secondary molecular orbital interactions.

These interactions, which are not directly involved in forming new bonds, are named secondary orbital interactions. In the case reported in Scheme 2, interactions occur between the C_2 and C_3 carbon atoms in the diene and the carbonyl carbon atoms of maleic anhydride (red dot line), making the *endo* approach kinetically favorable compared to the *exo* approach (Scheme 2).

In the Diels-Alder reactions the key factor in the prediction of the mechanism and reactivity is the consideration of the substituents that are attached to the diene and the dienophile. Firstly, the energy of the HOMO and LUMO changes according to the nature of the groups. In general:

- Extra conjugation raises the energy of the HOMO and lowers the energy of the LUMO
- An electron-withdrawing group (EWG) lowers the energy of both the HOMO and LUMO
- An electron-donating group (EDG) raises the energy of both the HOMO and LUMO

[9] Approximation made considering only the *suprafacial* approaches and based on the Hückel aromaticity model. See: M. B. Smith, J. March. Advanced Organic Chemistry: Reactions, Mechanisms and Structure. **2001** New York: Wiley.

[10] L. M. Stephenson, D. E. Smith, S. P. Current. *Endo* Preference in the Diels-Alder Cycloaddition of Butadiene and Maleic Anhydride. *J. Org. Chem.* **1982**, *47*, 4170.

In normal electron-demand Diels-Alder reactions, the HOMO is located in the diene, while the LUMO is in the dienophile. Considering unsubstituted butadiene and ethylene, the combination of HOMO-diene/LUMO-dienophile is preferred against the other possible one, where the LUMO is located into the diene and the HOMO in the dienophile (difference in energy ΔE between the two level is 10.6 vs 11.5 eV; Scheme 3a).

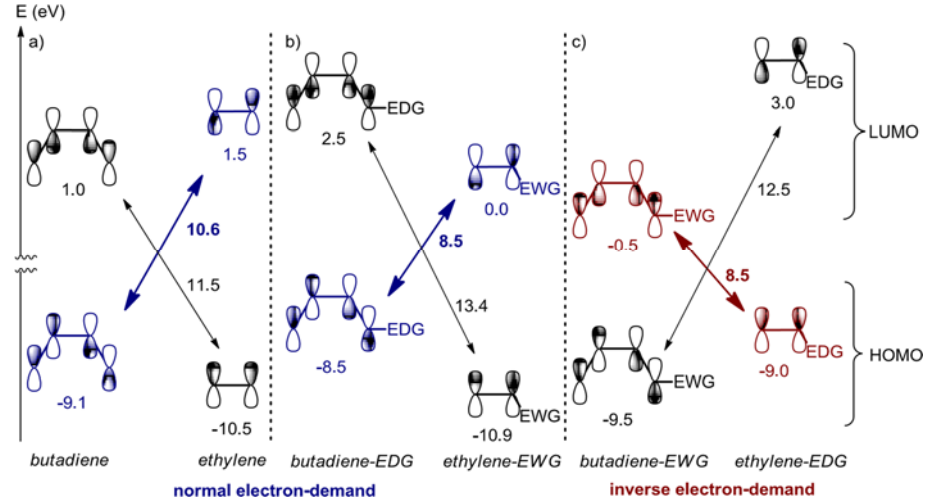

Scheme 3. Energy level of HOMO and LUMO: normal and inverse electron-demand Diels-Alder.

Thus, the optimal conditions to have a high reaction rate is a cycloaddition between a diene bearing an EDG (raising the HOMO) and a dienophile containing EWG (lowering the LUMO); ΔE: 8.5 vs 13.4 eV (Scheme 3b). In the opposite case (EWG-diene/EDG-dienophile), the difference in energy between the HOMO of the diene and the LUMO of the dienophile becomes too high (12.5 eV) and this reaction is described as an inverse electron-demand Diels-Alder reaction, where the LUMO is now centered on the diene and the HOMO on the dienophile (difference in energy: 8.5 eV, Scheme 3c).

Substituents not only introduce a change in energy of the HOMO and LUMO, but they also influence the coefficients of the atomic orbitals, which can determine the site-selectivity and regioselectivity of cycloadditions. For example, in the [4+2] cycloaddition that occurs between

1methoxybutadiene **3** and acrolein **4**, the only product observed experimentally is the "*ortho*" regioisomer 2-methoxycyclohex-3-enecarbaldehyde **5** (Scheme 4).[36]

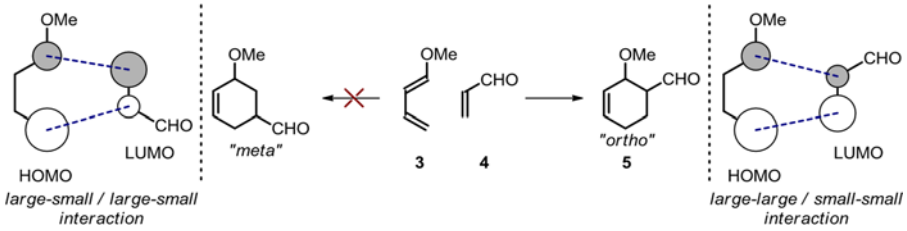

Scheme 4. Regioselectivity in the Diel-Alder reaction: atomic orbital coefficients.

According to the previous discussion regarding the two types of electron-demand Diels-Alder processes, the HOMO is located on the 1-methoxybutadiene and the LUMO on the acrolein. Considering the calculated atomic orbital coefficients, the interaction that predominates is the *large/large-small/small* one and defines the "*ortho*" regioselectivity against the "meta" adduct.

In general, the regioselectivity of a cycloaddition can be predicted by the following sequence:

1. Estimate the energy of the HOMO and the LUMO of both components.
2. Identify which HOMO/LUMO pair is closer in energy
3. Using this HOMO/LUMO pair, estimate the relative size of the atomic orbital coefficients of the atoms that participate in new bond formation
4. Match the larger coefficients of each component to give the predicted kinetic regioisomer of the reaction product.

2.2 State-Of-The-Art of Asymmetric Catalytic Diels-Alder Reactions

Following the first report by Diels and Alder in 1928, many methodologies have been developed to access a variety of cyclohexene derivatives. Among the available methods, of particular interest are those that provide [4+2] cycloadditions in both a catalytic and an enantioselective fashion.[37] In the last 20 years of the 20th century, the chemical community reported the first catalytic asymmetric examples of Diels-Alder reaction, mainly using the metal-based Lewis acid activation of the dienophile. The first example was reported in 1979 by Koga, who described the reaction

[36] S. D. Kahn, C. F. Pau, L. E. Overman, W. J. Hehre. Modeling Chemical Reactivity. 1. Regioselectivity of Diels-Alder Cycloadditions of Electron-Rich Dienes with Electron-Deficient Dienophiles. *J. Am. Chem. Soc.* **1986**, *108*, 7381.

[37] a) Y. Yamashita, S. Kobayashi. Handbook of Cyclization Reactions; S. Ma, Ed.; Wiley: New York, 2010; Vol. 1, pp 1−85. b) H. B. Kagan, O. Riant. Catalytic Asymmetric Diels-Alder Reactions. *Chem. Rev.* **1992**, *92*, 1007. c) G. Desimoni, G. Faita, K. A. Jørgensen. C2-Symmetric Chiral Bis(Oxazoline) Ligands in Asymmetric Catalysis. *Chem. Rev.* **2006**, *106*, 3561.

between cyclopentadiene **1** and methacrolein **6**. The chiral aluminium-based catalyst **7** was used as Lewis acid, affording the *exo* adduct **8** in 69% of yield and 72% *ee* (Scheme 5).[38]

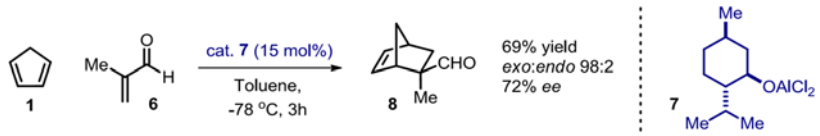

Scheme 5. The first enantioselective catalityc Diels-Alder reaction.

In 1989, Corey developed the novel Lewis acidic aluminum complex **11** based on chiral bissulfonamide with C_2 symmetry. The cycloaddition between the cyclopentadiene **9** and 3acryloyl-1,3-oxazolidin-2-one (**10**) in the presence of 10 mol% of **11** efficiently produced the chiral *endo* Diels-Alder adduct **12** in 94% yield and 96% *ee* (Scheme 6).[39]

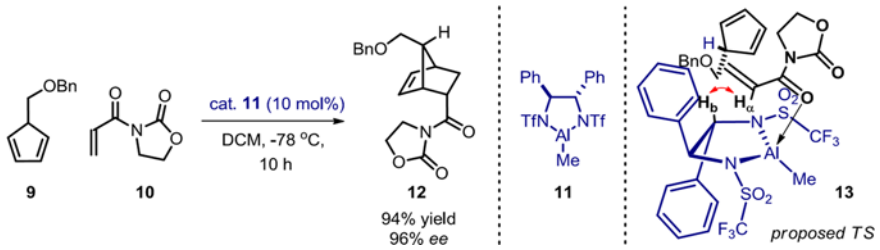

Scheme 6. The Diels-Alder reaction promoted by the chiral aluminum C_2 catalyst.

NMR experiments at low temperature of the 1:1 complex between catalyst **11** and the dienophile **10** showed a NOE interaction between the benzylic proton (H_b) and the proton in α position in the acrolein subunit (H_α). These studies prompted the authors to suggest the transition state assembly **13**, which is consistent with the observed stereochemical outcome.[40]

Titanium complexes represent another important class of Lewis acids used as chiral catalysts in [4+2] cycloadditions. Narasaka and collegues synthesized titanium dichloride complex **15** to promote the Diels-Alder reaction between cyclopentadiene **1** and the dienophile **14** (Scheme 7).[41]

---

[38] S. Hashimoto, N. Komeshima, K. Koga. Asymmetric Diels–Alder Reaction Catalysed by Chiral Alkoxyaluminium Dichloride. *J. Chem. Soc., Chem. Commun.* **1979**, 437.

[39] a) E. J. Corey, R. Imwinkelried, S. Pikul, Y. B. Xiang. Practical Enantioselective Diels-Alder and Aldol Reactions Using a New Chiral Controller System. *J. Am. Chem. Soc.* **1989**, *111*, 5493. b) E. J. Corey, N. Imai, S. Pikul. Catalytic Enantioselective Synthesis of a Key Intermediate for the Synthesis of Prostanoids. *Tetrahedron Lett.* **1991**, *32*, 7517.

[40] E. J. Corey, S. Sarshar, J. Bordner. X-ray Crystallographic and NMR Studies on the Origins of High Enantioselectivity in Diels-Alder Reactions Catalyzed by a Chiral Diazaaluminolidine. *J. Am. Chem. Soc.* **1992**, *114*, 7938.

[41] K. Narasaka, N. Iwasawa, M. Inoue, T. Yamada, M. Nakashima, J. Sugimori. Asymmetric Diels-Alder Reaction Catalyzed by a Chiral Titanium Reagent. *J. Am. Chem. Soc.* **1989**, *111*, 5340.

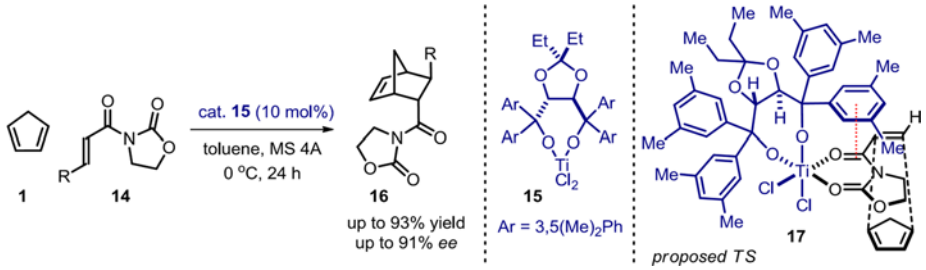

Scheme 7. Alkoxytitanium dichloride complexes in 4+2 cycloadditions.

The 1:1 complex between the catalyst **15** and 3-acryloyl-1,3-oxazolidin-2-one **14** was isolated and was proposed as the key intermediate toward the transition state **17**, which served to rationalize the stereochemical outcome of the Diels-Alder reaction.[42]

Later, Corey developed the new *B-n*-butyloxazaborolidine **19** from (*S*)-*N*-*p*toluenesulfonyltryptophan **18**.[18] Only 5 mol% of the oxazaborolidine sufficed for the acceleration and control of the reaction of cyclopentadiene **1** and 2-bromoacrolein **20** to enantioselectively form (more than 99% *ee*) the adduct **21** in high yield (Scheme 8).

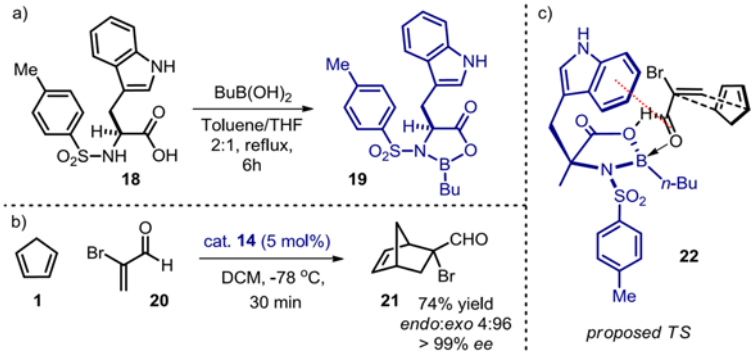

Scheme 8. New oxazaborolidine as catalyst for 4+2 cycloadditions.

In the proposed transition state **22**, the π-π interactions between the electron-rich indole scaffold within the catalyst and the α-bromo acrolein determines a well-structured TS to infer high stereocontrol in the cycloaddition. In 1991, Corey reported the first use of C_2-symmetric bis(oxazolines) (box) **25** as chiral ligands for metal-Lewis acid catalysis.[43] The Diels-Alder reaction between 3-acryloyl- 1,3-oxazolidin-2-one **10** and cyclopentadiene **1** was catalyzed by the *in situ* generated chiral iron(III) complex **23** (Scheme 9).

---

[42] E. J. Corey, Y. Mataumara. Evidence for the Importance of π-π Attractive Interactions in Enantioselective Diels-Alder Reactions Chiral Catalysts of Type $(RO)_2TiCl_2$. *Tetrahedron Lett.* **1991**, *32*, 6289. [18] E. J. Corey, T.-P. Loh. First Application of Attractive Intramolecular Interactions to the Design of Chiral Catalysts for Highly Enantioselective Diels-Alder Reactions. *J. Am. Chem. Soc.* **1991**, *113*, 8966.
[43] E. J. Corey, N. Imai, H.-Y. Zhang. Designed Catalyst for Enantioselective Diels-Alder Addition from a C_2-Symmetric Chiral Bis(oxazoline)-Iron(III) Complex. *J. Am. Chem. Soc.* **1991**, *113*, 728.

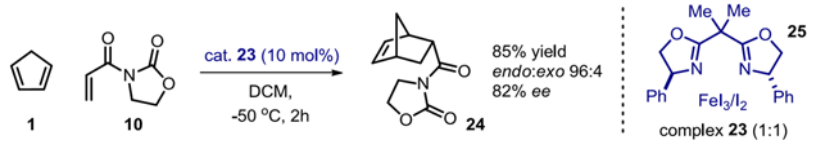

Scheme 9. Bis(oxazolines) as chiral ligand for Iron complex to provide Diels-Alder adducts.

From the year 2000, organocatalysis and specifically aminocatalysis greatly contributed to the development of asymmetric Diels-Alder cycloadditions. The first example was the intermolecular Diels-Alder reaction developed by MacMillan (Scheme 10).[44] This study introduced the concept of iminium ion activation. A series of chiral cyclohexene derivatives **27** were synthesized using a simple organic molecule (imidazolidinone **26**) as the catalyst for the [4+2] cycloaddition. According to the proposed mechanism, the transiently generated iminium ion **28**, characterized by a low LUMO energy, acted as a strong dienophile in a normal electron-demand Diels-Alder reaction. The two methyl groups on the catalyst scaffold defined the geometry of the iminium ion *via* steric effects, forcing the C-N double bond in a *trans* configuration. Concomitantly, the benzyl group shields the *Si*-face of the iminium ion (topicity at the β-carbon atom, priority given for R = Me), leaving the *Re*-face exposed to the cycloaddition.

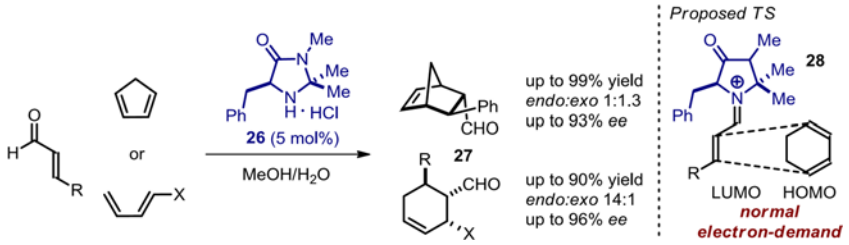

Scheme 10. First organocatalytic asymmetric Diels-Alder reaction.

After this pioneering example, many works appeared using different organocatalytic activations to obtain chiral [4+2] cycloadducts.[45] In 2003, Jørgensen described an inverse electron-demand hetero Diels-Alder reaction showing, for the first time, that a chiral enamine (**33**) could serve as the dienophile (Scheme 11).[46] The chiral secondary amine **31** catalyzed the cycloaddition between aliphatic aldehydes **29** and β,γ-unsaturated α-ketoesters **30** to give pyran-2-one derivatives **32** in high stereoselectivity after *in situ* PCC (pyridinium chlorochromate) oxidation of the corresponding hemiacetals.

---

[44] K. A. Ahrendt, C. J. Borths, D. W. C. MacMillan. New Strategies for Organic Catalysis: The First Highly Enantioselective Organocatalytic Diels−Alder Reaction. *J. Am. Chem. Soc.*, **2000**, *122*, 4243.
[45] J.-L. Li, T.-Y. Liu, Y.-C. Chen. Aminocatalytic Asymmetric Diels-Alder Reactions via HOMO Activation. *Acc. Chem. Res.* **2013**, *45*, 1491.
[46] K. Juhl, K. A. Jørgensen. The First Organocatalytic Enantioselective Inverse-electrondemand HeteroDiels_Alder Reaction. *Angew. Chem. Int. Ed.* **2003**, *42*, 1498.

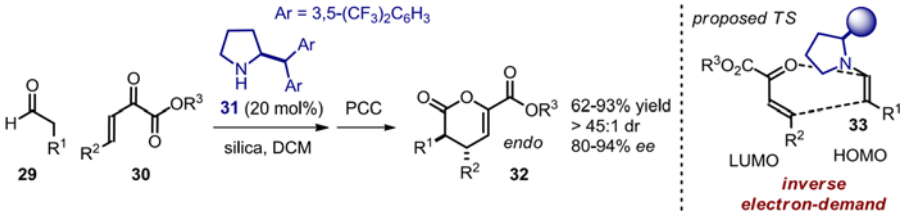

Scheme 11. First organocatalytic asymmetric IED Hetero Diels-Alder reaction.

In this case, the large diarylmethyl substituent in the pyrrolidine scaffold of the catalyst **31** controlled the geometry of the enamine **33** (*trans* configuration) and shielded the *Re*-face, leaving the enamine *Si*-face exposed to the cycloaddition (priority given for R^1 = Me). In 2006, the same group marked the beginning of the vinylogous reactivity in aminocatalysis, introducing the concept of dienamine activation.[47] In particular, a direct asymmetric γ-amination of α,βunsaturated aldehydes **34** with diethyl azodicarboxylate (DEAD) **35** was catalyzed by the chiral amine **36**, which forged the γ remote stereocenter in **37** (Scheme 12). For the first time, an organocatalytic remote fuctionalization of an α,β-unsaturated carbonyl compound was realized.

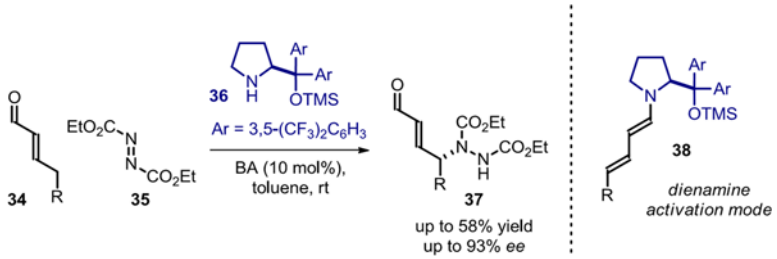

Scheme 12. γ-amination of α,β-unsaturated aldehydes *via* dienamine activation mode.

NMR studies showed the generation of the dienamine species **38** upon condensation of the secondary amine **36** and pentanal (R = Me in **34**), confirming the new activation mode. Dienamines, as with enamines, induce an increment of the HOMO energy, thus increasing the nucleophilicity of the substrate. Previous reactions using the chiral amine **36** as the organocatalyst for the α or β-functionalization of saturated aldehydes and α,β-unsaturated aldehydes, respectively, have all been very consistent with regard to the absolute configuration of the optically active products formed.[48] In all of these reactions, the catalyst **36** shielded the same face in the enamine or iminium ion intermediates (Scheme 13). The sense of the stereoinduction can be anticipated using

[47] S. Bertelsen, M. Marigo, S. Brandes, P. Dinér, K. A. Jørgensen. Dienamine Catalysis: Organocatalytic Asymmetric γ-Amination of α,β-Unsaturated Aldehydes. *J. Am. Chem. Soc.* **2006**, *128*, 12973.

[48] a) S. Brandau, A. Landa, J. Franzen, M. Marigo, K. A. Jørgensen. Organocatalytic Conjugate Addition of Malonates to α,β-Unsaturated Aldehydes: Asymmetric ormal Synthesis of (−)-Paroxetine, Chiral Lactams, and Lactones. *Angew. Chem., Int. Ed.* **2006**, *45*, 4305. b) J. Franzen, M. Marigo, D. Fielenbach, T. C. Wabnitz, A. Kjærsgaard, K. A. Jørgensen. A General Organocatalyst for Direct α-Functionalization of Aldehydes: Stereoselective C−C, C−N, C− , C−Br, and C−S Bond-Forming Reactions. Scope and Mechanistic Insights. *J. Am. Chem. Soc.* **2005**, *127*, 18296.

a steric control model, where the steric interactions of the transiently generated covalent intermediates are minimazed. However, the γ-amination reaction of the α,β-unsaturated aldehydes proceeded with a stereoselectivity that was opposite to the steric control approach, leading to the formation of the (*R*)-enantiomer of the γ-aminated product **37**. The high stereoselectivity (up to 93% *ee*) was rationalized by DFT calculations, which supported a concerted [4+2] cycloaddition pathway involving the dienamine intermediate **38**, characterized by an *s-cis* conformation of the single bond, as the activated diene (HOMO raising) and DEAD **35**, followed by facile hydrolysis of the aminal **39** to give γ-aminated product **37** (Scheme 14a).

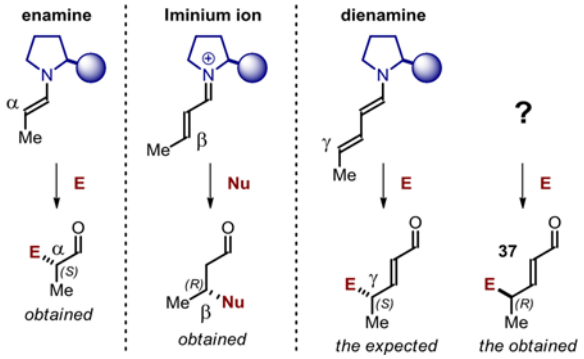

Scheme 13. Catalyst **36** always shields the top face of enamine and iminium ion; what happens with the dienamine?

To further support the hypothesis of a Diels-Alder reaction pathway for the γ-functionalization, the authors showed that, when *N*-methylmaleimide (often used as a good dienophile in [4+2] cycloadditions) was employed, the product **40** could be isolated (Scheme 14b). In this case, the C-C bond formation is irreversible, with the catalyst **36** permanently trapped within the cyclic adduct **40**.

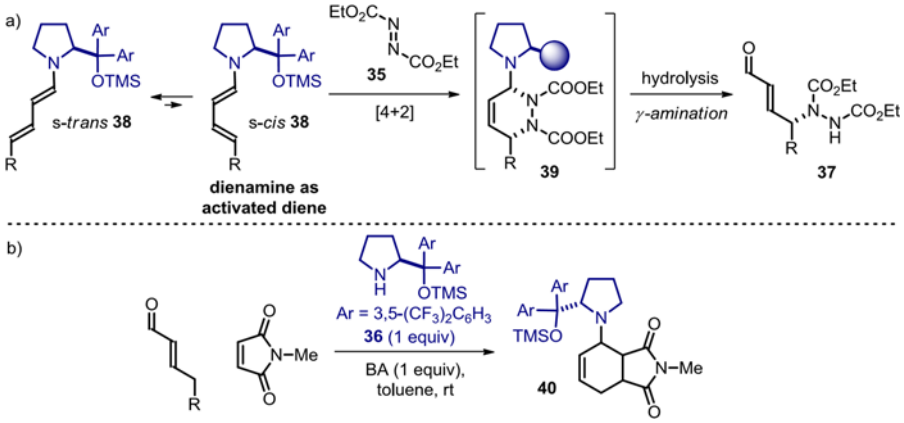

Scheme 14. γ-amination of α,β-unsaturated aldehydes via [4+2] cycloaddition: proposed mechanism and experimental evidence.

The continuous efforts to explore normal electron-demand Diels-Alder reactions via HOMOactivation of the diene led the groups of Chen and Jørgensen, in 2011, to the discovery of trienamine catalysis. In particular, the chiral secondary amine **43** catalyzed a [4+2] cycloaddition between 2,4-dienals **41** and oxindoles **42** (Scheme 15).[49] Highly functionalized products **44**, containing one spiro center, were synthesized with good yields and excellent enantioselectivities.

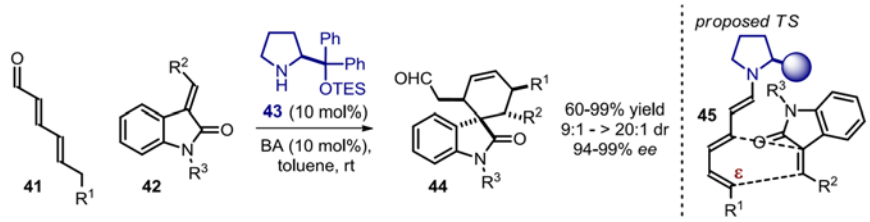

Scheme 15. Diels-Alder reaction via HOMO activation by trienamine.

As with enamine activation, the trienamine intermediate **45** allows the raising of the HOMO of the carbonyl compound, rendering the substrate active toward electrophilic partners. Given the additional unsaturation in the active species, not only the α and the γ positions are activated, but also the ε carbon atom. The Diels-Alder reaction exhibited exclusive β,ε-regioselectivity. Notably, excellent stereocontrol was maintained despite the C-C bond being formed at the remote ε-position of the 2,4-dienal skeleton, seven bonds away from the chiral center of the amine catalyst. This can be attributed to the concerted bond-forming reaction at the β-site of the trienamine intermediate, as proposed in Scheme 15.

2.3 Ortho-Quinodimethane Intermediates

Among all the dienes available for Diels-Alder reactions, *ortho*-quinodimethane (*o*-QDM) intermediates, or *ortho*-xylylenes, and their heterocyclic counterparts have been intensely employed in organic synthesis over the last 50 years. Due to their intrinsic high reactivity, *o*QDMs can react with a large number of dienophiles in an efficient and rapid manner, providing complex cyclic products.[5051] Because of their high reactivity, *o*-QDMs are usually generated *in situ* during the reaction. The *ortho*-quinodimethane intermediate (**I**) dimerizes at 123 K (-150 °C) and can coexist with the tautomer benzocyclobutene (**II**) at high temperature (Scheme 16).

[49] Z.-J. Jia, H. Jiang, J.-L. Li, B. Gschwend, Q.-Z. Li, X. Yin, J. Grouleff, Y.-C. Chen, K. A. Jørgensen. Trienamines in Asymmetric Organocatalysis: Diels-Alder and Tandem Reactions. *J. Am. Chem. Soc.* **2011**, *133*, 5053.
[50] J. L. Segura, N. Martin. *o*-Quinodimethanes: Efficient Intermediates in Organic Synthesis. *Chem. Rev.*
[51] , *99*, 3199.

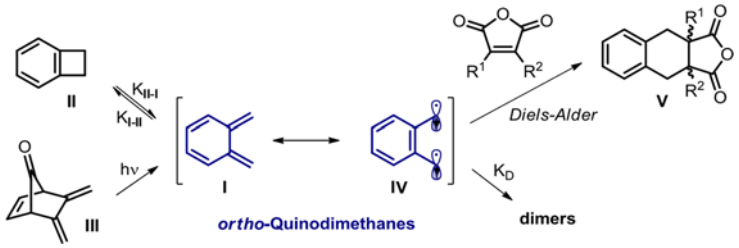

Scheme 16. General processes in the chemistry of *o*-QDMs.

Roth and coworkers observed that, at low temperature, the concentration of *o*-QDMs become considerable after decomposition of a suitable starting material (**III**), allowing the exploitation of the intermediate in useful chemical reactions such as Diels-Alder cycloadditions (**V**).[52] Flynn and Michl performed many studies and calculations on the ground state as well as the excited state of the *o*-QDMs, concluding that these intermediates can also be represented as biradicaloid species (**IV**).[53] Cava and coworkers first suggested in 1957 the participation of *ortho*quinodimethane intermediate **47** in the synthesis of *trans*-1,2-dibromobenzocyclobutene **48** starting from α,α,α',α'-tetrabromo-*o*-xylene **46** (Scheme 17).[54]

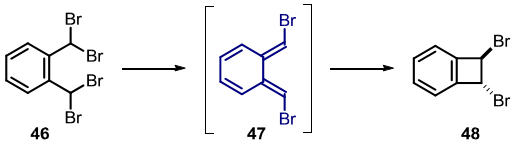

Scheme 17. First report of *o*-QDMs in synthetic processes.

Traditional methods for the generation of *o*-QDMs **49** and their heterocyclic analogues generally require harsh conditions, high reaction temperatures and high-intensity photon irradiations. They can be summarized into five main groups according to the different precursors used (Scheme 18): thermolysis of benzocyclobutenes (path A); ii) 1,4-elimination of α,α'-substituted *o*-xylenes (path B); iii) from benzo-fused heterocyclic compounds (retro Diels-Alder reaction and thermal cheletropic extrusion; path C and D); iv) from *o*-methylbenzaldehydes or *o*methylstyrenes (photoenolization and photorearrangement, respectively; path E); and v) from *o*xylylene-metal complexes (path F).[55]

---

[52] W. R. Roth, M. Biermann, H. Dekker, R. Jochems, C. Mosselman, H. Hermann. Das Energieprofil des oChinodimethan-Benzocyclobuten-Gleichgewichtes. *Chem. Ber.* **1978**, *111*, 3892.
[53] a) C. R. Flynn, J. Michl. Photochemical Preparation of *o*-Xylylene from 1,3-Dihydrophthalazine in Rigid Glass. *J. Am. Chem. Soc.* **1973**, *95*, 5802.
[54] M. P. Cava, D. R. Napier. Condensed Cyclobutane Aromatic Systems. II. Dihalo Derivatives of Benzocyclobutene and Benzocyclobutadiene Dimer. *J. Am. Chem. Soc.* **1957**, *79*, 1701.
[55] N. Martin, C. Seoane, M. Hanack. Recent Advances in *o*-Quinodimethane Chemistry. *Org. Prep. Proc. Int.* **1991**, *23*, 237.

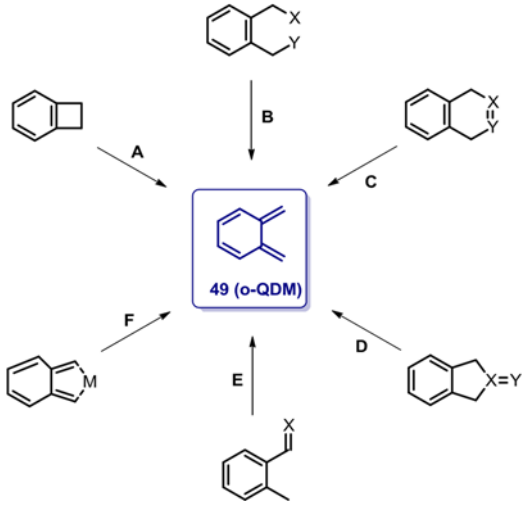

Scheme 18. Traditional methods for the generation of *o*-QDMs.

The termolysis of benzocyclobutenes **50** (path A) is based on reversible conrotatory opening of the cyclobutene ring (Scheme 19). Derivatives bearing substituent on the cyclobutene undergo a thermally allowed conrotatory ring opening to preferentially give the less steric hindered *E*isomer **51** of the diene. The nature of the substituents plays a crucial role in the ring opening.[56]

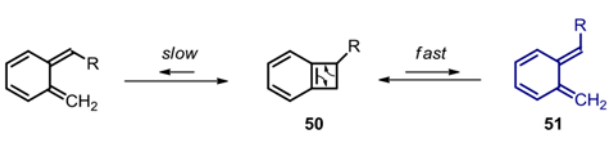

R	temperature
NH_2	25 °C
OH	80 °C
NHCOR'	110 °C
Alkyl	180 °C
CN	160 °C

Scheme 19. Conrotatory ring opening of benzocycobutenes to form *o*-QDMs.

The 1,4-elimination of α,α'-substituted *o*-xylenes (path B in Scheme 18) is one of the most important methods to generate *o*-QDMs because of the ready availability of the starting materials. The 1,4 elimination step can involve: (i) thermal eliminations, (ii) base-catalyzed eliminations, (iii) reductive eliminations, and (iv) ion-catalyzed eliminations (Scheme 20).

[56] T. Kametani, M. Tsukubi, Y. Shiratori, Y. Kato, H. Nemoto, M. Ihara, K. Fukumoto, F. Satoh, H. Inoue. Competitive Reactions between Sigmatropic Reaction and Cycloaddition Affected by Geometry of *o*Quinodimethanes. *J. Org. Chem.* **1977**, *42*, 2672.

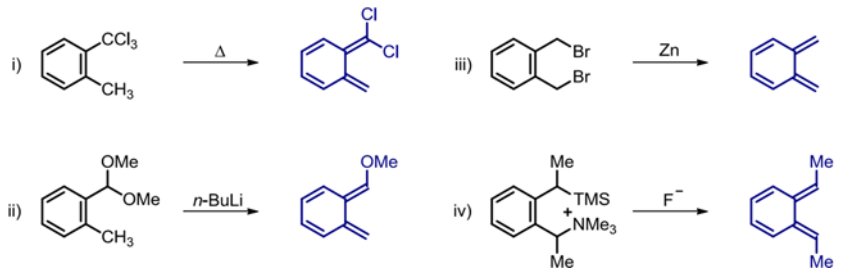

Scheme 20. 1,4 elimination processes to generate *o*-QDMs.

Retro Diels-Alder reactions and thermal cheletropic extrusion (path C and D in Scheme 18) from benzo-fused heterocyclic compounds have been also reported. Loss of nitrogen from 1,4dihydrophthalazine **52** through reverse cycloadditions have been used to generated o-QDMs either thermally[57] and photochemically (Scheme 21).[58] Isochromanones **53** also yield the dienes via flash vacuum pyrolysis at high temperature (500 ºC). Chelotropic elimination of sulfur dioxide from sulfones **54** was the first used methodology to generate *o*-QDMs and it was introduced by Cava and coworkers in 1959.[59] An alternative class of molecules has been developed to overcome the problems of high temperature requirement; the sulfinates or sultines **55** were indeed used to form the reactive dienes at 80 ºC.[60]

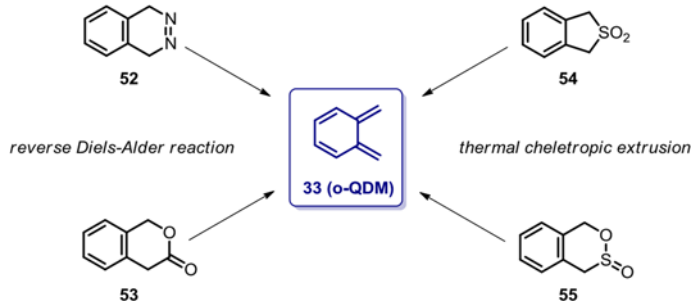

Scheme 21. Reverse Diels-Alder reaction and thermal cheletropic extrusion to form *o*-QDMs.

In general, the photochemical generation of reactive intermediates presents some advantages compared to thermal conditions; indeed, they can be generated under temperatures and concentrations that are not suitable to promote ground-state reactions. Among them,

[57] L. A. Carpino. 1,1,2-Triphenylbenzocyclobutene. *J. Org. Chem.* **1969**, *34*, 461.
[58] J. J. McCullough. o-Xylylenes and isoindenes as reaction intermediates. *Acc. Chem. Res.* **1980**, *13*, 270.
[59] M. P. Cava, A. A. Deana. Condensed Cyclobutane Aromatic Compounds. VI. The Pyrolysis of 1,3Dihydroisothianaphthene-2,2-dioxide: A New Synthesis of Benzocyclobutene. *J. Am. Chem. Soc.* **1959**, *81*, 4266.
[60] W. F. Jarvis, M. D. Hoey, A. L. Finocchio, D. C. Dittmer. Organic reactions of reduced species of sulfur dioxide. *J. Org. Chem.* **1988**, *53*, 5750.

photochemical extrusion of carbon monoxide from substituted 2-indanones **56** [61] and the photoenolization of o-alkylbenzaldehydes and o-alkylbenzophenones were employed to generate *o*-QDMs (**57**, Scheme 22).[62]

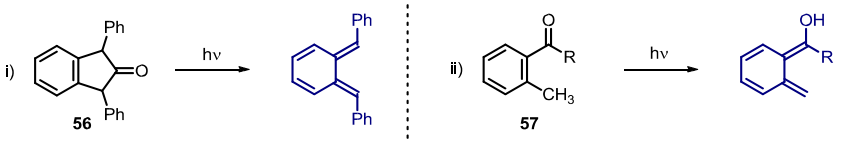

Scheme 22. Photochemical generation of *o*-QDMs.

The heterocyclic counterparts of *o*-QDMs (Het *o*-QDMs) have been extensively employed in organic synthesis since they provide a straightforward way to access a wide range of heterocyclic systems *via* Diels-Alder cycloadditions. The main generation routes of Het *o*-QDMs are similar to those used for the simple *o*-QDMs (see Scheme 18).

In 1980s, Magnus reported an interesting methodology that relied on the formation of heterocyclic *o*-QDMs in the synthesis of Aspidosperma alkaloids.[63] The imine-indole **58** served as the key substrate, whit the imino moiety installed at the 3 position of the *N*-protected-2methylindole (Scheme 23). The iminium ion **59** was formed upon addition of methyl chloroformate at 140 °C; the presence of the quaternarized positive nitrogen increased the acidity of the methyl protons at the 2 position, inducing the formation of indole-2,3quinodimetane intermediate **60** after deprotonation of **59**. The reactive diene was then trapped by the terminal alkene via an intramolecular [4+2] cycloaddition, leading to the adduct **61**. The so-called indole-2,3-quinodimethane strategy provided an effective and simple way to access reactive intermediates under mild reaction conditions, and it showed great synthetic potential toward the direct generation of complex architectures.

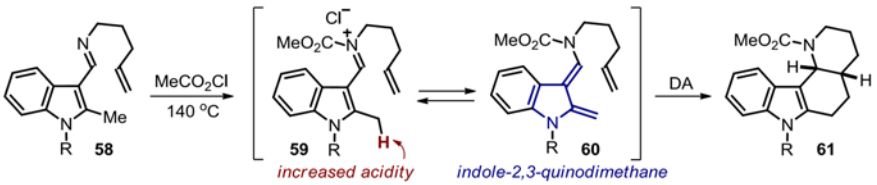

Scheme 23. Magnus's indole-2,3-quinodimethane strategy to generate heterocyclic *o*-QDMs.

[61] G. Quinkert, H. Stark. Stereoselective Synthesis of Enantiomerically Pure Natural Products-Estrone as Example. *Angew. Chem., Int. Ed. Engl.* **1983**, *22*, 637.
[62] J. L. Charlton, M. M. Alauddin. Orthoquinodimethanes. *Tetrahedron* **1987**, *43*, 2873.
[63] T. Gallagher, P. Magnus. Indole-2,3-Quinodimethan Route to Aspidosperma Alkaloids: Synthesis of dlAspidospermidine. *J. Am. Chem. Soc.* **1982**, *104*, 1140.

Despite the synthetic potential of this approach, the implementation of an enantioselective variant to access enantio-enriched *cis*-fused tetracyclic products **61** was limited to the use of chiral auxiliaries.[64]

2.4 Target of the Research Project

We recently recognized a mechanistic similarity between the synthetic plan engineered by Magnus and the iminium ion/enamine activation principles. Specifically, we wondered whether the underlying principle of the indole-2,3-quinodimetane strategy (Scheme 23) could be used to design a catalytic enantioselective Diels-Alder reaction, using aminocatalysis as the enabling strategy. We thought to *in situ* generated the indole-2,3-quinodimetane intermediate under mild reaction conditions. In particular, the indole-based unsaturated aldehyde **62** was identified as the best candidate for our proposal (Scheme 24).

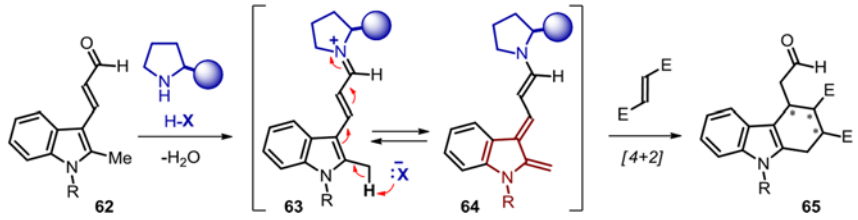

Scheme 24. Design blueprint for an asymmetric organocatalytic Diels-Alder reaction via *in situ* generated indole-2,3-quinodimetane intermediates.

The iminium ion **63** would be formed upon condensation with a chiral secondary amine in the presence of an acid. In analogy with Magnus' studies, we speculated that the quaternarized positive nitrogen would increase the acidity of the methyl protons at the 2 position of the indole scaffold. At this stage, an appropriate base (likely the conjugated base of the initial acid) would deprotonate the iminium ion **63** facilitating the formation of the key indole-2,3-quinodimetane trienamine intermediate **64**. In the presence of an appropriate dienophile, an asymmetric [4+2] cycloaddition reaction would occur to directly furnish the densely functionalized chiral tetrahydrocarbazole adduct **65**, which contains three contiguos stereogenic centers.

2.5 Results and Discussion

The reactivity of N-Boc protected 3-(2-methyl-indol-3-yl)acrylaldehyde **62a** toward the [4+2] cycloaddition with the electron-deficient trans-β-nitrostyrene **66a** was studied as the model reaction (Scheme 25a). The chiral secondary amine **67**, the commercially available JørgensenHayashi catalyst,[65] was selected as the catalyst because of its ability to impart high

[64] P. Magnus, P. M. Cairns. Methods for Indole Alkaloid Synthesis. Enantiospecific Synthesis of Pentacyclic Deethylaspidosperma-Type Alkaloids Using an Exceptionally Mild Retro-Diels-Alder Reaction. *J. Am. Chem. Soc.* **1986**, *108*, 217.

[65] a) M. Marigo, T. C. Wabnitz, D. Fielenbach, K. A. Jørgensen. Enantioselective Organocatalyzed αSulfenylation of Aldehydes. *Angew. Chem., Int. Ed.* **2005**, *44*, 794. b) Y. Hayashi, H. Gotoh, T. Hayashi, M.

stereocontrol and reactivity in a myriad of aminocatalyzed reactions proceeding through enamine and dienamine intermediates. Importantly, compound **62a**, bearing an α,β-unsaturated aldehyde substitution pattern in position 3 of the 2-methylindole scaffold, was chosen as the substrate instead of the 2-methylindole 3-carboxaldehyde **69** used by Magnus as the imine precursor. This is because we wished to make the strategy catalytic. Following the Magnus approach, the chiral aminocatalyst would be consumed by becoming part of the product as a substituent of the DielsAlder product **71** (Scheme 25b). Conversely, in our design plan (Scheme 25a), the use of the α,βunsaturated aldehyde **62a**, upon activation by the chiral amine catalyst **67**, would afford the cycloadduct bearing an enamine substituent (corresponding to product **68a**). This intermediate would subsequently release the amine through iminium ion hydrolysis, providing the necessary condition for the turnover of the catalyst.

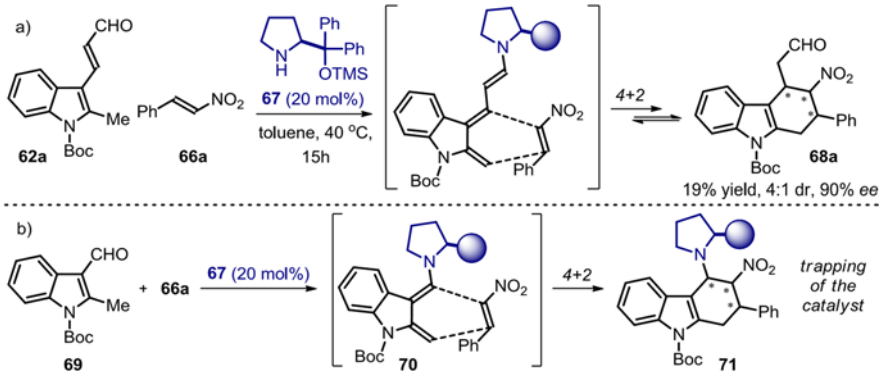

Scheme 25. Reaction design for developing the asymmetric organocatalytic 4+2 cycloaddition.

When aldehyde **62a**, nitrostyrene **66a**, amine **67** and toluene were placed in a normal vial at 40 °C for 15 hours, product **68a** was obtained in low yield (19%), moderate diastereoselectivity (4:1) and very good enantioselectivity (90% *ee*); Scheme 25. Encouraged by these initial results, we envisioned the possibility of using an acid as additive to improve the catalytic turnover and the *in situ* generation of *o*-QDM intermediate. Benzoic acid (BA) was tested and 20 mol% (equimolar with the catalyst) was found as the best amount (entry 3, Table 1). The acid not only improved the reactivity, but also the diastereoselectivity (from 4:1 to 12:1). This effect is not simple to rationalize, since the transiently generated trienamine is not a charged intermediate. Thus, the nature of the counteranion should not affect the diastereoselectivity. During the optimization studies, we observed a partial degradation of the starting aldehyde **62a**, probably through polymerization or oxidation pathways. To overcome this issue, we envisioned that a better

Shoji. Diphenylprolinol Silyl Ethers as Efficient Organocatalysts for the Asymmetric Michael Reaction of Aldehydes and Nitroalkenes. *Angew. Chem., Int. Ed.* **2005**, *44*, 4212.

reactivity would be achieved changing the stoichiometry of the substrates. When 1.5 equivalents of aldehyde **62a** were used, 44% of yield of the desired product was obtained (entry 6, Table 1).

Table 1. Role of acid in the reaction.

Entry[a]	**62a** (equiv.)	**66a** (equiv.)	Additive (mol%)	Yield (%)[b]	dr (%)[c]	*ee* (%)[d]
1	1	1.2 1.2	-	19	4:1	90
2	1	1.2	BA (10)	32	7:1	91
3	1	1.2	BA (20)	33	12:1	91
4	1		BA (30)	34	11:1	93
5	1.2	1	BA (20)	39	12:1	93
6	1.5	1	BA (20)	44	15:1	93

[a] [b] Reactions were carried out on a 0.1 mmol scale, [**62a-66a**]$_0$ = 0.5 M in toluene. Yield determined by ^{1}H NMR using 1,3,5-trimethoxybenzene as the internal standard. [c] Diastereomeric ratios (dr) were determined by means of ^{1}H NMR analysis of the crude mixture. [d] Enantiomeric excess (*ee*) values were determined after $NaBH_4$ reduction of compound **68a** to the corresponding alcohol and HPLC analysis on commercially available chiral stationary phases.

Evaluation of the conversion over the time indicated that the reaction reaches a stand-hill upon a certain time, without proceeding further. We attempted to increase the reactivity by raising the temperature, in order to obtain high yields before of the possible deactivation pathway (Table 2). 70 °C was found to be the optimal temperature for the system (entry 4), providing a good compromise between chemical yield and stereocontrol. The reaction at higher temperatures (80 °C) showed similar yield and diastereoselectivity, but offered lower enantiocontrol (entry 5). Under the optimized conditions (entry 4), the tetrahydrocarbazole **68a** was isolated after 40 h in 76% yield, with high diastereoselectivity (dr 16:1) and enantioselectivity (93% *ee*). With the best conditions in hand, we tested the generality of our method by evaluating a variety of indole derivatives **62** and nitroalkenes **66** (Table 3).

Table 2. Effect of the temperature on the reaction outcome.

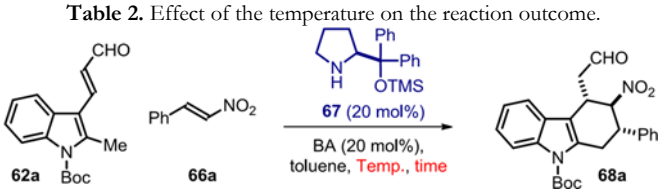

Entry[a]	Temperature (°C)	Time (h)	Yield (%)[b]	dr (%)[c]	*ee* (%)[d]

1	40	15 40	44 57	15:1	93
2	50	15 40	48 62	14:1	93
3	60	15 40	55 69	15:1	94
4	70	15 40	65 76	16:1	93
5	80	15 40	66 75	15:1	90

[a] [b]

Reactions were carried out with BA (20 mol%) on a 0.1 mmol scale, [**66a**]$_0$ = 0.5 M in toluene. Yield determined by ^{1}H NMR using 1,3,5-trimethoxybenzene as the internal standard. [c] Diastereomeric ratios (dr) were determined by means of ^{1}H NMR analysis of the crude mixture. [d] Enantiomeric excess (*ee*) values were determined after $NaBH_4$ reduction of compound **68a** to the corresponding alcohol and HPLC analysis on commercially available chiral stationary phases.

Both electron-donating groups (EDG) and electron-withdrawing groups (EWG) on the indole scaffold were well tolerated, affording the products **68** in a very good yield and stereoselectivity (entries 2 and 3). Changing the nature of the *N* substituent did not affect the reactivity; the *N*methyl indole-derived aldehyde reacted with nitrostyrene to afford the product **68d** in high enantioselectivity (entry 4). When an aldehyde bearing an unprotected indole was used, the desired product was not observed (entry 5). The absence of reactivity can be attributed to a competing process that can occur in the absence of a substituent on the *N* atom (Scheme 26).[66] Indeed, the reactive *o*-QDM intermediate **I**, having an s-*cis* conformation, is in equilibrium with the more stable species **II**, which, due to its s-*trans* conformation, cannot participate in the cycloaddition process. This observation was key to develop the chemistry details in Chapter IV.

We then evaluated the scope of nitroolefins; electron-rich substituents on the aromatic ring slightly decreased the reactivity of the system, in agreement with the mechanism of normal electron-demand cycloaddition, where the LUMO is centered on the dienophile (EDG raises the HOMO and LUMO, as discussed in section 2.1). However, the diastereo and enantioselectivity were not affected (entries 6 and 8).

Table 3. Generality of the Diels-Alder reaction with nitroolefins.

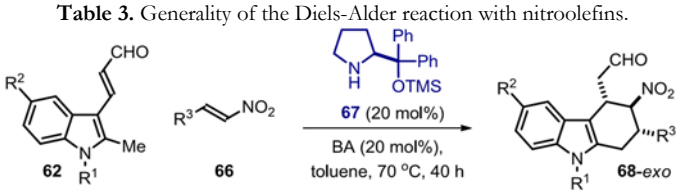

[66] G. N. Walker, M. A. Moore. 3-Aminomethylindoles and 2-(3-Indolyl)oxazokidines from Indole-3aldimines. Some Observations on the Acetylation of Schiff Bases. *J. Org. Chem.* **1961**, *26*, 432.

Entry[a]	R_1	R_2	R_3	**68**	Yield (%)[b]	dr (%)[c]	*ee* (%)[d]
1	Boc	H	Ph	**a**	76	16:1	93
2	Boc	OMe	Ph	**b**	84	11:1	92
3	Boc	Cl	Ph	**c**	80	17:1	90
4	Me	H	Ph	**d**	80	17:1	92
5	H	H	Ph	-	0	*nd*	*nd*
6	Boc	H	p-MeC_6H_4	**e**	72	>20:1	92
7	Boc	H	p-ClC_6H_4	**f**	83	>20:1	92
8	Boc	H	p-$OMeC_6H_4$	**g**	54	>20:1	93
9[e]	Boc	H	p-$NO_2C_6H_4$	**h**	88	10:1	92
10	Boc	H	o-BrC_6H_4	**i**	96	11:1	92
11	Boc	H	2-furanyl	**j**	55	17:1	92
12	Boc	H	3-thiophenyl	**k**	64	>20:1	92
13	Boc	H	CH_2CH_2Ph	**l**	22	14:1	92

[a] Reactions were carried out on a 0.1 mmol scale, [**66**]$_0$ = 0.5 M in toluene. [b] Yields of isolated product after chromatography. [c] Diastereomeric ratios (dr) were determined by means of ^{1}H NMR analysis of the crude mixture. [d] Enantiomeric excess (*ee*) values were determined after $NaBH_4$ reduction of compound **68** to the corresponding alcohol and HPLC analysis on commercially available chiral stationary phases. [e] The reaction required 16 h for completion. Selected reactions have been also performed using (*R*)-**67** as the catalyst to afford the opposite enantiomer of compounds **68**; see Table 5 in the experimental part 2.8 for details.

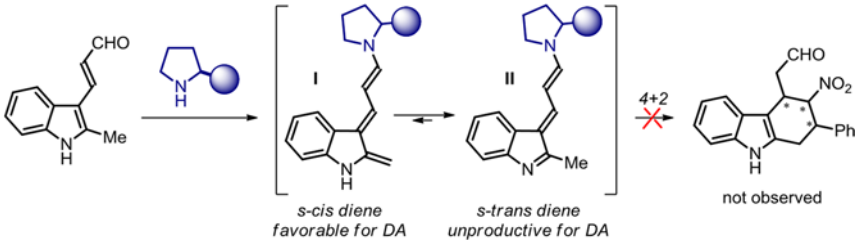

Scheme 26. Possible process in the absence of substituent in the *N* atom of the indole.

Nitroolefins bearing electron-withdrawing substituents showed better reactivity (entries 7, 9, 10). Remarkably, a nitroolefin bearing a nitro group on the aryl moiety was more reactive than the unsubstituted nitrostyrene, affording 88% of the product **68h** (entry 9). Heterocyclic moieties such as furanyl and thiophenyl were well tolerated, providing high level of stereoselectivity (entries 11, 12).

To further expand the synthetic value of our methodology, we investigated the reactivity of methyleneindolinone derivatives **72** as the dienophile. The resulting tetrahydrocarbazoles **73** would contain a spirocyclic oxindole moiety, which features in a large number of biologically active and natural products.[67] Methyleneindolinone **72a** was synthesized and tested in the optimized

[67] a) H. Lin, S. J. Danishefsky. Gelsemine: A Thought-Provoking Target for Total Synthesis. *Angew. Chem. Int. Ed.* **2003**, *42*, 36. b) C. V. Galliford, K. A. Scheidt. Pyrrolidinyl-Spirooxindole Natural Products as Inspirations for the Development of Potential Therapeutic Agents. *Angew. Chem. Int. Ed.* **2007**, *46*, 8748. c) M. M. C. Lo,

conditions at ambient temperature. We were pleased to find that the product **73a** was obtained in 59% of yield with almost perfect stereoselectivity (>20:1 dr, 96% *ee*). Fast screening of the solvents revealed that 1,1-dichloroethane was the best medium for conducting the Diels-Alder reaction with this class of dienophiles **72** (entry 6, table 4).

Table 4. Solvent screening for DA reaction with methyleneindolinones.

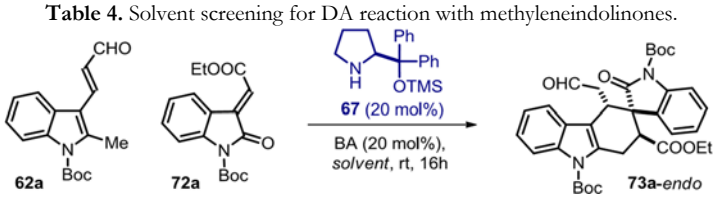

Entry[a]	Solvent	Yield (%)[b]	dr (%)[c]	*ee* (%)[d]
1	Toluene	59	>20:1	96
2	DCM	85	20:1	97
3	CH_3Cl	66	12:1	97
4	DCE	90	>20:1	97
5	THF	<5	nd	nd
6	1,4-dioxane	37	20:1	95

[a] [b] Reactions were carried out on a 0.1 mmol scale, $[\mathbf{72a}]_0$ = 0.5 M in toluene. Yield determined by ^{1}H NMR using 1,3,5-trimethoxybenzene as the internal standard. [c] Diastereomeric ratios (dr) were determined by means of ^{1}H NMR analysis of the crude mixture. [d] Enantiomeric excess (*ee*) values were determined with HPLC analysis on commercially available chiral stationary phases.

The complex products **73**, which contain two biological privileged structures such as spirooxindole and tetrahydrocarbazole, could be synthesized in a straightforward manner (Figure 1). The presence of different functional groups on the methyleneindolinone scaffold, including esters, aromatic ketones and nitriles, afforded excellent results in term of yield and enantioselectivity (products **73a**-**73h**). Notably, good results were obtained with unprotected methyleneindolinones (products **73e**, **73k** and **73l**). Diverse *N*-protecting groups as benzyl, allyl and carboxybenzyl did not alter the reactivity and stereoselectivity of the reaction (products **73m**-**73o**).

C. S. Neumann, S. Nagayama, E. O. Perlstein, S. L. Schreiber. A Library of Spirooxindoles Based on a Stereoselective Three-Component Coupling Reaction. *J. Am. Chem. Soc.* **2004**, *126*, 16077.

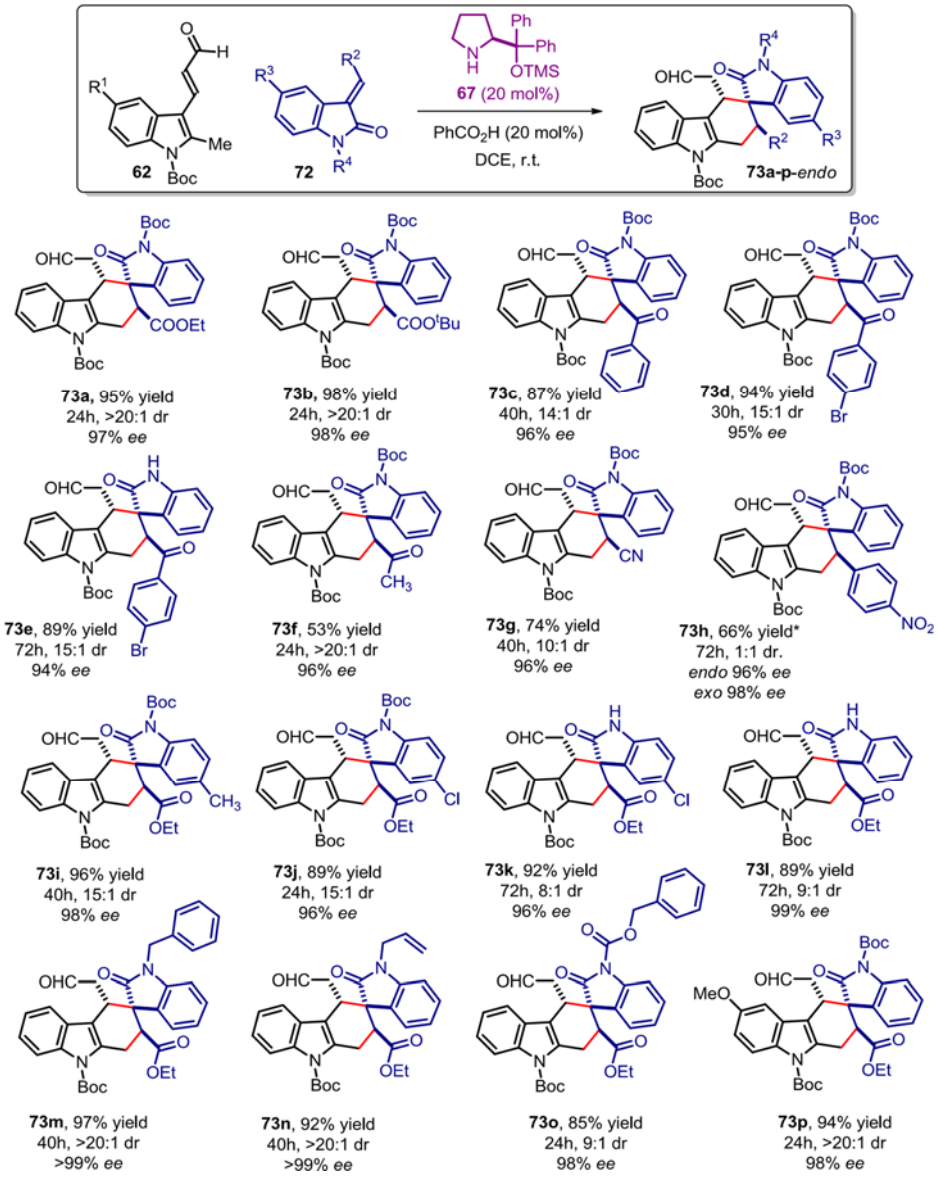

Figure 1. Methyleneindolinones as dienophiles in the Diels-Alder reaction: construction of tetrahydrocarbazole spirooxindoles. Reactions were performed on a 0.1 mmol scale and $[\mathbf{72}]_0$ = 0.5 M. Yields refer to the sum of the isolated diastereoisomers. Selected reactions have been also performed using (*R*)-**67** as the catalyst to afford the opposite enantiomer of compounds **73**; see Table 6 in the experimental part 2.8 for details. Compound **73h** and **73l** were prepared using trimethylacetic acid (TMAA) as the acidic additive. Additionaly, the reaction leading **73h** was carried out at 40 °C.

To expand the scope of our Diels-Alder approach, we explored the possibility of using the chiral amine catalyst **67** to induce the generation of different heteroaromatic-based *o*-QDMs from simple

starting aldehydes, while directing the pericyclic reactions with methyleneindolinones **72** toward a highly stereoselective pathway (Scheme 27). Pyrrole and furan-based *ortho*quinodimethanes were generated, leading to enantio-enriched products **74** and **75** in high yield, albeit with poor control over the relative stereochemistry.

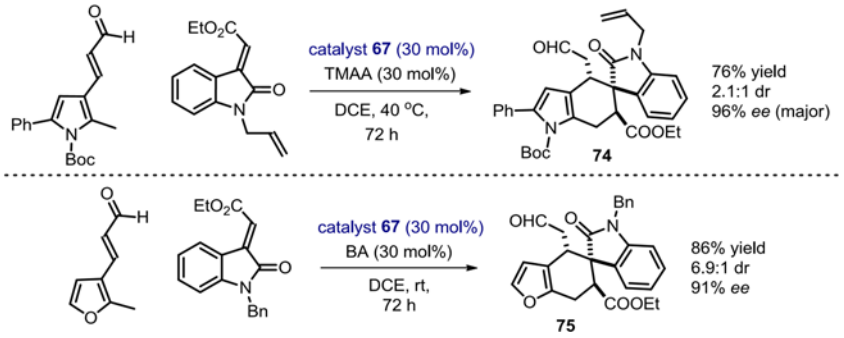

Scheme 27. Extending the scope of the Diels-Alder reaction to pyrrole and furan-based *o*-quinodimethanes.

2.6 Mechanistic Considerations

Crystal structures of derivatives **76** and **77** were obtained to determine the absolute configuration of cycloadducts **68a** and **73d**, respectively (Figure 2).

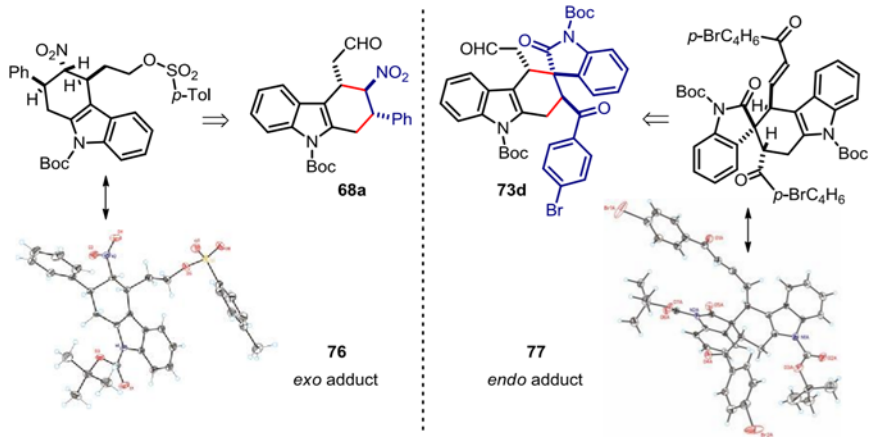

Figure 2. Stereochemical outcome of the Diels-Alder reaction with two different dienophiles.

Depending on the dienophiles, the stereochemical outcome of the Diels-Alder reaction changed from an *exo* (nitroolefins) to an *endo* (methyleneindolinones) selectivity. As alluded to above (Section 2.1), the reactivity and regioselectivity of cycloadditions can be explained considering the frontier molecular orbital theory. Since the reaction is a normal electron-demand cycloaddition, the HOMO of the diene (*o*-QDM/trienamine) and the LUMO of the dienophile (nitroolefin/oxindole-olefin) need to be considered. The major atomic orbital coefficient within the

HOMO of the trienamine is located on the methylene carbon atom ε because of three different electronic factors: i) the electron-realising effect in β position (enamine), ii) the contribution of the conjugated system in β position (enamine) and iii) the contribution of an EDG substituent bonded to δ carbon (nitrogen atom, Scheme 28a).

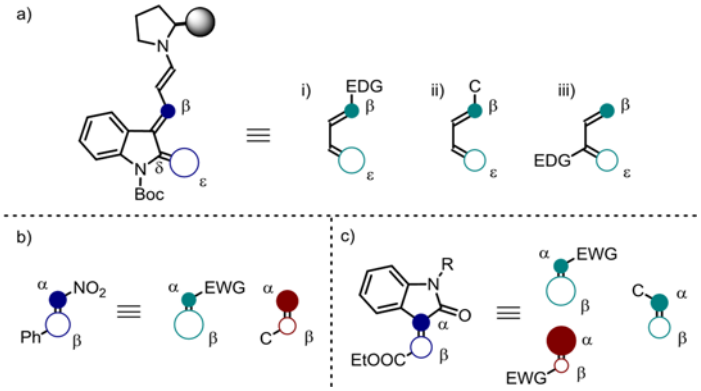

Scheme 28. Atomic orbital coefficients of *o*-QDM/trienamine and dienophiles. EDG = electron-donating group; EWG = electron-withdrawing group; C = conjugated system.

As for the LUMO of nitroolefins, the major atomic orbital coefficient is placed on the β carbon atom since the nitro substituent is a strong EWG (Scheme 28b). Regarding the LUMO of the methyleneindolinone (Scheme 28c), the assignment of the major atomic orbital coefficient is more difficult due to the presence of two EWG groups at both the α and β carbon atoms of the olefin. Considering the additional contribution of the conjugated system at the α carbon, the major atomic orbital coefficient is located on the β carbon of the oxindole-olefin. The assignment of the atomic orbital coefficients allows rationalizing the observed regioselectivity, applying the *large/large-small/small* interaction rule. Thus, the products are formed matching the methylene carbon atom ε of the *o*-QDM/trienamine and the β carbon atom of the dienophiles. As for the different stereoselectivity observed when using nitroolefins or methylenindolinones, the electrostatic interaction has to be considered in addition to the FMO interactions. The *endo* selectivity observed in the reaction with methyleneindolinones **72** can be explained considering the secondary orbital interactions (SOI) between the carbonyl of the oxindole moiety and the γ carbon of the *o*-QDM/trienamine (Scheme 29a). The *exo*-TS proposed for nitroolefins could instead be the result of repulsive electrostatic interactions between the electron-rich system of the trienamine and the negative charge delocalized in the nitro group (Scheme 29b).[68]

[68] Chen and coworkers proposed a similar explanation for the observed *exo* selectivity in the reaction of trienamine and nitroolefins, see: Z.-J. Jia, Q. Zhou, Q.-Q. Zhou, P-Q. Chen, Y.-C. Chen. *Exo*-Selective Asymmetric Diels-Alder Reaction of 2,4-Dienals and Nitroalkenes by Trienamine Catalysis. *Angew. Chem., Int. Ed.* **2011**, *50*, 8638.

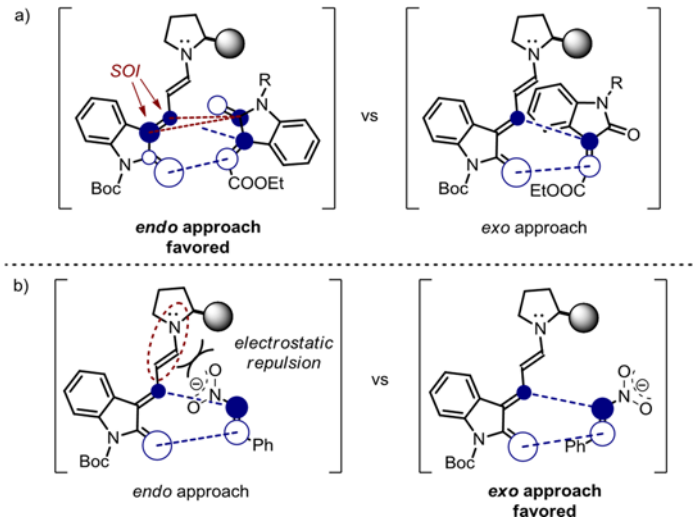

Scheme 29. *Endo* vs *Exo* approaches for methyleneindolinones and nitroolefins. SOI = secondary orbital interactions.

During the studies of the Diels-Alder reaction with methyleneindolinones, we found that oxindole-olefin **72h** gave two different diastereoisomers **73h** and **73h'** in a 1:1 ratio (Scheme 32). The low relative stereocontrol allowed us to isolate both diastereoisomers and to spectroscopically analyze them. This could help in better understanding the mechanism of the reaction: though we proposed a concerted pathway, a stepwise route cannot be excluded (both the diene and dienophile are highly polarized).

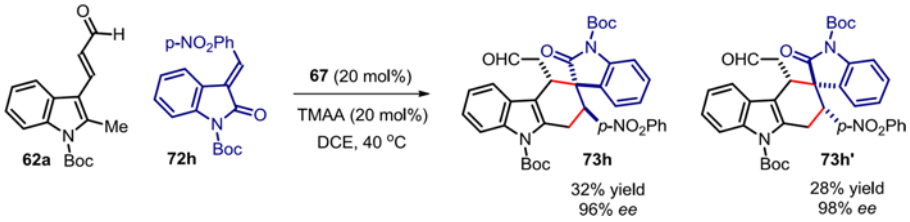

Scheme 32. Stereochemical outcome of Diels-Alder reaction with oxindole-olefin **7h**.

We analyzed products **73h** and **73h'** by NOE experiments in order to determine their relative configurations and have additional information on whether *exo-endo* geometries are exclusively formed. If different configurations are forged, a stepwise mechanism could be feasible instead. We began by investigating the NMR spectrum of compound **73c**. This was because a direct NMR correlation between the substrate **73d** (stereochemistry established by X-ray analysis, see Figure 2) and the corresponding isomer of **73h** was hampered by the complex proton patterns (overlap of many signals) within **73d**. We first analyzed compound **73c** because it was formed as a single isomer and showed clear proton NMR spectra. In addition, assuming a uniform reaction mechanism, we could infer for **73c** the same absolute and relative configuration as for **73d**.

Complete assignment of ^{1}H NMR signals was achieved for compound **73c**. The most indicative GOESY results (monodimensional NOESY) are shown in Figure 3. Saturation of the H_4 signal yielded a NOE on H_5, on H_2 and on the two protons H_C, however it did not show an enhancement of H_A or H_3, indicating that H_4 is on the opposite side than H_A and H_3.

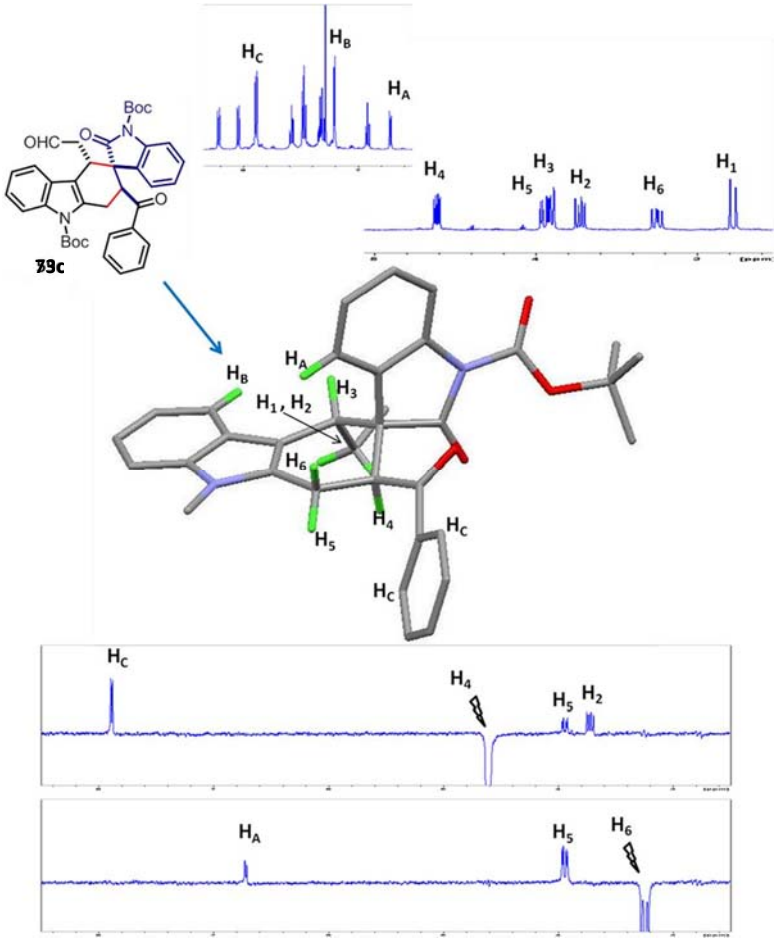

Figure 3. ^{1}H NMR assignment and NOE studies for compound **73c**. Structure drawn with Chem3D.

Saturation of the H_3 signal yielded NOEs on H_2, H_1, H_A and H_B, confirming the different side location with respect to H_4 and indicating that the aromatic system of oxindole was in the *endo* position. Saturation of H_6 showed NOE on H_A confirming the position of the oxindole moiety. This stereochemistry matched with a Diels-Alder approach through an *endo* transition state and it is consistent with the X-ray analysis for compound **73d**. As expected, GOESY experiments with compound **73h** showed the same NOEs as compound **73c**, consistent with a Diels-Alder cycloaddition through an *endo* TS (usual the major diastereoisomer). When saturating H_4, H_6 and H_3, the NOEs indicated a relative configuration in which H_3 and H_4 were in a *trans* relationship,

while the H_A proton of the oxindole moiety was located on the same side as H_3 and H_6. The most indicative spectra are shown in Figure 4.

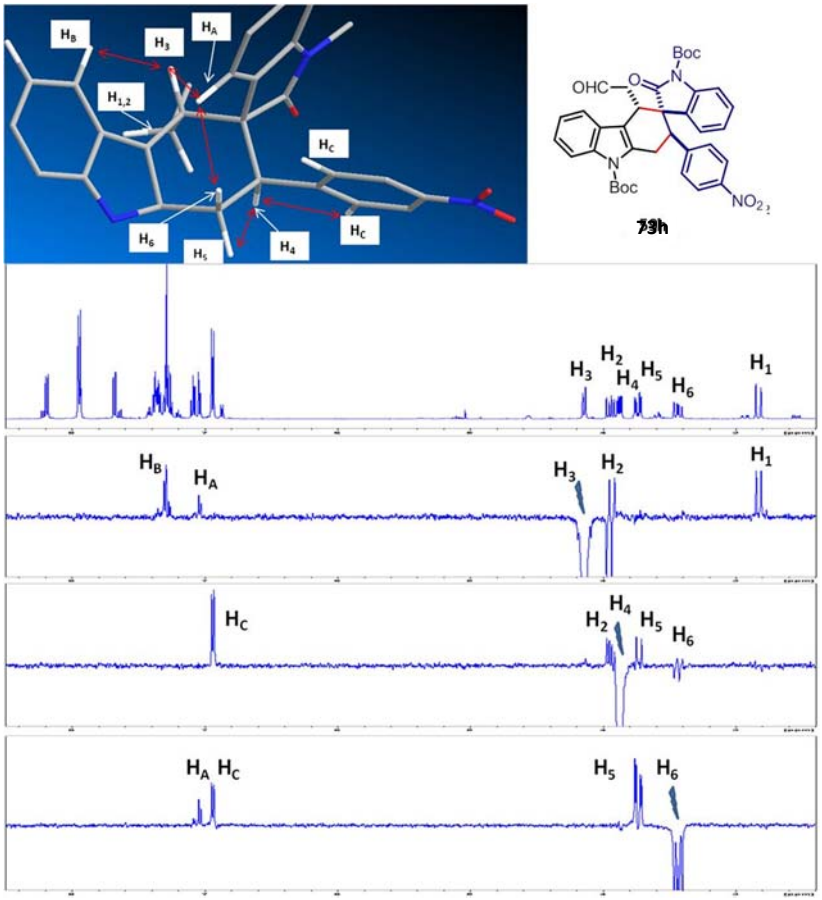

Figure 4. ^{1}H NMR assignment and NOE studies for compound **73h**; *endo* relative configuration. Structure drawn with Chem3D.

Analysis of compound **73h'** showed a different relative configuration. Saturation of the H_4 signal yielded a NOE on H_5, H_6, H_3, and on the two aromatic hydrogens H_C and H_B, but it did not show any interaction with H_A, indicating that H_4 is in the same side as H_3 and in opposite side than H_A. Saturation of the H_3 signal yielded NOEs on H_2, H_4, H_1 and H_B, confirming the same side location with respect to H_4 and indicating that the aromatic system of oxindole was in the *exo* position. This was confirmed also by the absence of a NOE on H_A when saturating H_6 proton. Selected spectra are shown in Figure 5.

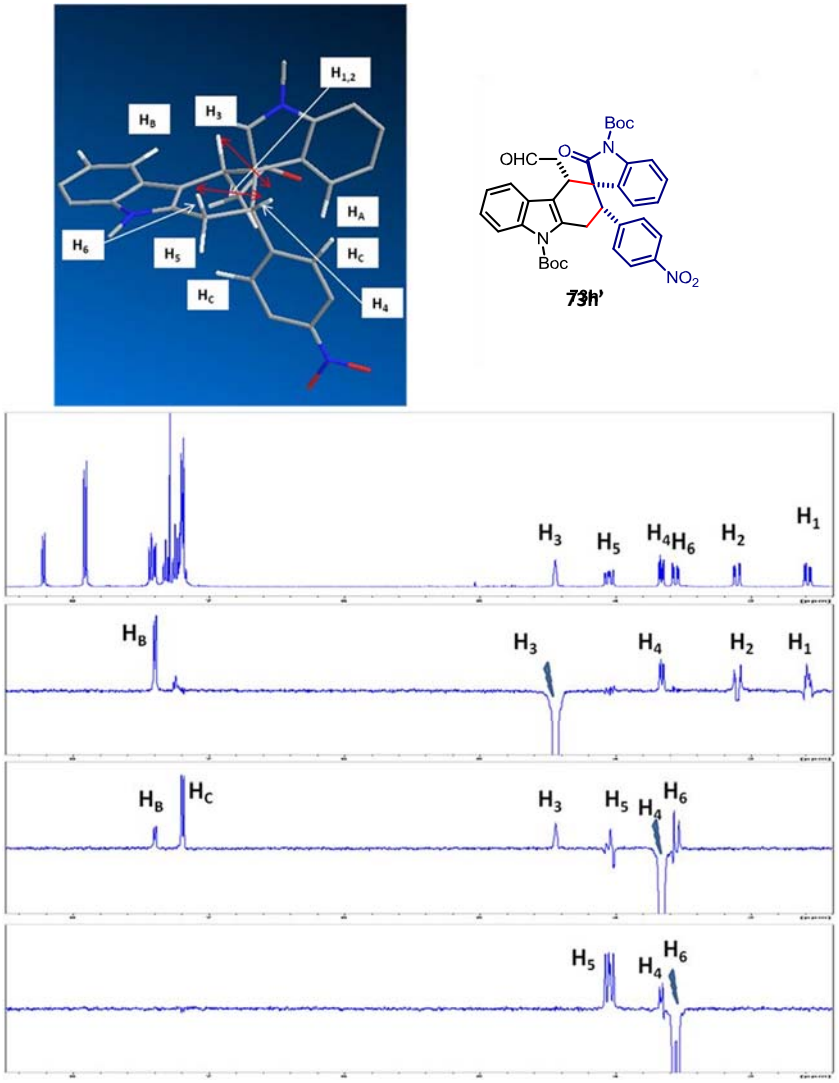

Figure 5. ^{1}H NMR assignment and NOE studies for compound **73h'**; *exo* relative configuration. Structure drawn with Chem3D.

The relative configurations of stereoisomers **73h** and **73h'** were found to be *endo* and *exo* respectively. These results suggest that both of the products are formed through a [4+2] concerted pathway, while they are not supportive of a stepwise mechanism.

2.7 Conclusions

Asymmetric aminocatalysis has allowed us to develop the hitherto elusive catalytic asymmetric Diels-Alder reaction of *in situ* generated *ortho*-quinodimethane intermediates. The indole-2,3quinodimethane strategy, originally conceived for the straightforward synthesis of indole alkaloids more than 30 years ago, can now be made catalytic using the chiral amine **67**. This

strategy was used to synthesize a structurally diverse range of complex spirooxindole-containing tetrahydrocarbazoles with high chemical yields and excellent stereoselectivities. The demonstration that this new strategy can be easily extended to access complex pyrrole- and furan-based heterocyclic compounds while using mild and simple reaction conditions may provide for the rapid application of this chemistry in synthetic and medicinal arenas.

2.8 Experimental Section

2.8.1 General Information

The ^{1}H and ^{13}C NMR spectra were recorded at 400 MHz and 500 MHz for ^{1}H or at 100 MHz and 125 MHz for ^{13}C, respectively. The chemical shifts (δ) for ^{1}H and ^{13}C are given in ppm relative to residual signals of the solvents ($CHCl_3$ @ 7.26 ppm ^{1}H NMR, 77.16 ppm ^{13}C NMR). Coupling constants are given in Hz. Carbon types were determined from DEPT ^{13}C NMR experiments. When necessary, ^{1}H and ^{13}C signals were assigned by means of g-COSY, 2D-NMR sequences. The following abbreviations are used to indicate the multiplicity: s, singlet; d, doublet; t, triplet; q, quartet; m, multiplet; bs, broad signal. High-resolution mass spectra (HRMS) were obtained from the ICIQ High Resolution Mass Spectrometry Unit on Waters GCT gas chromatograph coupled time-of-flight mass spectrometer (GC/MS-TOF) with electron ionization (EI). X-ray data were obtained from the ICIQ X-Ray Unit using a Bruker-Nonius diffractometer equipped with an APPEX 2 4K CCD area detector. Optical rotations are reported as follows: $[\alpha]^{rt}_{D}$ (c in g per 100 mL, solvent).

The ^{1}H, ^{13}C NMR spectra and the HPLC traces are available in the literature[1] and are not reported in the present thesis.

General Procedures. All the reactions were set up under air and using freshly distilled solvents, without any precautions to exclude moisture, unless otherwise noted - open air chemistry on the benchtop. Chromatographic purification of products was accomplished using force-flow chromatography (FC) on silica gel (60-200 mesh). For thin layer chromatography (TLC) analysis throughout this work, Merck precoated TLC plates (silica gel 60 GF254, 0.25 mm) were used, using UV light as the visualizing agent and an acidic mixture of ceric ammonium molybdate or basic aqueous potassium permangante ($KMnO_4$) as stain developing solutions. Organic solutions were concentrated under reduced pressure on a Büchi rotary evaporator.

Determination of Diastereomeric Ratios. The diastereomeric ratios were determined by ^{1}H NMR analysis of the crude reaction mixtures, and confirmed, after column chromatography purification, by HPLC analysis on chiral stationary phase columns.

Determination of Enantiomeric Purity. HPLC analyses on chiral stationary phase were performed on an Agilent 1200-series instrumentation. Daicel Chiralpak AD-H, IA, IB or IC columns with *i*-PrOH/hexane as the eluent were used. HPLC traces were compared to racemic samples prepared by mixture of two enantiomeric final products obtained using (*S*) and (*R*) catalysts.

Determination of Yield and Conversion in the Optimization Studies. The conversion of the starting materials and the yield of product in the optimization studies were determined by ^{1}H NMR spectroscopy using an internal standard in the crude reaction: 1,3,5-trimethoxybenzene: δ 6.10 ppm (s,3H). Since in all instances the conversion of nitrostyrene was equal to the yield of product, in some cases the yield was determined by integration of the signals of the unreacted nitrostyrene

in the ^{1}H NMR spectra. (Nitrostyrene ^{1}H NMR signal: δ 8.01 ppm (d) and oxindole NMR signal: δ 8.68 ppm (d)).

Materials. Commercial grade reagents and solvents were purchased from Sigma Aldrich, Fluka, and Alfa Aesar and used as received, without further purification.[69] Chiral secondary amines are commercially available (Aldrich or Alfa Aesar); they were purified by flash column chromatography prior to use. All the methyleneindolinones[70] and nitrostyrene[71] substrates were synthesized according to literature procedures.

2.8.2 General Procedure for the Synthesis of Enals

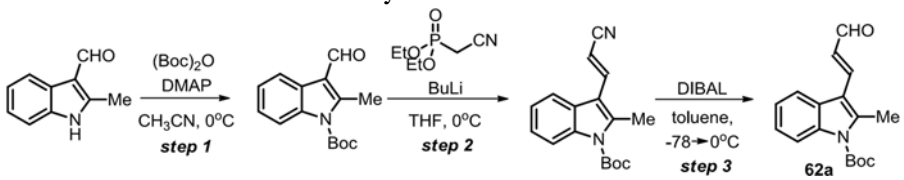

-1st step: The amine protection step was performed according to the literature procedure.[72]

-2nd step procedure: To a solution of diethylcyanomethyl phosphonate (3.58 g, 20.2 mmol) in anhydrous THF (30 mL) at 0°C, BuLi (18.6 mmol, 2.5M in hexanes) was added dropwise and the mixture was stirred for 1h at the same temperature. A solution of the aldehyde (15.5 mmol) in anhydrousTHF (20 mL) was prepared and the Witting solution was added dropwise via cannula. After the addition, the reaction mixture was stirred at 0°C for 4h. The reaction was then concentrated and the product was recrystalized from Hexane/Ethyl Acetate to give 3.67 g of the corresponding nitrile (84%).

-3rd step procedure: A solution of the nitrile (5 mmol) in anhydrous toluene (30 mL) was cooled down to -78 °C and at that temperature, a solution of di*iso*butylaluminium hydride in heptane (1M) (6 mL) was added dropwise for about 10 minutes. The reaction mixture was stirred at -78°C for 4 hours. After that time, the reaction was quenched with methanol (2 mL) at -78 °C The reaction flask was then allowed to warm to room temperature then stirred with 1M HCl (10 mL) for two minutes. The reaction was diluted with 20 mL of EtOAc and the organic phase was separated. The aqueous layer was extracted twice with 10 mL of EtOAc. The combined organics were washed with

---

[69] W. L. F. Armarengo, D. D. Perrin. *Purification of Laboratory Chemicals*, 4th ed.; Butterworth Heinemann: Oxford, 1996.
[70] Z. Chen, J. Fan, A. S. Kende. Total Synthesis of (±)-Alantrypinone by Hetero Diels−Alder eaction. *J. Org. Chem.* **2004**, *69*, 79.
[71] a) S. E. Denmark, L. R. Marcin. A general method for the preparation of 2,2-disubstituted 1-nitroalkenes. *J. Org. Chem.* **1993**, *58*, 3850. b) M. Fujii *Bull. Chem. Soc. Jpn.* **1988**, *61*, 4029.
[72] V. Dhayalan, A. J. Clement, R. Jagan, A. K. Mohanakrishnan. A Versatile Synthesis of Annulated Carbazole Analogs Involving a Domino Reaction of Bromomethylindoles with Arenes/Heteroarenes. *Eur. J. Org. Chem.* **2009**, 531.

brine and dried over Na_2SO_4. After concentration, the material was purified by column chromatography to give the desired product.

(*E*)-*tert*-butyl 2-methyl-3-(3-oxoprop-1-en-1-yl)-1*H*-indole-1-carboxylate (62a)

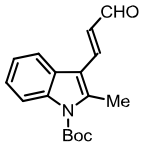

The title compound was isolated by flash column chromatography (Hexane/Ethyl acetate, 10:1-6:1) in 76% yield. ^{1}H NMR (400 MHz, $CDCl_3$): δ 9.69 (d, 1H, *J* = 7.65 Hz), 8.14 (m, 1H), 7.81 (m, 1H), 7.70 (d, 1H, *J* = 15.80 Hz), 7.33 (m, 2H), 6.86 (dd, 1H, J = 15.80, J = 7.65 Hz), 2.76 (s, 3H), 1.71 (s, 9H) ppm. ^{13}C NMR (400 MHz, $CDCl_3$): δ 194.38, 150.12, 144.58, 142.27, 136.46, 128.02, 126.79, 124.75, 123.98, 119.69, 115.73, 114.89, 85.36, 28.34, 14.54 ppm.

(*E*)-*tert*-butyl 5-methoxy-2-methyl-3-(3-oxoprop-1-en-1-yl)-1*H*-indole-1-carboxylate (62b)

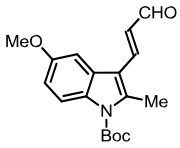

The title compound was isolated by flash column chromatography (Hexane/Ethyl acetate, 8:1) in 66% yield. ^{1}H NMR (400 MHz, $CDCl_3$): δ 9.68 (d, 1H, *J* = 7.74 Hz), 8.02 (d, 1H, *J* = 9.21 Hz), 7.69 (d, 1H, *J* = 15.84 Hz), 7.22 (s, 1H), 6.93 (d, 1H, *J* = 9.21 Hz), 6.79 (dd, 1H, J = 15.84, J = 7.74 Hz), 2.76 (s, 3H), 1.71 (s, 9H) ppm. ^{13}C NMR (400 MHz, $CDCl_3$): δ 194.44, 156.82, 150.06, 144.83, 142.91, 130.96, 127.64, 127.58, 116.58, 114.73, 113.00, 102.79, 85.23, 55.92, 28.33, 14.60 ppm.

(*E*)-*tert*-butyl 5-chloro-2-methyl-3-(3-oxoprop-1-en-1-yl)-1*H*-indole-1-carboxylate (62c)

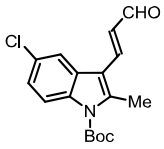

The title compound was isolated by flash column chromatography (Hexane/Ethyl acetate, 7:1) in 72% yield. ^{1}H NMR (400 MHz, $CDCl_3$): δ 9.69 (d, 1H, *J* = 7.70 Hz), 8.07 (d, 1H, *J* = 8.85 Hz), 7.77 (d, 1H, *J* = 2.06 Hz), 7.66 (d, 1H, J = 16.16), 7.29 (dd, 1H, *J* = 8.85, J = 2.06 Hz), 6.80 (dd, 1H, J = 16.16, J = 7.70 Hz), 2.75 (s, 3H), 1.71 (s, 9H) ppm. ^{13}C NMR (400 MHz, $CDCl_3$): δ 194.11, 149.78, 143.72, 143.14, 134.84, 129.78, 128.31, 127.97, 124.84, 119.37, 116.78, 114.23, 85.84, 28.31, 14.66 ppm.

(*E*)-3-(1,2-dimethyl-1*H*-indol-3-yl)acrylaldehyde (62d)

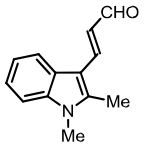

The title compound was isolated by flash column chromatography (Hexane/Ethyl acetate, 10:1-2:1) in 69% yield. ^{1}H NMR (400 MHz, $CDCl_3$): δ 9.61 (d, 1H, *J* = 8.02 Hz), 7.88 (m, 1H), 7.71 (d, 1H, *J* = 16.04 Hz), 7.34 (m, 1H), 7.32-7.25 (m, 2H, *J* = 9.21 Hz), 6.78 (dd, 1H, J = 16.04, J = 8.02 Hz), 3.74 (s, 3H), 2.58 (s, 3H) ppm. ^{13}C NMR (400 MHz, $CDCl_3$): δ 194.35, 146.15, 143.14, 137.90, 125.62, 123.42, 122.83, 122.13, 120.26, 109.79, 109.67, 30.20, 10.97 ppm.

(*E*)-*tert*-butyl 2-methyl-3-(3-oxoprop-1-en-1-yl)-5-phenyl-1*H*-pyrrole-1-carboxylate (62e)

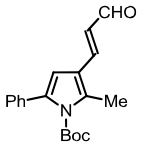

The title compound was synthetized from the corresponding 2-methyl-5phenyl-1*H*-pyrrole-3-carbaldehyde using the same general procedure described above. ^{1}H NMR (400 MHz, $CDCl_3$): δ 9.63 (d, 1H, *J* = 7.57 Hz), 7.49 (d, 1H, *J* =

15.63 Hz), 7.41-7.27 (m, 5H), 6.42 (dd, 1H, *J* = 15.63, *J* = 7.57 Hz), 6.36 (s, 1H), 2.58 (s, 3H), 1.24 (s, 9H) ppm. ^{13}C NMR (400 MHz, $CDCl_3$): δ 193.75, 149.57, 144.70, 136.56, 136.40, 134.17, 128.46, 128.15, 127.68, 126.45, 119.87, 109.55, 84.89, 27.35, 12.51 ppm. **(*E*)-3-(2-methylfuran-3-yl)acrylaldehyde (62f)**

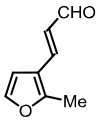

The title compound was synthetized from 2-methylfuran-3-carbaldehyde using tha same general procedure described above. ^{1}H NMR (400 MHz, $CDCl_3$): δ 9.61 (d, 1H, *J* = 7.85 Hz), 7.38-7.29 (m, 2H), 6.51 (d, 1H, *J* = 2.09 Hz), 6.35 (dd, 1H, J = 15.56, J = 7.85 Hz), 2.43 (s, 3H) ppm. ^{13}C NMR (400 MHz, $CDCl_3$): δ 193.48, 155.75, 143.16, 142.30, 127.41, 117.88, 108.04, 12.22 ppm.

2.8.3 General Procedure for the Diels-Alder Reaction with Nitroolefins

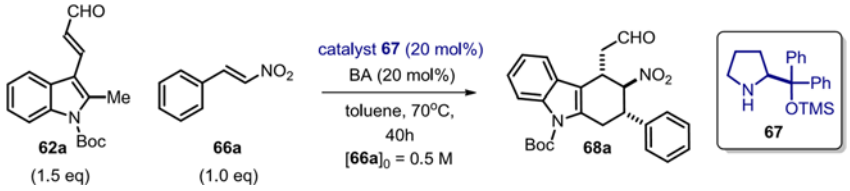

All the reactions were carried out in toluene of synthesis grade (>99%), without any precaution to exclude air and moisture (open air chemistry on the benchtop). An ordinary vial equipped with a Teflon-coated stir bar and a plastic screw cap was charged with (*S*)-2(diphenyl((trimethylsilyl)oxy)methyl)pyrrolidine **67** (0.02 mmol, 6.5 mg, 20 mol%). Then, benzoic acid (0.02 mmol, 2.4 mg, 20 mol%) and toluene (0.2 mL) were added in one portion and the resulting solution was stirred at ambient temperature for 5 minutes to allow the catalyst salt formation. The reaction was started by the sequential addition of the aldehyde **62a** (0.15 mmol, 42.8 mg, 1.5 eq) and the nitrostyrene **66a** (0.1 mmol, 14.9 mg). The vial was sealed and immerged in a oil bath (thermostated at 70°C). The crude mixture was flushed through a short plug of silica, using dichloromethane/diethyl ether 1:1 as the eluent (5 ml). Solvent was removed under reduced pressure and the crude mixture was analyzed by ^{1}H NMR spectroscopy to determine the diastereomeric ratio (d.r.) of the reaction. The product **68a** was isolated by flash column chromatography.

(2*S*,3*S*,4*S*)-*tert*-butyl-3-nitro-4-(2-oxoethyl)-2-phenyl-3,4-dihydro-1*H*-carbazole-9(2*H*)carboxylate (68a)

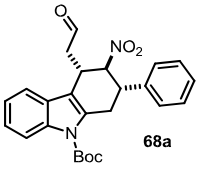

The reaction was carried out following the general procedure to furnish after 40 h the crude product as a 16:1 mixture of diastereoisomers; d.r. determined by integration of ^{1}H-NMR signals: δ_{major} 9.72 ppm (s), δ_{minor} 9.75 ppm (s). The title compound was isolated by flash column chromatography (Toluene/diethylether, 98:2) in 76% yield and 93% e.e..

The e.e. value was measured from the corresponding alcohol, prepared by reduction with $NaBH_4$ (see characterization data below) and was determined by HPLC analysis on a Daicel Chiralpak IA column: 90:10 hexane/*i*- rOH, flow rate 1.00 mL/min, λ = 254 nm: τ_{major} = 11.59 min, τ_{minor} = 13.40 min.
$[\alpha]_{26}^{D}$= -14.04 (*c* = 1.11, $CHCl_3$).

HRMS *calc* for ($C_{25}H_{26}N_2O_5Na$): 457.1739 *found* 457.1748.

^{1}H NMR (400 MHz, $CDCl_3$): δ 9.72 (s, 1H), 8.15 (d, 1H, *J* = 8.22 Hz), 7.40 (d, 1H, *J* = 7.73 Hz), 7.387.22 (m, 7H), 5.28 (m, 1H), 4.19 (m, 1H), 3.68-3.56 (m, 2H), 3.42-3.25 (m, 2H), 2.99 (dd, 1H, *J* = 18.69, *J* = 3.38), 1.64 (s, 9H) ppm. ^{13}C NMR (400 MHz, $CDCl_3$): δ 199.05, 150.12, 138.72, 136.34, 134.31, 128.99, 128.07, 127.59, 127.05, 124.28, 123.01, 118.18, 116.00, 114.05, 93.10, 84.53, 45.50, 44.18, 34.65, 32.33, 28.22 ppm.

(2*S*,3*S*,4*S*)-*tert*-butyl-4-(2-hydroxyethyl)-3-nitro-2-phenyl-3,4-dihydro-1*H*-carbazole-9(2*H*)carboxylate (68a')

Product **68a** was dissolved in MeOH/DCM (1:1); the resulting reaction mixture was cooled to 0 ^{o}C and $NaBH_4$ was introduced portionwise. After 30 min, the reaction was quenched with water and extracted with DCM (x3). The organic phases were collected and dried over $NaSO_4$; the solvent was then removed under reduced pression.

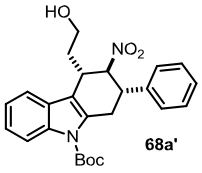

68a'

The title compound was isolated by flash column chromatography (Toluene/diethylether, 4:1).

$[\alpha]_{26}^{D}$= -28.68 (*c* = 1.32, $CHCl_3$);

HRMS *calc* for ($C_{25}H_{28}N_2O_5Na$): 459.1896 *found* 459.1896.

^{1}H NMR (400 MHz, $CDCl_3$): δ 8.14 (d, 1H, *J* = 8.22 Hz), 7.55 (d, 1H, *J* = 7.79Hz), 7.37-7.22 (m, 7H), 5.45 (m, 1H), 3.97 (m, 1H), 3.76-3.47 (m, 4H), 3.29 (m, 1H), 2.36 (m, 1H), 2.22 (m, 1H), 1.64 (s, 9H) ppm. ^{13}C NMR (400 MHz, $CDCl_3$): δ 150.20, 138.92, 136.23, 134.36, 128.92, 127.98, 127.68, 127.63, 124.16, 122.98, 118.95, 115.76, 114.94, 93.64, 84.39, 59.62, 46.17, 37.87, 32.70, 29.72, 28.23 ppm.

(2*S*,3*S*,4*S*)-*tert*-butyl 6-methoxy-3-nitro-4-(2-oxoethyl)-2-phenyl-3,4-dihydro-1*H*-carbazole9(2*H*)-carboxylate (68b)

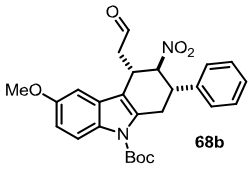

68b

The reaction was carried out following the general procedure to furnish after 40 h the crude product as a 11:1 mixture of diastereoisomers; d.r. determined by integration of ^{1}H-NMR signal: δ_{major} 9.73 ppm (s), δ_{minor} 9.76 ppm (s). The title compound was isolated by flash column chromatography (Toluene/diethylether, 97:3)

in 84% yield and 92% e.e.. The e.e. value was measured from corresponding alchol and was determined by HPLC analysis on a Daicel Chiralpak IC column: 80:20 hexane/*i*-PrOH, flow rate 1.00 mL/min, λ = 254 nm: τ_{major} = 25.13 min, τ_{minor} = 22.74 min.

$[\alpha]_{26}^{D}$= -9.62 (*c* = 1.04, $CHCl_3$).

HRMS *calc* for ($C_{26}H_{28}N_2O_6Na$): 487.1845 *found* 487.1830.

^{1}H NMR (400 MHz, $CDCl_3$): *δ* 9.73 (s, 1H), 8.02 (d, 1H, *J* = 9.19 Hz), 7.39-7.25 (m, 5H), 6.91 (dd, 1H, *J* = 9.19, *J* = 2.38), 6.84 (d, 1H, *J* = 2.38), 5.25 (m, 1H), 4.16 (m, 1H), 3.85 (s, 3H), 3.67-3.54 (m, 2H), 3.38-3.20 (m, 2H), 2.97 (dd, 1H, *J* = 18.83, *J* = 3.18 Hz), 1.63 (s, 9H) ppm. ^{13}C NMR (400 MHz, $CDCl_3$): *δ* 199.26, 156.01, 150.17, 138.78, 135.19, 131.04, 129.12, 128.19, 127.98, 127.70, 116.81, 113.96, 111.92, 102.06, 93.27, 84.47, 55.91, 45.55, 44.28, 34.60, 32.44, 28.35 ppm.

(2*S*,3*S*,4*S*)-*tert*-butyl 6-chloro-3-nitro-4-(2-oxoethyl)-2-phenyl-3,4-dihydro-1*H*-carbazole-9(2*H*)carboxylate (68c)

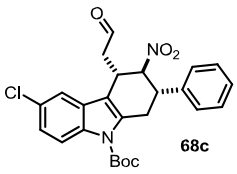

68c

The reaction was carried out following the general procedure to furnish after 40 h the crude product as a 17:1 mixture of diastereoisomers; d.r determined by integration of ^{1}H-NMR signal: δ_{major} 9.72 ppm (s), δ_{minor} 9.75 ppm (s). The title compound was isolated by flash column chromatography (Toluene/diethylether, 98:2) in 80% yield and 90% e.e.. The e.e. value was measured from corresponding alchol and was determined by HPLC analysis on a Daicel Chiralpak IC column: 90:10 hexane/*i*-PrOH, flow rate 1.00 mL/min, λ = 254 nm: τ_{major} = 49.06 min, τ_{minor} = 30.35 min.

$[\alpha]_{26}^{D}$= -6.35 (*c* = 1.09, $CHCl_3$).

HRMS *calc* for ($C_{25}H_{25}ClN_2O_5$): 491.1350 *found* 491.1333.

^{1}H NMR (400 MHz, $CDCl_3$): *δ* 9.72 (s, 1H), 8.06 (d, 1H, *J* = 8.81 Hz), 7.39-7.23 (m, 7H), 5.29 (m, 1H), 4.11 (m, 1H), 3.67-3.54 (m, 2H), 3.41-3.23 (m, 2H), 2.96 (dd, 1H, *J* = 19.05, *J* = 3.13 Hz), 1.63 (s, 9H) ppm. ^{13}C NMR (400 MHz, $CDCl_3$): *δ* 198.90, 149.86, 138.66, 135.93, 134.86, 129.18, 128.79, 128.38, 128.28, 127.68, 124.47, 117.31, 117.14, 113.64, 92.81, 85.15, 45.45, 43.96, 34.57, 32.34, 28.32 ppm.

2-((2*S*,3*S*,4*S*)-9-methyl-3-nitro-2-phenyl-2,3,4,9-tetrahydro-1*H*-carbazol-4-yl)acetaldehyde (68d)

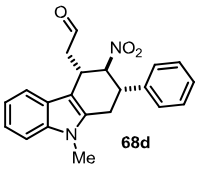

68d

The reaction was carried out following the general procedure to furnish after 40 h the crude product as a 17:1 mixture of diastereoisomers; d.r. determined by integration of ^{1}H-NMR signal: δ_{major} 9.74 ppm (s), δ_{minor} 9.77 ppm (s). The title compound was isolated by flash column chromatography (Toluene/diethyl ether 98:2) in 80% yield and 92% e.e.. The e.e. value was measured from corresponding alchol and was determined by HPLC analysis on a Daicel Chiralpak

IC column: 80:20 hexane/*i*- rOH, flow rate 1.00 mL/min, λ = 254 nm: τ_{major} = 41.45 min, τ_{minor} = 27.44 min.

$[\alpha]_{26}^{D}$= -70.40 (*c* = 1.31, CHCl3).

HRMS *calc* for (C38H37BrN2O7Na): 735.1682 *found* 735.1679.

^{1}H NMR (400 MHz, $CDCl_3$): *δ* 9.74 (s, 1H), 7.41 (d, 1H, *J* = 7.94 Hz), 7.40-7.30 (m, 6H), 7.24 (m, 1H), 7.13 (m, 1H), 5.32 (dd, 1H, *J* = 11.56, *J* = 9.45 Hz), 4.24 (m, 1H), 3.75 (m, 1H), 3.63 (s, 3H), 3.39 (dd, 1H, *J* = 18.35, *J* = 5.47 Hz), 3.22-3.08 (m, 2H), 2.96 (m, 1H) ppm. ^{13}C NMR (400 MHz, $CDCl_3$): *δ* 200.03, 139.05, 137.80, 133.83, 129.20, 128.30, 127.71, 125.14, 121.74, 119.88, 118.50, 109.54, 106.44, 93.53, 45.46, 44.26, 35.92, 29.63, 29.48 ppm.

(2*S*,3*S*,4*S*)-*tert*-butyl 3-nitro-4-(2-oxoethyl)-2-(*p*-tolyl)-3,4-dihydro-1*H*-carbazole-9(2*H*)carboxylate (68e)

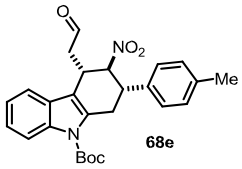

68e

The reaction was carried out following the general procedure to furnish after 40 h the crude product as a >20:1 mixture of diastereoisomers; d.r. determined by integration of ^{1}H-NMR signal: δ_{major} 5.24 ppm (m), δ_{minor} 5.35 ppm (m). The title compound was isolated by flash column chromatography (Toluene/diethylether, 98:2) in 72% yield and 92% e.e.. The e.e. value was measured from the corresponding alcohol and was determined by HPLC analysis on a Daicel Chiralpak IC column: 80:20 hexane/*i*-PrOH, flow rate 1.00 mL/min, λ = 254 nm: τ_{major} = 17.19 min, τ_{minor} = 13.02 min (product from R catalyst).

$[\alpha]_{26}^{D}$= -12.99 (*c* = 0.90, $CHCl_3$).

HRMS *calc* for ($C_{26}H_{28}N_2O_5Na$): 471.1896 *found* 491.1916.

^{1}H NMR (400 MHz, $CDCl_3$): *δ* 9.71 (s, 1H), 8.14 (d, 1H, *J* = 8.42 Hz), 7.39 (d, 1H, *J* = 7.77 Hz), 7.31 (m, 1H), 7.24 (m, 1H), 7.19 (m, 2H), 7.14 (m, 2H), 5.24 (m, 1H), 4.18 (m, 1H), 3.63-3.53 (m, 2H), 3.29-3.26 (m, 2H), 2.98 (dd, 1H, *J* = 18.85, *J* = 3.27), 2.33 (s, 3H), 1.64 (s, 9H) ppm. ^{13}C NMR (400 MHz, $CDCl_3$): *δ* 199.27, 150.21, 137.85, 136.44, 135.71, 134.51, 129.78, 127.55, 127.16, 124.36, 123.11, 118.29, 116.09, 114.12, 93.40, 84.60, 45.26, 44.29, 34.73, 32.47, 28.34, 21.25 ppm.

(2*S*,3*S*,4*S*)-*tert*-butyl 2-(4-chlorophenyl)-3-nitro-4-(2-oxoethyl)-3,4-dihydro-1*H*-carbazole-9(2*H*)carboxylate (68f)

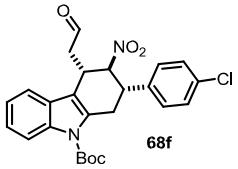

68f

The reaction was carried out following the general procedure to furnish after 40 h the crude product as a >20:1 mixture of diastereoisomers; d.r. determined by integration of ^{1}H-NMR signal: δ_{major} 9.71 ppm (s), δ_{minor} 9.73 ppm (s). The title compound was isolated by flash column chromatography (Toluene/diethylether, 98:2) in 83% yield and 92% e.e.. The e.e. value was measured from the corresponding alcohol and was

determined by HPLC analysis on a Daicel Chiralpak IA column: 80:20 hexane/*i*-PrOH, flow rate 1.00 mL/min, λ = 254 nm: τ_{major} = 7.00 min, τ_{minor} = 9.84 min.

$[\alpha]_{26}^{D}$= -11.60 (*c* = 0.90, $CHCl_3$).

HRMS *calc* for ($C_{25}H_{25}N_2O_5NaCl$): 491.1350 *found* 491.1370.

^{1}H NMR (400 MHz, $CDCl_3$): δ 9.71 (s, 1H), 8.15 (d, 1H, *J* = 8.33 Hz), 7.40 (d, 1H, *J* = 7.66 Hz), 7.367.20 (m, 6H), 5.25 (dd, 1H, *J* = 11.16, *J* = 9.20), 4.15 (m, 1H), 3.65-3.54 (m, 2H), 3.40-3.25 (m, 2H),

2.99 (dd, 1H, *J* = 18.81, *J* = 3.22), 1.65 (s, 9H) ppm. ^{13}C NMR (400 MHz, $CDCl_3$): δ 199.11, 150.18, 137.32, 136.38, 134.06, 134.01, 129.30, 129.07, 127.02, 124.47, 123.16, 118.30, 116.12, 114.10, 93.09, 84.74, 45.10, 44.11, 34.81, 32.50, 28.31 ppm.

(2*S*,3*S*,4*S*)-*tert*-butyl 2-(4-methoxyphenyl)-3-nitro-4-(2-oxoethyl)-3,4-dihydro-1*H*-carbazole9(2*H*)-carboxylate (68g)

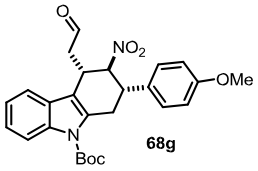

68g

The reaction was carried out following the general procedure to furnish after 40 h the crude product as a >20:1 mixture of diastereoisomers; d.r. determined by integration of ^{1}H-NMR signal: δ_{major} 5.21 ppm (dd), δ_{minor} 5.31 ppm (dd). The title compound was isolated by flash column chromatography (Toluene/diethylether, 98:2) in 54% yield and 93% e.e.. The e.e. value was measured from the corresponding alcohol and was determined by HPLC analysis on a Daicel Chiralpak IC column: 80:20 hexane/*i*-PrOH, flow rate 1.00 mL/min, λ = 254 nm: τ_{major} = 36.65 min, τ_{minor} = 25.48 min.

$[\alpha]_{26}^{D}$= -12.01 (*c* = 0.85, $CHCl_3$).

HRMS *calc* for ($C_{26}H_{28}N_2O_6Na$): 487.1845 *found* 487.1851.

^{1}H NMR (400 MHz, $CDCl_3$): δ 9.71 (s, 1H), 8.14 (d, 1H, *J* = 8.46 Hz), 7.39 (d, 1H, *J* = 8.05 Hz), 7.357.19 (m, 4H), 6.87 (m, 2H), 5.21 (dd, 1H, *J* = 10.94, *J* = 9.15), 4.17 (m, 1H), 3.79 (s, 3H), 3.63-3.51 (m, 2H), 3.38-3.24 (m, 2H), 2.97 (dd, 1H, *J* = 18.67, *J* = 3.26), 1.64 (s, 9H) ppm. ^{13}C NMR (400 MHz, $CDCl_3$): δ 199.23, 159.38, 150.23, 136.49, 134.51, 130.75, 128.78, 127.20, 124.38, 123.13, 118.30, 116.11, 114.50, 114.15, 93.58, 84.62, 55.39, 44.91, 44.34, 34.75, 32.53, 28.35 ppm.

(2*S*,3*S*,4*S*)-*tert*-butyl 3-nitro-2-(4-nitrophenyl)-4-(2-oxoethyl)-3,4-dihydro-1*H*-carbazole-9(2*H*)carboxylate (68h)

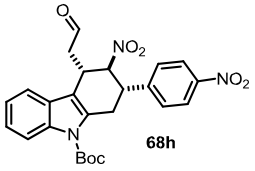

68h

The reaction was carried out following the general procedure to furnish after 16 h the crude product as a 10:1 mixture diastereoisomers; d.r. determined by integration of ^{1}H-NMR signal: δ_{major} 4.16 ppm (m), δ_{minor} 4.70 ppm (m). The title compound was isolated by flash column chromatography (Toluene/diethylether,

98:2) in 88% yield and 92% e.e.. The e.e. value was measured from the corresponding alcohol and was determined by HPLC analysis on a Daicel Chiralpak IB column: 80:20 hexane/*i*-PrOH, flow rate 1.00 mL/min, λ = 254 nm: τ_{major} = 13.97 min, τ_{minor} = 17.20 min.

$[\alpha]_{26}^{D}$= -8.59 (*c* = 0.77, $CHCl_3$).

HRMS *calc* for ($C_{25}H_{25}N_3O_7Na$): 502.1590 *found* 502.1588.

^{1}H NMR (400 MHz, $CDCl_3$): δ 9.73 (s, 1H), 8.22 (m, 2H), 8.13 (d, 1H, *J* = 8.39 Hz), 7.51 (m, 2H), 7.41 (d, 1H, *J* = 7.69 Hz), 7.33 (m, 1H), 7.26 (m, 1H), 5.39 (dd, 1H, *J* = 11.57, *J* = 9.26), 4.16 (m, 1H), 3.76 (td, 1H, *J* = 11.41, *J* = 5.19), 3.66 (dd, 1H, *J* = 17.90, *J* = 5.19), 3.47-3.30 (m, 2H), 3.03 (dd, 1H, *J* = 18.94, *J* = 3.11), 1.64 (s, 9H) ppm. ^{13}C NMR (400 MHz, $CDCl_3$): δ 198.90, 150.22, 147.87, 146.27, 136.40, 133.60, 128.83, 126.95, 124.68, 124.39, 123.30, 118.35, 116.23, 114.20,

92.63, 84.96, 45.65, 43.99, 35.01, 32.40, 28.35 ppm.

(2*S*,3*R*,4*S*)-*tert*-butyl 2-(2-bromophenyl)-3-nitro-4-(2-oxoethyl)-3,4-dihydro-1*H*-carbazole9(2*H*)-carboxylate (68i)

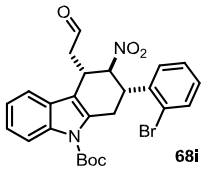

68i

The reaction was carried out following the general procedure to furnish after 40 h the crude product as ad 11:1 mixture of diastereoisomers; d.r. determined by integration of ^{1}H-NMR signal: δ_{major} 9.73 ppm (s), δ_{minor} 9.77 ppm (s). The title compound was isolated by flash column chromatography (Toluene/diethylether, 98:2) in 96% yield and 92% e.e.. The e.e. value was measured from the corresponding alcohol and was determined by HPLC analysis on a Daicel Chiralpak IA column: 90:10 hexane/*i*- rOH, flow rate 1.00 mL/min, λ = 254 nm: τ_{major} = 10.10 min, τ_{minor} = 12.07 min.

$[\alpha]_{26}^{D}$= -25.5 (*c* = 0.85, $CHCl_3$).

HRMS *calc* for ($C_{25}H_{25}N_2O_5NaBr$): 535.0845 *found* 535.0865.

^{1}H NMR (400 MHz, $CDCl_3$): δ 9.73 (s, 1H), 8.14 (d, 1H, *J* = 8.60 Hz), 7.59 (d, 1H, *J* = 8.21 Hz), 7.447.22 (m, 5H), 7.15 (m, 1H), 5.44 (m, 1H), 4.36 (m, 1H), 4.21 (m, 1H), 3.64 (m, 1H), 3.33 (dd, 1H, *J* = 19.02, *J* = 5.65), 3.14 (m, 1H), 3.01 (dd, 1H, *J* = 19.02, *J* = 3.08), 1.64 (s, 9H) ppm. ^{13}C NMR (400 MHz, $CDCl_3$): δ 199.11, 150.25, 138.27, 136.46, 134.13, 133.80, 129.43, 128.30, 127.15, 124.48, 123.18, 118.34, 116.16, 114.23, 91.13, 84.75, 44.08, 43.56, 34.81, 31.97, 28.37 ppm.

(2*R*,3*R*,4*S*)-*tert*-butyl 2-(furan-2-yl)-3-nitro-4-(2-oxoethyl)-3,4-dihydro-1*H*-carbazole-9(2*H*)carboxylate (68j)

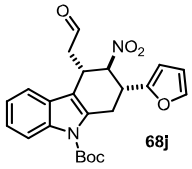

68j

The reaction was carried out following the general procedure to furnish after 40 h the crude product as a 17:1 mixture of diastereoisomers; d.r. determined by integration of ^{1}H-NMR signal: δ_{major} 5.25 ppm (m), δ_{minor} 5.32 ppm (m). The title compound was isolated by flash column chromatography

(Toluene/diethylether, 98:2) in 55% yield and 92% e.e.. The e.e. value was measured from the corresponding alcohol and was determined by HPLC analysis on a Daicel Chiralpak IC column: 80:20 hexane/*i*- rOH, flow rate 1.00 mL/min, λ = 254 nm: τ_{major} = 36.01 min, τ_{minor} = 20.48 min.

$[\alpha]_{26}^{D}$= -7.89 (*c* = 1.21, $CHCl_3$).

HRMS *calc* for ($C_{23}H_{24}N_2O_6Na$): 447.1532 *found* 447.1544.

^{1}H NMR (400 MHz, $CDCl_3$): δ 9.70 (s, 1H), 8.15 (d, 1H, *J* = 8.48 Hz), 7.40-7.33 (m, 2H), 7.30 (m, 1H), 7.23 (m, 1H), 6.31 (m, 1H), 6.18 (m, 1H), 5.25 (dd, 1H, *J* = 9.44, *J* = 7.13), 4.27 (m, 1H), 3.94 (m, 1H), 3.56 (m, 2H), 2.94 (dd, 1H, *J* = 19.05, *J* = 3.94), 2.79 (dd, 1H, *J* = 19.30, *J* = 7.01), 1.68 (s, 9H) ppm. ^{13}C NMR (400 MHz, $CDCl_3$): δ 199.12, 152.03, 150.28, 142.53, 136.48, 133.33, 127.21, 124.46, 123.14, 118.13, 116.12, 113.89, 110.72, 107.75, 89.68, 84.69, 44.61, 38.05, 32.77, 28.40, 28.20 ppm.

(2*S*,3*R*,4*S*)-*tert*-butyl 3-nitro-4-(2-oxoethyl)-2-(thiophen-3-yl)-3,4-dihydro-1*H*-carbazole-9(2*H*)carboxylate (68k)

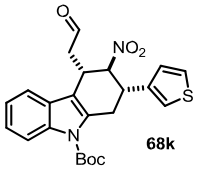

68k

The reaction was carried out following the general procedure to furnish after 40 h the crude product as a >20:1 mixture of diasteroisomers; d.r. determined by integration of ^{1}H-NMR signal: δ_{major} 5.17 ppm (m), δ_{minor} 5.27 ppm (m). The title compound was isolated by flash column chromatography (Toluene/diethylether, 98:2) in 64% yield and 92% e.e.. The e.e. value was measured from the corresponding alcohol and was determined by HPLC analysis on a Daicel Chiralpak IC column: 80:20 hexane/*i*-PrOH, flow rate 1.00 mL/min, λ = 254 nm: τ_{major} = 23.57 min, τ_{minor} = 38.26 min.

$[\alpha]_{26}^{D}$= -12.48 (*c* = 0.8, $CHCl_3$).

HRMS *calc* for ($C_{23}H_{24}N_2O_5NaS$): 463.1304 *found* 463.1317.

^{1}H NMR (400 MHz, $CDCl_3$): δ 9.70 (s, 1H), 8.15 (d, 1H, *J* = 8.31 Hz), 7.38 (d, 1H, *J* = 7.70 Hz), 7.357.28 (m, 2H), 7.24 (m, 1H), 7.16 (m, 1H), 7.06 (dd, 1H, *J* = 5.06, *J* = 1.45 Hz), 5.17 (dd, 1H, *J* = 10.85, *J* = 8.53 Hz), 4.19 (m, 1H), 3.84 (dt, 1H, *J* = 10.85, *J* = 5.35 Hz), 3.60 (dd, 1H, J = 18.51, J = 5.35 Hz), 3.39 (ddd, 1H, *J* = 18.51, *J* = 10.70, J = 2.60 Hz), 3.17 (dd, 1H, *J* = 18.95, *J* = 6.22 Hz), 2.96 (dd, 1H, J = 18.95, J= 3.33 Hz), 1.66 (s, 9H) ppm. ^{13}C NMR (400 MHz, $CDCl_3$): δ 199.07, 150.11, 139.39, 136.34, 133.94, 127.05, 126.69, 126.20, 124.31, 123.01, 122.63, 118.13, 116.00, 114.02, 92.94, 84.55, 44.21, 40.55, 34.13, 31.54, 28.24 ppm.

(2*R*,3*S*,4*S*)-*tert*-butyl 3-nitro-4-(2-oxoethyl)-2-phenethyl-3,4-dihydro-1*H*-carbazole-9(2*H*)carboxylate (68l)

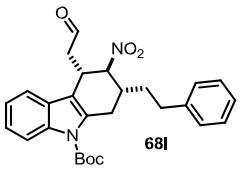

68l

The reaction was carried out following the general procedure to furnish after 40 h the crude product as a 14:1 mixture of diastereoisomers; d.r. determined after column by integration of ^{1}H-NMR signal: δ_{major} 9.70 ppm (s), δ_{minor} 9.73 ppm (s). The title compound was isolated by preparative TLC (Hexane/Acetone, 6:1) in 22% yield and 92% e.e.. The e.e. value was measured from the corresponding alcohol and was determined by HPLC analysis on a Daicel Chiralpak IB column: 90:10 hexane/*i*-PrOH, flow rate 1.00 mL/min, λ = 254 nm: τ_{major} = 13.21 min, τ_{minor} = 10.00 min.

$[\alpha]_{26}^{D}$= -36.19 (*c* = 0.73, $CHCl_3$).

HRMS *calc* for ($C_{27}H_{30}N_2O_5Na$): 485.2052 *found* 485.2043.

^{1}H NMR (400 MHz, $CDCl_3$): δ 9.72 (s, 1H), 8.15 (d, 1H, *J* = 8.46 Hz), 7.36 (d, 1H, *J* = 7.96 Hz), 7.327.27 (m, 3H), 7.23-7.15 (m, 4H), 4.83 (dd, 1H, *J* = 11.44, *J* = 9.20), 4.06 (m, 1H), 3.58 (dd, 1H, *J* = 17.91, *J* = 5.47), 3.29 (dd, 1H, J = 18.66, J = 5.72), 2.96-2.82 (m, 3H), 2.64 (m, 1H), 2.47 (m, 1H), 1.90-1.70 (m 2H), 1.71 (s, 9H) ppm. ^{13}C NMR (400 MHz, $CDCl_3$): δ 199.12, 150.13, 140.69, 136.43, 133.95, 128.59, 128.28, 127.00, 126.25, 124.23, 122.99, 118.17, 116.02, 113.98, 93.65, 84.38, 44.15, 37.91, 34.41, 33.71, 39.19, 29.70, 28.33 ppm.

Table 5. Results using catalyst ***ent*-67** to obtain the opposite enantiomer of the product (***ent*-68**)

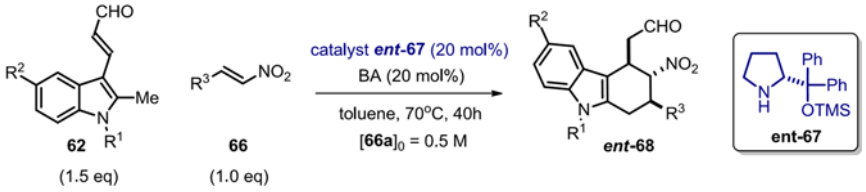

Entry	R1	R2	R3	**68**	Yield (%)[b]	dr (%)[c]	*ee* (%)[d]
1	Boc	H	Ph	**ent-a**	75	18:1	92
2	Boc	OMe	Ph	**ent-b**	84	11:1	92
3	Boc	Cl	Ph	**ent-c**	81	18:1	90
4	Boc	H	p-MeC_6H_4	**ent-e**	71	19:1	92
5	Boc	H	p-ClC_6H_4	**ent-f**	82	17:1	92
6	Boc	H	p-$OMeC_6H_4$	**ent-g**	52	19:1	93
7[e]	Boc	H	p-$NO_2C_6H_4$	**ent-h**	86	10:1	92
8	Boc	H	o-BrC_6H_4	**ent-i**	90	12:1	92
9	Boc	H	2-furanyl	**ent-j**	52	16:1	92
10	Boc	H	3-thiophenyl	**ent-k**	61	19:1	92
11	Boc	H	CH_2CH_2Ph	**ent-l**	14	14:1	92

[a] [b] Reactions were carried out on a 0.1 mmol scale, [**66**]$_0$ = 0.5 M in toluene. Yields of isolated products. [c] Diastereomeric ratios (dr) were determined by means of ^{1}H NMR analysis of the crude mixture. [d] Enantiomeric excess (*ee*) values were determined after $NaBH_4$ reduction of compound

68 to the corresponding alcohol and HPLC analysis on commercially available chiral stationary phases. [e] The reaction required 16 h for completion.

2.8.4 General Procedure for the Diels-Alder Reaction with Methyleneindolinones

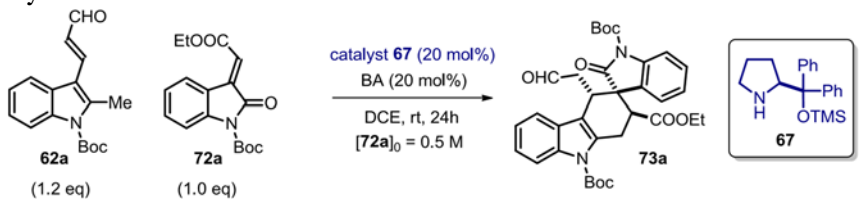

All the reactions were carried out in dichloroethane of synthesis grade (>99%), without any precaution to exclude air and moisture (open air chemistry on the benchtop). An ordinary vial equipped with a Teflon-coated stir bar and a plastic screw cap was charged with (*S*)-2(diphenyl((trimethylsilyl)oxy)methyl)pyrrolidine **67** (0.02 mmol, 6.5 mg, 20 mol%). Then, benzoic acid (0.02 mmol, 2.4 mg, 20 mol%) and DCE (0.2 mL) were added in one portion and the resulting solution was stirred at ambient temperature for 5 minutes to allow the catalyst salt formation. The reaction was started by the sequential addition of the aldehyde **62a** (0.12 mmol, 34.2 mg, 1.5 equiv) and the methyleneindolinone **72a** (0.1 mmol, 31.7 mg). The vial was sealed and left stirring at room temperature. The crude mixture was flushed through a short plug of silica, using dichloromethane/diethyl ether 1:1 as the eluent (5 ml). The solvent was removed under reduced pressure and the crude mixture was analyzed by ^{1}H NMR spectroscopy to determine the diastereomeric ratio (d.r.). The product **73a** was isolated by flash column chromatography.

(2*S*,3*S*,4*S*)-1',9-di-*tert*-butyl 2-ethyl 2'-oxo-4-(2-oxoethyl)-1,2-dihydrospiro[carbazole-3,3'indoline]-1',2,9(4*H*)-tricarboxylate (73a)

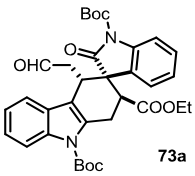

The reaction was carried out following the general procedure to furnish after 24 h the crude product as a single diastereoisomer (d.r. >20:1). The title compound was isolated by flash column chromatography (Hexane/ethyl acetate, 10:1) in 95% yield and 97% e.e.. The e.e. value was determined by HPLC analysis on a Daicel Chiralpak IA column: 95:5 hexane/*i*- rOH, flow rate 1.00 mL/min, λ = 254 nm: τ_{major} = 8.70 min, τ_{minor} = 5.70 min.

$[\alpha]_{26}^{D}$= -76.44 (*c* = 1.00, $CHCl_3$).

HRMS *calc* for ($C_{34}H_{38}N_2O_8$ Na): 625.2526 *found* 625.2534.

^{1}H NMR (400 MHz, $CDCl_3$): *δ* 9.76 (s, 1H), 8.21 (d, 1H, *J* = 8.52 Hz), 7.93 (d, 1H, *J* = 8.52 Hz), 7.30 (m, 1H), 7.26 (m, 1H), 7.20-7.13 (m, 2H), 6.88 (t, 1H, *J* = 7.57 Hz), 6.72 (d, 1H, *J* = 7.57 Hz), 4.043.80 (m, 3H), 3.86 (d, 1H, *J* = 10.08 Hz), 3.69 (dd, 1H, J = 11.91, J = 6.87 Hz), 3.58 (dd, 1H, J = 19.24, J = 10.08 Hz), 3.38 (dd, 1H, J = 19.24, J = 11.91 Hz), 2.62 (d, 1H, J = 19.24), 1.73 (s, 9H),

1.65 (s, 9H), 1.10 (t, 3H, *J* = 7.05 Hz) ppm. ^{13}C NMR (400 MHz, $CDCl_3$): δ 199.19, 177.62, 171.48, 150.42, 149.14, 139.75, 136.79, 132.92, 130.80, 128.44, 127.73, 124.70, 124.34, 123.12, 123.05, 117.64, 117.18, 115.97, 115.22, 84.54, 84.12, 61.40, 49.40, 45.75, 43.07, 35.17, 28.44, 28.21, 26.60, 13.91 ppm.

(2*S*,3*S*,4*S*)-tri-*tert*-butyl 2'-oxo-4-(2-oxoethyl)-1,2-dihydrospiro[carbazole-3,3'-indoline]1',2,9(4*H*)-tricarboxylate (73b)

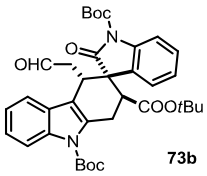

73b

The reaction was carried out following the general procedure to furnish after 24 h the crude product as a single diastereoisomer (d.r. >20:1). The title compound was isolated by flash column chromatography (Hexane/ethyl acetate, 7:1) in 98% yield and 98% e.e.. The e.e. value was determined by HPLC analysis on a Daicel Chiralpak IA column: 90:10 hexane/*i*- rOH, flow rate 1.00 mL/min, λ = 254 nm: τ_{major} = 6.89 min, τ_{minor} = 4.25 min.

$[\alpha]_{26}^{D}$= -90.45 (*c* = 1.16, $CHCl_3$).

HRMS *calc* for ($C_{36}H_{42}N_2O_8Na$): 653.2839 *found* 653.2850.

^{1}H NMR (400 MHz, $CDCl_3$): δ 9.75 (s, 1H), 8.20 (d, 1H, *J* = 8.62 Hz), 7.92 (d, 1H, *J* = 8.62 Hz), 7.317.23 (m, 2H), 7.19-7.12 (m, 2H), 6.87 (t, 1H, *J* = 7.66 Hz), 6.72 (d, 1H, *J* = 7.66 Hz), 3.89-3.79 (m, 2H), 3.62-3.53 (m, 2H), 3.42 (dd, 1H, J = 19.16, J = 11.49 Hz), 2.58 (d, 1H, *J* = 19.16 Hz), 1.73 (s, 9H), 1.65 (s, 9H), 1.20 (s, 9H) ppm. ^{13}C NMR (400 MHz, $CDCl_3$): δ 199.31, 177.37, 170.48, 150.41, 149.18, 139.46, 136.71, 133.21, 130.96, 128.30, 127.71, 124.57, 124.36, 123.13, 123.03, 117.57, 116.88, 115.90, 115.04, 84.45, 84.06, 82.18, 49.58, 45.79, 43.96, 35.21, 28.43, 28.18, 27.63, 26.63 ppm.

(2*S*,3*S*,4*S*)-di-*tert*-butyl 2-benzoyl-2'-oxo-4-(2-oxoethyl)-1,2-dihydrospiro[carbazole-3,3'indoline]-1',9(4*H*)-dicarboxylate (73c)

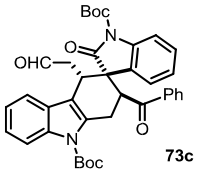

73c

The reaction was carried out following the general procedure to furnish after 40 h the crude product as a 14:1 mixture of diastereoisomers; d.r. determined by integration of ^{1}H-NMR signal: δ_{major} 9.80 ppm (s), δ_{minor} 9.39 ppm (m). The title compound was isolated by flash column chromatography (Hexane/ethyl acetate, 5:1) in 87% yield and 96% e.e.. The e.e. value was determined by HPLC analysis on a Daicel Chiralpak IB column: 80:20 hexane/*i*PrOH, flow rate 1.00 mL/min, λ = 254 nm: τ_{major} = 6.67 min, τ_{minor} = 13.05 min.

$[\alpha]_{26}^{D}$= -76.27 (*c* = 1.31, $CHCl_3$).

HRMS *calc* for ($C_{38}H_{38}N_2O_7Na$): 657.2577 *found* 657.2607.

^{1}H NMR (400 MHz, $CDCl_3$): δ 9.80 (s, 1H), 8.20 (d, 1H, *J* = 8.49 Hz), 8.03 (d, 1H, *J* = 8.49 Hz), 7.87 (d, 2H, *J* = 7.76 Hz), 7.56 (t, 1H, *J* = 7.52 Hz), 7.45 (m, 2H), 7.34-7.27 (m, 2H), 7.19 (m, 2H), 6.90 (t, 1H, *J* = 7.52 Hz), 6.70 (d, 1H, *J* = 7.52 Hz), 4.59 (dd, 1H, *J* = 12.62, *J* = 6.07 Hz), 3.98-3.84 (m, 2H), 3.71

(dd, 1H, *J* = 18.92, *J* = 10.19 Hz), 3.23 (dd, 1H, *J* = 18.24, *J* = 12.86 Hz), 2.76 (d, 1H, *J* = 18.92 Hz), 1.62 (s, 9H), 1.54 (s, 9H) ppm. ^{13}C NMR (400 MHz, $CDCl_3$): δ 199.88, 199.14, 177.89, 150.32, 149.08, 139.65, 136.80, 136.27, 133.37, 133.02, 131.85, 128.83, 128.67, 128.11, 127.78, 124.80, 124.30, 123.18, 122.69, 117.74, 117.70, 116.00, 115.38, 84.52, 84.07, 49.94, 49.41, 45.63, 35.70, 28.24, 28.18, 28.08 ppm.

(2*S*,3*S*,4*S*)-di-*tert*-butyl 2-(4-bromobenzoyl)-2'-oxo-4-(2-oxoethyl)-1,2-dihydrospiro[carbazole3,3'-indoline]-1',9(4*H*)-dicarboxylate (73d)

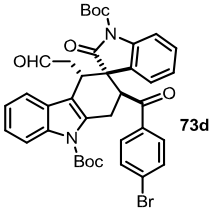

73d

The reaction was carried out following the general procedure to furnish after 30 h the crude product as a 15:1 mixture of diastereoisomers; d.r. determined by integration of ^{1}H-NMR signal: δ_{major} 9.79 ppm (s), δ_{minor} 9.39 ppm (m). The title compound was isolated by flash column chromatography (Hexane/ethyl acetate, 10:1) in 94% yield and 94% e.e..

The e.e. value was determined by HPLC analysis on a Daicel Chiralpak IA column: 90:10 hexane/*i*-PrOH, flow rate 1.00 mL/min, λ = 254 nm: τ_{major} = 10.00 min, τ_{minor} = 12.38 min.

$[\alpha]_{26}^{D}$= -70.40 (*c* = 1.31, $CHCl_3$).

HRMS *calc* for ($C_{38}H_{37}BrN_2O_7Na$): 735.1682 *found* 735.1679.

^{1}H NMR (400 MHz, $CDCl_3$): δ 9.79 (s, 1H), 8.18 (d, 1H, *J* = 8.05 Hz), 8.02 (d, 1H, *J* = 8.05 Hz), 7.75 (d, 2H, *J* = 8.67 Hz), 7.60 (d, 2H, *J* = 8.67 Hz), 7.34-7.27 (m, 2H), 7.22-7.17 (m, 2H), 6.90 (t, 1H, *J* = 7.43 Hz), 6.71 (d, 1H, *J* = 7.43 Hz), 4.53 (dd, 1H, *J* = 12.38, *J* = 5.57 Hz), 3.94-3.85 (m, 2H), 3.69 (dd, 1H, *J* = 19.19, *J* = 9.90 Hz), 3.25 (dd, 1H, *J* = 18.24, *J* = 12.86 Hz), 2.76 (d, 1H, *J* = 18.57 Hz), 1.62 (s, 9H), 1.59 (s, 9H) ppm. ^{13}C NMR (400 MHz, $CDCl_3$): δ 199.07, 198.85, 177.83, 150.36, 148.99, 139.57, 136.71, 134.95, 132.89, 132.16, 131.62, 130.20, 128.62, 128.20, 127.73, 124.86, 124.37, 123.21, 122.73, 117.76, 117.67, 116.03, 115.38, 84.65, 84.18, 50.01, 46.23, 45.58, 35.64, 28.29, 28.16, 27.87 ppm.

(2*S*,3*S*,4*S*)-*tert*-butyl 2-(4-bromobenzoyl)-2'-oxo-4-(2-oxoethyl)-1,2-dihydrospiro[carbazole3,3'-indoline]-9(4*H*)-carboxylate (73e)

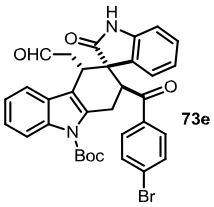

73e

The reaction was carried out following the general procedure to furnish after 72 h the crude product as a 15:1 mixture of diastereoisomers; d.r. determined by integration of ^{1}H-NMR *signal*: δ_{major} 9.79 ppm (s), δ_{minor} 9.32 ppm (m). The title compound was isolated by flash column chromatography (Hexane/ethyl acetate, 10:1) in 89% yield and 94% e.e..

The e.e. value was determined by HPLC analysis on a Daicel Chiralpak IB column: 80:20 hexane/*i*- rOH, flow rate 1.00 mL/min, λ = 254 nm: τ_{major} = 11.41 min, τ_{minor} = 38.11 min.

$[\alpha]_{26}^{D}$= -83.18 (*c* = 1.31, $CHCl_3$).

HRMS *calc* for ($C_{33}H_{29}BrN_2O_5Na$): 635.1158 *found* 635.1172.

^{1}H NMR (400 MHz, $CDCl_3$): δ 9.79 (s, 1H), 8.17 (d, 1H, *J* = 8.37 Hz), 7.79 (d, 2H, *J* = 8.74 Hz), 7.68 (bs, 1H), 7.60 (d, 2H, *J* = 8.74 Hz), 7.32 (m, 1H), 7.25-7.17 (m, 3H), 6.94 (d, 1H, *J* = 7.64 Hz), 6.81 (t, 1H, *J* = 7.64 Hz), 6.69 (d, 1H, *J* = 7.64 Hz), 4.51 (dd, 1H, *J* = 12.74, *J* = 5.46 Hz), 3.92 (d, 1H, *J* = 9.83), 3.88-3.72 (m, 2H), 3.27 (dd, 1H, J = 18.57, J = 12.74 Hz), 2.73 (d, 1H, *J* = 18.93 Hz), 1.60 (s, 9H) ppm. ^{13}C NMR (400 MHz, $CDCl_3$): δ 199.58, 198.93, 180.18, 150.42, 140.43, 136.64, 135.01, 133.11, 133.00, 132.17, 130.32, 130.25, 128.72, 128.09, 127.81, 124.76, 123.59, 123.17, 122.64, 118.01, 117.84, 116.00, 110.23, 84.59, 49.90, 45.29, 45.12, 34.95, 28.37, 28.32, 27.95 ppm.

(2*S*,3*S*,4*S*)-di-*tert*-butyl 2-acetyl-2'-oxo-4-(2-oxoethyl)-1,2-dihydrospiro[carbazole-3,3'indoline]-1',9(4*H*)-dicarboxylate (73f)

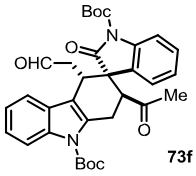

73f

The reaction was carried out following the general procedure to furnish after 24 h the crude product as a single diastereoisomer (d.r. >20:1). The title compound was isolated by flash column chromatography (Toluene/Diethyl ether, 85:15) in 53% yield and 96% e.e.. The e.e. value was determined by HPLC analysis on a Daicel Chiralpak IB column: 80:20 hexane/*i*- rOH, flow rate 1.00 mL/min, λ = 254 nm: τ_{major} = 9.60 min, τ_{minor} = 19.20 min.

$[\alpha]_{26}^{D}$= -80.71 (*c* = 0.93, $CHCl_3$).

HRMS *calc* for ($C_{33}H_{36}N_2O_7Na$): 595.2420 *found* 595.2419.

^{1}H NMR (400 MHz, $CDCl_3$): δ 9.75 (s, 1H), 8.16 (d, 1H, *J* = 8.24 Hz), 7.95 (d, 1H, *J* = 8.24 Hz), 7.31 (m, 1H), 7.24 (m, 1H), 7.20-7.14 (m, 2H), 6.85 (t, 1H, *J* = 7.59 Hz), 6.63 (d, 1H, *J* = 7.66 Hz), 4.01 (dd, 1H, *J* = 18.23, *J* = 6.58 Hz), 3.82-3.70 (m, 2H), 3.54 (dd, 1H, *J* = 19.07, *J* = 9.79 Hz), 3.30 (dd, 1H, J = 18.23, J = 12.49 Hz), 2.62 (d, 1H, *J* = 19.07 Hz), 2.21 (s, 3H), 1.74 (s, 9H), 1.65 (s, 9H) ppm.

^{13}C NMR (400 MHz, $CDCl_3$): δ 206.06, 199.09, 178.01, 150.58, 149.13, 139.77, 136.69, 132.77, 131.18, 128.62, 128.18, 127.76, 124.81, 124.20, 123.20, 122.65, 117.94, 117.81, 116.03, 115.37, 84.68, 84.07, 51.23, 49.32, 45.64, 35.26, 28.49, 28.26, 28.22, 26.20 ppm.

(2*S*,3*S*,4*S*)-di-*tert*-butyl 2-cyano-2'-oxo-4-(2-oxoethyl)-1,2-dihydrospiro[carbazole-3,3'indoline]-1',9(4*H*)-dicarboxylate (73g)

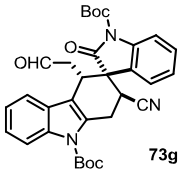

73g

The reaction was carried out following the general procedure to furnish after 40 h the crude product as a 10:1 mixture of diastereoisomers; d.r. determined by integration of ^{1}H-NMR signal: δ_{major} 9.75 ppm (s), δ_{minor} 9.39 ppm (m). The title compound was isolated by flash column chromatography (Hexane/ethyl acetate, 8:1-5:1) in 74% yield and 96% e.e.. The e.e. value was

determined by HPLC analysis on a Daicel Chiralpak IA column: 95:5 hexane/*i* rOH, flow rate 1.00 mL/min, λ = 254 nm: τ_{major} = 18.39 min, τ_{minor} = 10.08 min.

$[\alpha]_{26}^{D}$= -59.27 (*c* = 0.97, $CHCl_3$).

HRMS *calc* for ($C_{32}H_{33}N_3O_6Na$): 578.2267 *found* 578.2277.

^{1}H NMR (400 MHz, $CDCl_3$): δ 9.75 (s, 1H), 8.18 (d, 1H, *J* = 8.28 Hz), 7.98 (d, 1H, *J* = 8.28 Hz), 7.407.30 (m, 2H), 7.25-7.13 (m, 2H), 7.01 (t, 1H, *J* = 7.71 Hz), 6.86 (d, 1H, *J* = 7.71 Hz), 4.05-3.91 (m, 2H), 3.65 (dd, 1H, *J* = 11.08, *J* = 6.14 Hz), 3.58-3.42 (m, 2H), 2.74 (d, 1H, *J* = 19.28 Hz), 1.73 (s, 9H), 1.66 (s, 9H) ppm. ^{13}C NMR (400 MHz, $CDCl_3$): δ 199.01, 175.49, 150.26, 148.54, 139.62, 136.54, 130.65, 129.91, 127.60, 127.32, 125.17, 125.12, 123.65, 123.33, 118.26, 117.73, 116.62, 116.13, 115.79, 85.16, 85.00, 50.08, 45.29, 33.69, 30.85, 28.43, 28.16, 26.77 ppm.

(2*R*,3*R*,4*S*)-di-*tert*-butyl 2-(4-nitrophenyl)-2'-oxo-4-(2-oxoethyl)-1,2-dihydrospiro[carbazole3,3'-indoline]-1',9(4*H*)-dicarboxylate (73h)

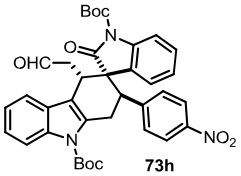

73h

The reaction was carried out following the general procedure to furnish after 72 h the crude product as a 1:1 mixture of diastereoisomers; d.r. determined by integration of ^{1}H-NMR signal: δ_{major} 9.83 ppm (s), δ_{minor} 9.50 ppm (m). The mixture was isolated by flash column chromatography (Hexane/ethyl acetate, 10:1-6:1) in 66% overall yield. The title compound was after separated by flash column chromatography (Toluene/diethyl ether, 98:2) in 32% yield (d.r.: 5:1). The e.e. values (96, 94%, respectively) were determined by HPLC analysis on a Daicel Chiralpak IA column: 90/10 hexane/*i*-PrOH, flow rate 1.00 mL/min, λ = 254 nm: τ_{major} = 6.10 min, τ_{minor} = 7.49 min (Major diastereoisomer); τ_{major} = 24.50 min, τ_{minor} = 8.43 min (Minor diastereoisomer).

$[\alpha]_{26}^{D}$= -99.3 (*c* = 0.98, CHCl3).

HRMS *calc* for ($C_{37}H_{37}N_3O_8Na$): 674.2478 *found* 674.2493.

^{1}H NMR (400 MHz, $CDCl_3$): δ 9.83 (s, 1H), 8.16 (d, 1H, *J* = 8.51 Hz), 7.92 (d, 2H, *J* = 8.97 Hz), 7.65 (d, 1H, *J* = 8.11 Hz), 7.37-7.30 (m, 2H), 7.29-7.21 (m, 2H), 7.06 (t, 1H, *J* = 7.56 Hz), 7.01 (d, 1H, *J* = 7.56 Hz), 6.91 (d, 2H, *J* = 8.97 Hz), 4.12 (d, 1H, *J* = 10.15 Hz), 3.92 (dd, 1H, *J* = 19.41, *J* = 10.15 Hz), 3.85 (dd, 1H, *J* = 11.94, *J* = 5.67 Hz), 3.71 (dd, 1H, *J* =18.51, *J* = 5.67 Hz), 3.41 (dd, 1H, *J* = 18.51, *J* = 11.94 Hz), 2.80 (d, 1H, *J* = 19.41 Hz), 1.68 (s, 9H), 1.45 (s, 9H) ppm. ^{13}C NMR (400 MHz, $CDCl_3$): δ 199.67, 176.24, 150.63, 148.13, 147.40, 146.17, 139.40, 136.45, 133.87, 130.01, 129.27, 129.19, 127.77, 125.03, 124.76, 123.99, 123.23, 123.12, 117.82, 117.23, 116.08, 115.28, 84.71, 84.47, 52.64, 45.45, 44.39, 34.55, 30.14, 28.44, 27.97 ppm.

(2*S*,3*S*,4*S*)-di-*tert*-butyl 2-(4-nitrophenyl)-2'-oxo-4-(2-oxoethyl)-1,2-dihydrospiro[carbazole3,3'-indoline]-1',9(4*H*)-dicarboxylate (73h')

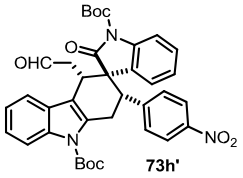

73h'

The reaction was carried out following the general procedure to furnish after 72 h the crude product as a 1:1 mixture of diastereoisomers; d.r. determined by integration of ^{1}H-NMR signal: δ_{major} 9.83 ppm (s), δ_{minor} 9.51 ppm (m). The mixture was isolated by flash column chromatography (Hexane/ethyl acetate, 10:1-6:1) in 66% overall yield. The title compound was after separated by flash column chromatography (Toluene/diethyl ether, 98:2) in 28% yield and 98% e.e.. The e.e. value was determined by HPLC analysis on a Daicel Chiralpak IB column: 90:10 hexane/*i*- rOH, flow rate 1.00 mL/min, λ = 254 nm: τ_{major} = 17.22 min, τ_{minor} = 16.05 min (product from R catalyst).

$[\alpha]_{26}^{D}$= +190.3 (*c* = 0.88, CHCl3).

HRMS *calc* for ($C_{37}H_{37}N_3O_8Na$): 674.2478 *found* 674.2497.

^{1}H NMR (400 MHz, $CDCl_3$): *δ* 9.50 (s, 1H), 8.19 (d, 1H, *J* = 8.57 Hz), 7.87 (d, 2H, *J* = 8.57 Hz), 7.427.36 (m, 2H), 7.29 (m, 1H), 7.25-7.15 (m, 6H), 4.42 (m, 1H), 4.02 (dd, 1H, *J* = 17.65, *J* = 11.63 Hz), 3.64 (dd, 1H, *J* = 11.63, *J* = 4.90 Hz), 3.53 (dd, 1H, *J* =17.65, *J* = 4.90 Hz), 3.08 (dd, 1H, *J* = 18.85, *J* = 4.09 Hz), 2.56 (dd, 1H, *J* = 18.85, *J* = 6.13 Hz), 1.66 (s, 9H), 1.60 (s, 9H) ppm. ^{13}C NMR (400 MHz, $CDCl_3$): *δ* 199.75, 174.56, 150.47, 148.47, 147.15, 146.52, 139.48, 136.45, 135.31, 129.44, 129.33, 128.61, 127.74, 124.88, 124.01, 123.15, 123.03, 122.88, 118.31, 116.13, 114.83, 114.80, 84.99, 84.38, 56.41, 50.11, 44.61, 35.72, 28.47, 28.40, 28.24 ppm.

(2*S*,3*S*,4*S*)-1',9-di-*tert*-butyl 2-ethyl 5'-methyl-2'-oxo-4-(2-oxoethyl)-1,2dihydrospiro[carbazole-3,3'-indoline]-1',2,9(4*H*)-tricarboxylate (73i)

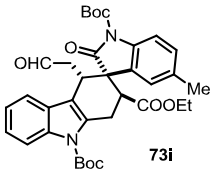

73i

The reaction was carried out following the general procedure to furnish after 40 h the crude product as a 15:1 mixture of diastereoisomers; d.r. determined by integration of ^{1}H-NMR signal: δ_{major} 9.75 ppm (s), δ_{minor} 9.33 ppm (m). The title compound was isolated by flash column chromatography (Hexane/ethyl acetate, 7:1) in 96% yield and 98% e.e.. The e.e. value was determined by HPLC analysis on a Daicel Chiralpak IB column: 80:20 hexane/*i*PrOH, flow rate 1.00 mL/min, λ = 254 nm: τ_{major} = 8.37 min, τ_{minor} = 9.66 min.

$[\alpha]_{26}^{D}$= -92.84 (*c* = 0.81, $CHCl_3$).

HRMS *calc* for ($C_{35}H_{40}N_2O_8Na$): 639.2682 *found* 639.2700.

^{1}H NMR (400 MHz, $CDCl_3$): *δ* 9.75 (s, 1H), 8.21 (d, 1H, *J* = 8.51 Hz), 7.81 (d, 1H, *J* = 8.04 Hz), 7.31 (m, 1H), 7.21-7.14 (m, 2H), 7.06 (d, 1H, *J* = 8.04 Hz), 6.52 (s, 1H), 4.05-3.89 (m, 3H), 3.85 (d, 1H, *J* = 9.93 Hz), 3.65 (dd, 1H, *J* = 11.82, *J* = 6.62 Hz), 3.57 (dd, 1H, *J* = 18.91, *J* = 10.40 Hz), 3.38 (dd, 1H,

J = 18.91, *J* = 11.82 Hz), 2.61 (d, 1H, *J* = 19.38 Hz), 2.12 (s, 3H), 1.73 (s, 9H), 1.65 (s, 9H), 1.11 (s, 3H, *J* = 7.56) ppm. ^{13}C NMR (400 MHz, $CDCl_3$): δ 199.21, 177.78, 171.50, 150.48, 149.17, 137.36, 136.85, 133.72, 132.91, 130.82, 129.02, 127.78, 124.63, 123.60, 123.08, 117.74, 117.20, 115.99, 114.98, 84.52, 83.95, 61.37, 49.50, 45.81, 43.09, 35.21, 28.45, 28.22, 26.48, 21.51, 13.91 ppm.

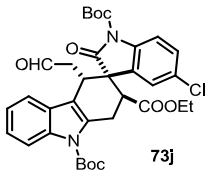

73j

(2*S*,3*S*,4*S*)-1',9-di-*tert*-butyl 2-ethyl 5'-chloro-2'-oxo-4-(2-oxoethyl)-1,2-dihydrospiro[carbazole3,3'-indoline]-1',2,9(4*H*)-tricarboxylate (73j)

The reaction was carried out following the general procedure to furnish after 24 h the crude product as a 15:1 mixture of diastereoisomers; d.r. determined by integration of ^{1}H-NMR signal:

δ_{major} 9.74 ppm (s), δ_{minor} 9.34 ppm (m). The title compound was isolated by flash column chromatography (Hexane/ethyl acetate, 6:1) in 89% yield and 96% e.e.. The e.e. value was determined by HPLC analysis on a Daicel Chiralpak IA column: 95:5 hexane/*i* rOH, flow rate 1.00 mL/min, λ = 254 nm: τ_{major} = 7.99 min, τ_{minor} = 5.91 min.

$[\alpha]_{26}^{D}$= -43.59 (*c* = 0.93, $CHCl_3$).

HRMS *calc* for ($C_{34}H_{37}ClN_2O_8Na$): 659.2136 *found* 659.2163.

^{1}H NMR (400 MHz, $CDCl_3$): δ 9.74 (s, 1H), 8.21 (d, 1H, *J* = 8.19 Hz), 7.92 (d, 1H, *J* = 9.01 Hz), 7.33 (m, 1H), 7.25 (m, 1H), 7.22-7.13 (m, 2H), 6.70 (d, 1H, *J* = 2.46 Hz), 4.07-3.94 (m, 3H), 3.85 (d, 1H, *J* = 9.93 Hz), 3.66 (dd, 1H, *J* = 11.88, *J* = 6.96 Hz), 3.54 (dd, 1H, *J* = 18.84, *J* = 10.24 Hz), 3.33 (dd, 1H, *J* = 18.84, *J* = 11.88 Hz), 2.64 (d, 1H, *J* = 19.25 Hz), 1.74 (s, 9H), 1.65 (s, 9H), 1.14 (s, 3H, *J* = 6.96) ppm. ^{13}C NMR (400 MHz, $CDCl_3$): δ 199.07, 177.07, 171.38, 150.40, 148.96, 138.49, 136.89, 132.70, 132.62, 130.31, 129.61, 128.57, 127.54, 124.88, 123.14, 117.60, 116.75, 116.46, 116.18, 84.71, 84.49, 61.59, 49.58, 45.71, 43.15, 34.96, 28.45, 28.18, 26.35, 13.97 ppm. **(2*S*,3*S*,4*S*)-9-*tert*-butyl 2-ethyl 5'-chloro-2'-oxo-4-(2-oxoethyl)-1,2-dihydrospiro[carbazole-3,3'indoline]-2,9(4*H*)-dicarboxylate (73k)**

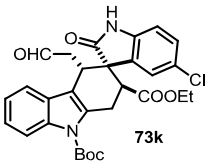

73k

The reaction was carried out following the general procedure to furnish after 72 h the crude product as a 8:1 mixture of diastereoisomers; d.r. determined by integration of ^{1}H-NMR signal: δ_{major} 9.76 ppm (s), δ_{minor} 9.36 ppm (m). The title compound was isolated by flash column chromatography (Hexane/ethyl acetate, 10:1) in 92% yield and 96%. The e.e. value was determined by HPLC analysis on a Daicel Chiralpak IA column: 80:20 hexane/*i* rOH, flow rate 1.00 mL/min, λ = 254 nm: τ_{major} = 14.20 min, τ_{minor} = 22.29 min.

$[\alpha]_{26}^{D}$= -38.04 (*c* = 1.00, $CHCl_3$).

HRMS *calc* for ($C_{29}H_{29}ClN_2O_6Na$): 559.1612 *found* 559.1599.

^{1}

H NMR (400 MHz, $CDCl_3$): δ 9.76 (s, 1H), 8.21 (d, 1H, *J* = 8.15 Hz), 8.07 (bs, 1H), 7.33 (m, 1H), 7.20 (d, 2H, *J* = 4.35 Hz), 7.16 (dd, 1H, *J* = 8.35, *J* = 2.02 Hz), 6.85 (d, 1H, *J* = 8.15 Hz), 6.67 (d, 1H, *J* = 2.02 Hz), 4.05 (m, 2H), 3.99-3.86 (m, 2H), 3.66-3.53 (m, 2H), 3.33 (dd, 1H, *J* = 19.23, *J* = 11.78 Hz), 2.64 (d, 1H, *J* = 19.23 Hz), 1.74 (s, 9H), 1.17 (s, 3H, *J* = 7.07) ppm. ^{13}C NMR (400 MHz, $CDCl_3$): δ 199.42, 180.05, 171.63, 150.44, 139.50, 136.80, 133.98, 132.72, 128.40, 127.67, 127.57, 124.81, 124.14, 123.15, 117.67, 117.22, 116.14, 110.97, 84.64, 61.44, 49.61, 45.37, 42.69, 34.39, 28.45, 26.52, 14.09 ppm.

(2*S*,3*S*,4*S*)-9-*tert*-butyl 2-ethyl 2'-oxo-4-(2-oxoethyl)-1,2-dihydrospiro[carbazole-3,3'-indoline]2,9(4*H*)-dicarboxylate (73l)

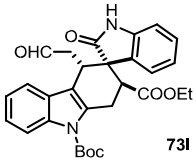

73l

The reaction was carried out following the general procedure to furnish after 72 h the crude product as a 9:1 mixture of diastereoisomers; d.r. determined by integration of ^{1}H-NMR signal: δ_{major} 9.79 ppm (s), δ_{minor} 9.22 ppm (m). The title compound was isolated by flash column chromatography (Hexane/ethyl acetate, 10:1) in 89% yield and 99% e.e.. The e.e. value was determined by HPLC analysis on a Daicel Chiralpak IA column: 80/20 hexane/*i*- rOH, flow rate 1.00 mL/min, λ = 254 nm: τ_{major} = 14.14 min, τ_{minor} = 15.80 min.

$[\alpha]_{26}^{D}$= -82.22 (*c* = 1.00, $CHCl_3$).

HRMS *calc* for ($C_{29}H_{30}N_2O_6Na$): 525.2002 *found* 525.1996.

^{1}H NMR (400 MHz, $CDCl_3$): δ 9.79 (s, 1H), 8.40 (bs, 1H), 8.21 (d, 1H, *J* = 8.29 Hz), 7.30 (m, 1H), 7.24-7.13 (m, 3H), 6.92 (d, 1H, *J* = 8.29 Hz), 6.77 (t, 1H, *J* = 7.46 Hz), 6.70 (d, 1H, *J* = 7.46 Hz), 4.04 (q, 2H, *J* = 7.39), 3.96-3.86 (m, 2H), 3.72-3.62 (m, 2H), 3.40 (dd, 1H, J = 19.13, J = 11.74 Hz), 2.60 (d, 1H, J = 18.70), 1.73 (s, 9H), 1.14 (t, 3H, *J* = 7.39 Hz) ppm. ^{13}C NMR (400 MHz, $CDCl_3$): δ 199.50, 180.50, 171.69, 150.44, 140.86, 136.68, 133.00, 132.15, 128.27, 127.77, 124.58, 123.83, 123.04, 122.42, 117.70, 117.65, 115.91, 110.11, 84.43, 61.21, 49.31, 45.39, 42.52, 34.60, 28.41, 26.75, 14.01 ppm.

(2*S*,3*S*,4*S*)-9-*tert*-butyl 2-ethyl 1'-benzyl-2'-oxo-4-(2-oxoethyl)-1,2-dihydrospiro[carbazole-3,3'indoline]-2,9(4*H*)-dicarboxylate (73m)

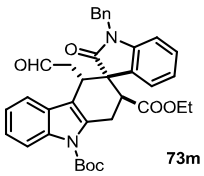

73m

The reaction was carried out following the general procedure to furnish after 40 h the crude product as a single diastereoisomer (d.r. >20:1). The title compound was isolated by flash column chromatography (Hexane/ethyl acetate, 10:1) in 97% yield and >99% e.e.. The e.e. value was determined by HPLC analysis on a Daicel Chiralpak IA column: 70:30 hexane/*i*- rOH, flow rate 1.00 mL/min, λ = 254 nm: τ_{major} = 13.71 min, τ_{minor} = 5.51 min.

$[\alpha]_{26}^{D}$= -70.78 (*c* = 1.00, $CHCl_3$).

HRMS *calc* for ($C_{36}H_{36}N_2O_6Na$): 615.2471 *found* 615.2494.

^{1}

H NMR (400 MHz, $CDCl_3$): δ 9.80 (s, 1H), 8.22 (d, 1H, *J* = 8.51 Hz), 7.46 (d, 2H, J = 7.61 Hz), 7.39 (t, 2H, 7.61 Hz), 7.34-7.27 (m, 2H), 7.24-7.17 (m, 2H), 7.10 (t, 1H, *J* = 7.54 Hz), 6.80-6.70 (m, 3H), 5.10 (d, 1H, *J* = 15.86 Hz), 4.80 (d, 1H, *J* = 15.86 Hz), 4.04-3.90 (m, 4H), 3.79-3.68 (m, 2H), 3.40 (dd, 1H, *J* = 19.04, *J* = 11.40 Hz), 2.61 (d, 1H, *J* = 19.04 Hz), 1.74 (s, 9H), 1.10 (t, 3H, *J* = 7.09 Hz) ppm. ^{13}C NMR (400 MHz, $CDCl_3$): δ 199.32, 178.57, 171.47, 150.39, 142.91, 136.56, 135.79, 132.94, 131.56, 128.71, 128.09, 127.68, 127.46, 127.42, 124.51, 123.47, 122.96, 122.44, 117.78, 117.65, 115.83, 109.54, 84.35, 61.01, 48.74, 45.39, 44.39, 42.66, 34.43, 28.33, 26.86, 14.01 ppm.

(2*S*,3*S*,4*S*)-9-*tert*-butyl 2-ethyl 1'-allyl-2'-oxo-4-(2-oxoethyl)-1,2-dihydrospiro[carbazole-3,3'indoline]-2,9(4*H*)-dicarboxylate (73n)

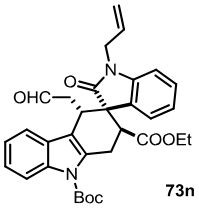

73n

The reaction was carried out following the general procedure to furnish after 40 h the crude product as a single diastereoisomer (d.r. >20:1). The title compound was isolated by flash column chromatography (Hexane/ethyl acetate, 10:1) in 92% yield and >99%. The e.e. value was determined by HPLC analysis on a Daicel Chiralpak IA column: 80:20 hexane/*i*- rOH, flow rate 1.00 mL/min, λ = 254 nm: τ_{major} = 8.68 min, τ_{minor} = 5.12 min. $[\alpha]_{26}^{D}$= -79.68 (*c* = 1.00, $CHCl_3$);

HRMS *calc* for ($C_{32}H_{34}N_2O_6Na$): 565.2315 *found* 565.2336.

^{1}H NMR (400 MHz, $CDCl_3$): δ 9.76 (s, 1H), 8.21 (d, 1H, *J* = 8.30 Hz), 7.30 (m, 1H), 7.23-7.15 (m, 3H), 6.90 (d, 1H, J = 7.91 Hz), 6.79 (t, 1H, *J* = 7.51 Hz), 6.73 (d, 1H, J = 7.51 Hz), 5.91 (m, 1H), 5.41 (d, 1H, *J* = 17.39 Hz), 5.29 (d, 1H, *J* = 10.28 Hz), 4.48 (m, 1H), 4.22 (dd, 1H, *J* = 16.21, *J* = 5.53 Hz), 4.00 (m, 2H), 3.91 (dd, 1H, *J* = 18.58, *J* = 6.72 Hz), 3.83 (d, 1H, *J* = 10.28 Hz), 3.71-3.62 (m, 2H), 3.38 (dd, 1H, *J* = 18.58, *J* = 11.56 Hz), 2.56 (d, 1H, *J* = 18.58 Hz), 1.73 (s, 9H), 1.12 (t, 3H, *J* = 7.12 Hz) ppm. ^{13}C NMR (400 MHz, $CDCl_3$): δ 199.27, 178.21, 171.52, 150.48, 142.97, 136.70, 133.07, 131.93, 137.76, 128.16, 127.81, 124.58, 123.51, 123.04, 122.44, 117.87, 117.80, 117.71, 115.93, 109.33, 84.42, 61.05, 48.79, 45.41, 42.89, 42.58, 34.63, 28.43, 26.90, 14.12 ppm. **(2*S*,3*S*,4*S*)-1'-benzyl 9-tert-butyl 2-ethyl 2'-oxo-4-(2-oxoethyl)-1,2-dihydrospiro[carbazole-3,3'indoline]-1',2,9(4*H*)-tricarboxylate (73o)**

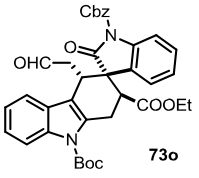

73o

The reaction was carried out following the general procedure to furnish after 24 h the crude product as a 9:1 mixture of diastereoisomers; d.r. determined by integration of ^{1}H-NMR signal: δ_{major} 9.75 ppm (s), δ_{minor} 9.22 ppm (m). The title compound was isolated by flash column chromatography (Hexane/ethyl acetate, 8:1-5:1) in 85% yield and 98% e.e.. The e.e. value was determined by HPLC analysis on a Daicel Chiralpak IA column: 95:5 hexane/*i*-PrOH, flow rate 1.00 mL/min, λ = 254 nm: τ_{major} = 38.65 min, τ_{minor} = 18.93 min.

$[\alpha]_{26}^{D}$= -51.9 (*c* = 0.91, CHCl3).

HRMS *calc* for ($C_{37}H_{36}N_2O_8Na$): 659.2369 *found* 659.2399.

^{1}H NMR (400 MHz, $CDCl_3$): δ 9.75 (s, 1H), 8.21 (d, 1H, *J* = 8.46 Hz), 8.00 (d, 1H, *J* = 8.46 Hz), 7.51 (m, 2H), 7.45-7.24 (m, 5H), 7.20-7.13 (m, 2H) 6.91 (t, 1H, *J* = 7.53), 6.73 (d, 1H, J = 7.53), 5.47 (d, 1H, *J* = 4.08), 4.02-3.91 (m, 3H), 3.88 (d, 1H, *J* = 9.69 Hz), 3.70 (dd, 1H, *J* = 11.73, *J* = 6.63 Hz), 3.60 (dd, 1H, *J* = 18.87, *J* = 10.20 Hz), 3.37 (dd, 1H, *J* = 19.38, *J* = 11.73 Hz), 2.60 (d, 1H, *J* = 19.38 Hz), 1.73 (s, 9H), 1.05 (s, 3H, *J* = 7.05) ppm. ^{13}C NMR (400 MHz, $CDCl_3$): δ 199.37, 177.56, 171.45, 150.78, 150.42, 139.36, 136.80, 135.38, 132.89, 130.86, 128.81, 128.70, 128.64, 128.37, 127.97, 127.67, 124.76, 123.15, 123.11, 117.65, 117.06, 116.00, 115.40, 84.60, 68.60, 61.49, 49.44, 45.76, 43.38, 35.08, 28.44, 26.55, 13.89 ppm.

(2*S*,3*S*,4*S*)-1',9-di-*tert*-butyl 2-ethyl 6-methoxy-2'-oxo-4-(2-oxoethyl)-1,2dihydrospiro[carbazole-3,3'-indoline]-1',2,9(4*H*)-tricarboxylate (73p)

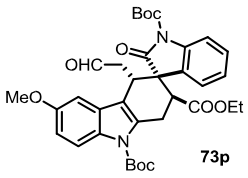

73p

The reaction was carried out following the general procedure to furnish after 24 h the crude product as a single diastereoisomer (d.r. >20:1). The title compound was isolated by flash column chromatography (Hexane/ethyl acetate, 6:1-4:1) in 94% yield and 98% e.e.. The e.e. value was determined by HPLC analysis on a Daicel Chiralpak IA column: 90:10 hexane/*i*- rOH, flow rate 1.00 mL/min, λ = 254 nm: τ_{major} = 7.97 min, τ_{minor} = 5.52 min.

$[\alpha]_{26}^{D}$= - 30.8 (*c* = 0.73, CHCl3).

HRMS *calc* for ($C_{35}H_{40}N_2O_9Na$): 655.2632 *found* 655.2662.

^{1}H NMR (400 MHz, $CDCl_3$): δ 9.74 (s, 1H), 8.08 (d, 1H, *J* = 9.33 Hz), 7.93 (d, 1H, *J* = 8.20 Hz), 7.26 (m, 1H), 6.91-6.85 (m, 2H), 6.71 (d, 1H, *J* = 7.63 Hz) 6.58 (d, 1H, *J* = 2.54), 4.03-3.87 (m, 3H), 3.823.72 (m, 4H), 3.68 (dd, 1H, *J* = 11.61, *J* = 6.91 Hz), 3.58 (dd, 1H, *J* = 18.52, *J* = 9.73 Hz), 3.33 (dd, 1H, *J* = 19.15, *J* = 11.61 Hz), 2.60 (d, 1H, *J* = 19.15 Hz), 1.71 (s, 9H), 1.65 (s, 9H), 1.10 (s, 3H, *J* = 6.91) ppm. ^{13}C NMR (400 MHz, $CDCl_3$): δ 199.35, 177.65, 171.50, 156.18, 150.37, 149.14, 139.73, 133.55, 131.32, 130.82, 128.57, 128.45, 124.37, 123.07, 117.00, 116.78, 115.22, 112.93, 110.56, 84.37, 84.16, 61.41, 55.77, 49.45, 45.62, 43.00, 35.17, 28.45, 28.21, 26.65, 13.92 ppm.

(3'*S*,4*S*,6*S*)-1-*tert*-butyl 6-ethyl 1'-allyl-2'-oxo-4-(2-oxoethyl)-2-phenyl-6,7-dihydrospiro[indole5,3'-indoline]-1,6(4*H*)-dicarboxylate (74)

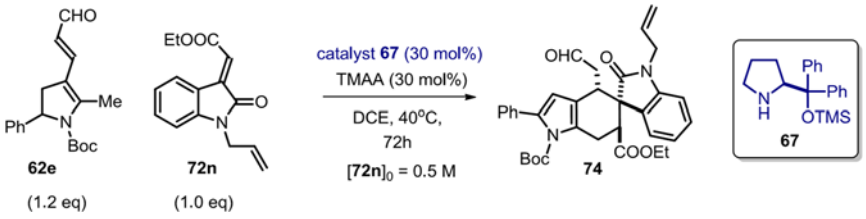

The reaction was carried out following the general procedure to furnish after 72 h (40 °C) the crude product as a 2.1:1 mixture of diastereoisomers; dr determined by integration of ^{1}H-NMR signal: δ_{major} 9.71 ppm (s), δ_{minor} 9.55 ppm (m). The title compound was isolated by flash column chromatography (Hexane/ethyl acetate, 8:1-5:1) in 76% yield and 96% ee. The ee value was determined by HPLC analysis on a Daicel Chiralpak IA column: 85:15 hexane/*i*-PrOH, flow rate 1.00 mL/min, λ = 254 nm: τ_{major} = 8.96 min, τ_{minor} = 6.31 min.

$[\alpha]_{26}^{D}$= -59.6 (*c* = 1.0, CHCl3).

^{1}H NMR (400 MHz, $CDCl_3$): δ 9.71 (s, 1H), 7.36-7.28 (m, 5H), 7.23 (m, 1H), 6.93-6.83 (m, 3H), 5.93-5.82 (m, 2H), 5.36 (dd, 1H, *J* = 17.25, *J* = 1.23 Hz) 5.25 (dd, 1H, *J* = 10.33, *J* = 1.23 Hz), 4.464.38 (m, 1H), 4.24 (ddt, 1H, J = 16.28, J = 5.58, J = 1.5 Hz), 4.05-3.93 (m, 2H), 3.72-3.43 (m, 4H), 3.24 (dd, 1H, *J* = 18.19, *J* = 11.33 Hz), 2.52 (dd, 1H, *J* = 18.19, *J* = 4.02 Hz), 1.32 (s, 9H), 1.11 (s, 3H, *J* = 7.15) ppm. ^{13}C NMR (400 MHz, $CDCl_3$): δ 199.73, 178.26, 171.87, 149.91, 142.93, 136.11, 134.83, 131.94, 128.74, 128.55, 128.12, 127.87, 127.23, 123.82, 122.55, 122.45, 117.79, 112.94, 109.24, 84.13, 60.98, 49.58, 47.30, 42.82, 42.61, 36.01, 27.61, 26.05, 14.12 ppm.

(3'*S*,4*S*,6*S*)-ethyl 1'-benzyl-2'-oxo-4-(2-oxoethyl)-6,7-dihydro-4H-spiro[benzofuran-5,3'indoline]-6-carboxylate (75)

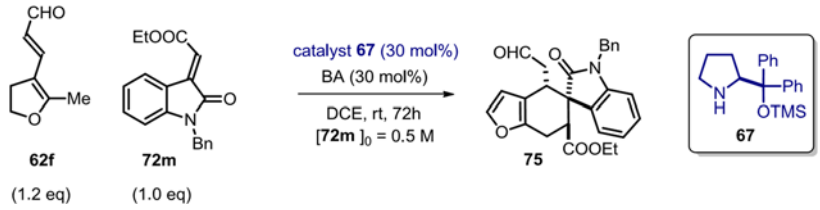

The reaction was carried out following the general procedure to furnish after 72 h the crude product as a 6.9:1 mixture of diastereoisomers; dr determined by integration of ^{1}H-NMR signal: δ_{major} 9.73 ppm (s), δ_{minor} 9.55 ppm (m). The title compound was isolated by flash column chromatography (Hexane/ethyl acetate, 10:1) in 86% yield and 91% ee. The ee value was determined by HPLC analysis on a Daicel Chiralpak IA column: 70:30 hexane/*i*-PrOH, flow rate 1.00 mL/min, λ = 254 nm: τ_{major} = 15.41 min, τ_{minor} = 10.13 min.

$[\alpha]_{26}^{D}$= -33.4 (*c* = 1.0, CHCl3).

^{1}H NMR (400 MHz, $CDCl_3$): δ 9.73 (s, 1H), 7.42-7.31 (m, 5H), 7.30-7.24 (m, 1H), 7.13 (t, 1H, *J* = 7.72 Hz), 6.84 (t, 1H, *J* = 7.72 Hz), 6.70 (m, 2H) 6.16 (d, 1H, *J* = 1.80), 5.02 (d, 1H, J = 15.80 Hz), 4.80 (d, 1H, J = 15.80 Hz), 4.01-3.89 (m, 2H), 3.65-3.47 (m, 3H), 3.36 (dd, 1H, *J* = 17.34, *J* = 6.68 Hz), 3.07 (dd, 1H, *J* = 17.34, *J* = 11.30 Hz), 2.52 (dd, 1H, *J* = 16.70, *J* = 2.83 Hz), 1.05 (s, 3H, *J* = 7.06) ppm. ^{13}C NMR (400 MHz, $CDCl_3$): δ 199.69, 178.22, 171.38, 147.73, 142.94, 142.58, 135.89, 131.59, 128.82, 128.33, 127.62, 127.50, 123.66, 122.57, 119.51, 110.17, 109.60, 61.15,

50.23, 46.91, 44.39, 42.61, 35.61, 24.37, 14.04 ppm.

Table 6. Results using catalyst ***ent*-67** to obtain the opposite enantiomer of the product (***ent*-73**)

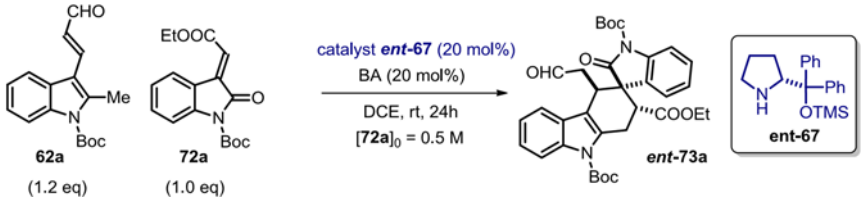

Entry	**73**	Yield (%)[b]	dr (%)[c]	*ee* (%)[d]
1	**ent-a**	93	>20:1	97
2	**ent-b**	94	>20:1	98
3	**ent-f**	45	>20:1	96
4	**ent-g**	72	10:1	96
5	**ent-h**	30	5:1	96(94)
6	**ent-h'**	26	1	98
7	**ent-i**	91	15:1	98
8	**ent-j**	82	15:1	96
9	**ent-k**	83	9:1	98
10	**ent-l**	89	>20:1	98

[a] Reactions were carried out on a 0.1 mmol scale, [**72**]$_0$ = 0.5 M in toluene. [b] Yields of isolated products [c] Diastereomeric ratios (dr) were determined by means of ^{1}H NMR analysis of the crude mixture. [d] Enantiomeric excess (*ee*) values were determined on commercially available chiral stationary phases.

2.8.5 Single Crystal X-ray Diffraction Data for Compounds 76 and 77

X-ray structure determinations: Crystals of **76** were obtained from hexane-DCM by slow evaporation of DCM at room temperature. The measured crystals were stable under atmosphere conditions.

Data Collection. Measurements were made on a Bruker-Nonius diffractometer equipped with an APPEX 2 4K CCD area detector, a FR591 rotating anode with Mo radiation, Montel mirrors and a Cryostream Plus low temperature device (*T* = -173 ˚C). Full-sphere data collection was used and scans.

Programs used: Data collection Apex2 V2010 7.0 (Bruker-Nonius 2008), data reduction Saint + Version 7.60A (Bruker AXS 2008) and absorption correction SADABS.

Structure Solution. SIR2007 program was used.[73]

Structure Refinement. SHELXTL-97.[49]

---

[73] R.Caliandro, B. Carrozzini, G.L.Cascarano, L. De Caro, C. Giacovazzo and D. Siliqi. Advances in ab Initio Protein Phasing by Patterson Deconvolution Techniques *J. Appl. Cryst.* **2007**, *40*, 883. [49] G.M. Sheldrick. A Short History of SHELX. *Acta Crys.* **2008**, A64, 112.

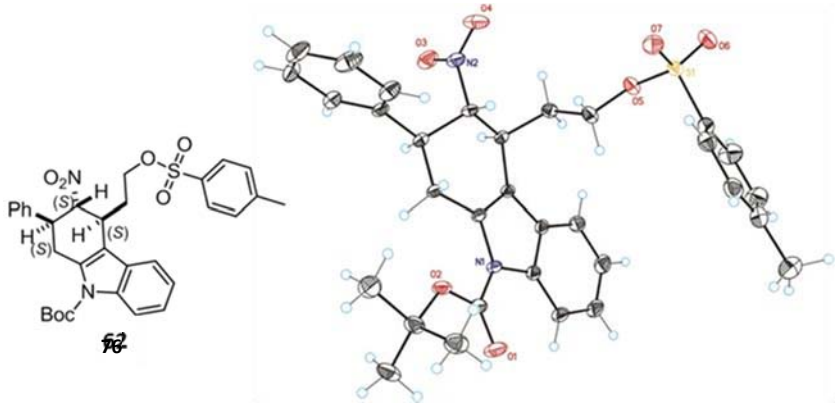

X-ray structure determinations: Crystals of **77** were obtained from hexane-diethyl ether by slow evaporation of diethyl ether at room temperature. The measured crystals were stable under atmosphere conditions.

Data Collection. Measurements were made on a Bruker-Nonius diffractometer equipped with an APPEX 2 4K CCD area detector, a FR591 rotating anode with $Mo_{K\square}$ radiation, Montel mirrors and a Cryostream Plus low temperature device (*T* = 100K). Full-sphere data collection was used with □ and □ scans.

Programs used: Data collection Apex2 V2009.11 (Bruker-Nonius 2008), data reduction Saint + Version 7.60A (Bruker AXS 2008) and absorption correction TWINABS V. 2008-1 (2008).

Structure Solution. SIR2008

Structure Refinement. SHELXTL V6.14

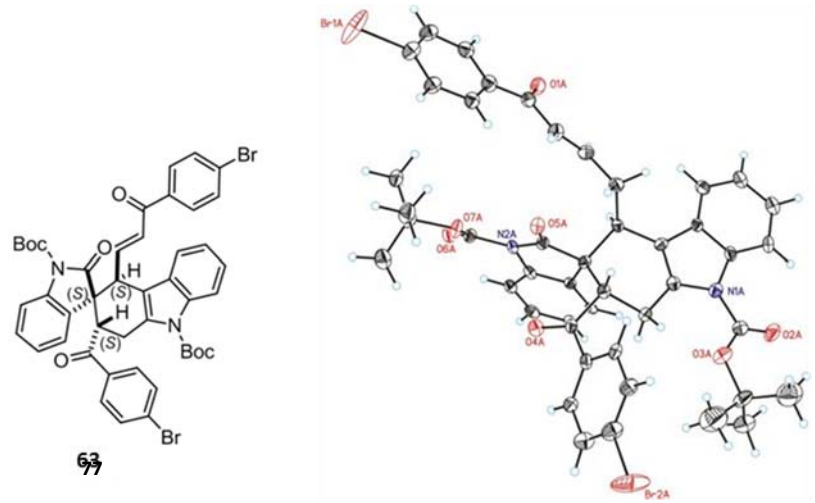

Crystal data for **77** at 100 K: CCDC 831383

Chapter III Multicatalytic Asymmetric Synthesis of Complex Tetrahydrocarbazoles via the Combination of Aminocatalysis and NHC Catalysis

Target

Enantioselective synthesis of polycyclic complex structures *via* a Diels-Alder/benzoin condensation tandem sequence.

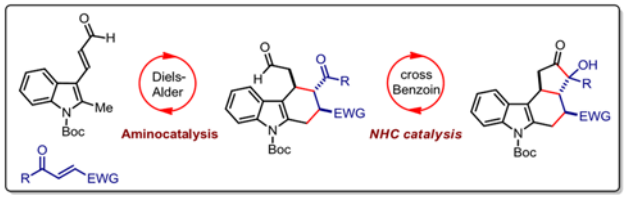

Tool

Ability of trienamine activation to *in situ* generate *ortho*-quinodimethane (*o*-QDMs) intermediates, followed by the umpolung activation of carbonyl compounds with *N*-heterocyclic carbenes (NHCs) *via* the transient formation of the Breslow intermediate.[74]

One of the main advantages of aminocatalysis is the high tolerance to different reaction conditions, allowing the combination with others organocatalytic activation modes. Among the reported approaches, the combined use of chiral secondary amines and *N*-heterocyclic carbenes (NHC) has shown great potential for the construction of complex molecular skeletons. While aminocatalysis induces the classical reactivity of carbonyl compounds, NHC catalysis allows the umpolung activation of the carbonyl group favoring the formation of the well-known Breslow intermediate.[75] Introduced to chemistry by Wittig *et al.* in 1951,[76] the word "umpolung" was then popularized by Seebach,[77] who described with it the synthetic equivalence of dithianes with acyl anions (Scheme 1). [78] Encompassing other seminal works by Eschenmoser [79], Stork and

[74] The work discussed in this chapter has been published, see: Y. Liu, M. Nappi, E. C. Escudero-Adán, P. Melchiorre. Multicatalytic Asymmetric Synthesis of Complex Tetrahydrocarbazoles via a Diels-Alder Benzoin Reaction Sequence. *Org. Lett.* **2012**, *14*, 1310. Experimental part developed together with Y. Liu.
[75] R. Breslow. On the Mechanism of Thiamine Action. IV. Evidence from Studies on Model Systems. *J. Am. Chem. Soc.* **1958**, *80*, 3719.
[76] G. Wittig, P. Davis, G. Koenig Phenanthrensynthesen über intraionische Isomerisationen. *Chem. Ber.* **1951**, *84*, 627.
[77] First used by Dieter Seebach at a lecture, given in the University of Hamburg, July 7th, **1972**.
[78] E. J. Corey, D. Seebach. Carbanions of 1,3-Dithianes. Reagents for C-C Bond Formation by Nucleophilic Displacement and Carbonyl Addition. *Angew. Chem., Int. Ed. Engl.* **1965**, *4*, 1075.
[79] J. Schreiber, M. Pesaro, W. Leimgruber, A. Eschenmoser. Über eine neue Bildungsweise des Troponsystems. Vorläufige Mitteilung. *Helv. Chim. Acta* **1958**, *41*, 2103.

Maldonado,[80] the term umpolung now refers to a powerful strategy in organic synthesis that consists in the inversion of the innate reactivity of a functional group.[81]

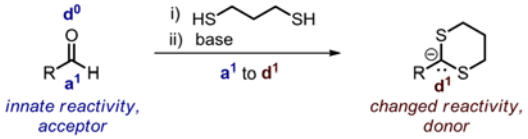

Scheme 1. Umpolung reactivity. a = acceptor carbon; d = donor carbon

The presence of lone pairs on heteroatoms, such as nitrogen and oxygen, offers them the possibility of donating electrons. As a consequence, the successive atoms of the skeleton of the initial molecule are alternatively defined as being donor (d^{2n}) and acceptor (a^{2n+1}) positions. Any process that enables the interchange of this normal reactivity falls under the definition of umpolung reactivity.[82] Since *N*-heterocyclic carbenes (NHC) chemistry is a useful and established strategy to induce umpolung reactivity of carbonyl compounds, part of the history that led to the discovery of the key Breslow intermediate and some basic principles on the reactivity and stability of NHC intermediates will be discussed in the next section.

3.1 N-Heterocyclic Carbenes

Nature was the main inspiration for the development of the *N*-heterocyclic carbenes chemistry. In 1936, Williams discovered and elucidated the structure of thiamin (vitamin B1) and thiamin diphosphate (TDP). [83] In 1937, Lohmann and Schuster established that the coenzyme "cocarboxylase" in pyruvate decarboxylase is TD (Scheme 2).[84] Decarboxylation of pyruvate is a common primary metabolic process whose outcome amounts to electrophilic substitution on acyl carbanion synthon **1**.[85]

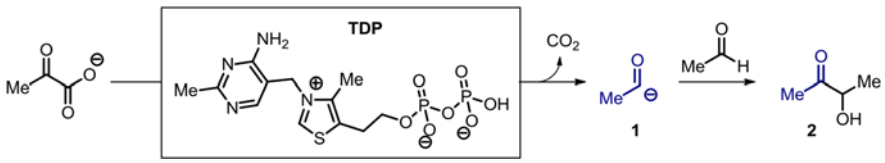

[80] G. Stork and L. Maldonado. Anions of protected cyanohydrins as acyl carbanion equivalents and their use in a new synthesis of ketones. *J. Am. Chem. Soc.* **1971**, *93*, 5286.
[81] The late 1960's and early 1970's have been an important time for the theorization of the strategies used in organic synthesis. For a timeless account see: E. J. Corey. General Methods for the Construction of Complex Molecules. *Pure Appl. Chem.* **1967**, *14*, 19.
[82] a) B.-T. Gröbel, D. Seebach. Umpolung of the Reactivity of Carbonyl Compounds Through SulfurContaining Reagents. *Synthesis* **1977**, 357; b) D. Seebach. Methods of Reactivity Umpolung. *Angew. Chem., Int. Ed. Engl.* **1979**, *18*, 239.
[83] a) R. R.Williams. Structure of Vitamin B. *J. Am. Chem. Soc.* **1935**, *57*, 229. b) R. R.Williams. Structure of Vitamin B1. *J. Am. Chem. Soc.* **1936**, *58*, 1063.
[84] a) K. Lohmann, P. Schuster. *Biochem. Z.* **1937**, *294*, 188. b) K. Lohmann, P. Schuster. *Naturwissenschaften* **1937**, *25*, 26.
[85] R. Kluger, K. Tittmann. Thiamin Diphosphate Catalysis: Enzymic and Nonenzymic Covalent Intermediates. *Chem. Rev.* **2008**, *108*, 1797.

Scheme 2. TDP is responsible for the production of acyl carbanion equivalents in biological processes.

In 1943, Ugai demonstrated for the first time that thiamin **3**, derived from TDP, and other thiazolium compounds could promote the α-condensation of an aldehyde to produce αhydroxyketones **4** (Scheme 3).[86] The reaction was reminiscent of the formation of acetoin **2** (Scheme 2) in the enzymatic decarboxylation of pyruvate catalyzed by TDP, suggesting the intermediacy of a common acetyl carbanion intermediate.

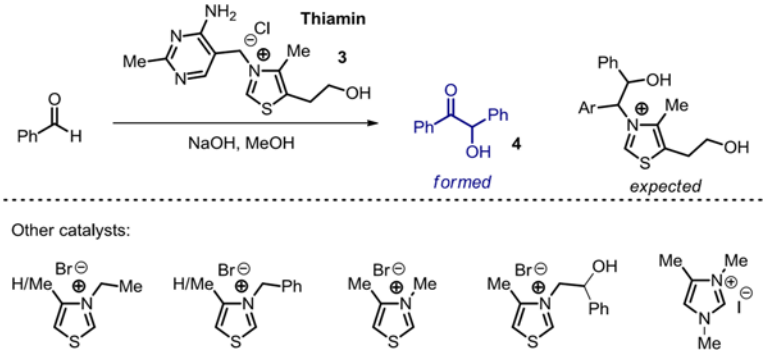

Scheme 3. Thiamin and thiazolium compounds can catalyze the benzoin condensation.

In 1958, Breslow proposed the modern and accepted mechanism of the benzoin condensation catalyzed by thiamin and derivatives (Scheme 4).[1] The ylide or carbene **5** is formed under basic conditions; after nucleophilic attack of **5** to benzaldehyde, the zwitterionic intermediate **6** is generated. A protonation and deprotonation sequence provided the famous "Breslow intermediate" **7**, which is a formal nucleophilic enolamine that reacts with the second equivalent of benzaldehyde to give **8**. The intermediate **8** then rearranges to yield the benzoin product **4** and the ylide **5**, which can restart another catalytic cycle.

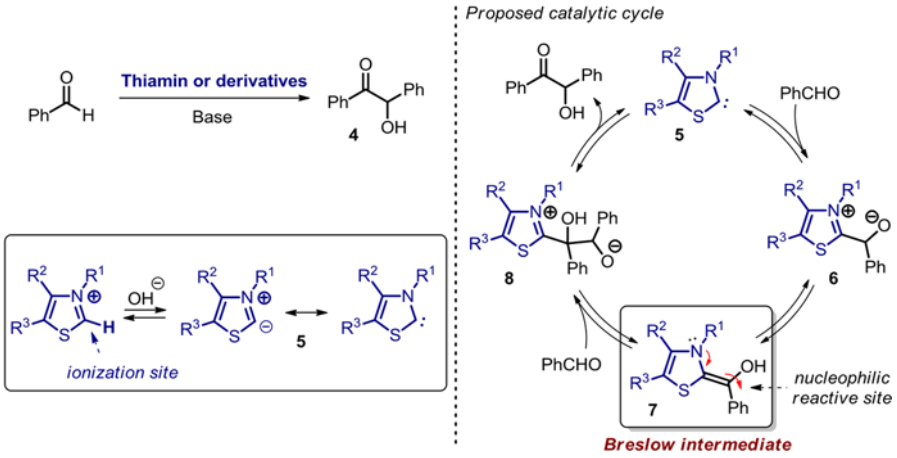

[86] T. Ugai, R. Tanaka, T. Dokawa. *J. Pharm. Soc. Jpn.* **1943**, *63*, 296.

Scheme 4. Accepted mechanism of the benzoin condensation via the Breslow intermediate **7**.

After the seminal work of Breslow, the chemical community accepted carbenes as highly reactive intermediates and chemists tried to isolated them.

The first carbenes ever isolated were into metal complexes of mercury and chromium, reported by Wanzlick and Öfele in 1968 (Scheme 5).[87]

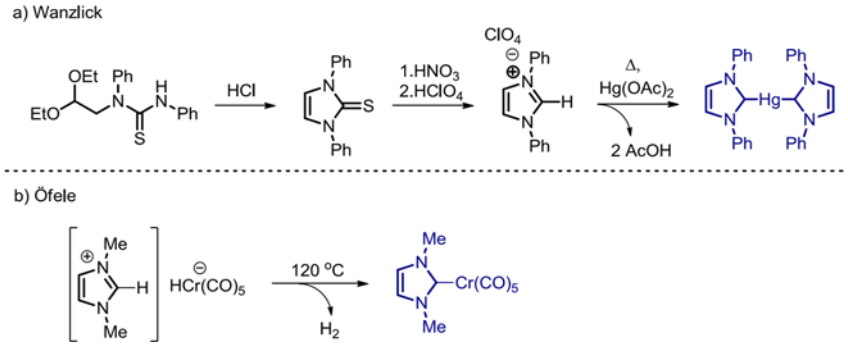

Scheme 5. Synthesis and isolation of carbenes as lingands in metal complexes.

Nevertheless, only in 1991 Arduengo isolated a stable carbene.[88] The major problem was the dimerization occurring as soon as the carbene was formed. Arduengo solved this issue synthesizing a precursor **9** which contained two adamantyl groups; in this manner, when carbene **10** was generated, the dimerization was hindered by the strong steric congestion (Scheme 6). Following this first example, other carbenes have been successfully isolated.[16]

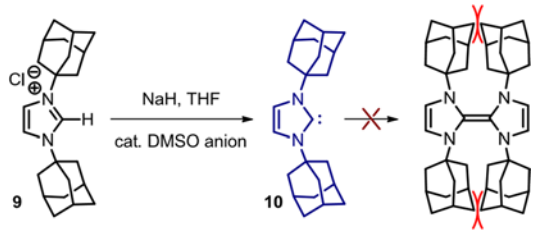

Scheme 6. The first isolated stable carbene.

As for the reactivity, NHC have found different application in asymmetric catalysis. Singlet carbenes are exceptionally good σ donors and can form strong metal–carbon bonds giving much more stable and active complexes compared to those containing phosphines. Moreover, singlet carbenes of NHCs are distinct Lewis bases that show both σ basicity and π acidity allowing for the

[87] a) H.-W.Wanzlick,, H.-J. Schönherr. Direct Synthesis of a Mercury Salt-Carbene Complex. *Angew. Chem. Int. Ed.* **1968**, *7*, 141. b) K. Öfele. 1,3-Dimethyl-4-imidazolinyliden-(2)-pentacarbonylchrom ein neuer übergangsmetall-carben-komplex. *J. Organomet. Chem.* **1968**, *12*, 42.
[88] A. J. Arduengo III, R. Harlow, M. Kline. A Stable Crystalline Carbene. *J. Am. Chem. Soc.* **1991**, *113*, 361. [16] D. Bourissou, O. Guerret, F. P. Gabbai, G. Bertrand. Stable Carbenes. *Chem. Rev.* **2000**, *100*, 39.

generation of a nucleophilic intermediate (*i.e.* the Breslow intermediate). This unique ability allows NHCs to act as powerful organocatalysts.

3.2 NHCs as Organocatalysts in Benzoin Condensation

The first application of NHCs as organocatalysts was the benzoin condensation catalyzed by thiamin derivatives, reported by Ugai in 1943 (Scheme 3). In 1974, Sheenan achieved for the first time the benzoin product **4** with moderate enantioselectivity, though low yield was obtained using the chiral carbene precursor **11** (Scheme 7).[89]

Scheme 7. First enantioselective benzoin condensation.

In 1998, Leeper and coworkers designed a new chiral carbene catalyst based on a byclic triazolium scaffold (**12** and **13**) that allowed to reach high enantioselectivity (80% *ee*) with moderate yield (45%, Scheme 8).[90]

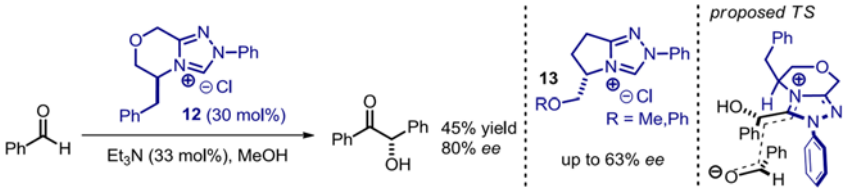

Scheme 8. Chiral byclic asymmetric triazolium carbenes introduced by Leeper.

In the proposed transition state, the benzyl group shields the upper face of the Breslow intermediate, forcing the aldehyde to approach from the lower face. Calculations suggest that the favoured approach of the aldehyde is *anti* to the enolamine with the phenyl group in the opposite side of the perpendicular *N*-aromatic ring of the catalyst.

This study prompted many research groups to design other chiral byclic triazolium carbenes. A highly efficient NHC catalytic system was designed by Enders and coworkers in 2002, using an evolution of the Leeper scaffold **13**.[91] The carbene precursor **14** was employed in 10 mol% to give the benzoin product **4** with 83% of yield and 90% of enantioselectivity (Scheme 9).

---

[89] J. C. Sheehan, T. Hara. Asymmetric Thiazolium Salt Catalysis of the Benzoin Condensation. *J. Org. Chem* **1974**, *39*, 1196.

[90] R. L.Knight, F. J. Leeper. Comparison of Chiral Thiazolium and Triazolium Salts as Asymmetric Catalysts for the Benzoin Condensation. *J. Chem. Soc., Perkin Trans. 1* **1998**, 1891.

[91] D .Enders, U. Kallfass. An Efficient Nucleophilic Carbene Catalyst for the Asymmetric Benzoin Condensation. *Angew. Chem. Int. Ed.* **2002**, *41*, 1743.

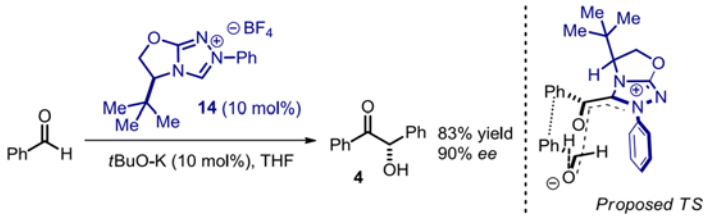

Scheme 9. Highly efficient asymmetric benzoin condensation.

In the proposed transition state, the *Si*-face of the nucleophilic intermediate is sterically shielded by the *tert*-butyl group of the bicyclic catalyst. Accordingly, the aldehyde molecule would attack the Breslow intermediate at its *Re*-face.

In 2009, Connon demonstrated that the NHC **15**, bearing alcohol directing groups, exert exceptional levels of enantioinduction (Scheme 10).[92] Remarkably, an electron-withdrawing *N*substituent in the catalyst was necessary to obtain high yield of the benzoin **4**.

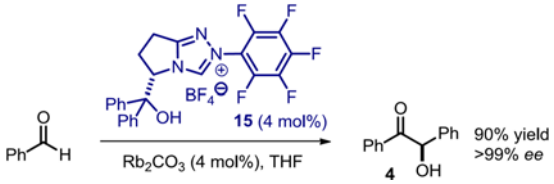

Scheme 10. Best results achieved with NHCs in asymmetric benzoin condensation.

In the same year, capitalizing upon the high tolerance to various reaction conditions and the robustness of chiral secondary amines, Rovis coupled aminocatalysis with *N*-heterocyclic carbenes for the asymmetric synthesis of cyclopentanones **20** (Scheme 11).[93] The condensation of the chiral secondary amine **18** with the α,β-unsaturated aldehyde **16** led to the formation of the iminium ion **21**. This activated electrophile was attacked by a malonate derivative **17** *via* a Michael addition to yield the aldehyde **23** after the hydrolysis of the corresponding iminium ion **22**. Amine **18** returned to the aminocatalytic cycle while the aldehyde **23** generated the Breslow intermediate **24** upon nucleophilic addition of the carbene **19'** (generated under basic conditions from **19**).

[92] L. Baragwanath, C. A. Rose, K. Zeitler, S. J. Connon. Highly Enantioselective Benzoin Condensation Reactions Involving a Bifunctional Protic Pentafluorophenyl-Substituted Triazolium Precatalyst. *J. Org. Chem.* **2009**, *74*, 9214.
[93] S. P. Lathrop, T. Rovis. Asymmetric Synthesis of Functionalized Cyclopentanones via a Multicatalytic Secondary Amine/N-Heterocyclic Carbene Catalyzed Cascade Sequence. *J. Am. Chem. Soc.* **2009**, 131, 13628.

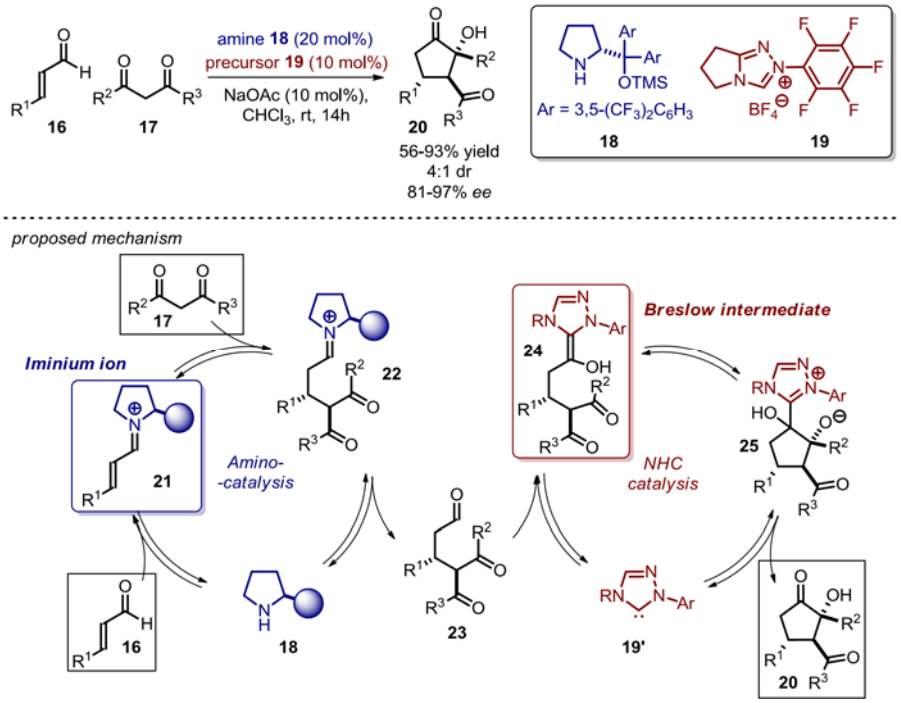

Scheme 11. Synthesis of cyclopentanones via the merger of NHCs catalysis and aminocatalysis.

The resulting intramolecular benzoin condensation led to the intermediate **25**, which consequently released the cyclopentanone **20** and the carbene **19'** through a protonationdeprotonation processes. Notably, the stepwise procedure (isolation of aldehyde **23** and addition of precursor **19**) afforded the cyclopentanone **20** in a modest 46% yield (93% yield using the cascade sequence) with a lower enantioselectivity than the cascade procedure (58% vs 86% *ee*). These results indicated a synergistic correlation between the two catalysts, which function more efficiently in the presence of each other than they do independently.

After the seminal work of Rovis, the groups of Enders and Jørgensen expanded the scope of the NHC-aminocatalytic sequence to other classes of nucleophiles such as (phenylsulfonyl)ketones **26**, showing the synthetic utility and the power of the merged methodologies (Scheme 12).[94]

[94] a) D. Enders, A. Grossmann, H. Huang, G. Raabe. Dual Secondary Amine/N-Heterocyclic Carbene Catalysis in the Asymmetric Michael/Cross-Benzoin Cascade eaction of β-Oxo Sulfones with Enals. *Eur. J. Org. Chem.* **2011**, 4298. b) C. B. Jacobsen, K. L. Jensen, J. Udmark, K. A. Jørgensen. Organocatalytic Iminium Ion/Carbene Reaction Cascade for the Formation of Optically Active 2,4-Disubstituted Cyclopentenones. *Org. Lett.* **2011**, *13*, 4790.

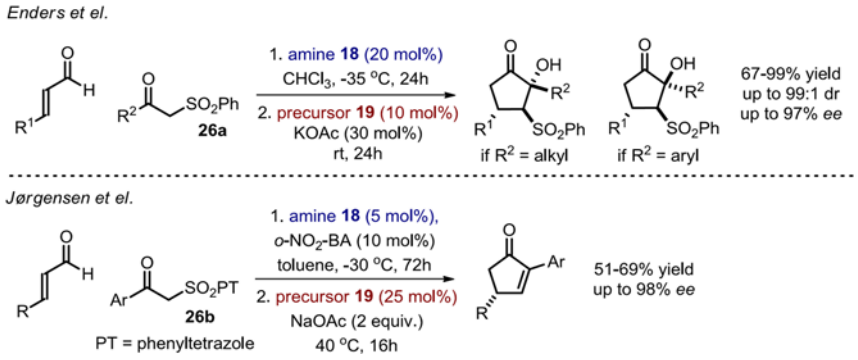

Scheme 12. Further expansion of the iminium ion/carbene catalysis sequence.

In 2011, Rovis extended the strategy to also merge enamine activation and NHCs. An enamine/carbene cascade reaction was engineered for the diastereo- and enantioselective synthesis of functionalized cyclopentanones **30** (Scheme 13).[95] Key to this new methodology was the use of highly reactive electrophiles **27** which were attacked by the enamine **31** to form the new aldehyde **32**.

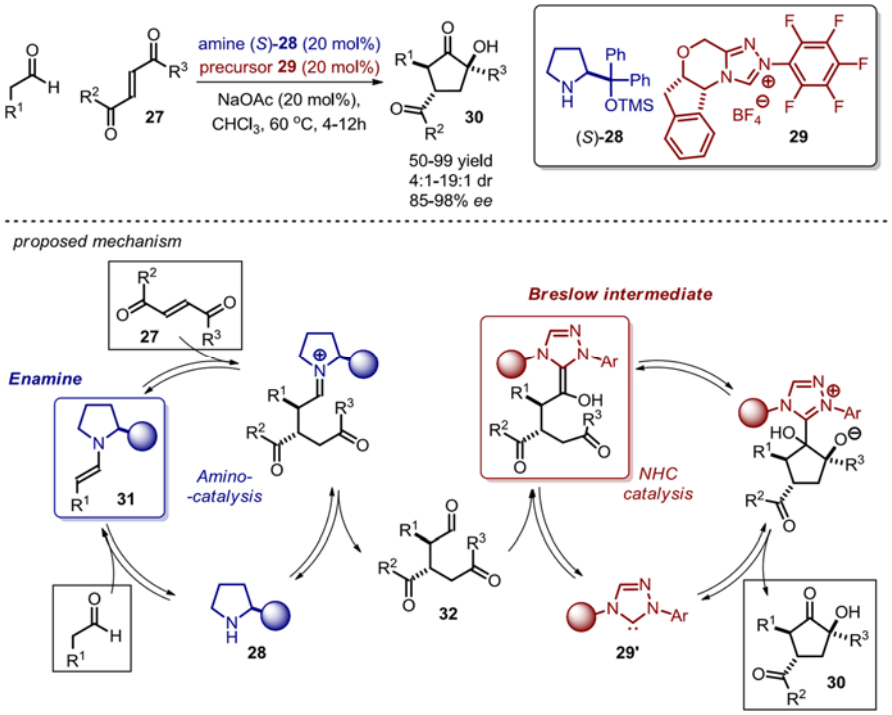

Scheme 13. Enamine/carbene cascade reaction for the asymmetric synthesis of cyclopentanones.

[95] K. E. Ozboya, T. Rovis. Enamine/Carbene Cascade Catalysis in the Diastereo- and Enantioselective Synthesis of Functionalized Cyclopentanones. *Chem. Sci.* **2011**, *2*, 1835.

This intermediate underwent an intramolecular benzoin condensation catalyzed by the chiral carbene **29'**. The use of the catalyst **29** was necessary to achieve good diastereoselectivity. Also in this case, the authors showed that the cascade procedure gave better results than the stepwise procedure in term of diastereoselectivity.

3.3 Target of the Research Project

Inspired by these precedents, we evaluated the possibility to couple our asymmetric Diels-Alder reaction strategy, discussed in Chapter II of this thesis, with NHC catalysis. Recognition of the directness and versatility of the aminocatalytic indole-2,3-quinodimethane strategy for the stereocontrolled annulations of indole systems prompted us to further investigate its synthetic potential. In particular, we wondered if the complexity-generating power of the chemistry could be further expanded by integration into a multicatalytic reaction sequence. Our previous studies indicated that the reactive *ortho*-quinodimethane (trienamine) intermediate **35** could be formed *in situ* upon condensation of a chiral secondary amine with an indole based unsaturated aldehyde **33**. Reaction of the transiently *o*-QDM species with an appropriate dienophile **34** would generate the Diels-Alder adduct **36** (Scheme 14). If a ketone moiety is present on the dienophile **34**, a NHC catalyzed benzoin condensation would then be possible, leading to densely functionalized tetracyclic structures **38**. In particular, *in situ* formation of the Breslow intermediate **37** would activate the remaining aldehyde moiety within the tetrahydrocarbazole **36** toward an umpolung reactivity, promoting the nucleophilic attack on the ketone at the original dienophile.

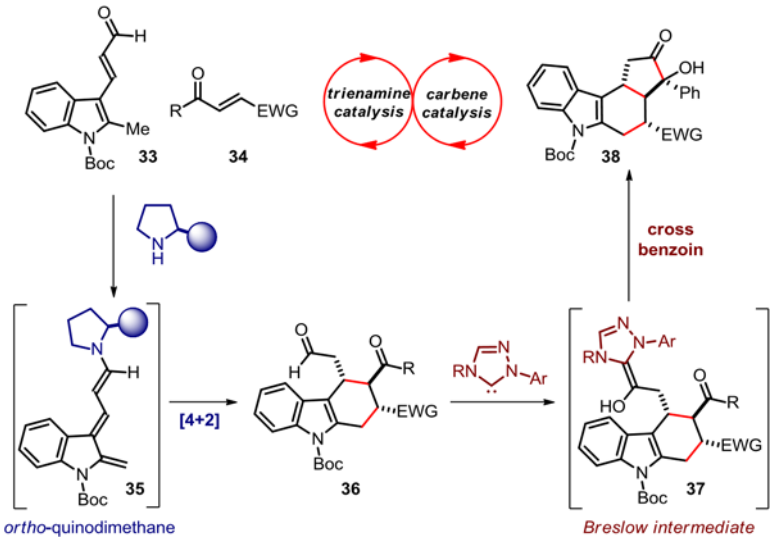

Scheme 14. Design plan for the asymmetric Diels-Alder/benzoin reaction sequence.

As for the synthetic interest of the process, polycyclic indole architectures, including tetrahydrocarbazole derivatives,[96] are key structural elements of many natural alkaloids and synthetic biologically active compounds. There is thus great interest in developing catalytic asymmetric methodologies to efficiently access these privileged molecular scaffolds.

3.4 Results and Discussion

To test the feasibility of our strategy, we selected the unsaturated aldehyde **33** and the dienophile **34** as the model substrates. The N-Boc protected 3-(2-methyl-indol-3-yl)acrylaldehyde **33a** was selected because of its ability to generate *in situ* the highly reactive indole-2,3-quinodimethane intermediate (**35**) upon condensation with the Jørgensen-Hayashi catalyst **28**. The selection of the commercially available alkene **34a** was motivated by the requirement for the ketone moiety, so to make the next benzoin condensation step feasible. Initially, we tested only the Diels-Alder process with the intention of confirming the reactivity of the new class of dienophiles **34**. The substrates were combined with the chiral secondary amine **28** (20 mol%), benzoic acid (BA, equimolar to **28**) and toluene in a normal glass vial at ambient temperature. The desired *exo* cycloadduct **36a** was formed in 38% yield, 5.6:1 diasteroisomeric ratio and excellent enantioselectivity after 16 hours (97% *ee*, entry 1, Table 1). A solvent screening revealed that toluene was the appropriate reaction medium (entry 1).

Table 1. Solvent screening for the Diels-Alder reaction of aldehyde **33a** and dibenzoylethylene **34a**

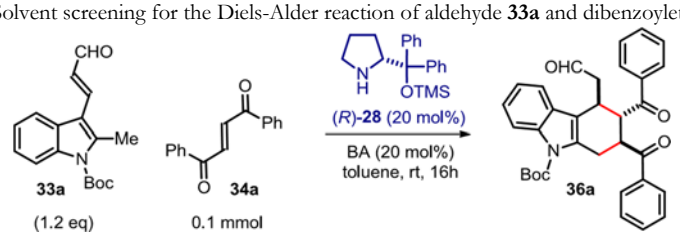

Entry	Solvent	Yield (%)[b]	dr (%)[c]	*ee* (%)[d]
1	Toluene	38	5.6:1	97
2	DCE	48	6.3:1	94
3	CH_3Cl	40	6.5:1	96
4	THF	17	3:1	92
5	TBME	22	5.4:1	96

[a] [b] Reactions were carried out on a 0.1 mmol scale, [**34a**]$_0$ = 0.5 M in toluene. Yield determined by ^{1}H NMR using 1,3,5-trimethoxybenzene as the internal standard. [c] Diastereomeric ratios (dr) were determined by means of ^{1}H NMR analysis of the crude mixture. [d] Enantiomeric excess (*ee*) values were determined with HPLC analysis on commercially available chiral stationary phases.

[96] a) J. Bonjoch, D. Sole. Synthesis of Strychnine. *Chem. Rev.* **2000**, *100*, 3455. b) D. Kato, Y. Sasaki, D. L. Boger. Asymmetric Total Synthesis of Vindoline. *J. Am. Chem. Soc.* **2010**, *132*, 3685. c) S. B. Jones, B. Simmons, A. Mastracchio, D. W. C. MacMillan. Collective Synthesis of Natural Products by Means of Organocascade Catalysis. *Nature* **2011**, *475*, 183.

We then investigated the role of the acid (Table 2). In agreement with the previous studies on the 2,3-indole-quinodimethane reactivity (Chapter II, Table 1), the absence of the acid completely suppressed the reactivity (entry 1, Table 2). 2,4,6-trimethyl benzoic acid gave the best results in term of reactivity, providing 52% of the desired product **36a** in almost enantiopure form (entry 5). Though the enantioselectivity of the cycloaddition was clearly not affected by the acid, the diastereoselectivity was sensitive to the nature of the additive. The same behavior was also observed in the previous optimization studies discussed in Chapter II. Finally, higher temperatures (40°C) and longer times (48 hours) were crucial to obtain the desired *exo* cycloadduct **36a** in good yield (85%, entry 6).

Table 2. Role of the acid and temperature in the Diels-Alder reaction of aldehyde **33a** and dibenzoylethylene **34a**

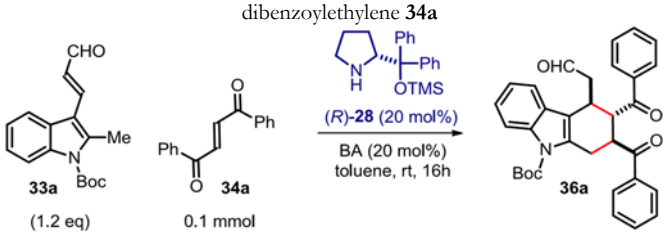

Entry	Acid	Yield (%)[b]	dr (%)[c]	*ee* (%)[d]
1	-	< 5%	nd	nd
2 3[e]	*o*-NO_2-BA *o*-NO_2-	42	8:1	97
4	BA	73	7.3:1	97
5	*o*-F-BA	47	6.7:1	96
	2,4,6-trimethyl-BA	52	8:1	96
6[e]	2,4,6-trimethyl-BA	85	8:1	98
7	*o*-Bn-BA	48	6.4:1	95
8	Pivalic acid	21	3.4:1	94
9	*N*-Boc-1-amino-AcOH	51	7:1	96
10[e]	*N*-Boc-1-amino-AcOH	95	6.7:1	96

[a] Reactions were carried out on a 0.1 mmol scale, [**34a**]$_0$ = 0.5 M in toluene. [b] Yield determined by ^{1}H NMR using 1,3,5-trimethoxybenzene as the internal standard. [c] Diastereomeric ratios (dr) were determined by means of ^{1}H NMR analysis of the crude mixture. [d] Enantiomeric excess (*ee*) values were determined with HPLC analysis on commercially available chiral stationary phases.
[e] Reaction was carried out at 40 °C in 48 hours.

The conditions in entry 6 (Table 2) were selected to examine the scope of the Diels-Alder process by evaluating a variety of keto-containing dienophiles **34** (Figure 1). There appears to be significant tolerance toward structural and electronic variations of the substitution patterns on the dienophiles **34**. Different substituents at the aromatic moiety of the symmetric *trans*-1,2dibenzoylethylene derivatives (EWG = COAr) were well-tolerated. Tetrahydrocarbazoles **36a-d** were obtained in almost perfect enantiocontrol (98-99% *ee*) with satisfactory yields (64-84%). Unsymmetrical dienophiles were also evaluated, where benzoylacrylic esters (EWG = COOR)

showed almost perfect levels of chemo-, diastereo-, and enantioselectivity (products **36e-l**). The synthetic utility of the methodology was confirmed by the results obtained using a larger scale (1 mmol) for products **36c** and **36e**; the catalytic system maintained its efficiency showing comparable yields and optical purity (results between parentheses refer to a 0.1 mmol scale).

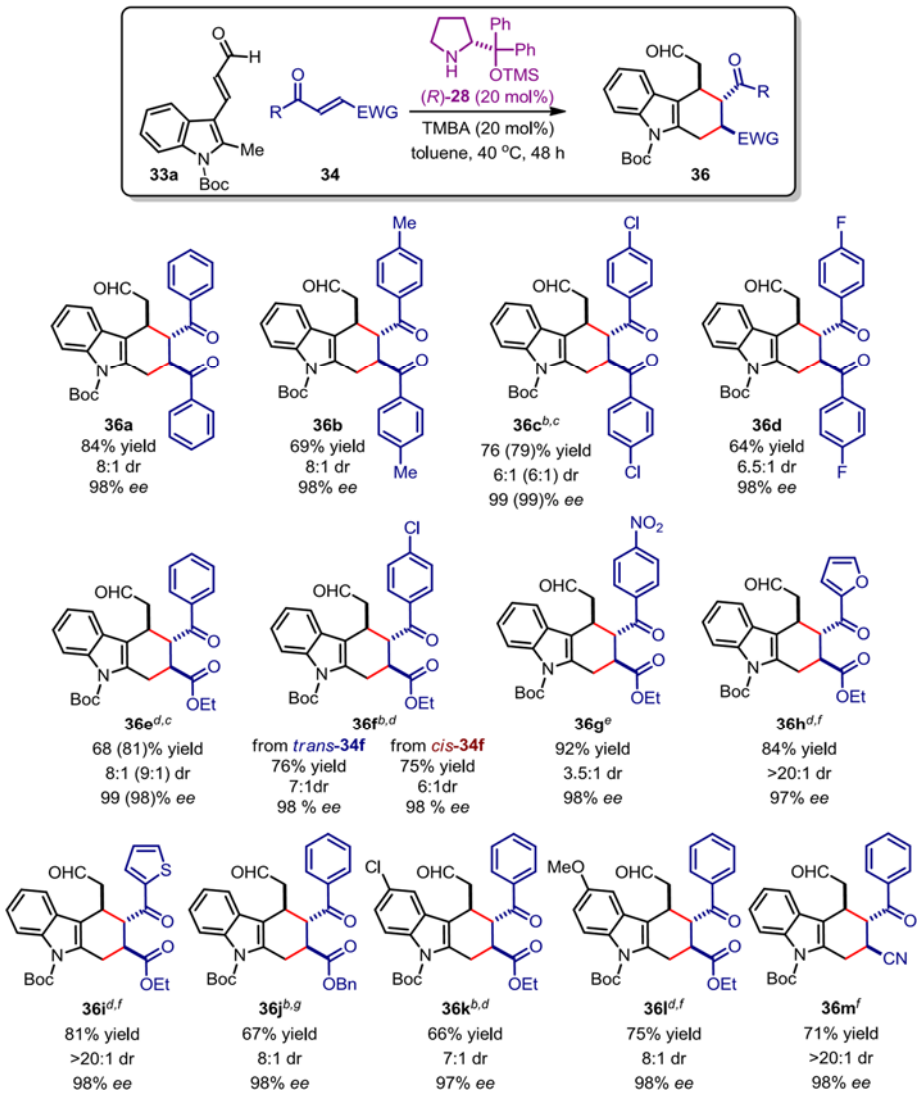

Figure 1. Extending the aminocatalytic indole-2,3-quinodimethane strategy to new classes of dienophiles. [a] Unless noted otherwise, reactions performed on a 0.1 mmol scale and $[\mathbf{34}]_0$ = 0.5M. Yields refer to the sum of the isolated diastereoisomers **36** and reflect the degree of conversion. [b] Yield of the isolated single, major diastereoisomer. [c] 1 mmol scale reaction: results between brackets refer to 0.1 mmol scale reaction. [d] Reaction at 50 °C. [e] 2,6-Bis(trifluoromethyl) benzoic acid (20 mol %) was used. [f] Yield and *ee* were determined after *in situ* homologation of aldehydes **36h-i,l-m** with a Wittig reagent (PPh_3=$CHCO_2Et$, 0.14 mmol, rt, 16 h). [g] Reaction at 60 °C. TMBA = 2,4,6-trimethylbenzoic acid.

Moreover, the geometry of the initial dienophile did not influence the stereochemical outcome of the reaction; tetrahydrocarbazole **36f** was obtained either starting from *trans*-**34f** or *cis*-**34f**. Monitoring the reaction by ^{1}H NMR spectroscopy, we observed a fast isomerization of the *cis*-benzoylacrylic ester **34f** to the *trans* related compound. Thus, in both of the tested reactions, the species that reacted as the dienophile was the *trans* alkene, as deduced by the geometry of the final product **36**. Notably, the indole-2,3-quinodimethane strategy can also be applied to benzoylacrylonitrile (EWG = CN), the corresponding product **36m** formed with perfect regioselectivity. Different substituents at the indole core were also well-tolerated, furnishing products **36k** and **36l** from *trans*-benzoylacrylic ester derivatives.

After exploring the generality of the asymmetric Diels-Alder reaction with the new class of dienophiles, we turned our attention to the development of the proposed multicatalytic system. In analogy with the conditions used by Rovis (Schemes 11 and 13), we performed the cascade protocol adding 20 mol% of NHC achiral precursor **19** to the reaction mixture (Scheme 15).

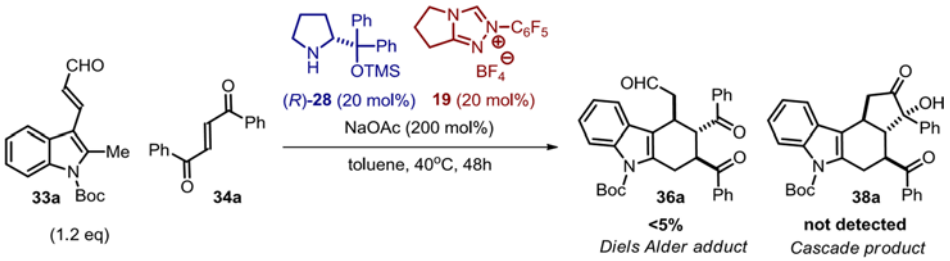

Scheme 15. Initial trial of the *cascade* Diels-Alder/benzoin sequence.

However, the Diels-Alder reaction proceeded sluggishly in the presence of a base (sodium acetate), required to *in situ* form the active carbene catalyst from **19**. This is because an acid cocatalyst is necessary to have a fast formation of the *o*-QDM intermediate and consequently to obtain the pericyclic product (as previously detailed in Table 2). Under the conditions reported in Scheme 15, only trace amounts of the adduct **36a** were detected, with no formation of the cascade product **38a**. Since it was not possible to optimize a cascade protocol to combine the Diels-Alder and the benzoin condensation, we focused on the development of a one-pot sequence.

One-pot operations are effective for carrying out several transformations and forming several bonds in a single pot, while at the same time cutting out several purification steps, minimizing chemical waste generation, and saving time. The potential of one-pot methodologies was demonstrated in the past in the synthesis of complex and biologically active compounds. For example, in 2009, Hayashi developed a remarkable one-pot procedure to synthesize the antiinfluenza neuramidase inhibitor (-)-Oseltamivir or Tamiflu.[97] The synthesis was completed by

[97] H. Ishikawa, T. Suzuki, Y. Hayashi. High-Yielding Synthesis of the Anti-Influenza Neuramidase Inhibitor (-)-Oseltamivir by Three "One-Pot" Operations. *Angew. Chem. Int. Ed.* **2009**, *48*, 1304.

employing three one-pot reaction sequences with a total yield of 57%. The Hayashi synthesis of Tamiflu nicely illustrated the power of asymmetric organocatalysis combined with one-pot reaction sequences.

With the aim to develop a one-pot strategy, the achiral triazolium salt **19** and a base (necessary to activate the NHC precursor) were added in a sequential one-pot manner at elevated temperature after completion of the initial Diels-Alder reaction. As showed in Figure 1, the DielsAlder step led to the almost quantitative formation of the adduct **36a**. Critical parameters to identify a productive benzoin condensation (thus, an effective one-pot sequence) were the use of NaOAc as the base, the dilution of the benzoin reaction system ([**34a**] = 0.2 M), and the reaction temperature (Table 3).

Table 3. Base, temperature and concentration study of the one pot Diels-Alder/Benzoin condensation of aldehyde **33a** and dibenzoylethylene **34a**

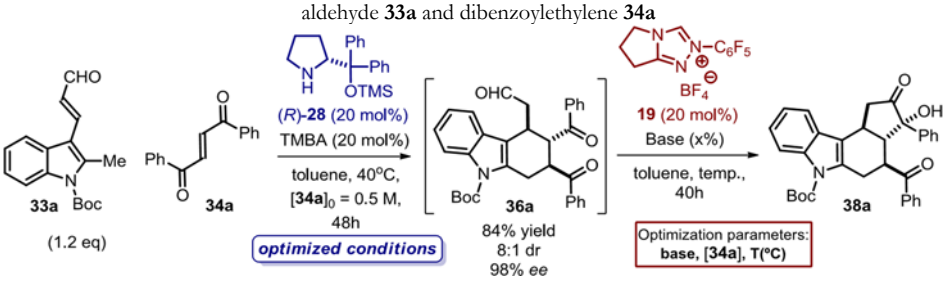

Entry	Base (x%)	Temp. (°C)	Conc. **34a** (M)	Yield (%)[b]	dr (%)[c]	*ee* (%)[d]
1	NaOAc (200)	rt	0.2 0.2	< 5%	nd	nd
2	NaOAc (200)	40	0.2	37	8:1	99
3	Na_2CO_3 (200)	40	0.2	< 5%	nd nd	nd
4	DIPEA (200)	40		< 5%		nd
5	NaOAc (20)	40	0.2	< 5%	nd	nd
6	NaOAc (200)	40	0.5	< 5%	nd	nd
7	NaOAc (200)	50	0.2	41	8:1	99
8	NaOAc (200)	60	0.2	40	8:1	99

[a] Reactions were carried out on a 0.1 mmol scale. [b] Overall yield determined by ^{1}H NMR using 1,3,5-trimethoxybenzene as the internal standard. [c] Diastereomeric ratios (dr) were determined by means of ^{1}H NMR analysis of the crude mixture. [d] Enantiomeric excess (*ee*) values were determined with HPLC analysis on commercially available chiral stationary phases.

With the optimized conditions for the carbene catalyzed benzoin reaction in hand (entry 7), we explored the generality of the one-pot multicatalytic system. While symmetric *trans*dibenzoylethylene (EWG = COAr) derivatives **34** worked well in the multicatalytic sequence (products **38a-d**, Scheme 16), *trans*-benzoylacrylic esters (EWG = COOR, **34e** and **34f**) led to complex product mixtures. This is probably due to a transesterification event between the ester group and the newly generated OH group under basic conditions. Further optimization studies were not successful to improve the results with the *trans*-benzoylacrylic ester substrates.

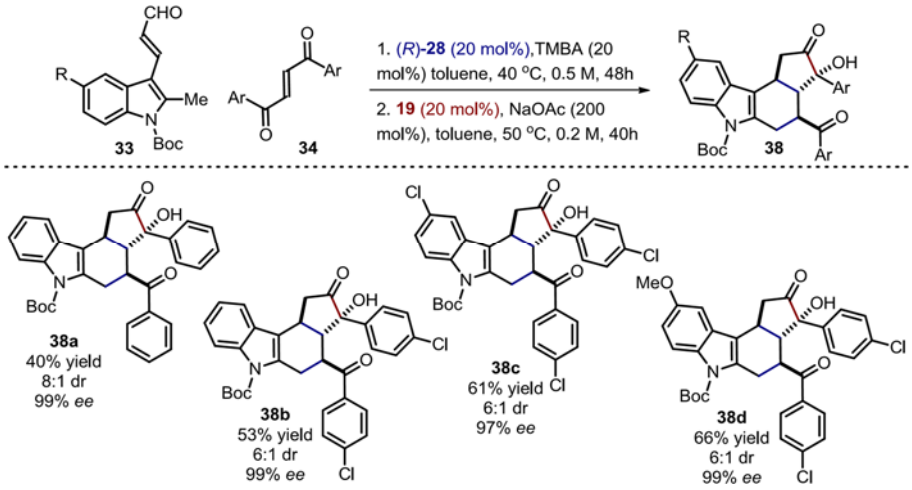

Scheme 16. Multicatalytic Diels-Alder/cross-benzoin reaction sequence to *trans*-fused tetracyclic products.

3.5 Mechanistic Considerations

An X-ray crystal structure analysis of the dichlorosubstituted cycloadduct **38b** allowed the unambiguous determination of the stereochemical outcome of the multicatalytic process. An *exo*-selective Diels-Alder process is followed by a completely stereoselective benzoin condensation, proceeding through a substrate-directed pathway. The explanation of the regioselectivity and the *exo* stereochemical outcome of the cycloaddition step are not simple since the absence of a charged substituent (i.e. the nitro group in the previous study with nitroolefins) rules out any consideration of additional electrostatic interactions. The major atomic orbital coefficient in the o-QDM intermediate is at the ε carbon (Scheme 17a, see also Section 2.6).

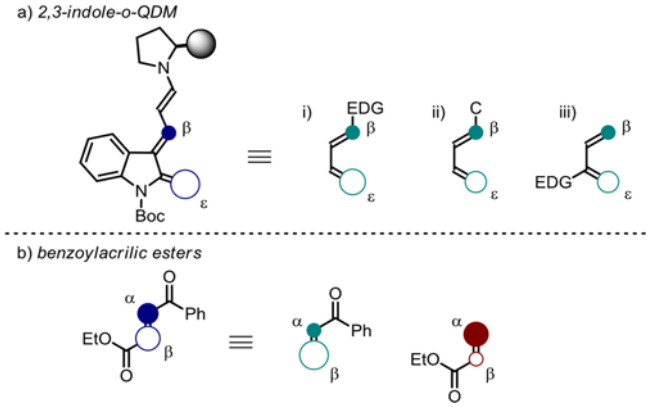

Scheme 17. Atomic orbital coefficients of *o*-QDM/trienamine and dienophiles. EDG = electron-donating group; EWG = electron-withdrawing group; C = conjugated system.

Regarding the regioselectivity of non-symmetric benzoylacrilic esters, the atomic orbital coefficient with higher value is located at the β position respect to the ketone moiety (ketone is more electron-withdrawing than an ester, the major contribution is from the first one, Scheme 17b). According to the *large/large-small/small* interaction rule (see Section 2.1) it is straightforward to explain the regioselectivity observed with non-symmetric benzoylacrilate esters. Thus, the products are formed matching the methylene ε carbon atom of the *o*QDM/trienamine and the β carbon atom of the dienophiles (Scheme 17).

As for the *exo* selectivity, considerations of the possible secondary orbital interaction (SOI) in both the transition states are needed. In the *endo*-TS, secondary orbital interactions can be hypothesized between the carbonyl of the ketone and the γ carbon of the *o*-QDM. In the *exo*-TS, the same type of interactions can be present. Considering the contribution of the atomic orbital coefficients, it seems reasonable that stronger secondary orbital interactions are those of the *exo*-TS, being the atomic orbital coefficient of the ε carbon much higher than the γ carbon of the o-QDM. Thus, the *exo* transition state may be kinetically favored against the *endo* approach (Scheme 18), suggesting the observed *exo* selectivity with non-symmetric and symmetric dienophiles.

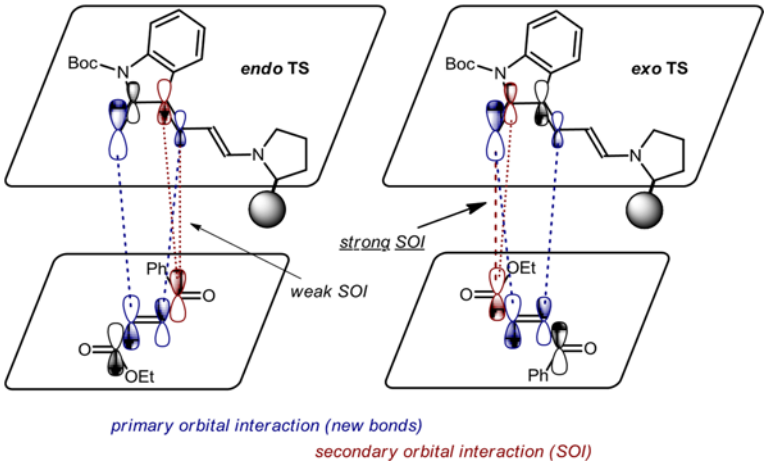

Scheme 18. The importance of secondary orbital interactions (SOI) in *endo* and *exo* transition states.

In order to confirm the observed regioselectivity of the reaction and the relative configuration of the cycloadducts obtained in the Diels-Alder reaction with benzoylacrylic esters (X-ray structure obtained only for symmetric ketone derivatives), the major isolated diastereoisomer of compound **36f** was selected for a deep NMR analysis. Full assignment of the proton signals was obtained by g-COSY, 2D-NMR spectra. Figure 2 shows the protons under study in structure **36f** along with the more relevant ^{1}H NMR regions with the corresponding proton assignment. The fact that proton H_5 and proton H_6 completely overlap introduces a difficulty to these studies (however, all the similar products **36e-l** showed similar spectroscopic patterns, with some of the signals overlapping). The most indicative GOESY results are shown in Figure 2. Saturation of the H_4 signal yields strong NOE

on aromatic hydrogen H_A and weak NOE on H_3, H_5, H_6, H_1, and H_2, confirming the position of ketone and ester moieties within the molecular framework and the regioselectivity of the pericyclic process. Moreover, the weak NOE yielded with all the other protons indicate a *trans*-disposition of proton H_4 with respect to the protons H_3 and H_5. Saturation of the H_3 signal yields NOE on protons H_5 or H_6 (the two signals overlap). To confirm that the saturation of the H_3 only yields NOE on H_5 (and not on H_6), GOESY experiments were carried out on similar products (**39** and **40**, Figure 3) synthesized in our previous work.

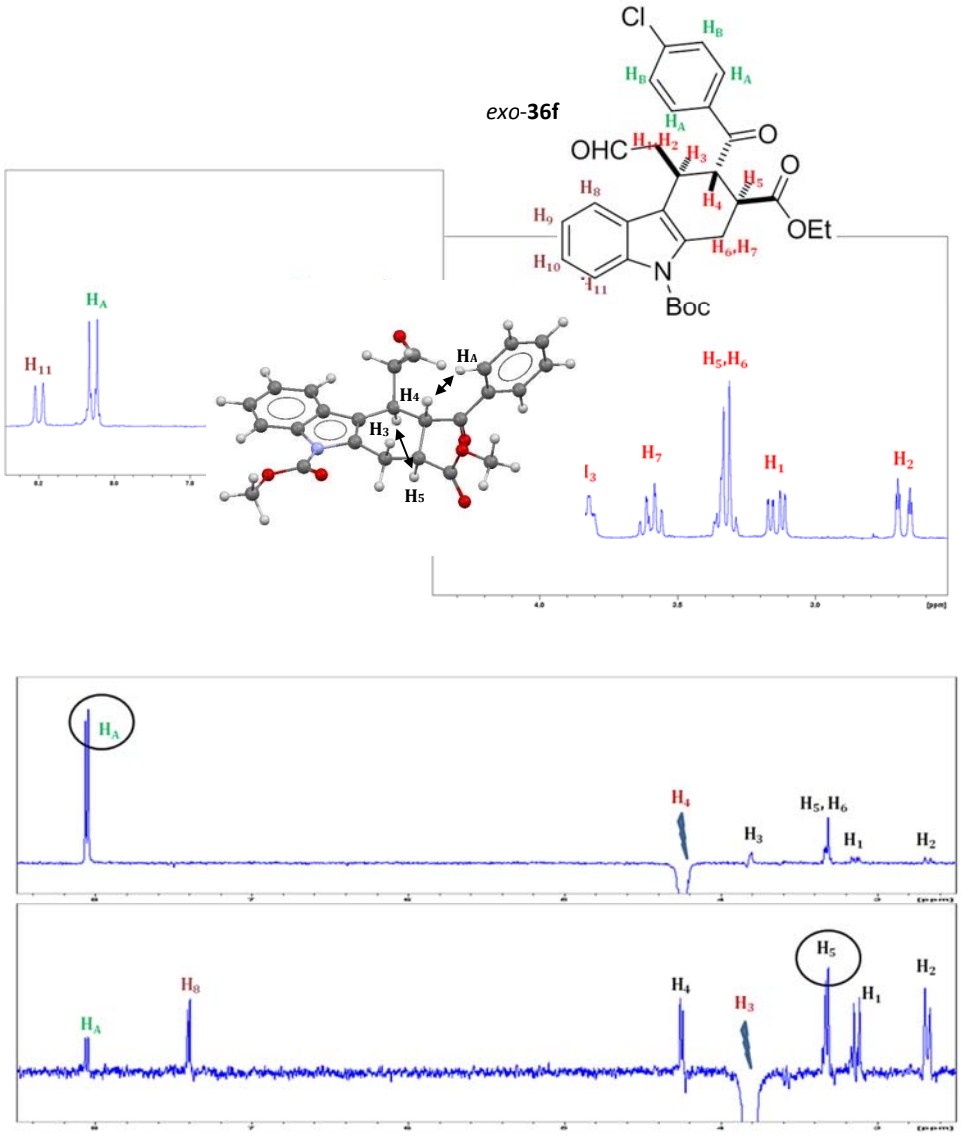

Figure 2. ^{1}H NMR assignment and NOE studies for compound **36f**; *exo* relative configuration.

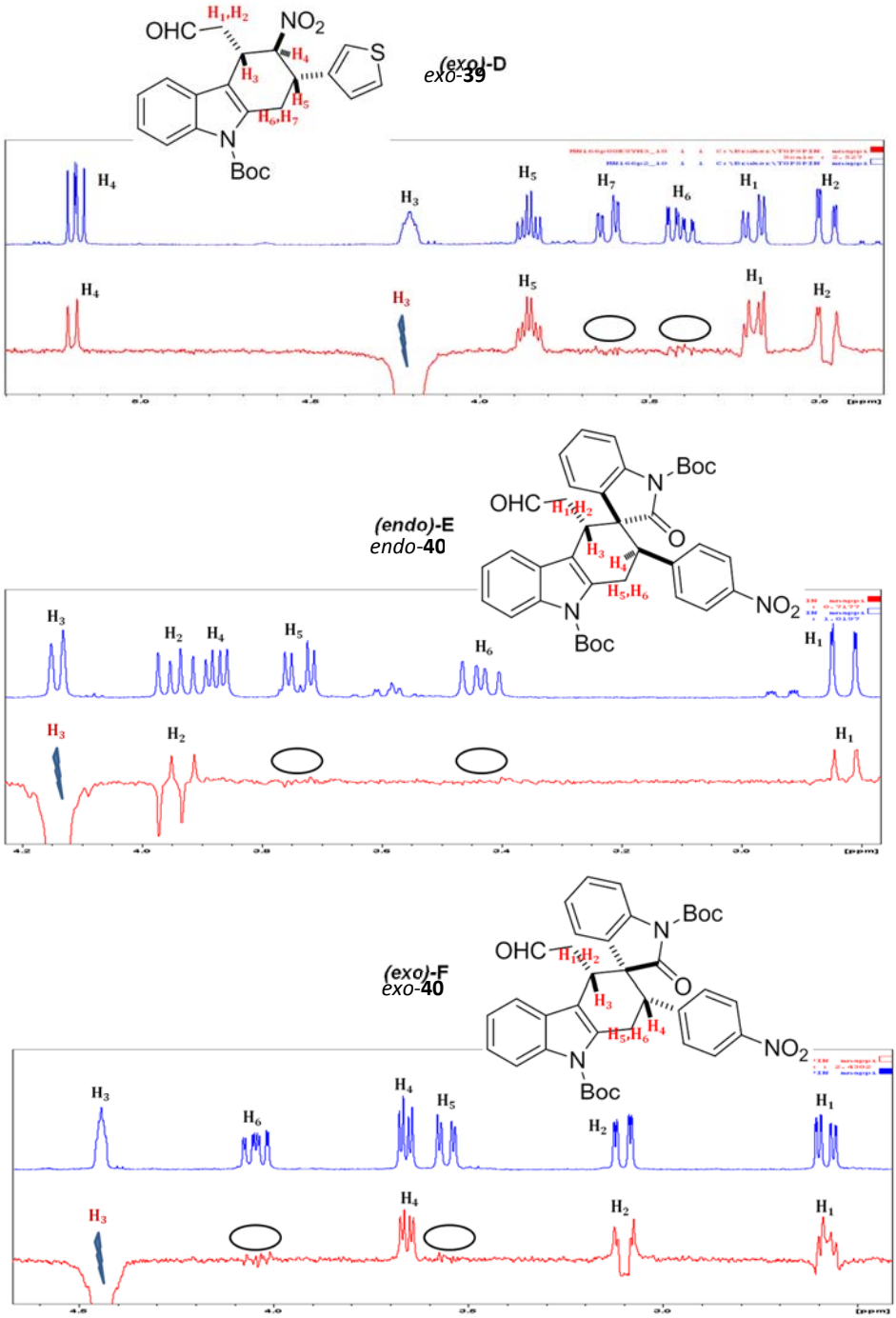

Figure 3. NOE studies for compound **39** and **40**; irradiation of H_3 never yielded H_6 or H_7 (H_5 and H_6 for compounds *endo* and *exo* **40**).

All the experiments detailed in Figure 3 confirm that, when proton H_3 in the corresponding products was saturated, it never yielded NOE on protons H_6 and H_7 (H_5 and H_6 for compounds *endo* and *exo* **40**). This notion points to a *cis* relation of proton H_3 and H_5 in the studied compound **36f**. The stereochemistry matches with a Diels-Alder approach through an *exo* transition state. The *exo*-adduct structure for compound **36f** was optimized with semi-empirical method PM3 (Figure 4).[98] The conformation with the lowest energy shows a short distance between proton H_4 and proton H_A (1.728 Å) and between proton H_3 and proton H_5 (2.730 Å), confirming the strong NOE yielded on the NMR experiments.

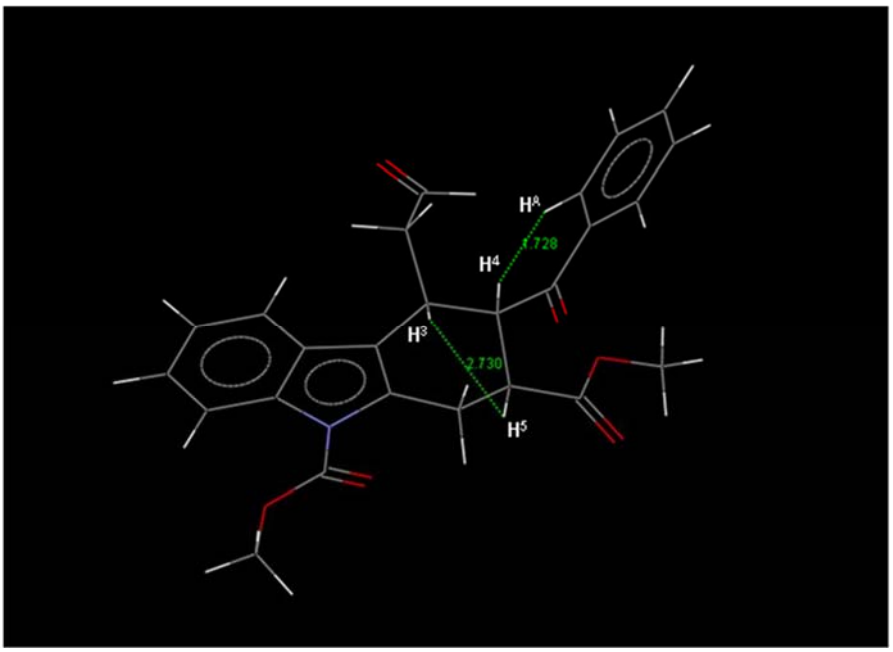

Figure 4. *exo*-adduct structure for compound **36f** optimized with semiempirical method PM3.

We also investigated the structure and the stereochemistry of the cyano-adduct **36m**, in order to confirm the relative configuration and the site-selectivity (X-ray crystal obtained only for symmetric ketone derivatives). Full assignment of the proton signals was obtained by g-COSY, 2D-NMR spectra. Figure 5 shows the protons under study in structure **36m** and the more relevant ^1H NMR regions with the corresponding proton assignment. Proton H_3 and proton H_7 partly overlapped, as also proton H_5 and proton H_6, representing a limitation for these studies. The most indicative GOESY results are shown in Figure 5. Saturation of the H_4 signal yields strong NOE on the aromatic proton H_A and weak NOE on H_3, H_5, H_6, H_1, H_2, H_8 and H_9, thus confirming the relative position of the ketone and cyano moiety. After elucidating the regioselectivity, we focused on the relative spatial arrangement. The weak NOE yielded with all the other protons indicates a *trans*-

[98] We thank Dr. Jamin Krinsky for useful discussions and theoretical models.

disposition of proton H_4 respect to the protons H_3 and H_5. The *exo* selectivity was further confirmed by the multiplicity of the proton H_4, which perfectly matched the one of the corresponding proton (H_4) within compound **36f** (Figure 2). The *exo*-adduct structure for compound **36m** was optimized with semi-empirical method PM3 (Figure 6).[26] The conformation with the lowest energy shows a short distance between proton H_4 and proton H_A (1.727 Å), confirming the strong NOE yielded on the NMR experiments.

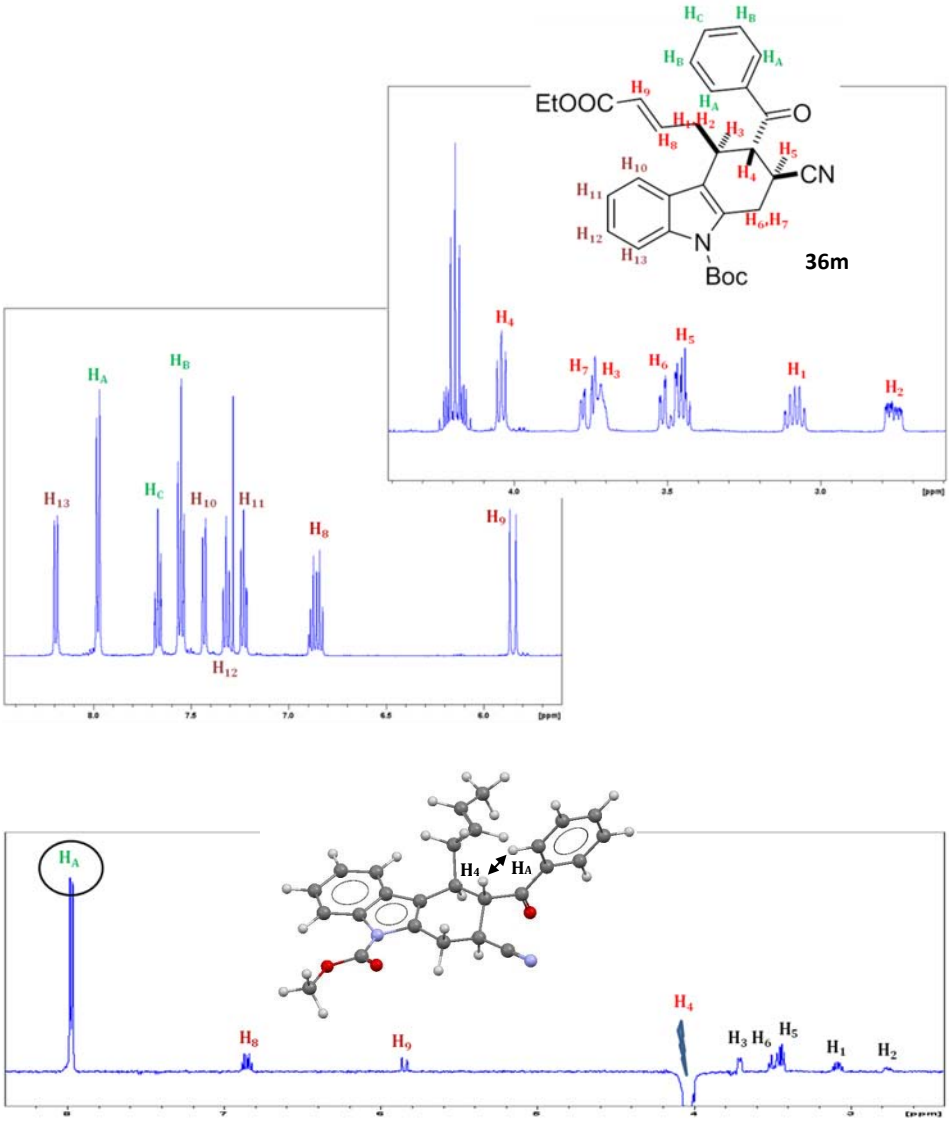

Figure 5. ^{1}H NMR assignment and NOE studies for compound **36m**; *exo* relative configuration.

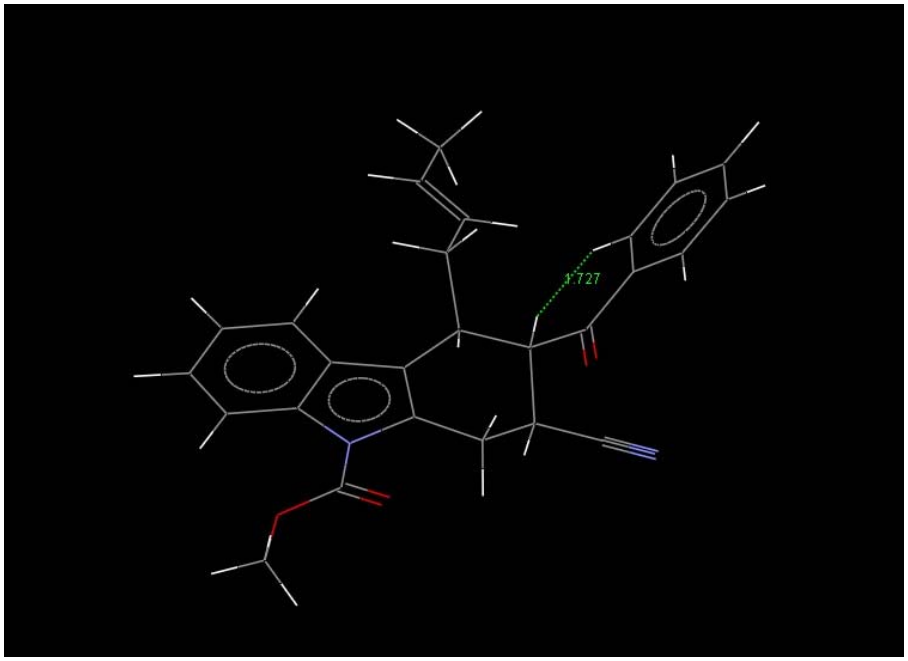

Figure 6. *exo*-adduct structure for compound **36m** optimized with semiempirical method PM3.[26]

3.6 Conclusions

In the previous chapter, we demonstrated that the aminocatalytic indole-2,3-quinodimethane strategy can rapidly build up complex frameworks from simple starting materials. Here, we have shown how its potential can be expanded to include a variety of different dienophiles. The implementation of a multicatalytic, one-pot Diels-Alder/benzoin reaction sequence, based upon the unprecedented combination of trienamine and carbene catalysis, led to the highly stereoselective preparation of complex tetrahydrocarbazole derivatives.

3.7 Experimental Section

3.7.1 General Information

The ^{1}H and ^{13}C NMR spectra were recorded at 400 MHz and 500 MHz for ^{1}H or at 100 MHz and 125 MHz for ^{13}C, respectively. The chemical shifts (δ) for ^{1}H and ^{13}C are given in ppm relative to residual signals of the solvents ($CHCl_3$ @ 7.26 ppm ^{1}H NMR, 77.16 ppm ^{13}C NMR). Coupling constants are given in Hz. Carbon types were determined from DEPT ^{13}C NMR experiments. When necessary, ^{1}H and ^{13}C signals were assigned by means of g-COSY, 2D-NMR sequences. The following abbreviations are used to indicate the multiplicity: s, singlet; d, doublet; t, triplet; q, quartet; m, multiplet; bs, broad signal. High-resolution mass spectra (HRMS) were obtained from the ICIQ High Resolution Mass Spectrometry Unit on Waters GCT gas chromatograph coupled time-of-flight mass spectrometer (GC/MS-TOF) with electron ionization (EI). X-ray data were obtained from the

ICIQ X-Ray Unit using a Bruker-Nonius diffractometer equipped with an APPEX 2 4K CCD area detector. Optical rotations are reported as follows: $[\alpha]^{rt}_{D}$ (c in g per 100 mL, solvent).

The ^{1}H, ^{13}C NMR spectra and the HPLC traces are available in the literature[1] and are not reported in the present thesis.

General Procedures. All the reactions were set up under air and using freshly distilled solvents, without any precautions to exclude moisture, unless otherwise noted - open air chemistry on the benchtop. Chromatographic purification of products was accomplished using force-flow chromatography (FC) on silica gel (60-200 mesh). For thin layer chromatography (TLC) analysis throughout this work, Merck precoated TLC plates (silica gel 60 GF254, 0.25 mm) were used, using UV light as the visualizing agent and an acidic mixture of ceric ammonium molybdate or basic aqueous potassium permangante ($KMnO_4$) as stain developing solutions. Organic solutions were concentrated under reduced pressure on a Büchi rotary evaporator.

Determination of Diastereomeric Ratios. The diastereomeric ratios were determined by ^{1}H NMR analysis of the crude reaction mixtures, and confirmed, after column chromatography purification, by HPLC analysis on chiral stationary phase columns.

Determination of Enantiomeric Purity. HPLC analyses on chiral stationary phase were performed on an Agilent 1200-series instrumentation. Daicel Chiralpak AD-H, IA, IB or IC columns with *i*-PrOH/hexane as the eluent were used. HPLC traces were compared to racemic samples prepared by mixture of two enantiomeric final products obtained using (*S*) and (*R*) catalysts.

Determination of Yield and Conversion in the Optimization Studies. The conversion of the starting materials and the yield of product in the optimization studies were determined by ^{1}H NMR spectroscopy using an internal standard in the crude reaction: 1,3,5-trimethoxybenzene: δ 6.10 ppm (s,3H). Since in all instances the conversion of dibenzoylethylene **34a** was equal to the yield of product, in some cases the yield was determined by integration of the signals of the unreacted dibenzoylethylene in the ^{1}H NMR spectra (dibenzoylethylene ^{1}H NMR signal: δ 8.02 ppm (s, 2H))

Materials. Commercial grade reagents and solvents were purchased from Sigma Aldrich, Fluka, and Alfa Aesar and used as received, without further purification.[99] Chiral secondary amine **28** is commercially available in both the enantiomeric forms (Aldrich or Alfa Aeser); the catalyst was purified by flash column chromatography prior to use. All the aldehydes,[100] dibenzoylethylenes[101] and benzoylacrylic esters[102] were synthesized according to literature procedures.

---

[99] W. L. F. Armarengo, D. D. Perrin, In *Purification of Laboratory Chemicals*, 4th ed.; Butterworth Heinemann: Oxford, 1996.
[100] Y. Liu, M. Nappi, E. Arceo, S. Vera, P. Malchiorre. Asymmetric Catalysis of Diels-Alder Reactions with *in Situ* Generated Heterocyclic ortho-Quinodimethanes. *J. Am. Chem. Soc.* **2011**, *133*, 15212.
[101] R. E. Lutz. *Trans*-Dibenzoylethylene. *Org. Synth.* **1940**, *20*, 29.
[102] a) K. A. Runcie, R. J. K. Taylor. The *in Situ* Oxidation–Wittig eaction of α-Hydroxyketones. *Chem. Commun.* **2002**, 974. b) W. Kroutil, M. E. Lasterra-Sánchez, S. J. Maddrell, P. Mayon, P. Morgan, S. M. Roberts, S. R.

3.7.2 General Procedure for the Diels-Alder Reaction

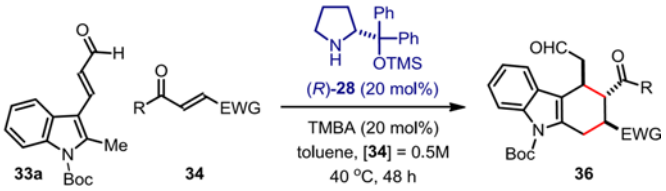

All the reactions were carried out in toluene (synthesis grade, >99%), without any precaution to exclude air and moisture (open air chemistry on the benchtop). An ordinary vial equipped with a Teflon-coated stir bar and a plastic screw cap was charged with (*R*)-2-(diphenyl((trimethylsilyl)oxy)methyl)pyrrolidine **28** (0.02 mmol, 6.5 mg, 20 mol%). Then, 2,4,6trimethylbenzoic acid (TMBA, 0.02 mmol, 3.2 mg, 20 mol%) and toluene (0.2 mL) were added in one portion and the resulting solution was stirred at ambient temperature for 5 minutes to allow the catalyst salt formation. The reaction was started by the sequential addition of the aldehyde **33a** (0.12 mmol, 34.2 mg, 1.2 eq) and the dibenzoylethylene derivative **34** (0.1 mmol, 23.6 mg). The vial was sealed and immerged in a oil bath (thermostated at 40°C), and stirred over 48 hours. Then the crude mixture was flushed through a short plug of silica, using dichloromethane/diethyl ether 1:1 as the eluent (5 ml). Solvent was removed under reduced pressure and the crude mixture was analyzed by ^{1}H NMR spectroscopy to determine the diastereomeric ratio (d.r.) of the reaction. The product **36** was isolated by flash column chromatography.

(2*S*,3*S*,4*S*)-*tert*-butyl 2,3-dibenzoyl-4-(2-oxoethyl)-3,4-dihydro-1H-carbazole-9(2H)-carboxylate (36a)

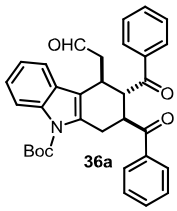

The reaction was carried out following the general procedure to furnish after 48 h the crude product as a 8:1 mixture of diastereoisomers; d.r. determined by integration of ^{1}H-NMR signals: δ_{major} 9.51 ppm (m), δ_{minor} 9.61 ppm (s). The title compound was isolated by flash column chromatography (Hexane/ Ethyl Acetate, 12:1-10:1) in 84% yield and 98% e.e.. The e.e. was determined by HPLC analysis on a Daicel Chiralpak IA column: 80:20 hexane/*i*- rOH, flow rate 1.00 mL/min, λ = 254 nm: τ_{major} = 9.3 min, τ_{minor} = 20.3 min.

$[\alpha]_{26}^{D}$= -42.5 (*c* = 1.01, $CHCl_3$, dr = 8:1, ee = 98%).

HRMS *calc* for ($C_{33}H_{31}NO_5Na$): 544.2100 *found* 544.2101.

[1]

Thornton, C. J. Todd, M. Tüter. Development of the Juliá Asymmetric Epoxidation Reaction. Part 2. Application of the Oxidation to Alkyl Enones, Enediones and Unsaturated Keto-Esters. *J. Chem. Soc., Perkin Trans. 1* **1996**, 2837.

H NMR (400 MHz, $CDCl_3$): δ 9.51 (m, 1H), 8.18 (d, 1H, *J* = 8.19 Hz), 8.07 (m, 2H), 7.90 (m, 2H), 7.62-7.37 (m, 7H), 7.29 (m, 1H), 7.22 (m, 1H), 4.50-4.34 (m, 2H), 3.84 (m, 1H), 3.62 (dd, 1H, *J* = 17.72 Hz, *J* = 4.83 Hz), 3.21-3.10 (m, 2H), 2.71 (dt, 1H, *J* = 17.72 Hz, *J* = 2.30 Hz), 1.58 (s, 9H) ppm.

^{13}C NMR (400 MHz, $CDCl_3$): δ 204.77, 202.14, 200.90, 150.26, 138.23, 136.61, 136.01, 134.36, 133.69, 133.62, 129.00, 128.91, 128.86, 128.76, 127.60, 124.16, 123.00, 118.60, 116.83, 116.02, 84.32, 48.27, 47.11, 45.37, 33.61, 29.97, 28.30 ppm.

(2*S*,3*S*,4*S*)-*tert*-butyl 2,3-bis(4-methylbenzoyl)-4-(2-oxoethyl)-3,4-dihydro-1H-carbazole-9(2H)carboxylate (36b)

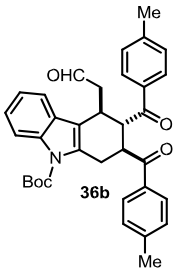

The reaction was carried out following the general procedure using 1 eq of aldehyde and 1.2 eq of dibenzoylethylene to furnish after 48 h the crude product as a 8:1 mixture of diastereoisomers; d.r. determined by integration of ^{1}H-NMR signals: δ_{major} 9.51 ppm (m), δ_{minor} 9.59 ppm (s). The title compound was isolated by flash column chromatography (Hexane/ Ethyl Acetate, 12:1) in 69% yield and 98% e.e.. The e.e. was determined by HPLC analysis on a Daicel Chiralpak IA column: 80:20 hexane/*i*-PrOH, flow rate 1.00 mL/min, λ = 254 nm: τ_{major} = 9.9 min, τ_{minor} = 27.3 min.

$[\alpha]_{26}^{D}$= -63.7 (*c* = 0.95, $CHCl_3$, dr = 8:1, ee = 98%).

HRMS *calc* for ($C_{36}H_{39}NO_6Na$): 604.2675 *found* 604.2689.

^{1}H NMR (400 MHz, $CDCl_3$): δ 9.51 (m, 1H), 8.17 (d, 1H, *J* = 8.42 Hz), 7.96 (d, 2H, *J* = 8.32 Hz), 7.80 (d, 2H, *J* = 8.32 Hz), 7.40 (d, 1H, *J* = 7.82 Hz), 7.28 (m, 3H), 7.22 (m, 3H), 4.45-4.28 (m, 2H), 3.82 (m, 1H), 3.58 (dd, 1H, *J* = 17.65 Hz, *J* = 4.79 Hz), 3.20-3.09 (m, 2H), 2.69 (dt, 1H, *J* = 17.65 Hz, *J* = 2.52 Hz),2.41 (s, 3H), 2.39 (s, 3H), 1.58 (s, 9H) ppm. ^{13}C NMR (400 MHz, $CDCl_3$): δ 204.20, 201.64, 201.11, 150.28, 144.61, 144.48, 136.61, 135.76, 134.54, 133.54, 129.61, 129.51, 129.15, 128.92, 127.67, 124.10, 122.96, 118.63, 116.86, 115.99, 84.27, 48.23, 46.85, 45.33, 33.69, 30.08, 28.32, 21.84, 21.79 ppm.

(2*S*,3*S*,4*S*)-*tert*-butyl 2,3-bis(4-chlorobenzoyl)-4-(2-oxoethyl)-3,4-dihydro-1H-carbazole-9(2H)-carboxylate (36c)

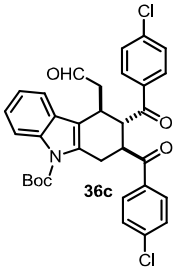

The reaction was carried out following the general procedure to furnish after 48 h the crude product as a 6:1 mixture of diastereoisomers; d.r. determined by integration of ^{1}H-NMR signals: δ_{major} 9.50 ppm (m), δ_{minor} 9.60 ppm (s). The major diastereoisomer was isolated by flash column chromatography (Hexane/ Ethyl Acetate, 20:1-15:1) in 79% yield and 99% e.e.. The e.e. was determined by HPLC analysis on a Daicel Chiralpak IA column: 80:20 hexane/*i*-PrOH, flow rate 1.00 mL/min, λ = 254 nm: τ_{major} = 12.0 min, τ_{minor} = 35.1 min.

$[\alpha]_{26}^{D}$= -79.2 (*c* = 0.85, $CHCl_3$, dr = 1, ee = 99%).

HRMS *calc* for ($C_{34}H_{33}NO_6Cl_2Na$): 644.1583 *found* 644.1588.

^{1}H NMR (400 MHz, $CDCl_3$): δ 9.50 (m, 1H), 8.16 (d, 1H, *J* = 8.26 Hz), 8.01 (m, 2H), 7.84 (m, 2H), 7.46 (m, 2H), 7.41 (m, 3H), 7.30 (m, 1H), 7.23 (m, 1H), 4.42-4.25 (m, 2H), 3.81 (m, 1H), 3.60 (dd, 1H, *J* = 17.91 Hz, *J* = 4.83 Hz), 3.24-3.07 (m, 2H), 2.67 (dt, 1H, *J* = 17.91 Hz, *J* = 2.27 Hz), 1.60 (s, 9H) ppm. ^{13}C NMR (400 MHz, $CDCl_3$): δ 203.67, 200.87, 150.25, 140.40, 140.33, 136.55, 136.44, 134.17, 134.15, 130.44, 130.18, 129.27, 127.50, 124.29, 123.08, 118.61, 116.67, 116.08, 84.50, 48.24, 47.27, 45.24, 33.79, 29.97, 28.34 ppm.

(2*S*,3*S*,4*S*)-*tert*-butyl 2,3-bis(4-fluorobenzoyl)-4-(2-oxoethyl)-3,4-dihydro-1H-carbazole-9(2H)carboxylate (36d)

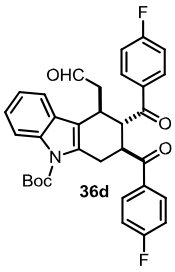

36d

The reaction was carried out following the general procedure to furnish after 48 h the crude product as a 6.5:1 mixture of diastereoisomers; d.r. determined by integration of ^{1}H-NMR signals: δ_{major} 9.51 ppm (s), δ_{minor} 9.61 ppm (s). The major diastereoisomer was isolated as a single isomer by flash column chromatography (Toluene/ diethyl ether, 99:1) in 64% yield and 98% e.e.. The e.e. was determined by HPLC analysis on a Daicel Chiralpak IA column: 80:20 hexane/*i*-PrOH, flow rate 1.00 mL/min, λ = 254 nm: τ_{major} = 10.6 min, τ_{minor} = 27.5 min.

$[\alpha]_{26}^{D}$= -51.6 (*c* = 1.00, $CHCl_3$, dr = 1, ee = 98%).

HRMS *calc* for ($C_{34}H_{33}NO_6F_2Na$): 612.2174 *found* 612.2170.

^{1}H NMR (400 MHz, $CDCl_3$): δ 9.51 (m, 1H), 8.16 (d, 1H, *J* = 8.26 Hz), 8.10 (m, 2H), 7.93 (m, 2H), 7.42 (d, 1H, *J* = 7.78 Hz), 7.30 (m, 1H), 7.23 (m, 1H), 7.16 (m, 2H), 7.11 (m, 2H), 4.43-4.25 (m, 2H), 3.83 (m, 1H), 3.60 (dd, 1H, *J* = 17.74 Hz, *J* = 4.86 Hz), 3.24-3.09 (m, 2H), 2.67 (dt, 1H, *J* = 17.74 Hz, *J* = 2.43 Hz), 1.60 (s, 9H) ppm. ^{13}C NMR (400 MHz, $CDCl_3$): δ 203.23, 200.96, 200.46, 167.22, 165.19, 150.28, 136.58, 134.61, 134.26, 132.31, 131.83, 131.76, 131.54, 131.46, 127.55, 124.27, 123.08, 118.63, 116.69, 116.08, 84.47, 48.33, 47.16, 45.25, 33.84, 30.05, 28.35 ppm.

(2*S*,3*S*,4*S*)-9-*tert*-butyl 2-ethyl 3-benzoyl-4-(2-oxoethyl)-3,4-dihydro-1H-carbazole-2,9(2H)-dicarboxylate (36e)

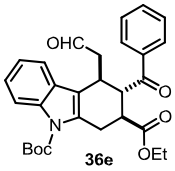

36e

The reaction was carried out following the general procedure at 50 °C to furnish after 48 h the crude product as a 9:1 mixture of diastereoisomers; d.r. determined after column by integration of ^{1}H-NMR signals: δ_{major} 2.69 ppm (dt), δ_{minor} 2.55 ppm (dd). The title compound was isolated (d.r 9:1) by flash column chromatography (Hexane/ Ethyl Acetate, 12:1-10:1) in 81% yield and 98% e.e.. The e.e. was determined by HPLC analysis on a Daicel Chiralpak IC column: 70:30 hexane/*i*- rOH, flow rate 1.00 mL/min, λ = 254 nm: τ_{major} = 14.7 min, τ_{minor} = 27.4 min.

$[\alpha]_{26}^{D}$= 3.8 (*c* = 1.03, $CHCl_3$, dr = 9:1, ee = 98%).

HRMS *calc* for ($C_{29}H_{31}NO_6Na$): 512.2049 *found* 512.2049.

^{1}H NMR (400 MHz, $CDCl_3$): δ 9.57 (m, 1H), 8.18 (d, 1H, *J* = 8.42 Hz), 8.07 (m, 2H), 7.60 (m, 1H), 7.51 (m, 2H), 7.38 (d, 1H, *J* = 7.81 Hz), 7.27 (m, 1H), 7.20 (m, 1H), 4.28 (m, 1H), 4.05-3.87 (m, 2H), 3.83 (m, 1H), 3.55 (m, 1H), 3.38-3.26 (m, 2H), 3.09 (dd, 1H, *J* = 17.77 Hz, *J* = 7.05 Hz), 2.69 (dt, 1H, *J* = 17.77 Hz, *J* = 2.45 Hz), 1.69 (s, 9H), 1.10 (t, 3H, *J* = 7.20) ppm. ^{13}C NMR (400 MHz, $CDCl_3$): δ 203.19, 201.17, 173.68, 150.32, 137.66, 136.56, 133.97, 133.65, 128.93, 128.88, 127.67, 124.09, 122.90, 118.41, 116.16, 116.01, 84.28, 61.31, 47.25, 45.48, 44.04, 32.61, 28.41, 28.09, 14.03 ppm.

(2*S*,3*S*,4*S*)-9-*tert*-butyl 2-ethyl 3-(4-chlorobenzoyl)-4-(2-oxoethyl)-3,4-dihydro-1H-carbazole2,9(2H)-dicarboxylate (36f)

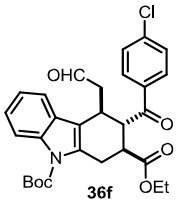

36f

The reaction was carried out following the general procedure at 50 °C to furnish after 48 h the crude product as a 7:1 mixture of diastereoisomers; d.r. determined by integration of ^{1}H-NMR signals: δ_{major} 9.56 ppm (m), δ_{minor} 9.58 ppm (s). The major diastereoisomer was isolated by flash column chromatography (Toluene/ Diethyl ether, 98:2) in 76% yield and 98% e.e.. The e.e. was determined by HPLC analysis on a Daicel Chiralpak IC column: 80:20 hexane/*i*- rOH, flow rate 1.00 mL/min, λ = 254 nm: τ_{major} = 13.6 min, τ_{minor} = 24.7 min.

$[\alpha]_{26}^{D}$= 4.1 (*c* = 0.88, $CHCl_3$, dr = 1, ee = 98%).

HRMS *calc* for ($C_{29}H_{30}NO_6ClNa$): 546.1659 *found* 546.1677.

^{1}H NMR (400 MHz, $CDCl_3$): δ 9.56 (m, 1H), 8.18 (d, 1H, *J* = 8.44 Hz), 8.03 (m, 2H), 7.48 (m, 2H), 7.38 (d, 1H, *J* = 7.94 Hz), 7.28 (m, 1H), 7.21 (m, 1H), 4.22 (m, 1H), 4.09-3.91 (m, 2H), 3.80 (m, 1H), 3.57 (m, 1H), 3.35-3.25 (m, 2H), 3.12 (dd, 1H, *J* = 17.56 Hz, *J* = 7.18 Hz), 2.66 (dt, 1H, *J* = 17.54 Hz, *J* = 2.39 Hz), 1.69 (s, 9H), 1.13 (t, 3H, *J* = 7.11) ppm. ^{13}C NMR (400 MHz, $CDCl_3$): δ 202.23, 201.20, 173.69, 150.30, 140.19, 136.56, 136.03, 133.97, 130.34, 129.26, 127.59, 124.16, 122.95, 118.39, 116.04, 115.96, 84.34, 61.40, 47.16, 45.38, 44.08, 32.82, 28.41, 28.13, 14.11 ppm.

(2*S*,3*S*,4*S*)-9-*tert*-butyl 2-ethyl 3-(4-nitrobenzoyl)-4-(2-oxoethyl)-3,4-dihydro-1H-carbazole2,9(2H)-dicarboxylate (36g)

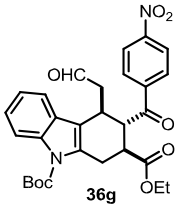

36g

The reaction was carried out following the general procedure using 2,6-bis (trifluoromethyl) benzoic acid as a cocatalyst at 50 °C to furnish after 30 h the crude product as a 3.5:1 mixture of diastereoisomers; d.r. determined after column by integration of ^{1}H-NMR signals: δ_{major} 9.56 ppm (m), δ_{minor} 9.56 ppm (s). The mixture of diastereoisomers was isolated by flash column chromatography (Hexane/ Ethyl acetate, 10:1) in 92% yield, 98% e.e. of

major diastereoisomer and 53% e.e. of minor diastereoisomer. The e.e. was determined by HPLC analysis on a Daicel Chiralpak IC column: 80:20 hexane/*i*- rOH, flow rate 1.00 mL/min, λ = 254 nm; Major diastereoisomer: τ_{major} = 25.5 min, τ_{minor} = 49.7 min; Minor diasteroisomer: τ_{major} = 19.7 min, τ_{minor} = 49.1 min.

$[\alpha]_{26}^{D}$= 2.2 (*c* = 0.88, $CHCl_3$, dr = 3.5:1, ee_1 = 98%, ee_2 = 53%).

HRMS *calc* for ($C_{29}H_{30}N_2O_8Na$): 557.1900 *found* 557.1896.

^{1}H NMR (400 MHz, $CDCl_3$): δ 9.56 (m, 1H), 8.35 (m, 2H), 8.26 (m, 2H), 8.18 (d, 1H, *J* = 8.42 Hz), 7.37 (d, 1H, *J* = 8.02 Hz), 7.29 (m, 1H), 7.21 (m, 1H), 4.28 (m, 1H), 4.10-3.96 (m, 2H), 3.81 (m, 1H), 3.62 (m, 1H), 3.39-3.28 (m, 2H), 3.14 (dd, 1H, *J* = 17.25 Hz, *J* = 7.26 Hz), 2.65 (m, 1H), 1.70 (s, 9H), 1.16 (t, 3H, *J* = 7.07) ppm. ^{13}C NMR (400 MHz, $CDCl_3$): δ 202.36, 201.10, 173.71, 150.54, 150.25, 142.17, 136.56, 133.96, 129.97, 127.44, 124.29, 124.08, 123.02, 118.27, 116.10, 115.63, 84.46, 61.59, 47.59, 45.53, 44.03, 32.76, 28.41, 28.39, 14.16 ppm.

(2*S*,3*S*,4*S*)-2-benzyl 9-*tert*-butyl 3-benzoyl-4-(2-oxoethyl)-3,4-dihydro-1H-carbazole-2,9(2H)-dicarboxylate (36j)

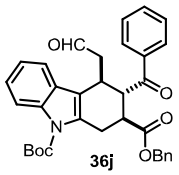

36j

The reaction was carried out following the general procedure at 60 °C using 1 eq of aldehyde and 1.2 eq of 3-benzoylacrylic esters to furnish after 48 h the crude product as a 8:1 mixture of diastereoisomers; d.r. determined by integration of ^{1}H-NMR signals: δ_{major} 9.45 ppm (dt), δ_{minor} 9.57 ppm (dd). The major diastereoisomer was isolated by flash column chromatography (Hexane/ Ethyl Acetate, 12:1-10:1) in 67% yield and 98% e.e.. The e.e. was determined by HPLC analysis on a Daicel Chiralpak IA column: 95:5 hexane/*i*- rOH, flow rate 1.00 mL/min, λ = 254 nm: τ_{major} = 18.9, τ_{minor} = 20.4 min.

$[\alpha]_{26}^{D}$= 2.4 (*c* = 0.8, $CHCl_3$, dr = 1, ee = 98%).

HRMS *calc* for ($C_{35}H_{37}NO_7Na$): 606.2468 *found* 606.2496.

^{1}H NMR (400 MHz, $CDCl_3$): δ 9.45 (m, 1H), 8.18 (d, 1H, *J* = 8.42 Hz), 8.04 (m, 2H), 7.59 (m, 1H), 7.48 (m, 2H), 7.34 (d, 1H, *J* = 7.72 Hz), 7.32-7.16 (m, 7H), 4.96 (complex system, 2H), 4.28 (m, 1H), 3.82 (m, 1H), 3.50 (m, 1H), 3.42-3.33 (m, 2H), 2.98 (dd, 1H, *J* = 17.96 Hz, *J* = 7.36 Hz), 2.66 (m, 1H), 1.64 (s, 9H), ppm. ^{13}C NMR (400 MHz, $CDCl_3$): δ 202.91, 201.09, 173.60, 150.30, 137.45, 136.62, 135.35, 133.73, 123.62, 128.95, 128.90, 128.70, 128.63, 128.54, 127.66, 124.11, 122.88, 118.34, 116.14, 116.00, 84.24, 67.10, 47.19, 45.66, 43.68, 32.10, 28.39, 27.75 ppm.

(2*S*,3*S*,4*S*)-9-*tert*-butyl 2-ethyl 3-benzoyl-6-chloro-4-(2-oxoethyl)-3,4-dihydro-1H-carbazole2,9(2H)-dicarboxylate (36k)

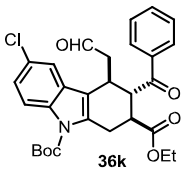

36k

The reaction was carried out following the general procedure at 50 °C to furnish after 48 h the crude product as a 7:1 mixture of diastereoisomers;

d.r. determined by integration of ^{1}H-NMR signals: δ_{major} 9.59 ppm (m), δ_{minor} 9.55 ppm (s).The major diasteroisomer was isolated by flash column chromatography (Toluene/ Diethyl ether, 98:2) in 66% yield and 97% e.e.. The e.e. was determined by HPLC analysis on a Daicel Chiralpak IA column: 80:20 hexane/*i*-PrOH, flow rate 1.00 mL/min, λ = 254 nm: τ_{major} = 6.3 min, τ_{minor} = 7.1 min.

$[\alpha]_{26}^{D}$= 17.2 (*c* = 0.80, $CHCl_3$, dr = 1, ee = 97%).

HRMS *calc* for ($C_{30}H_{34}NO_7NaCl$): 578.1922 *found* 578.1938.

^{1}H NMR (400 MHz, $CDCl_3$): *δ* 9.56 (m, 1H), 8.10 (d, 1H, *J* = 8.93 Hz), 8.06 (m, 2H), 7.60 (m, 1H), 7.51 (m, 2H), 7.32 (d, 1H, *J* = 2.01 Hz), 7.21 (dd, 1H, *J* = 8.93 Hz, *J* = 2.01 Hz), 4.32 (m, 1H), 4.073.89 (m, 2H), 3.78 (m, 1H), 3.50 (dd, 1H, *J* = 17.90 Hz, *J* = 5.30 Hz), 3.40-3.26 (m, 2H), 3.03 (dd, 1H, *J* = 17.90 Hz, *J* = 7.29 Hz), 2.69 (m, 1H), 1.68 (s, 9H), 1.11 (t, 3H, *J* = 7.07) ppm. ^{13}C NMR (400 MHz, $CDCl_3$): *δ* 202.72, 200.71, 173.58, 149.98, 143.72, 137.38, 135.42, 134.95, 133.71, 128.97, 128.85, 128.51, 124.11, 117.92, 117.02, 115.55, 84.72, 61.40, 46.76, 45.46, 43.48, 31.97, 28.38, 27.71, 14.05 ppm.

Table 4. Results using catalyst (*S*)-**28** to obtain the opposite enantiomer of the product (***ent*-36**)

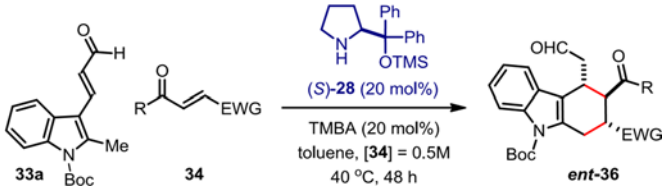

Entry	**36**	Yield (%)[b]	dr (%)[c]	*ee* (%)[d]
1	**ent-a**	85	8:1	98
2	**ent-b**	70	8:1	98
3	**ent-c**	81	6:1	99
4	**ent-e**	65	6.5:1	98
5	**ent-f**	80	9:1	98
6	**ent-g**	78	7:1	98
7[e]	**ent-h**	91	3.5:1	98
8	**ent-i**	69	8:1	98
9	**ent-j**	68	7:1	97

[a] Reactions were carried out on a 0.1 mmol scale. [b] Yields of isolated products [c] Diastereomeric ratios (dr) were determined by means of ^{1}H NMR analysis of the crude mixture. [d] Enantiomeric excess (ee) values were determined with HPLC analysis on commercially available chiral stationary phases.

3.7.3 General Procedure for One-Pot Diels-Alder/Wittig Reaction

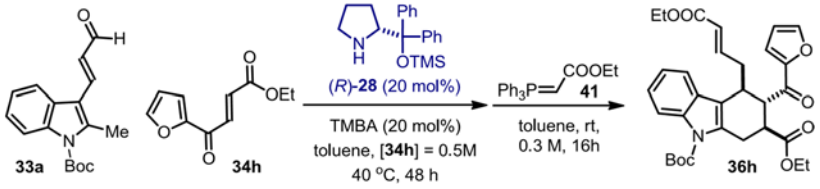

All the reactions were carried out in toluene of (synthesis grade, >99%), without any precaution to exclude air and moisture (open air chemistry on the benchtop). An ordinary vial equipped with a Teflon-coated stir bar and a plastic screw cap was charged with (*R*)-2(diphenyl((trimethylsilyl)oxy)methyl)pyrrolidine **28** (0.02 mmol, 6.5 mg, 20 mol%). Then, 2,4,6trimethylbenzoic acid (0.02 mmol, 3.2 mg, 20 mol%) and toluene (0.2 mL) were added in one portion and the resulting solution was stirred at ambient temperature for 5 minutes to allow the catalyst salt formation. The reaction was started by the sequential addition of the aldehyde **33a** (0.12 mmol, 34.2 mg, 1.2 eq) and the 3-furanylacrylic ester **34h** (0.1 mmol, 20.4 mg). The vial was sealed and immerged in a oil bath (thermostated at 40°C). After 48 hours stirring, the vial was removed from the oil bath and cooled until room temperature. Then, 0.1 ml of toluene and ethyl 2-(triphenylphosphoranylidene) acetate **41** (0.144 mmol, 50 mg, 1.44 eq) were added sequentially and the resulting solution was stirred at room temperature for 16 hours. The corresponding product **36h** was directly isolated by flash column chromatography. **(2*S*,3*S*,4*S*)-9-*tert*-butyl 2-ethyl 4-((E)-4-ethoxy-4-oxobut-2-en-1-yl)-3-(furan-2-carbonyl)-3,4dihydro-1H-carbazole-2,9(2H)-dicarboxylate (36h)**

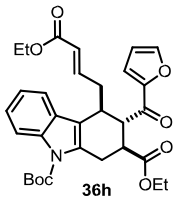

The reaction was carried out following the general procedure at 50 °C to furnish after 64 h the crude product as a >20:1 mixture of diastereoisomers. The title compound was isolated by flash column chromatography (Hexane/ Ethyl Acetate, 10:1-6:1) in 86% yield and 97% e.e.. The e.e. was determined by HPLC analysis on a Daicel Chiralpak IB column: 70:30 hexane/*i*-PrOH, flow rate 1.00 mL/min, λ = 254 nm: τ_{major} = 8.6 min, τ_{minor} = 6.1 min.

$[\alpha]_{26}^{D}$= -14.7 (*c* = 0.96, $CHCl_3$, dr = 1, ee = 97%).

HRMS *calc* for ($C_{31}H_{35}NO_8Na$): 572.2260 *found* 572.2274.

^{1}H NMR (400 MHz, $CDCl_3$): δ 8.18 (d, 1H, *J* = 8.71 Hz), 7.65 (m, 1H), 7.45 (d, 1H, *J* = 7.72 Hz), 7.307.25 (m, 2H), 7.20 (m, 1H), 6.67 (m, 1H), 6.59 (dd, 1H, *J* = 3.65 Hz, *J* = 1.66 Hz), 5.65 (d, 1H, *J* = 15.69 Hz), 4.10 (m, 2H), 4.06-3.90 (m, 2H), 3.78 (m, 1H), 3.68 (m, 1H), 3.59 (m, 1H), 3.24-3.15 (m, 2H), 2.97 (m, 1H), 2.57 (ddd, 1H, *J* = 15.66 Hz, *J* = 8.47, *J* = 2.95 Hz), 1.69 (s, 9H), 1.23 (t, 3H, *J* = 7.24), 1.09 (t, 3H, *J* = 7.15) ppm. ^{13}C NMR (400 MHz, $CDCl_3$): δ 191.65, 173.50, 166.12, 153.59, 150.31, 146.95, 144.52, 136.61, 134.13, 127.92, 124.61, 124.00, 122.81, 118.86, 118.18, 116.40, 115.88, 112.86, 84.19, 61.19, 60.33, 47.91, 44.19, 36.60, 34.66, 28.61, 28.41, 14.36, 13.99 ppm.

(2*S*,3*S*,4*S*)-9-*tert*-butyl 2-ethyl 4-((E)-4-ethoxy-4-oxobut-2-en-1-yl)-3-(thiophene-2-carbonyl)3,4-dihydro-1H-carbazole-2,9(2H)-dicarboxylate (36i).

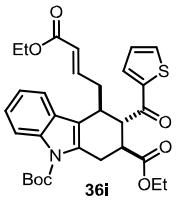

36i

The reaction was carried out following the general procedure at 50 °C to furnish after 64 h the crude product as a >20:1 mixture of diastereoisomers. The title compound was isolated by flash column chromatography (Hexane/ Ethyl Acetate, 10:1) in 81% yield and 98% e.e.. The e.e. was determined by HPLC analysis on a Daicel Chiralpak IB column: 70:30 hexane/*i*-PrOH, flow rate 1.00 mL/min, λ = 254 nm: τ_{major} = 7.6 min, τ_{minor} = 6.2 min.

$[\alpha]_{26}^{D}$= -36.5 (*c* = 0.83, $CHCl_3$, dr = 1, ee = 98%).

HRMS *calc* for ($C_{31}H_{35}NO_7NaS$): 588.2032 *found* 588.2057.

^{1}H NMR (400 MHz, $CDCl_3$): δ 8.18 (d, 1H, *J* = 8.14 Hz), 7.80 (d, 1H, *J* = 3.72 Hz), 7.71 (d, 1H, *J* = 4.96 Hz), 7.46 (d, 1H, *J* = 7.59 Hz), 7.32-7.13 (m, 3H), 6.65 (m, 1H), 5.63 (d, 1H, *J* = 15.67 Hz), 4.10 (m, 2H), 4.04-3.80 (m, 2H), 3.80-3.68 (m, 2H), 3.54 (m, 1H), 3.33-3.11 (m, 2H), 3.01 (m, 1H), 2.58 (dd, 1H, *J* = 15.63 Hz, *J* = 8.67), 1.70 (s, 9H), 1.22 (t, 3H, *J* = 6.96), 1.06 (t, 3H, *J* = 7.20) ppm. ^{13}C NMR (400 MHz, $CDCl_3$): δ 195.41, 173.52, 166.04, 150.32, 145.50, 144.38, 136.61, 135.04, 134.05, 133.24, 128.44, 127.92, 124.89, 124.01, 122.83, 118.91, 116.32, 115.89, 84.22, 61.20, 60.36, 49.33, 44.64, 36.58, 34.50, 28.67, 28.41, 14.35, 13.94 ppm.

(2*S*,3*S*,4*S*)-9-*tert*-butyl 2-ethyl 3-benzoyl-4-((E)-4-ethoxy-4-oxobut-2-en-1-yl)-6-methoxy-3,4dihydro-1H-carbazole-2,9(2H)-dicarboxylate (36l)

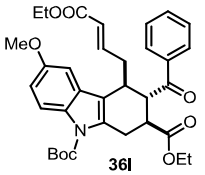

36l

The reaction was carried out following the general procedure at 50 °C to furnish after 64 h the crude product as a 8:1 mixture of diastereoisomers; d.r. determined before add the corrispondenting ylide by integration of ^{1}H-NMR signals: δ_{major} 5.48 ppm (d), δ_{minor} 5.62 ppm (d). The title compound was isolated by flash column chromatography (Toluene/ Diethyl ether, 98:2) in 75% yield and 98% e.e.. The e.e. was determined by HPLC analysis on a Daicel Chiralpak IB column: 80:20 hexane/*i*- rOH, flow rate 1.00 mL/min, λ = 254 nm: τ_{major} = 8.7 min, τ_{minor} = 6.5 min.

$[\alpha]_{26}^{D}$= -14.9 (*c* = 1.18, $CHCl_3$, dr = 8:1, ee = 98%).

HRMS *calc* for ($C_{34}H_{39}NO_8Na$): 612.2573 *found* 612.2581.

^{1}H NMR (400 MHz, $CDCl_3$): 8.03 (m, 3H), 7.60 (m, 1H), 7.49 (m, 2H), 6.88 (m, 2H), 6.61 (m, 1H), 5.48 (d, 1H, *J* = 15.71 Hz), 4.10 (m, 2H), 3.96 (m, 2H), 3.90-3.77 (m, 4H), 3.67-3.45 (m, 2H), 3.293.15 (m, 2H), 2.90 (m, 1H), 2.42 (m, 1H), 1.69 (s, 9H), 1.23 (t, 3H, *J* = 6.87), 1.07 (t, 3H, *J* = 7.13) ppm. ^{13}C NMR (400 MHz, $CDCl_3$): δ 203.81, 173.81, 166.07, 155.84, 150.29, 144.39, 137.99, 135.00, 133.57, 131.32, 128.90, 128.78, 124.93, 116.57, 116.27, 111.57, 102.74, 84.04, 61.23,

60.36, 55.90, 46.89, 44.48, 36.96, 34.37, 28.45, 14.37, 14.02 ppm.

(2*S*,3*S*,4*S*)-*tert*-butyl 2-benzoyl-3-cyano-4-((E)-4-ethoxy-4-oxobut-2-en-1-yl)-3,4-dihydro-1Hcarbazole-9(2H)-carboxylate (36m)

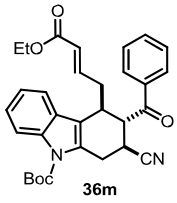

36m

The reaction was carried out following the general procedure at 50 °C to furnish after 64 h the crude product as a >20:1 mixture of diastereoisomers. The title compound was isolated by flash column chromatography (Hexane/ Ethyl Acetate, 10:1) in 71% yield and 98% e.e.. The e.e. was determined by HPLC analysis on a Daicel Chiralpak IB column: 70:30 hexane/*i*-PrOH, flow rate 1.00 mL/min, λ = 254 nm: τ_{major} = 9.9 min, τ_{minor} = 7.4 min.

$[\alpha]_{26}^{D}$= +10.1 (*c* = 1.00, $CHCl_3$, dr = 1, ee = 98%).

HRMS *calc* for ($C_{31}H_{32}N_2O_5Na$): 535.2209 *found* 535.2207.

^{1}H NMR (400 MHz, $CDCl_3$): *δ* 8.17 (d, 1H, *J* = 8.17 Hz), 7.95 (d, 2H, *J* = 7.91 Hz), 7.65 (m, 1H), 7.52 (m, 2H), 7.41 (d, 1H, *J* = 7.39 Hz), 7.30 (m, 1H), 7.20 (m, 1H), 6.83 (m, 1H), 5.82 (d, 1H, *J* = 15.82 Hz), 4.16 (m, 2H), 4.02 (m, 1H), 3.81-3.63 (m, 2H), 3.55-3.36 (m, 2H), 3.06 (m, 1H), 2.73 (m, 1H), 1.71 (s, 9H), 1.28 (t, 3H, *J* = 6.87) ppm. ^{13}C NMR (400 MHz, $CDCl_3$): *δ* 200.46, 166.01, 150.20, 144.42, 136.45, 136.35, 134.23, 131.50, 129.16, 128.81, 127.64, 125.63, 124.55, 122.98, 121.08, 118.56, 116.03, 116.00, 84.70, 60.56, 45.53, 35.60, 35.50, 28.42, 27.44, 14.38 ppm.

Table 5. Results using catalyst (*S*)-**28** to obtain the opposite enantiomer of the product (***ent*-36**)

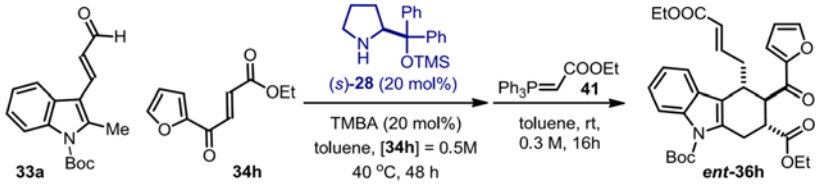

Entry	**36**	Yield (%)[b]	dr (%)[c]	*ee* (%)[d]
1	**ent-h**	88	>20:1	97
2	**ent-i**	80	>20:1	98
3	**ent-l**	86	8:1	98
4	**ent-m**	72	>20:1	98

a b c

Reactions were carried out on a 0.1 mmol scale. Yields of isolated products Diastereomeric ratios (dr) were determined by means of ^{1}H NMR analysis of the crude mixture. [d] Enantiomeric excess (*ee*) values were determined with HPLC analysis on commercially available chiral stationary phases.

3.7.4 General Procedure for One-Pot Diels Alder/Benzoin Condesation

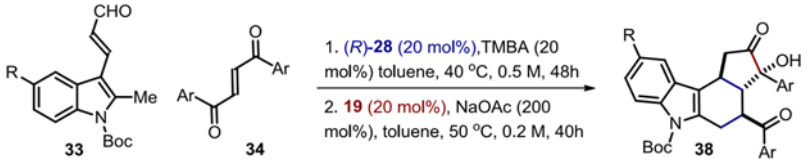

All the reactions were carried out in toluene of synthesis grade (>99%), without any precaution to exclude air and moisture (open air chemistry on the benchtop). An ordinary vial equipped with a Teflon-coated stir bar and a plastic screw cap was charged with (*R*)-2(diphenyl((trimethylsilyl)oxy)methyl)pyrrolidine **28** (0.02 mmol, 6.5 mg, 20 mol%). Then, 2,4,6trimethylbenzoic acid (TMBA, 0.02 mmol, 3.2 mg, 20 mol%) and toluene (0.2 mL) were added in one portion and the resulting solution was stirred at ambient temperature for 5 minutes to allow the catalyst salt formation. The reaction was started by the sequential addition of the aldehyde **33a** (0.12 mmol, 34.2 mg, 1.2 eq) and the dibenzoylethylenes **34** (0.1 mmol, 23.6 mg). The vial was sealed and immerged in a oil bath (thermostated at 40°C). After 48 hours the vial was removed from the oil bath and cooled until room temperature. Then, 0.3 ml of toluene, sodium acetate (0.2 mmol, 16.4 mg, 2 eq) and 6,7-dihydro-2-pentafluorophenyl-5H-pyrrolo[2,1c]-1,2,4-triazolium tetrafluoroborate **19** (0.02 mmol, 7.2 mg, 20 mol%) were added sequentially and the resulting solution was stirred at 50°C for 40 hours. The reaction was cooled down to ambient temperature and quenched with an aqueous solution of sodium bicarbonate (0.2 mmol, 16.8 mg, 2 eq in 1ml of water). The mixture was stirred for 30 minutes and the crude product was extracted 3 times with ethyl acetate. The organic phase was dried with anhydrous sodium sulfate, filtered and the solvent was removed under vacuum. The product **38** was isolated by flash column chromatography.

(3*S*,3a*S*,4*S*,10c*S*)-*tert*-butyl 4-benzoyl-3-hydroxy-2-oxo-3-phenyl-1,3,3a,4,5,10chexahydrocyclopenta[c]carbazole-6(2H)-carboxylate (38a)

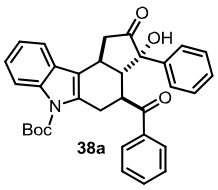

38a

The reaction was carried out following the general procedure to furnish after 88 h the crude product as a 8:1 mixture of diastereoisomers. The title compound was isolated by flash column chromatography (Hexane/ Ethyl Acetate, 12:1-10:1) in 40% yield and 99% e.e.. The e.e. was determined by HPLC analysis on a Daicel Chiralpak IC column: 80:20 hexane/*i*- rOH, flow rate 1.00 mL/min, λ = 254 nm: τ_{major} = 6.5 min,

τ_{minor} = 10.7 min.

$[\alpha]_{26}^{D}$= -24.4 (*c* = 0.56, $CHCl_3$, dr = 1, ee = 99%).

HRMS *calc* for ($C_{33}H_{31}NO_5Na$): 544.2100 *found* 544.2100.

^{1}H NMR (400 MHz, $CDCl_3$): *δ* 8.19 (d, 1H, *J* = 8.17 Hz), 7.86 (d, 2H, *J* = 8.08 Hz), 7.59 (m, 1H), 7.517.42 (m, 3H), 7.32-7.25 (m, 2H), 7.23 (m, 1H), 7.17 (m, 2H), 6.89 (d, 2H, *J* = 7.56 Hz), 4.38 (m, 1H), 3.78 (m, 1H), 3.50-3.41 (m, 2H), 3.34 (ddd, 1H, *J* = 18.19 Hz, *J* = 10.63 Hz, *J* = 3.08 Hz), 2.87 (m, 1H), 2.68 (dd, 1H, *J* = 17.07 Hz, *J* = 13.15 Hz), 2.50 (bs, 1H), 1.59 (s, 9H) ppm. ^{13}C NMR (400 MHz, $CDCl_3$): *δ* 215.88, 201.30, 150.47, 140.20, 137.41, 136.21, 134.04, 133.37, 128.84, 128.56, 128.30, 128.09, 127.91, 125.93, 123.93, 123.00, 118.50, 117.66, 116.02, 84.21, 80.14, 55.94,
42.86, 40.74, 34.51, 29.84, 28.32 ppm.

(3*S*,3a*S*,4*S*,10c*S*)-*tert*-butyl 4-(4-chlorobenzoyl)-3-(4-chlorophenyl)-3-hydroxy-2-oxo1,3,3a,4,5,10c-hexahydrocyclopenta[c]carbazole-6(2H)-carboxylate (38b)

The reaction was carried out following the general procedure to furnish after 88 h the crude product as a 6:1 mixture of diastereoisomers. The title compound was isolated by flash column chromatography (Hexane/ Ethyl Acetate, 12:1) in 53% yield and 99% e.e.. The e.e. was determined by HPLC analysis on a Daicel Chiralpak IC column: 80:20 hexane/*i*- rOH, flow rate 1.00 mL/min, λ = 254 nm: τ_{major} = 5.2 min, τ_{minor} = 8.1 min.

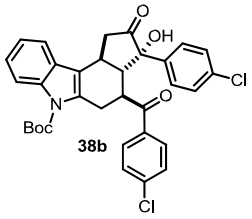

$[\alpha]_{26}^{D}$= -26.3 (*c* = 1.02, $CHCl_3$, dr = 1, ee = 99%).

HRMS *calc* for ($C_{33}H_{29}NO_5NaCl_2$): 612.1320 *found* 612.1309.

^{1}H NMR (400 MHz, $CDCl_3$): δ 8.17 (d, 1H, *J* = 8.18 Hz), 7.82 (d, 2H, *J* = 8.73 Hz), 7.48-7.41 (m, 3H), 7.31 (m, 1H), 7.27 (m, 1H), 7.13 (d, 2H, *J* = 8.65 Hz), 6.81 (d, 2H, *J* = 8.65 Hz), 4.30 (m, 1H), 3.74 (m, 1H), 3.44 (m, 2H), 3.33 (ddd, 1H, *J* = 18.29 Hz, *J* = 10.52 Hz, *J* = 3.01 Hz), 2.80 (m, 1H), 2.702.60 (m, 2H), 1.60 (s, 9H) ppm. ^{13}C NMR (400 MHz, $CDCl_3$): δ 215.36, 200.18, 150.45, 140.10, 138.78, 136.14, 135.47, 133.85, 133.81, 130.28, 128.99, 128.28, 128.16, 126.72, 124.04, 123.06, 118.49, 117.46, 116.05, 84.35, 79.85, 55.85, 42.71, 40.65, 34.46, 31.70, 28.32 ppm. **(3*S*,3a*S*,4*S*,10c*S*)-*tert*-butyl 9-chloro-4-(4-chlorobenzoyl)-3-(4-chlorophenyl)-3-hydroxy-2-oxo-1,3,3a,4,5,10c-hexahydrocyclopenta[c]carbazole-6(2H)-carboxylate (38c)**

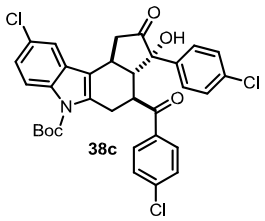

The reaction was carried out following the general procedure to furnish after 88 h the crude product as a 6:1 mixture of diastereoisomers. The title compound was isolated by flash column chromatography (Hexane/ Ethyl Acetate, 12:1) in 61% yield and 97% e.e.. The e.e. was determined by HPLC analysis on a Daicel Chiralpak IA column: 80:20 hexane/*i*-PrOH, flow rate 1.00 mL/min, λ = 254 nm: τ_{major} = 9.8 min, τ_{minor} = 7.1 min. $[\alpha]_{26}^{D}$= -28.7 (*c* = 0.54, $CHCl_3$, dr = 1, ee = 97%).

HRMS *calc* for ($C_{33}H_{27}NO_5Cl_3$): 622.0955 *found* 622.0939.

^{1}H NMR (400 MHz, $CDCl_3$): δ 8.08 (d, 1H, *J* = 8.95 Hz), 7.81 (d, 1H, *J* = 8.50 Hz), 7.44 (d, 1H, *J* = 8.50 Hz), 7.42 (d, 1H, *J* = 1.93 Hz), 7.25 (m, 1H), 7.13 (d, 2H, *J* = 8.32 Hz), 6.80 (d, 2H, *J* = 8.32 Hz), 4.29 (m, 1H), 3.71 (m, 1H), 3.42 (m, 2H), 3.32 (ddd, 1H, *J* = 18.40 Hz, *J* = 10.44 Hz, *J* = 3.01 Hz), 2.78 (m, 1H), 2.64 (dd, 1H, *J* = 17.65 Hz, *J* = 13.34 Hz), 2.54 (bs, 1H), 1.59 (s, 9H) ppm. ^{13}C NMR (400 MHz, $CDCl_3$): δ 214.69, 199.99, 150.09, 140.23, 138.59, 135.39, 135.35, 134.55, 133.94, 130.29, 129.32, 129.02, 128.68, 128.33, 126.70, 124.10, 118.12, 117.06, 116.91, 84.84, 79.79, 55.80, 42.46, 40.44, 34.27, 31.71, 28.30 ppm.

(3*S*,3a*S*,4*S*,10c*S*)-*tert*-butyl 4-(4-chlorobenzoyl)-3-(4-chlorophenyl)-3-hydroxy 9-methoxy-2oxo-1,3,3a,4,5,10c-hexahydrocyclopenta[c]carbazole-6(2H)-carboxylate (38d)

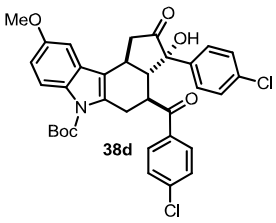

The reaction was carried out following the general procedure to furnish after 88 h the crude product as a 6:1 mixture of diastereoisomers. The title compound was isolated by flash column chromatography (Hexane/ Ethyl Acetate, 8:1-6:1) in 66% yield and 99% e.e.. The e.e. was determined by HPLC analysis on a Daicel Chiralpak IA column: 80:20 hexane/*i*-PrOH, flow rate 1.00 mL/min, λ = 254 nm: τ_{major} = 13.8 min, τ_{minor} = 10.2 min.

$[\alpha]_{26}^{D}$= -35.7 (*c* = 0.88, $CHCl_3$, dr = 1, ee = 99%).

HRMS *calc* for ($C_{34}H_{30}NO_6Cl_2$): 618.1450 *found* 618.1462.

^{1}H NMR (400 MHz, $CDCl_3$): δ 8.05 (d, 1H, *J* = 9.85 Hz), 7.81 (d, 1H, *J* = 8.62 Hz), 7.44 (d, 1H, *J* = 8.62 Hz), 7.15 (d, 2H, *J* = 8.45 Hz), 6.91 (m, 2H), 6.82 (d, 2H, *J* = 8.45 Hz), 4.29 (m, 1H), 3.88 (s, 3H), 3.72 (m, 1H), 3.44 (m, 2H), 3.31 (ddd, 1H, *J* = 18.30 Hz, *J* = 10.66 Hz, *J* = 3.02 Hz), 2.80 (m, 1H), 2.67 (dd, 1H, *J* = 17.50 Hz, *J* = 13.48 Hz), 2.44 (bs, 1H), 1.59 (s, 9H) ppm. ^{13}C NMR (400 MHz, $CDCl_3$): δ 215.25, 200.13, 156.07, 150.37, 140.11, 138.75, 135.47, 134.60, 133.87, 130.82, 130.27, 128.99, 128.30, 126.69, 117.24, 116.77, 111.82, 101.92, 84.18, 79.85, 55.89, 55.84, 42.65, 40.62, 34.42, 31.77, 28.34 ppm.

Table 6. Results using catalyst (*S*)-**28** to obtain the opposite enantiomer of the product (***ent*-38**)

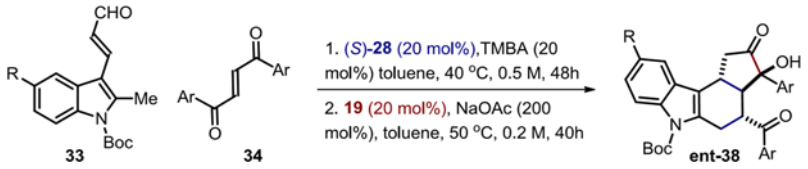

Entry	**38**	Yield (%)[b]	dr (%)[c]	*ee* (%)[d]
1	**ent-a**	42	8:1	99
2	**ent-b**	54	6:1	99
3	**ent-c**	62	6:1	97
4	**ent-d**	66	6:1	99

[a] Reactions were carried out on a 0.1 mmol scale. [b] Yields of isolated products. [c] Diastereomeric ratios (dr) were determined by means of ^{1}H NMR analysis of the crude mixture. [d] Enantiomeric excess (*ee*) values were determined with HPLC analysis on commercially available chiral stationary phases.

3.7.5 Single Crystal X-Ray Diffraction Data for Compound 37b

X-ray structure determinations: Crystals of **38b** (obtained by using aminocatalyst (*R*)-**28**) were obtained by slow evaporation of DCM at room temperature. The measured crystals were stable under atmosphere conditions.

Data Collection. Measurements were made on a Bruker-Nonius diffractometer equipped with an APPEX 2 4K CCD area detector, a FR591 rotating anode with Mo radiation, Montel mirrors and a

Cryostream Plus low temperature device (*T* = -173 ˚C). Full-sphere data collection was used and scans.

Programs used: Data collection Apex2 V2010 7.0 (Bruker-Nonius 2008), data reduction Saint + Version 7.60A (Bruker AXS 2008) and absorption correction SADABS.

Structure Solution. SIR2007 program was used.[103]

Structure Refinement. SHELXTL-97.[32]

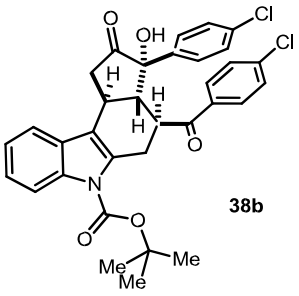

38b

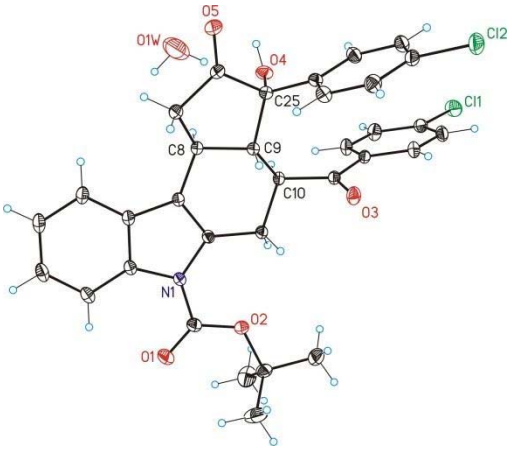

Crystal data for **38b** at 293(2) K: **CCDC 862664**

[103] R.Caliandro, B. Carrozzini, G.L.Cascarano, L. De Caro, C. Giacovazzo and D. Siliqi. Advances in ab Initio Protein Phasing by Patterson Deconvolution Techniques *J. Appl. Cryst.* **2007**, *40*, 883. [32] G.M. Sheldrick. A Short History of SHELX. *Acta Crys.* **2008**, A64, 112.

UNIVERSITAT ROVIRA I VIRGILI
NOVEL AMINOCATALYTIC AND PHOTOCHEMICAL REACTIONS
Manuel Nappi

Chapter V Direct β-Functionalization of Cyclic Ketones with Aryl Ketones via the Merger of Photoredox and Organocatalysis

Target

Developing a formal β-aldol reaction by the direct β-coupling of cyclic ketones with aryl ketones to produce γ-hydroxyketones.

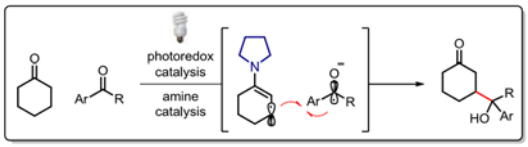

Tool

The synergistic combination of photoredox catalysis and aminocatalysis to transiently generate β-enaminyl radical (5πe⁻) species and ketyl radicals.[104]

Chemists have been always fascinated by the possibility to promote organic reactions using the energy of the light. Since most of the organic molecules only absorb UV light, almost all the photochemical reactions discovered are based on the use of high energy photons and harmful UV lamps in harsh protocols. Only few methods are available to exploit the more convenient and readily available visible light. One of these methodologies relies upon the use of metalbased complexes that, upon absorption of visible light, can transfer or accept an electron to promote a redox reaction. The most studied one-electron photoredox catalysts are ruthenium- and iridium-based complexes. These inorganic complexes have facilitated important advances in the areas of energy storage, hydrogen and oxygen evolution from water, and methane production from carbon dioxide.[105] Only very recently, they found application in organic chemistry and their combination with other types of catalysis (i.e. aminocatalysis, acid and metal catalysis) [106] allowed the development of unprecedented transformations.

During a research period at Princeton University, I had the chance to get involved in research dealing with the use of visible light-photocatalysts to develop novel synthetic transformation. To provide the

[104] The ork discussed in this chapter has been published. see: . . Petroni evic , M. Nappi, D. W. C. MacMillan. Direct β-Functionalization of Cyclic Ketones with Aryl Ketones via the Merger of Photoredox and Organocatalysis. *J. Am. Chem. Soc.* **2013**, *135*, 323. . . Petroni evic finished the optimization studies of the aryl-alkyl ketone system and developed almost the entire scope of the reaction.

[105] a) K. Kalyanasundaram. Photophysics, Photochemistry and Solar Energy Conversion with Tris(bipyridyl)ruthenium(II) and its Analogues. *Coord. Chem. Rev.* **1982**, *46*, 159; b) A. Juris, V. Balzani, F. Barigelletti, S. Campagna, P. Belser, A. von Zelewsky. Ru(II) Polypyridine Complexes: Photophysics, Photochemistry, Eletrochemistry, and Chemiluminescence. *Coord. Chem. Rev.* **1988**, *84*, 85.

[106] M. N. Hopkinson, B. Sahoo, J.-L. Li, F. Glorius. Dual Catalysis Sees the Light: Combining Photoredox with Organo-, Acid, and Transition-Metal Catalysis. *Chem. Eur. J.* **2014**, *20*, 3874.

readers with an overview of the emerging field of visible light-photoredox catalysis, some basic principles will be discussed in the next section. In particular, the discussion will explain how visible light, interacting with matter, can promote chemical reactions and the photochemical mode of action of ruthenium- and iridium- based inorganic complexes.

5.1 Principles of Photochemistry and Photoredox Catalysis

The interaction of the light with a molecule can lead to photophysical and photochemical processes, depending if the molecular structure remains unchanged or not, respectively. In 1935, Jablonski introduced the homonymous diagram to simply describe how the light interacts with matter (Figure 1).[107] According to the Stark-Einstein law, a molecule only absorbs light that leads to a single electron transition; this means that the energy of the light has to match the difference in energy between the ground state (S_0, if singlet state) and a specific excited state
(S_1, S_2, etc.; Figure 1, transition 1)

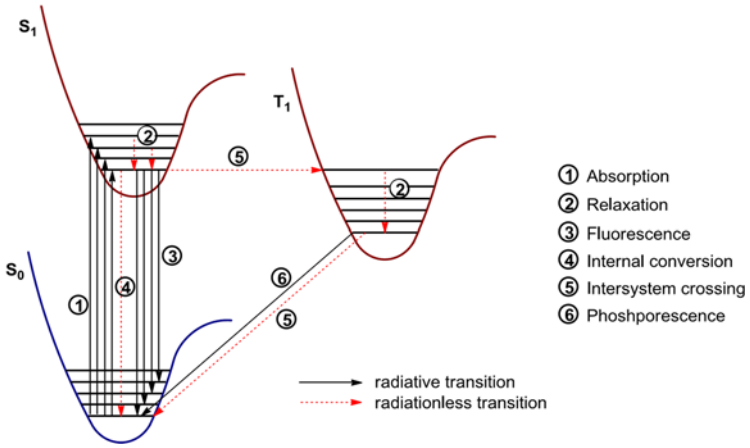

Figure 1. Jablonski diagram: interaction of light with matter.[4]

After absorption, according to the Kasha's rule, the relaxations of high energy excited states (S_2, S_3, etc.) to the lowest one in energy (S_1), as well as the relaxations of high energy vibrational levels to the minimum one (transitions 2), are usually very fast in comparison with all the other processes that can occur. Different transitions can then happen when a molecule reaches its minimum vibrational level within the lowest excited state (S_1): i) *fluorescence* (transition 3) radiative decay to the ground state (S_0) which emits a photon of a specific energy; ii) *internal conversion* (transition 4) - radiationless decay to the ground state producing heat in the media; or iii) *intersystem crossing* (ISC, transition 5) - interconversion to a different spin state (i.e. T_1,

[107] E. V. Anslyn, D. A. Dougherty, In *Modern Physical Organic Chemistry*, 3rd ed.; University science books, Sausalito-California, 2006.

triplet state). The intersystem crossing is a spin forbidden transition, thus the triplet state is a long-life state. The radiative decay of the excited triplet state to the ground singlet state is called *phosphorescence* (transition 6). In this case, the energy of the photon equals the energy difference of the two states; consequently, *phosphorescence* is a lower energy radiative decay than *fluorescence*.

In addition to the previously discussed monomolecular photophysical behavior, further multimolecular processes exist; *e.g.* bimolecular interactions, which are strictly connected with the possibility to have a productive chemical reaction. In productive bimolecular photophysical processes, when an excited molecule in its single or triplet state (E) meets another molecule in its ground state (G), three different general transitions, or quenching of the excited state of E, are normally possible (Scheme 1): i) energy transfer (or sensitization), ii) oxidative quenching via photoinduced electron transfer (PET) and iii) reductive quenching via PET. Bimolecular photophysical processes can occur only if they are faster or at least they can compete with the rate of all the radiative and radiationless monomolecular decays (fluorescence, internal conversion, ISC and phosphorescence).

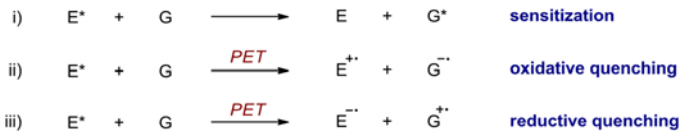

Scheme 1. Bimolecular photophysical processes between a molecule in its excited states (E*) and another molecule in its ground state (G).

The photoinduced electron transfer processes involve molecules in the excited state that have an electron in an anti-bonding molecular orbital (often the LUMO). The excited state exhibits a significantly different reduction potential than the ground state. Indeed, the fact that the highenergy electron is relatively easy to remove, makes the excited state a good donor and reductant. On the other hand, due to the vacancy in the bonding molecular orbital (HOMO), the excited state is also easier to reduce, which makes it also a good acceptor and oxidant.

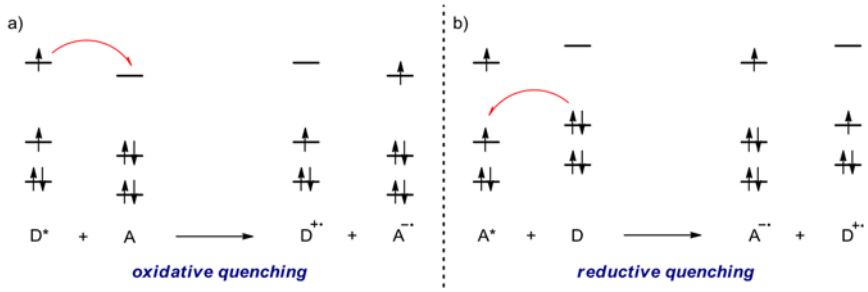

Figure 2. Oxidative and reductive quenching via photoinduced elctron transfer (PET).

Consequently, the excited state can easily participate in electron transfer processes: when the ground state of another molecule has a low energy LUMO, the excited state becomes a donor (D)

and reduces the molecule (A, *oxidative quenching*, Figure 2a); while if the ground state of the other molecule has a high energy HOMO, the excited state acts as acceptor (A) and oxidizes the partner (D, *reductive quenching*, Figure 2b).

The photoinduced electron transfer is a key process to promote a redox reaction catalyzed by light. It allows the reduction or the oxidation of an initial substrate, which product could undergo consequent chemical transformations. The most studied one-electron photoredox catalysts, which can absorb visible light and promote chemical transformations via PET, are ruthenium- and iridium-based complexes. In particular, polypyridyl complexes are the most employed in organic chemistry.[108] Absorption of photons in the high-energy visible region (454 and 375 nm for Ru and Ir, respectively) promotes a metal-to-ligand electronic transition (MLCT) leading to the formation of stable, long lifetime (τ) triplet states *via* ISC (1100 and 1900 ns for Ru and Ir, Figure 3).

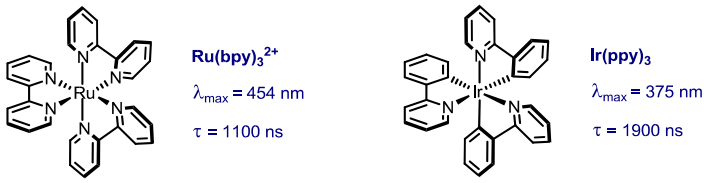

Figure 3. Polypyridyl complexes of ruthenium and iridium: $Ru(bpy)_3$ and $Ir(ppy)_3$.

While the ground states of these complexes are practically inactive in redox processes, the unique properties of their excited triplet states allow their use as photocatalysts in many organic reactions. The excited triplet state of $Ru(bpy)_3^{2+}$ is a good donor and a good acceptor at the same time, given its negative reduction potential for the *oxidative quenching* ($E_{1/2}^{III/II*}$ = -0.76 V) and its positive reduction potential in the *reductive quenching* ($E_{1/2}^{II*/I}$ = +0.67 V), Scheme 2.

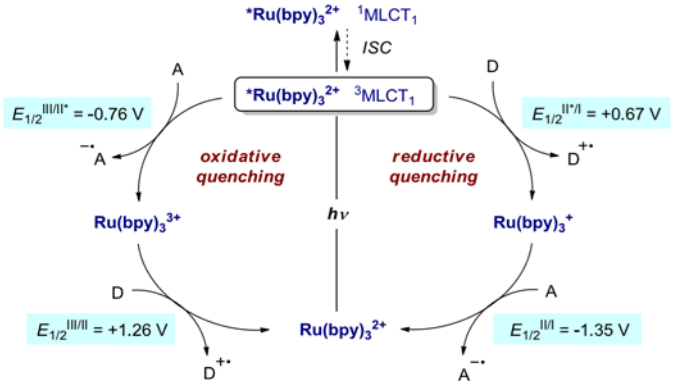

Scheme 2. Oxidative and reductive quenching cycle of $Ru(bpy)_3^{2+}$. A = acceptor; D = donor.

[108] a) C. K. Prier, D. A. Rankic, D. W. C. MacMillan. Visible Light Photoredox Catalysis with Transition Metal Complexes: Applications in Organic Synthesis. *Chem. Rev.* **2013**, *113*, 5322. b) J. W. Tucker, C. R. J. Stephenson. Shining Light on Photoredox Catalysis: Theory and Synthetic Applications. *J. Org. Chem.* **2012**, *77*, 1617.

This means that two different photocatalytic cycles are accessible depending on the type of redox process needed for the chemical reaction to proceed. For instance, if the first step requires the reduction of an acceptor (A), the excited $*Ru(bpy)_3^{2+}$ is oxidized to $Ru(bpy)_3^{3+}$ in the first photoinduced electron transfer (PET) (*oxidative quenching* cycle). The resulting Ru(III) complex is a powerful oxidant ($E_{1/2}^{III/II}$ = +1.26 V), which can oxidize a donor (D) and return to its ground state Ru(II). However, if the first step requires the oxidation of a donor (D), the excited $*Ru(bpy)_3^{2+}$ is reduced to $Ru(bpy)_3^{+}$ via PET (*reductive quenching* cycle). At this point, the Ru(I) complex acts as a powerful reductant ($E_{1/2}^{II/I}$ = -1.35 V), which can reduce an acceptor (A) and return to its Ru(II) ground state. Note that both of the cycles are redox neutral; for each cycle one donor is oxidized and one acceptor is reduced. Thus, the participation of one of the quenching cycle against the other completely depends on the reduction potentials of the donor and the acceptor. For example, an acceptor that has $E_{1/2}$ = -1.05 V cannot be reduced directly by the excited $*Ru(bpy)_3^{2+}$ ($E_{1/2}^{III/II*}$ = -0.76 V) in the *oxidative quenching* cycle, but can be only reduced by $Ru(bpy)_3^{+}$ ($E_{1/2}^{II/I}$ = -1.35 V) in the *reductive quenching* cycle. Consequently, the *reductive quenching* cycle is the only possible pathway for the reduction of that acceptor. Of course, the appropriate donor ($E_{1/2}^{D}$ < $E_{1/2}^{II*/I}$ = +0.67 V) has to be present in the reaction to start the *reductive quenching* cycle and reduce the excited $*Ru(bpy)_3^{2+}$ to $Ru(bpy)_3^{+}$.

The flexibility of the ruthenium and iridium based photocatalysts to undergo both *oxidative* and *reductive quenching* furnishing two different photocatalytic cycles, explains why they served to promote many organic transformations. Iridium photocatalysts, such as $Ir(ppy)_3$ (ppy = 2phenylpyridinato-C^2,*N*), are useful to achieve the reduction of particular challenging substrates, due to their strong reducing ability. The potential energy associated with the oxidative quenching of the excited triplet state is very low ($E_{1/2}^{+1/0*}$ = -1.73 V),[109] which makes $Ir(ppy)_3$ a very strong reductant (Scheme 3).

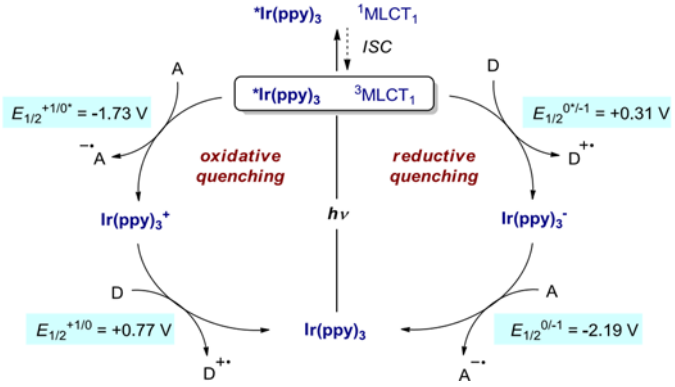

[109] The standard reduction potential of $Ir(ppy)_3$ refers to the overall **charge** of the complex, and not to the oxidation state of the Ir (in this case Ir III). It is worthy of note that ppy is an anionic ligand. This notion will be followed within the entire Chapter.

Scheme 3. Oxidative and reductive quenching cycle of $Ir(ppy)_3$. A = acceptor; D = donor.

Moreover, $Ir(ppy)_3^-$ formed during the *reductive quenching* is even a better donor, having a extremely negative reduction potential; $E_{1/2}^{0/-1}$ = -2.19 V.

As with all the chemical processes, the occurrence of electron transfers is governed not only by thermodynamic factors but also by the kinetics of the system.

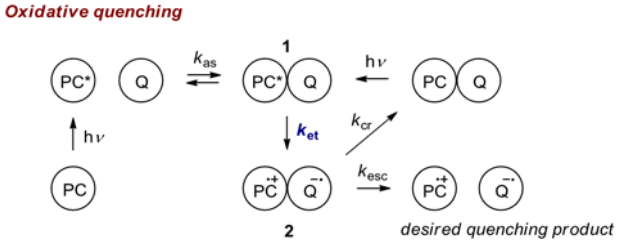

Scheme 4. Processes involved in oxidative quenching photoinduced electron transfer. PC = photocatalyst; Q = quencher.

As described in Scheme 4, after the excitation of the photoredox catalyst *via* light absorption, the reaction begins with the association of the excited photocatalyst and the quencher. The formation of the solvated complex **1** is required to allow the electron transfer. The PET generates the charged diradical complex **2**. At this point, the components in **2** could escape from the solvent cage yielding the desired quenching products. Alternatively, charge recombination (back electron transfer) can occur to regenerate the quencher along with the ground-state photocatalyst. The relative rates of all these processes are critical in order to have the productive generation of the quenching products. The rate of electron transfer is well predicted by the Marcus theory (not discussed within this chapter).[110]

In summary, while favorable thermodynamics are critical, the successful implementation of a reaction design and mechanistic understanding requires the consideration of the proper kinetics for the various steps associated with the net electron-transfer process. Indeed, as described in Schemes 2 and 3, for any closed photoredox catalytic cycle there are at least two outer-sphere electron transfer processes that must occur: i) an electron transfer to quench the excited state of the photocatalyst and ii) a subsequent electron transfer to regenerate the ground-state species.

[110] Marcus, R.A. On the Theory of Oxidation-Reduction Reactions Involving Electron Transfer. *J.Chem.Phys.* **1956**, *24*, 966.

5.2 Background of Visible Light Photoredox Catalysis

In 2008, the groups of MacMillan[111] and Yoon[112] independently demonstrated that visible light photoredox catalysis can impact modern organic synthesis. Yoon and coworkers described a photocatalyzed formal [2+2] cycloaddition of enones **3** (Scheme 5). $Ru(bpy)_3^{2+}$ was employed as the photocatalyst to reduce the starting ketones **3** and obtain radical anions **4** using a standard 275 W floodlight; no specialized high-pressure UV photolysis apparatus was required. A subsequent stepwise cyclization/protonation sequence afforded the substituted cyclobutane derivatives **5** in a good yield and in short reaction times.

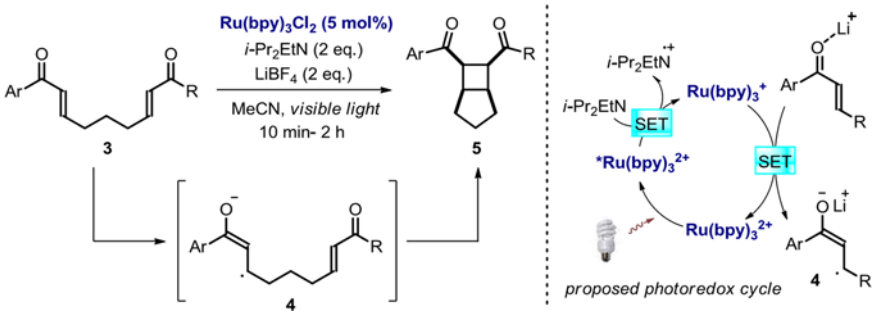

Scheme 5. Visible light photocatalyzed formal [2+2] cycloaddition of enones. SET = single electron transfer.

Control experiments revealed that all the components of the reaction were necessary to achieve reactivity. The authors suggested that the reductive quenching cycle of the photocatalyst was operative under the reaction conditions. No reactivity was observed in the absence of a suitable donor (the Hünig base), needed to reductively quench the excited $*Ru(bpy)_3^{2+}$. Moreover, it was proposed that the coordination of the lithium cation to the carbonyl increased the reduction potential of the vinyl-aryl ketone in order to allow the reduction with $Ru(bpy)_3^{+}$ ($E_{1/2}^{II/I}$ = -1.35 V).

Independently and concurrently with these studies, MacMillan and Nicewicz merged the use of visible light photoredox catalysis with an aminocatalytic system (Scheme 6).[8] This combination allowed the realization of the enantioselective α-alkylation of aldehydes, a sought-after yet elusive transformation in asymmetric catalysis. A simple compact fluorescence lamp (15 W CFL) was used as the source of visible light. According to the proposed mechanism, the imidazolidinone catalyst **8** activates the aldehyde via enamine (**9**) formation while the radical **10** is generated by the ruthenium (I) complex. In particular, the electron-deficient bromocompound **6** is reduced by $Ru(bpy)_3^{+}$ to the corresponding radical anion (not shown), which, upon rapid fragmentation (mesolysis) of the C-Br bond, releases the electrophilic radical **10** and the bromide. The

[111] D. Nicewicz, D. W. C. MacMillan. Merging Photoredox Catalysis with Organocatalysis: The Direct Asymmetric Alkylation of Aldehydes. *Science*, **2008**, *322*, 77.
[112] M. A. Ischay, M. E. Anzovino, J. Du, T. P. Yoon. Efficient Visible Light Photocatalysis of [2+2] Enone Cycloadditions. *J. Am. Chem. Soc.* **2008**, *130* (39), 12886.

combination of the chiral electron-rich enamine **9** with the radical **10** yields the α-amino radical **11**, which is prone to oxidation from the excited $Ru(bpy)_3^{2+}$. The photoredox cycle is thus closed. The hydrolysis of the iminium ion **12** provides the desired alkylated aldehyde **7** with high optical purity while the imidazolidinone **8** can restart another catalytic cycle. The first photoredox cycle is supposed to start with the oxidation of a sacrificial amount of enamine **9**, which leads to the formation of the strongly reducing Ru(I) (this step is not shown in Scheme 6).

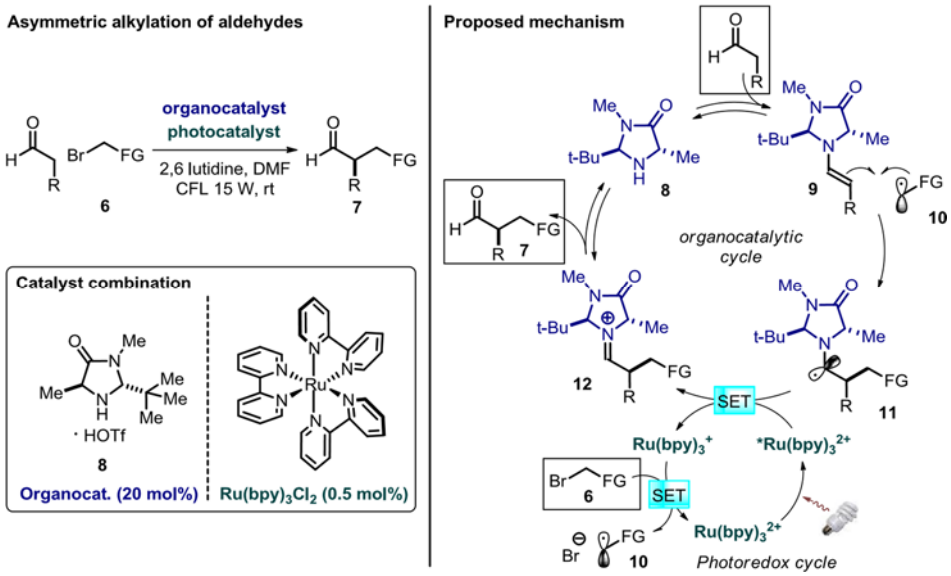

Scheme 6. Asymmetric organocatalytic photoredox alkylation of aldehydes and the proposed reaction mechanism. CFL = compact fluorescence lamp; SET = single electron transfer.

After the seminal works by Yoon and MacMillan, other reactions were developed using the photoredox strategy extending the number of transformations available in organic chemistry.[5] A major area in which photoredox catalysis has been employed is the oxidation of amines. Due to their electron-rich properties, amines are good donors and readily undergo single-electron oxidation to yield an aminium radical cation **13** (scheme 7).

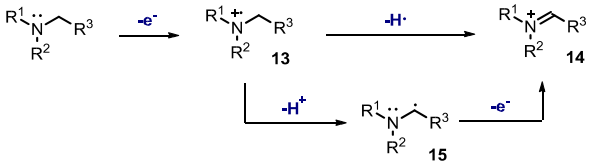

Scheme 7. Pathways of Amine Oxidation to Iminium Ions.

The oxidation of an amine has the effect of dramatically lowering the bond dissociation energy (BDE) of the C–H bonds at the amine α-position.[113] Thus, if a good hydrogen atom (H·) acceptor is present in the reaction media, the iminium ion **14** could be directly obtained. However, single electron oxidation of an amine also decreases the pK_a of the C-H bond in the α-position; typically the pK_a values range from 3 to 13 depending on the substrate.[114] Consequently, an appropriate base could deprotonate the aminium radical cation **13** to yield the α-amino radical **15**, which could be readily oxidized via a second single electron transfer to give the iminium ion **14**.

Stephenson and coworkers were the first to apply this strategy for trapping the photogenerated iminium ion of type **14** with a series of nucleophiles.[115] They developed in 2010 an aza-Henry reaction *via* the addition of nitromethane to a catalytically generated iminium ion **20** from Nphenyltetrahydroisoquinoline **16** (Scheme 8).

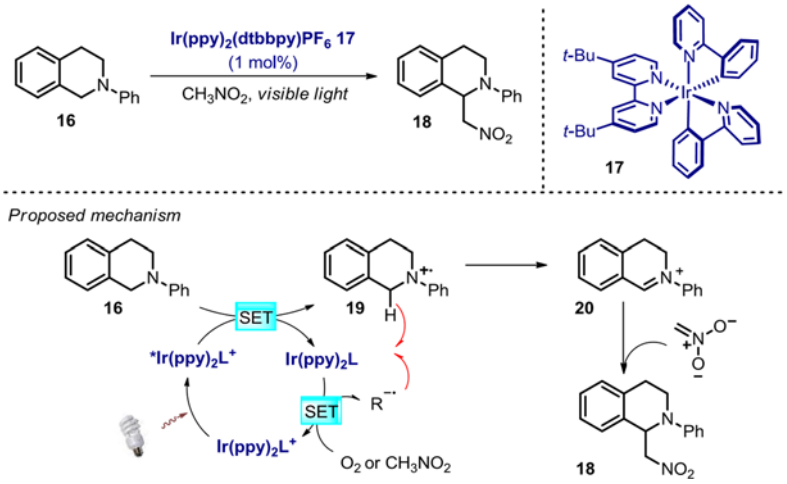

Scheme 8. Photoredox aza-Henry reaction via iminium intermediate. L = (dtbbpy)

As for the mechanism, Ir(ppy)$_2$(dtbbpy)$^+$ **17** oxidized amine **16** to afford the aminium radical **19** *via* reductive quenching. To close the photoredox cycle, Ir(ppy)$_2$(dtbbpy) reduced molecular oxygen or nitromethane. The corresponding radical anions then abstracted a hydrogen atom from the aminium radical **19** to generate the iminium ion **20**, which was then trapped by nitromethane anion to yield product **18**. After this example, other photoredox reactions have been published employing different nucleophiles to trap the photogenerated iminium ions.[5]

---

[113] J. P. Dinnocenzo, T. E. Banach. Deprotonation of Tertiary Amine Cation Radicals. A Direct Experimental Approach. *J. Am. Chem. Soc.* **1989**, *111*, 8646.
[114] V. D. Parker, M. Tilset. Facile Proton-Transfer Reactions of N,N-Dimethylaniline Cation Radicals. *J. Am. Chem. Soc.* **1991**, *113*, 8778.
[115] A. G. Condie, J. C. Gonzalez-Gomez, C. R. J. Stephenson. Visible-Light Photoredox Catalysis: AzaHenry Reactions *via* C-H Functionalization. *J. Am. Chem. Soc.* **2010**, *132*, 1464.

As describe in Scheme 7, α-amino radicals **15** can be obtained by simple deprotonation of the aminium radical cation **13**. Although these species often serve as intermediates along the path to iminium ions, they may also be employed as reactive intermediates in their own right to perform unique transformations. In 2011, MacMillan and colleagues reported an unprecedented photocatalyzed α-arylation of tertiary amines (Scheme 9).[116] $Ir(ppy)_3$ was used as the visible light photocatalyst to promote the reaction of cyclic amines, such as N-phenylpyrrolidine **21,** and benzonitriles, such as 1,4-dicyanobenzene **22,** to give benzylic amine products **23**. The key step was the C-C bond formation between the α position of the amine and the *ipso* position in the benzonitriles, displacing cyanide as a leaving group (Scheme 9). Crucial was the choice of $Ir(ppy)_3$ ($E_{1/2}{}^{0*/+1}$ = -1.73 V) for the reduction of 1,4-dicyanobenzene **22**, given its relatively low reduction potential to generate the long-lived radical anion **24** ($E_{1/2}$ = -1.61 V). $Ir(ppy)_3{}^+$ ($E_{1/2}{}^{0/+1}$ = +0.77 V) then oxidized N-phenylpyrrolidine **21** to its aminium radical cation **25**; the C–H bonds adjacent to the nitrogen in **25** are weakened by about 40 kcal/mol and could undergo deprotonation by sodium acetate to give the α-amino radical **26**.

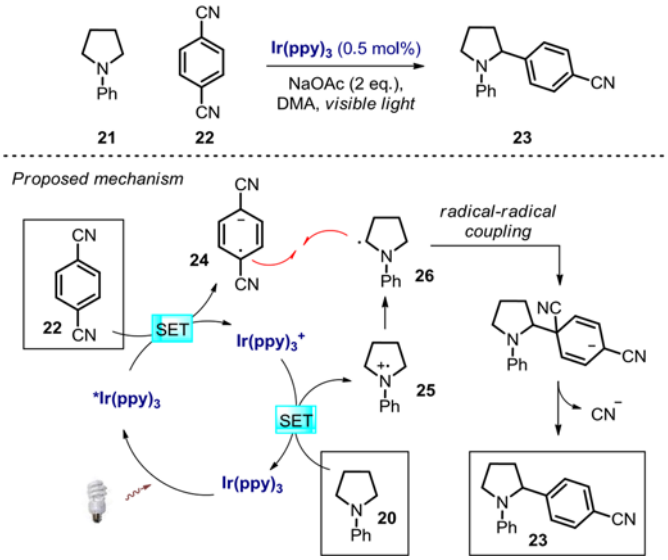

Scheme 9. Photoredox α-amino C–H arylation reaction of tertiary amines.

Radical-radical coupling between the persistent radical anion **24**[117] and α-amino radical **26** was the central C-C bond forming step to obtain the α-arylated products **23** upon rearomatization and leaving of the cyanide.

---

[116] A. McNally, C. K. Prier, D. W. C. MacMillan. Discovery of an α-Amino C–H Arylation Reaction Using the Strategy of Accelerated Serendipity. *Science* **2011**, *334*, 1114.

[117] E. V. Panteleeva, T. A. Vaganova, V. D. Shteingarts, I. I. Bilkis. Evidence for the Transition from S_N to ET Mechanism in the Reaction of Arene Radical Anion with Alkyl Halide Evoked by the Introduction of an Electron Withdrawing Substituent into Radical Anion. *Tetrahedron Lett.* **1995**, *36*, 8465.

The chemistry relies upon the radical-radical hetero-coupling between two open-shell intermediates. This bimolecular event is possible only when one of the species is a persistent radical, as described by the persistent radical effect (PRE).[118] The PRE is a general principle that explains the highly specific formation of the cross-coupling product (R^1-R^2) between two radicals R^1 and R^2, when one species is persistent (long lived) while the other is transient, and assuming that the two radicals are formed at equal rates. The initial buildup in concentration of the persistent species, caused by the self-termination of the transient radical, steers the reaction to follow a single pathway, that is, the cross reaction. In the chemistry of Scheme 9, the radical anion **24** acts as the long-lived intermediate, a feature which allowed **24** to participate in the cross coupling reactions, *e.g.* **24** is the long-lived radical species involved in the reported photochemical nucleophile-olefin combination, aromatic substitution (photo-NOCAS) reaction.[119]

Inspired by the mechanistic insights of the α-amino C–H arylation, MacMillan and coworkers developed in 2013 the unprecedented direct β-arylation of ketones and aldehydes.[17] Mixing simple saturated ketones and aldehydes **27** with 1,4-dicyanobenzene **22**, an organocatalyst (secondary amines **29** and **30**), $Ir(ppy)_3$ and the appropriated base (DABCO) under visible light illumination, afforded the β-arylated carbonyl compounds **28** (Scheme 10). Again, the merger of two types of methodologies, *i.e.* photoredox and organocatalysis, led to the discovery of an elusive transformation. Indeed, the direct β-functionalization of a saturated ketone or aldehyde had never been successfully developed before. As in the α-amino C–H arylation, the choice of $Ir(ppy)_3$ was crucial for the single electron reduction of electron-poor cyanobenzene derivatives **22** to their corresponding long-lived radical anions **24**. Concurrent with the first photoreduction step, the secondary amine catalysts **29** or **30** could condense with the aldehyde **27** to generate the electron-rich enamine **31**.

---

[118] A. Studer. The Persistent Radical Effect in Organic Synthesis. *Chem. Eur. J.* **2001**, *7*, 1159.
[119] D. Mangion, D. R. Arnold. Photochemical Nucleophile-Olefin Combination, Aromatic Substitution Reaction. Its Synthetic Development and Mechanistic Exploration *Acc. Chem. Res.* **2002**, *35*, 297. [17] M. T. Pirnot, D. A. Rankic, D. B. C. Martin, D. W. C. MacMillan. Photoredox Activation for the Direct β-Arylation of Ketones and Aldehydes. *Science* **2013**, *339*, 1593.

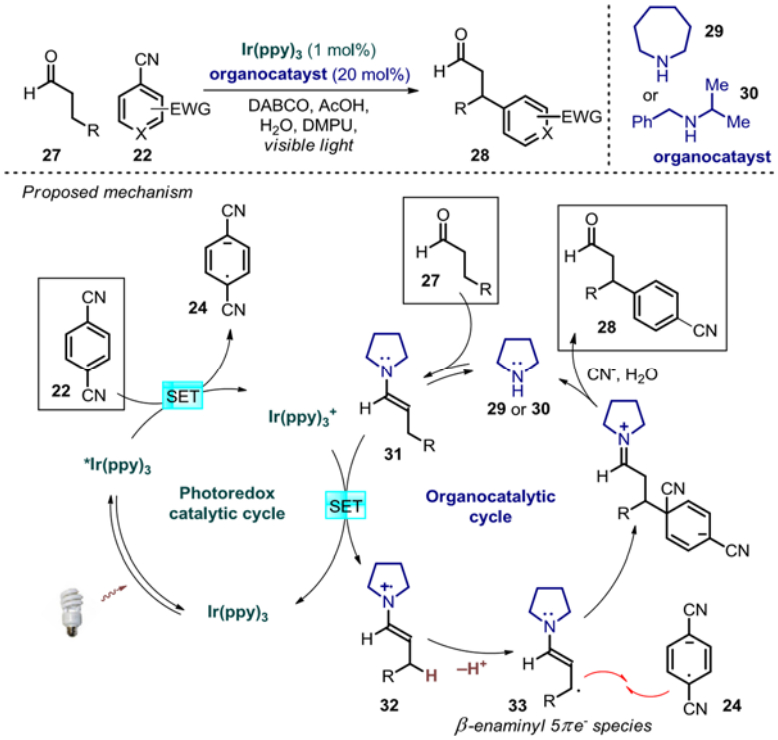

Scheme 10. Direct photoredox β-arylation of ketones and aldehydes.

Given that the reduction potential of the enamine **31** ($E_{1/2}$ = +0.35 to +0.6 V)[120] is lower than the reduction potential of $Ir(ppy)_3^+$ ($E_{1/2}^{0/+1}$ = +0.77 V), it could be oxidized to radical cation **32**, which can be seen as the vinylogous version of aminium radical **13** (compare Schemes 7 and 10). As a key mechanistic consideration, formation of the enaminyl radical cation **32** would sufficiently weaken the allylic C–H bonds (at the original carbonyl β-position) so as to allow deprotonation by DABCO and formation of the β-enaminyl radical **33**, which represents the critical 5πe⁻ intermediate to achieve the β-functionalization. Consequently, radical-radical coupling between the persistent radical anion **24** and the electron-rich β-enamine radical **33** furnished β-arylated carbonyl compound **28** *via* rearomatization, elimination of the cyanide, and hydrolysis of the organocatalyst. The authors presented a broad scope of aldehydes and ketones, though the aryl partner had to be electron-poor enough to be reduced by the excited $Ir(ppy)_3$. Moreover, an asymmetric catalytic example of β-arylation of ketone was reported, showing moderate enantioselectivity (50% *ee*) using the quinine-derived organocatalysts **34** (Scheme 11).

[120] W. W. Schoeller, J. Niemann. On the Electrochemical Oxidation of Enamines. *J. Chem. Soc. Perkin Trans. 2*, **1988**, 369.

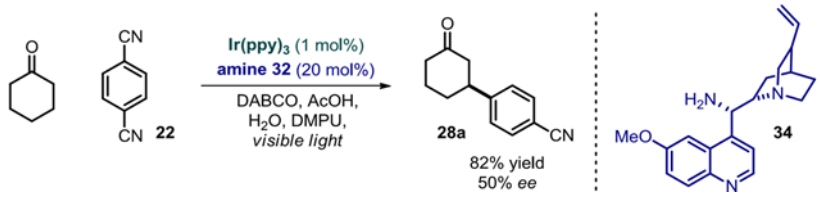

Scheme 11. Preliminary studies on the asymmetric version of photoredox direct β-arylation of ketones.

5.3 Target of the Research Project and Initial Trials

I had the chance to spend a 6 months research period at Princeton University working in the group of Professor MacMillan. We were interested in the use of the transiently generated 5πe⁻ carbonyl intermediate **33** (see Scheme 10) to achieve new β-coupling reactions. Indeed, the development of a general catalytic platform for the direct β-functionalization of saturated aldehydes and ketones would represent a conceptual and practical advance for organic chemistry.

Our strategy was based on the idea that the key β-enaminyl species **33** is inherently nucleophilic. Thus, we initially planned to trap it with electron-deficient olefins (Scheme 12).

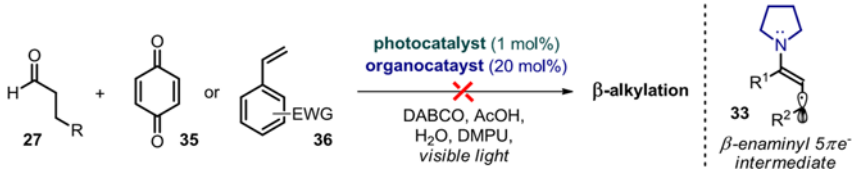

Scheme 12. Initial trials for the β-alkylation reactions using electron-deficient olefins.

In particular, benzoquinone derivatives **35** and styrenes **36**, bearing electron-withdrawing groups on the aromatic ring, were chosen to achieve a formal β-alkylation reaction. Unfortunately, no product formation was observed using the optimized reaction conditions previously developed for the β-arylation, even changing the photocatalyst (both ruthenium and iriudium complexes were tested) and trying different secondary amines as organocatalysts. We then speculated that electron-poor radicals could couple with the β-enaminyl open-shell species **33**. We considered trifluoromethyl radicals, easily available from reduction of trifluoromethansulfonyl chloride **37**,[121] as good candidates for the β-functionalization of saturated aldehydes (Scheme 13).

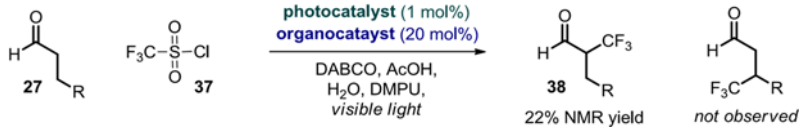

Scheme 13. Initial trials for the β-trifluoromethylation reaction.

[121] D. A. Nagib, D. W. C. MacMillan. Trifluoromethylation of Arenes and Heteroarenes by Means of Photoredox Catalysis. *Nature* **2011**, *480*, 224.

In this case, the α-trifluoromethylated aldehyde **38** was the only product observed under the standard reaction conditions. Product **38** probably arose from the reaction of the photochemically generated electron-deficient trifluoromethyl radical with the electron-rich enamine, a transformation already reported by MacMillan in 2009 (trifluoromethyl iodide was used as the source of CF_3 radical).[122]

We then focused on the generation of the long-lived diphenyl ketyl radical anion **40** from benzophenone **39a** as a possible coupling partner (Scheme 14). It is reported that the radical anion **40** is a persistent species in the absence of oxygen and in basic conditions,[123] while protonated diphenyl ketyl radical **42**, which is predominant in neutral or acidic condition, has a moderate lifetimes in the order of milliseconds[124] (80 msec in ethylene glycol).[125]

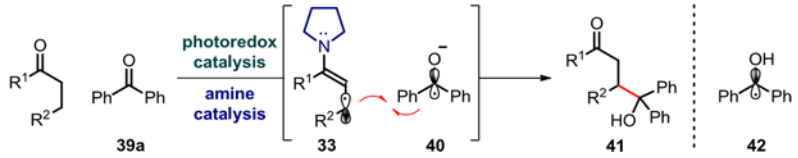

Scheme 14. Direct photoredox β-aldol coupling between β-enamine 5πe⁻ species and ketyl radicals.

Thus, we speculated that the excited $Ir(ppy)_3$, acting as a strong reductant ($E_{1/2}^{0*/+1}$ = -1.73 V), could reduce diaryl ketones, such as benzophenone **39a**, which has a compatible reduction potential ($E_{1/2}$ = -1.83 V),[126] to generate the correspondig diphenyl ketyl radical **40**. Subsequently, the transiently generated nucleophilic β-enaminyl 5πe⁻ species **33** might intercept the long-lived ketyl radical **40** to directly form a γ-hydroxyketone adduct **41**. This would formally constitute a direct β-aldol reaction.

Although the aldol reaction has been widely exploited for the α-functionalization of carbonyl substrates for over 140 years, analogous "homo-aldol" transformations that allow for the direct β-functionalization of carbonyls remain elusive. Classical synthons for the homoaldol reaction are

---

[122] D. A. Nagib, M. E. Scott, D. W. C. MacMillan. Enantioselective α-Trifluoromethylation of Aldehydes via Photoredox Organocatalysis. *J. Am. Chem. Soc.* **2009**, *131*, 10875.

[123] a) A. Beckett, G. Porter. Primary Photochemical Processes in Aromatic Molecules. Part 9. Photochemistry of Benzophenone in Solution. *Trans. Faraday Soc.* **1963**, 59, 2038. b) M. K. Kalinowski, Z. R. Grabowski. Reactivity of Ketyl Free Radicals. Part 2. Dimerization and Dismutation of Fluorenone and Xanthone Ketyls. *Trans. Faraday Soc.* **1966**, *62*, 926.

[124] A. V. Buettner, J. Dedinas. Photoreduction of Benzophenone in Benzene. II. Flash Photolysis Study of Primary Photochemical Reactions. *J. Phys. Chem.* **1971**, *76*(1), 187.

[125] G. Porter, F. Wilkinson. Primary Photochemical Processes in Aromatic Molecules Part 5. Flash Photolysis of Benzophenone in Solution *Trans. Faraday Soc.* **1961**, 57, 1686.

[126] P. J. Wagner, R. J. Truman, A. E. Puchalski, R. Wake. Extent of Charge Transfer in the Photoreduction of Phenyl Ketones by Alkylbenzenes. *J. Am. Chem. Soc.* **1986**, *108*, 7727.

accessed *via* carbene catalysis (Scheme 15a),[127] nucleophilic addition of acetal protected Grignard reagents (b),[128] or stoichiometric metal activated homoenolate equivalents (c).[129]

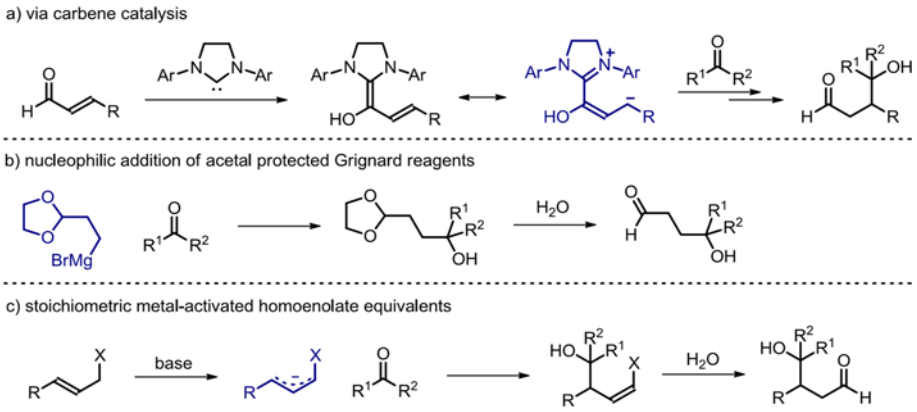

Scheme 15. Typical homoaldol-type synthons.

We first explored the proposed direct β-aldol reaction using octanal **43** and benzophenone **39a** as the substrates (Scheme 16). Our starting point was the reaction conditions employed to achieve the general direct β-arylation (Scheme 10): $Ir(ppy)_3$ as the photocatalyst (1 mol%), *N*benzyl-*N*-isopropyl amine **30** as the organocatalyst (20 mol%), acetic acid, water, 1,4diazabicyclo[2.2.2]octane (DABCO) as the base and 1,3-dimethyl-3,4,5,6-tetrahydro-2(1H)pyrimidinone (DMPU) as the solvent. After 20 hours under visible light irradiation from a compact fluorescence lamp (CFL) of 26 W, trace amounts of the desired product **44** were detected by mass spectroscopy, but not cleanly isolated.

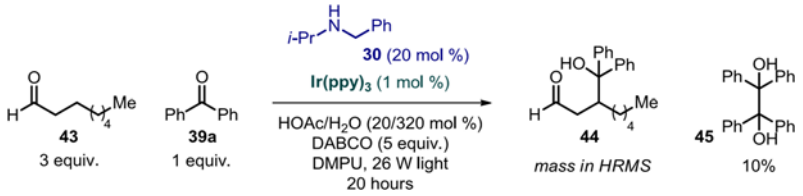

Scheme 16. Preliminary test of the direct β-aldol reaction with octanal and benzophenone.

Interestingly, the benzopinacol dimer **45** was isolated in 10% yield, indicating that somehow (probably by single electron reduction) the desired ketyl radicals **40** and **42** were generated (considering that **45** arises from the combination of two molecules of ketyl radical **42**). The

[127] a) C. Burstein, . Glorius. Organocatalyzed Con ugate Umpolung of α,β-Unsaturated Aldehydes for the Synthesis of γ-Butyrolactones. *Angew. Chem., Int. Ed.* **2004**, *43*, 6205. b) S. S. Sohn, E. L. Rosen, J. W. Bode. N-Heterocyclic Carbene-Catalyzed Generation of Homoenolates: γ-Butyrolactones by Direct Annulations of Enals and Aldehydes. *J. Am. Chem. Soc.* **2004**, *126*, 14370.
[128] G. Büchi, H. Wüest. Synthesis of (±)-Nuciferal. *J. Org. Chem.* **1969**, *34*, 1122.
[129] a) D. Hoppe. The Homoaldol Reaction, or How to Overcome Problems of Regio- and Stereo-selectivity. *Angew. Chem., Int. Ed. Engl.* **1984**, *23*, 932.

absence of the β-aldol product could be justified with a possible deactivation pathway where the intramolecular cyclization of the iminium ion of the product **46** could compete with the hydrolysis of the organocatalyst (Scheme 17). Consequently, the secondary amine would be trapped in the hemiaminal **47**, deactivating both the photoredox and the organocatalytic cycles.

Consistently with this possibility, intermediate **47** was detected by HRMS analysis.

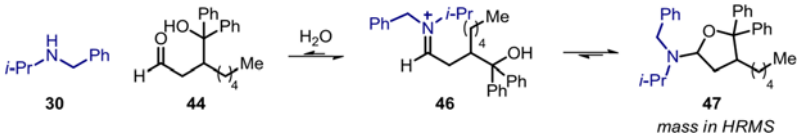

Scheme 17. Possible deactivation pathway of the β-aldol reaction with octanal **43** and benzophenone **39a**.

We reasoned that the use of a more rigid substrate could decrease the rate of the intramolecular cyclization in favor of the hydrolysis of the iminium ion of type **46**. Thus, cyclohexanone **48a** was tested under the same reaction conditions (Scheme 18). Due to its negative reduction potential ($E_{1/2}$ = -2.79 V)[130] cyclohexanone is not competitive with benzophenone **39a** ($E_{1/2}$ = -1.83 V) for the first single electron reduction step by the excited $Ir(ppy)_3$.

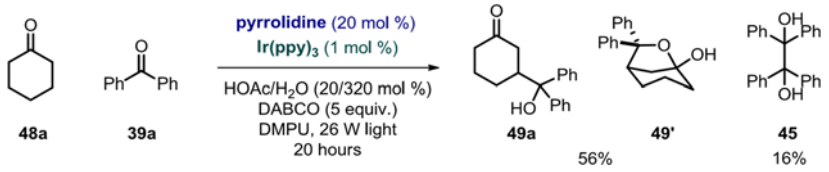

Scheme 18. Preliminary test of direct β-aldol reaction with cyclohexanone and benzophenone.

We were pleased to find that the β-coupling product **49a** was formed in 56% of NMR yield along with 16% of the benzopinacol dimer **45** after 20 hours under irradiation from a 26 W CFL. The desired compound was isolated as an inseparable 9:1 mixture with the corresponding cyclic hemiacetal **49'** (NMR studies suggested that the products are in equilibrium), confirming the ability of this type of compound to undergo intramolecular cyclization.

5.4 Results and Discussion

Encouraged by the initial results, we first examined a range of organocatalysts and photocatalysts; the best results were obtained using the combination of azepane **29** and $Ir(ppy)_3$ (67% yield, entry 2, table 1). Azepane and pyrrolidine are particularly nucleophilic amines because of their capacity to donate electrons from nitrogen to alleviate ring strain (not found to the same level with piperidine). We believe that the use of an azepane catalyst leads to a more nucleophilic $5\pi e^-$ system as a result of this phenomenon.

Table 1. Examination of organocatalysts and photocatalysts.

[130] A. J. Bard. Encyclopedia of Electrochemistry of the Elements; Marcel Dekker: New York, 1978.

Direct β-Aldol of Cyclic Ketones via the Merger of Photoredox and

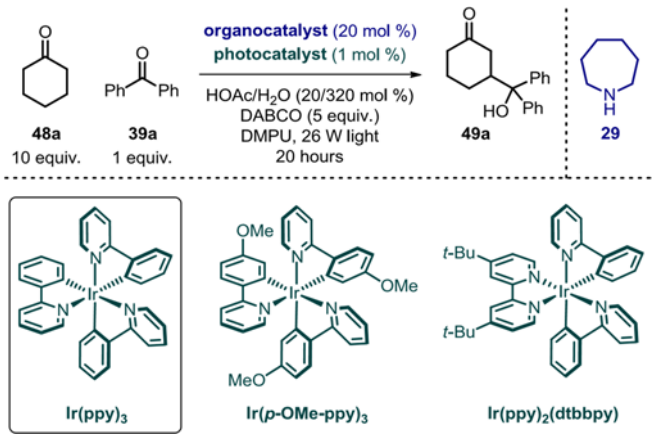

Entry	Organocatalyst (20 mol%)	Photocatalyst (1 mol %)	Yield (%)[b]
1	Pyrrolidine	$Ir(ppy)_3$	56
2	Azepane **29**	$Ir(ppy)_3$	67
3	Morpholine	$Ir(ppy)_3$	26
4	*N*-Benzyl-*N*-*i*-Pr amine	$Ir(ppy)_3$	traces
5	Azepane	Ir(*p*-MeO-ppy)$_3$	65
6	Azepane	$Ir(ppy)_2$(dtbbpy)	59
7	Azepane	$Ir(ppy)_2$(bpy)	56

[a] Reactions were carried out on a 0.25 mmol scale, [**39a**]$_0$ = 0.5 M in DMPU. [b] Yield determined by ^{1}H NMR analysis of the crude mixture using 1,3-benzodioxole as the internal standard.

Having identified the best catalysts combination for the direct β-aldol reaction, we performed a series of control experiments to ensure the necessity of each reaction component for the good outcome of the reaction (Table 2).

Our starting point was the optimized conditions of the previously developed β-arylation (Scheme 10),[16] where 5 equivalents of 1,4-diazabicyclo[2.2.2]octane (DABCO) were used as the base to deprotonate the radical cation **32** and furnish the β-enaminyl 5πe$^-$ intermediate **33** and for quenching the HCN, derived from the mesolysis process. Moreover, 20 mol% of acetic acid (AcOH) and 3.2 equivalents of water increased the rate of the β-arylation, presumably by favouring organocatalytic turnover.

Table 2. Control experiments.

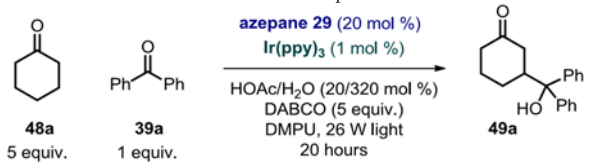

Entry	Reaction conditions	Yield (%)[b]
1	normal	67

2	no light	0
3	no photocatalyst	0
4	no organocatalyst	0
5	no DABCO	42
6	no AcOH	54
7	no H_2O	62
8	open to air	7

[a] [b]

Reactions were carried out on a 0.25 mmol scale, $[\mathbf{39a}]_0$ = 0.5 M in DMPU. Yield determined by ^{1}H NMR analysis of the crude mixture using 1,3-benzodioxole as the internal standard.

The exclusion of light, photocatalyst, and organocatalyst from the β-aldol reaction completely suppressed the reactivity (entries 2, 3 and 4, Table 2). DABCO, AcOH and water were important but not fundamental for the β-coupling, since the corresponding reactions conducted in their absence afforded moderate yields (entries 4, 5 and 6). It is interesting to note that the reaction without DABCO (pK_a = 8.82 in water) still provided some reactivity; probably the ketyl radical anion **40** (pK_a = 9.25 in water)[131] can deprotonate the radical cation **50** thus promoting itself the formation of the key β-enaminyl 5πe⁻ radical **51** (Scheme 19).

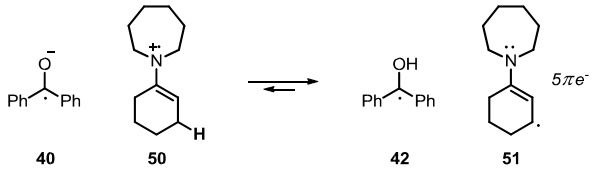

40 **50** **42** **51**

Scheme 19. Plausible formation of 5πe⁻ radical *via* deprotonation of **50** by the ketyl radical anion **40**.

The presence of oxygen quenched the reactivity almost completely (entry 8), indicating the importance to carefully exclude it from the reaction medium. On the basis of these studies, we revised the amount of each components as well as the type of base and solvent (Table 3). Decreasing the amount of water and DABCO to 2 and 1 equivalents, respectively, did not change the yield (entry 1), while the use of DMPU as the solvent increased the reactivity (67% yield, entry 1).

Table 3. Final optimization of standard parameters; screening of bases and solvents.

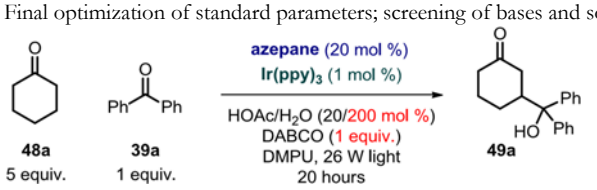

48a 5 equiv. **39a** 1 equiv. **49a**

Entry	Base	Solvent	Yield (%)[b]
1	DABCO	DMPU	67

[131] E. Hayon, T. Ibata, N. N. Lichtin, M. Simica. Electron and Hydrogen Atom Attachment to Aromatic Carbonyl Compounds in Aqueous Solution. Absorption Spectra and Dissociation Constants of Ketyl Radicals. *J. Phys. Chem.* **1972**, *76*, 2072.

2	DMAP	DMPU	44
3	NaOAc	DMPU	52
4	Na_2CO_3	DMPU	28
5	DABCO	DMSO	66
6	DABCO	CH_3CN	14
7	DABCO	DCM	12

[a] [b] Reactions were carried out on a 0.25 mmol scale, [**39a**]$_0$ = 0.5 M in DMPU. Yield determined by ^{1}H NMR analysis of the crude mixture using 1,3-benzodioxole as the internal standard.

Since we did not reach the desired level of reactivity changing the standard reaction parameters, we focused on the byproducts of the reaction. We noticed the concomitant formation of the benzopinacol dimer **45** in all the examples where the conversion of the starting benzophenone **39a** was almost complete (Table 4). To minimize the by-product formation, we tested different additives.

Table 4. Test of different additives in order to decrease the dimerization rate.

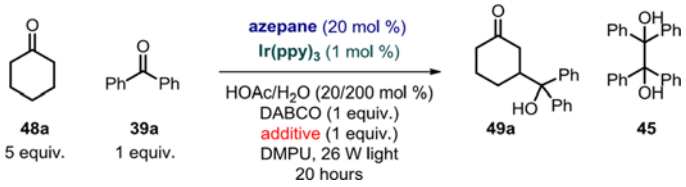

Entry	Additive	Yield **49a** (%)[b]	Yield **45** (%)[c]
1	no	67	12
2	LiCl	55	15
3	$LiBF_4$	70	11
4	$LiAsF_6$	79	8
5	$NaAsF_6$	79	8
6	$KAsF_6$	75	9
7	$AlCl_3$	20	12
8	$Sc(Tf)_3$	42	13

[a] [b] Reactions were carried out on a 0.25 mmol scale, [**39a**]$_0$ = 0.5 M in DMPU. Yield of **49a** determined by ^{1}H NMR analysis of the crude mixture using 1,3-benzodioxole as the internal standard. [c] Yield of **45** determined by HPLC using 1,3-benzodioxole as the internal standard (maximum yield 50%).

We found that lithium hexafluoroarsenate ($LiAsF_6$, entry 4) increased the yield of the desired βaldol product **49a** (79%) against the benzopinacol dimer **45** (8%). Presumably, the production of a lithium alkoxide ketyl radical decreased the dimerization rate (dimerization constants for radical anion **40** systems are considered negligible compared to those of protonated ketyl radicals, rending the radical more persistent)[20] favoring the product formation (Scheme 20).

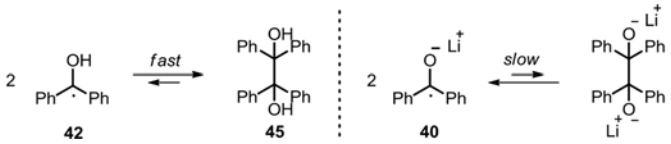

Scheme 20. Dimerization of ketyl radicals and ketyl radical anions.

Examination of the quantity of $LiAsF_6$ and DABCO indicated that the use of 1 and 2 equivalents, respectively, was the best combination, leading to product **49a** in 81% yield. Having identified the optimum conditions for this photoredox direct β-aldol reaction, we aimed at defining the scope of the enaminyl radical precursor (Figure 4).

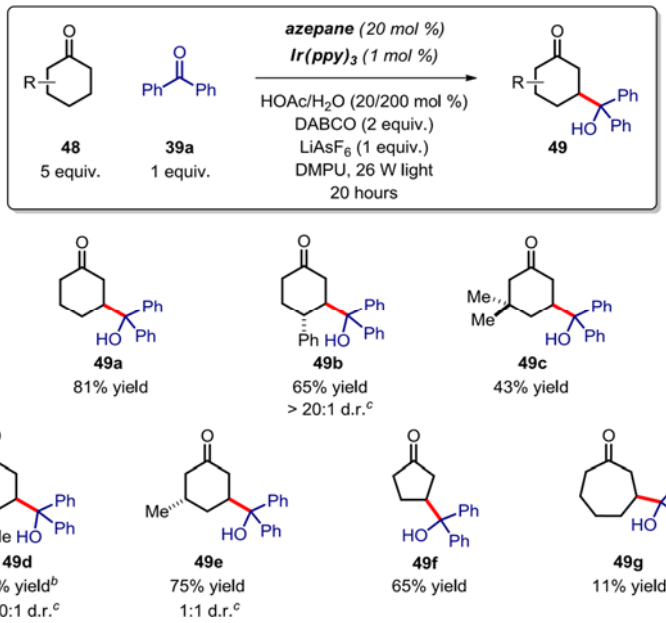

Figure 4. Scope of the keto-enaminyl radical precursor. [a] Reactions were carried out on a 0.75 mmol scale, $[\mathbf{39a}]_0$ = 0.5 M in DMPU. [b] Reaction performed with 10 equiv. of water. [c] Diastereoselectivity determined by ^1H NMR analysis.

A series of differently substituted cyclohexanone derivatives **48** efficiently coupled with benzophenone **39a**. Methyl and phenyl groups were well tolerated in position 3 and 4 (**49b**, **49d** and **49e**). As expected, substituents in position 4 (**49b** and **49d**) induced higher levels of diastereoselectivity than substituents at position 3 (**49e**). Cyclopentanone (**49f**) was a suitable substrate for the β-coupling reaction while the 7 membered ring anologue showed lower yield (**49g**). We next turned our attention to the generality of the ketyl radical substrate; a range of substituted benzophenones was well tolerated (**49h**, **49i** and **49j**) to furnish γ-hydroxyketones in high levels of efficiency (Figure 5). Remarkably, substituted *para*-methoxybenzophenone (**49i**)

showed lower yield, probably due to the electron-donating substituent that decreases the reduction potential of the ketone.

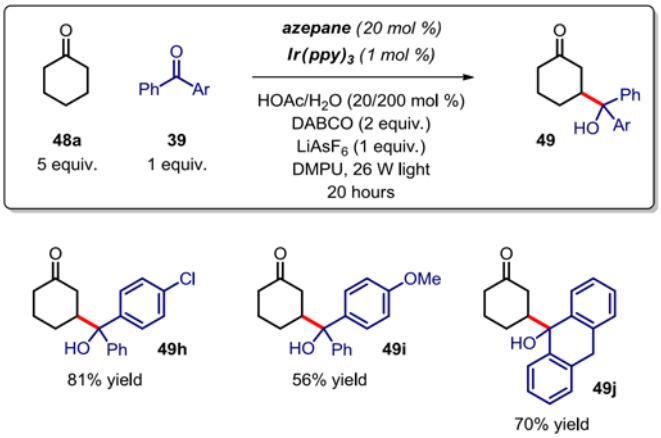

Figure 5. Scope of the diaryl radical coupling precursor. [a] Reactions were carried out on a 0.75 mmol scale, $[\mathbf{39a}]_0$ = 0.5 M in DMPU.

To further increase the synthetic potential of the direct β-aldol reaction, we turned our attention to the aryl-alkyl ketones, a more challenging substrate class given that the ketyl radical formation is thermodynamically disfavored with respect to the analogous benzophenone system. Initial efforts using acetophenone **52a** met with little success using our previously optimized conditions (only 9% yield, result not shown). We recognized that the excited state of $Ir(ppy)_3$ ($E_{1/2}^{0*/+1}$ = -1.73 V) was not sufficiently reducing to induce ketyl radical **53** formation from acetophenone *via* SET ($E_{1/2}$ = −2.14 V),[20] since **53** has a reduction potential that is considerably lower than that of benzophenone **39a** ($E_{1/2}$ = -1.83 V, Scheme 21). We identified Ir(*p*-MeO-ppy)$_3$ as an effective photocatalyst for the reduction of aryl-alkyl ketones, which showed a remarkable increasing of yield with respect to $Ir(ppy)_3$ (27% yield under the same reaction conditions). We initially speculated that the incorporation of an EDG in the ligand of the photocatalyst could enhance the reducing power of its excited state, thus allowing the reduction of acetophenone. Further mechanistic proofs indicated instead that another mechanism was operative, probably a reductive quenching cycle initiated by the oxidation of the enamine (see Section 5.5 for more details).

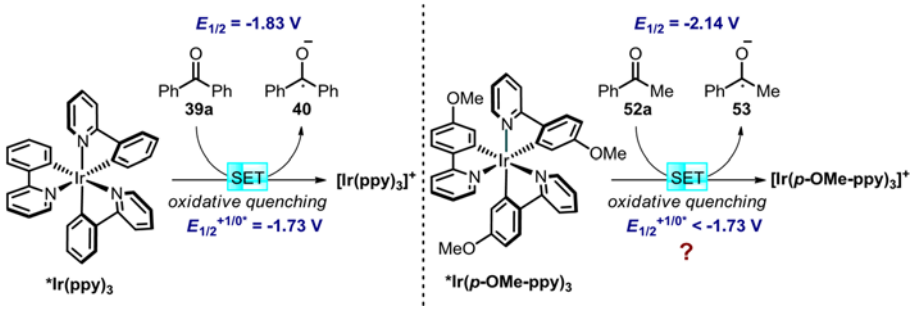

Scheme 21. Rational choice of Ir(*p*-MeO-ppy)$_3$ for the single electron reduction of acetophenone **52** via oxidative quenching cycle.

The use of Ir(*p*-MeO-ppy)$_3$ allowed us to further extend the scope after a second optimization of the reaction parameters (*I will not discuss the details of the studies on the reactivity of acetophenone because they were conducted by Dr. ilip . etronijevi , who was involved in the project after my departure from Princeton University*).

With the new optimized conditions, product **49k** was formed in 77% yield (Figure 6), while both electron-deficient (**49l** and **49n**) and electron-rich (**49o** and **49p**) acetophenone derivatives βcoupled with cyclohexanone **48a** with good efficiency (65-79% yield). Moreover, heterocyclic furan derivatives were well tolerated in this transformation (**49m** and **49q**). Though higher alkyl homologues of acetophenone did not show desiderable reactivity, substrates bearing an electron-withdrawing group at the α position provided the corresponding products in good yields (**49r** and **49s**, 54-62% yield).

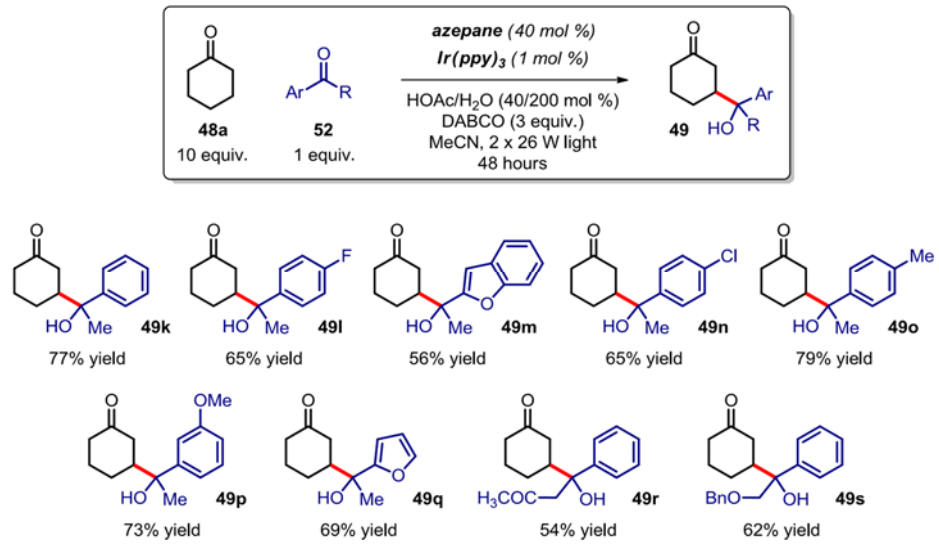

Figure 6. Scope of the ketyl radical coupling precursor. [a] Reactions were carried out on a 0.75 mmol scale, [**52**]$_0$ = 0.167 M in DMPU.

5.5 Mechanistic Considerations

The proposed mechanism for the photoredox direct β-aldol reaction is highlighted in Scheme 22. The first step is the reduction of benzophenone **39a** ($E_{1/2}$ = -1.83 V) by Ir(ppy)$_3$ ($E_{1/2}^{0^*/+1}$ = -1.73 V) in the oxidative quenching cycle. Though the electron transfer is slightly endergonic, in acidic medium and under appropriate reaction conditions the reduction potential of ketone can be elevated and therefore it might be easier to reduce it, rendering this step experimentally feasible.[132] Concurrently, the enamine **54** is formed upon condensation with the aminocatalyst. Its oxidation by Ir(ppy)$_3^+$ ($E_{1/2}^{0/+1}$ = +0.77 V) generates the radical cation **50**. Subsequent deprotonation of **50** with the base provides the key β-enaminyl 5πe$^-$ radical **51**, which undergoes a radical-radical coupling with the persistent ketyl radical **40** to yield the desired γhydroxyketone adduct **49** after hydrolysis of the amine catalyst.

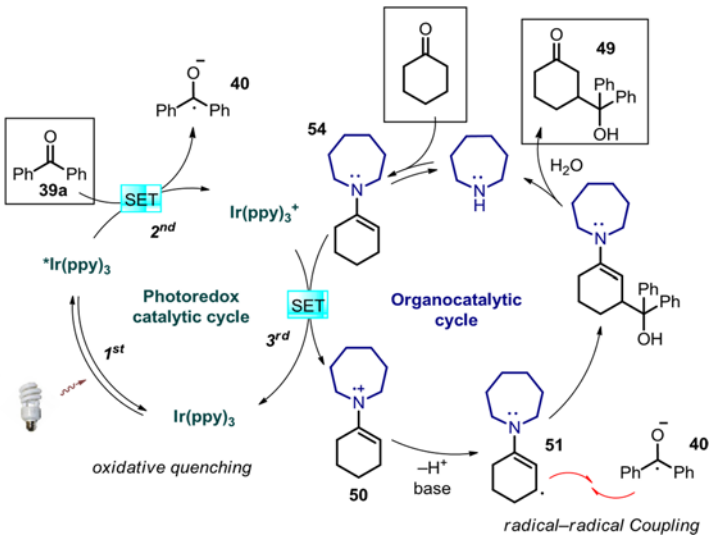

Scheme 22. Proposed mechanism for photoredox direct β-aldol reaction with benzophenone derivatives.

To further probe the proposed mechanism, we performed a series of Stern-Volmer quenching studies. Fluorescence quenching (or Stern–Volmer) studies are commonly employed in photochemistry to have evidence of interaction between a general photoexcited molecule and the compound that is supposed to interact with.[133] As mentioned in Section 5.1, bimolecular interactions, or quenching, happen *via* energy transfers and oxidative/reductive quenching by photoinduced electron transfer. In a photoredox reaction, the photocatalyst can donate (oxidative quenching) or remove (reductive quenching) an electron from the substrate. In our

[132] a) J. J. Warren, T. A. Tronic, J. M. Mayer. Thermochemistry of Proton-Coupled Electron Transfer Reagents and its Implications. *Chem. Rev.* **2010**, *110*, 6961. b) K. T. Tarantino, P. Liu, R. R. Knowles. Catalytic Ketyl-Olefin Cyclizations Enabled by Proton-Coupled Electron Transfer. *J. Am. Chem. Soc.* **2013**, *135*, 10022.
[133] N. J. Turro. *Modern Molecular Photochemistry*; Benjamin/Cummings: Menlo Park, CA, 1978.

specific case, we hypothesized that the excited $Ir(ppy)_3$ donates an electron to the benzophenone (BP) **39a** *via* oxidative quenching. The fluorescence quenching technique examines the competition between two possible deactivation pathways of the photoexcited state of $Ir(ppy)_3$: the quenching *via* electron transfer (bimolecular process with BP **39a**) and the emission (unimolecular process); Figure 7.

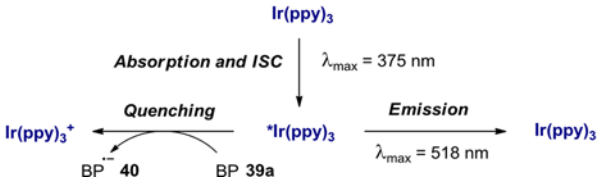

Figure 7. Deactivation of the excited state of $Ir(ppy)_3$ by emission (unimolecular process) and oxidative quenching (bimolecular process).

In the absence of the BP **39a**, excited $Ir(ppy)_3$ undergoes emission, with a specific λ_{max} = 518 nm and with an inherent intensity. However, in the presence of a molecule that can interact with the excited photocatalyst in a bimolecular process, the inherent intensity of the emission at 518 nm would decease. This is what we observed when adding different amounts of benzophenone **39a**. The relationship between the concentration of BP **39a** and the emission intensity is given by the Stern–Volmer equation (Eq. 1)

$$I_0 / I = 1 + k_{BP}\tau_0[BP] \qquad \text{(Eq. 1)}$$

where I_0 and I are the emission intensity in the absence and the presence of benzophenone **39**, respectively, k_{BP} is the quenching rate constant, τ_0 is the excited-state lifetime in the absence of BP, and [BP] is the concentration of benzophenone **39a**. In the case of electron transfer between the excited $Ir(ppy)_3$ and BP, plotting the ratio I_0/I against the [BP] would give a straight line having a *y*-intercept equal to 1 and a slope, termed the Stern–Volmer constant (K_{SV}), equal to $k_{BP}\tau_0$. In our Stern–Volmer quenching studies, we observed a relationship between the concentration of BP **39a** and the emission intensity, which confirmed that benzophenone was an efficient quencher of $*Ir(ppy)_3$ (Figure 8). When enamine **54** was used as the quencher, no decrease in emission intensity of the excited $Ir(ppy)_3$ was observed, excluding the reductive quenching as a possible mechanism for this transformation.

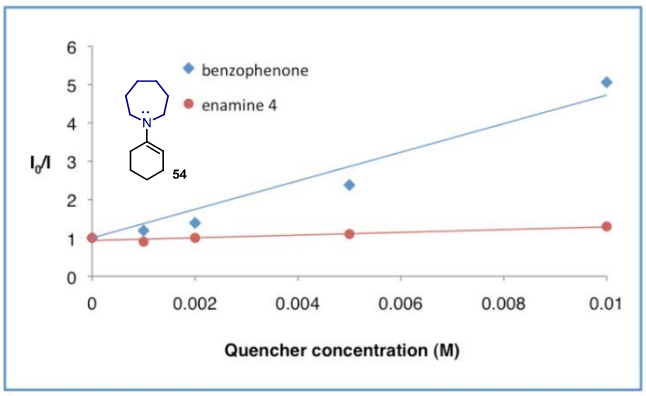

Figure 8. luorescence quenching (or Stern−Volmer) studies of excited Ir(ppy)3.

A different situation was found when the same study was performed using Ir(*p*-MeO-ppy)3 (Figure 9). Acetophenone **52a** could not directly quench the excited state of Ir(*p*-MeO-ppy)3, also in the presence of acetic acid (in acidic medium the reduction potential of ketone is elevated and therefore it might be easier to reduce).[20] Enamine **54** was found to quench the excited photocatalyst instead, suggesting that in the case of acetophenone the two single elctron transfer processes are inverted. Thus, a probable mechanism for the photoredox direct β-aldol reaction with aryl-alkyl ketones would be through the reductive quenching cycle of the Ir(*p*MeO-ppy)3 (Scheme 23).

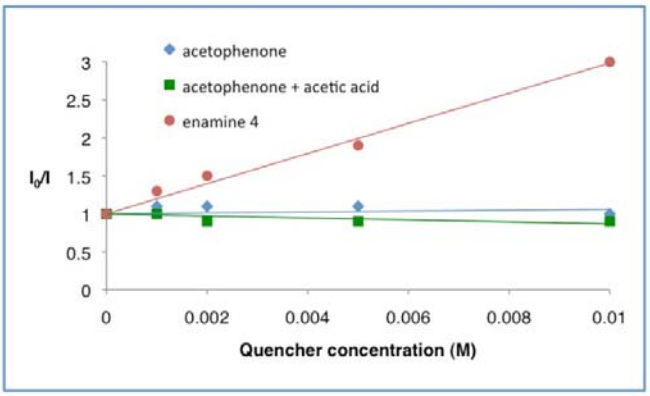

Figure 9. Stern−Volmer quenching studies of excited Ir(*p*-MeO-ppy)3.

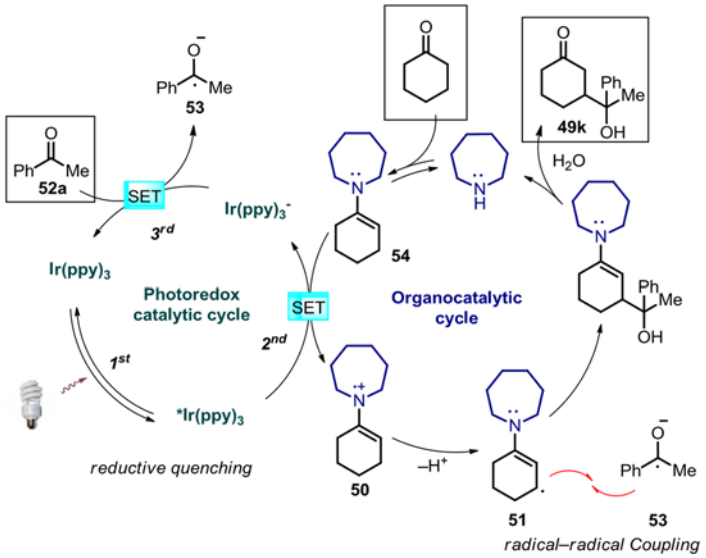

Scheme 23. Proposed mechanism for photoredox direct β-aldol reaction with aryl-alkyl ketones.

5.6 Conclusions

The direct β-aldol reaction between cyclic ketones and aryl ketones has been developed *via* the synergistic combination of photoredox catalysis and organocatalysis. Diaryl oxymethyl or aryl–alkyl oxymethyl radicals, generated *via* single-electron reduction of ketone precursors, readily combine with β-enaminyl 5πe⁻ radical species, transiently generated by enamine oxidation, to produce γ-hydroxyketone adducts. Experimental evidences indicate that two discrete reaction pathways can be operable in this process depending upon the nature of the ketyl radical precursor and the photocatalyst.

5.7 Experimental Section

5.7.1 General Information

The work has been performed at Princeton University, Merck Center of catalysis, under the supervision of Professor MacMillan.

Commercial reagents were purchased from Sigma Aldrich and purified prior to use following the guidelines of Perrin and Armarego.[134] All solvents were purified according to the method of Grubbs.[135] Organic solutions were concentrated under reduced pressure on a Büchi rotary evaporator using an acetone-dry ice bath. Chromatographic purification of products was

[134] W. L. F. Armarengo, D. D. Perrin, In *Purification of Laboratory Chemicals*, 4th ed.; Butterworth Heinemann: Oxford, 1996.
[135] A. B. Pangborn, M. A. Giardello, R. H. Grubbs, R. K. Rosen, F. J. Timmers. Safe and Convenient Procedure for Solvent Purification. *Organometallics* **1996**, *15*, 1518.

accomplished using forced-flow chromatography according to the method of Still[136] on ICN 60 3264 mesh silica gel 63. Thin-layer chromatography (TLC) was performed on Silicycle 250 mm silica gel F-254 plates. Visualization of the developed plates was performed by fluorescence quenching, potassium permanganate, or ceric ammonium molybdate stain. ^{1}H and ^{13}C NMR spectra were recorded on a Bruker 500 (500 and 125 MHz), and are internally referenced to residual protio solvent signals (for CDCl3, δ 7.27 and 77.0 ppm, respectively). Data for ^{1}H NMR are reported as follows: chemical shift (δ ppm), multiplicity (s = singlet, d = doublet, t = triplet, q = quartet, h = heptet, m = multiplet, br = broad), integration, coupling constant (Hz). ^{13}C spectra were reported as chemical shifts in ppm and multiplicity where appropriate. High Resolution Mass spectra were obtained from the Princeton University Mass Spectral Facility.

The ^{1}H and ^{13}C NMR spectra are available in the literature[1] and are not reported in the present thesis.

5.7.2 General Procedure for the β-Aldol Reaction of Diaryl Ketones

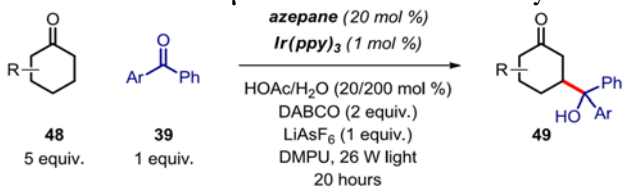

A solution of tris[2-phenylpyridinato-C^2,N]iridium(III) (4.8 mg, 7.5 µmol, 0.010 equiv.), DABCO (168.0 mg, 1.500 mmol, 2.000 equiv.), $LiAsF_6$ (147.0 mg, 0.7500 mmol, 1.000 equiv.), benzophenone **39** (0.75 mmol, 1.00 equiv.), azepane (18.0 µL, 0.150 mmol, 0.200 equiv.), cyclohexanone **48** (3.9 mmol, 5.0 equiv.), acetic acid (9.0 µL, 0.15 mmol, 0.20 equiv.) and water (27 µL, 1.5 mmol, 2.0 equiv.) in DMPU (1.5 mL) was degassed 3 times (freeze-pump-thaw: cooled to –78 °C and degassed via vacuum evacuation (5 min), backfilled with argon, and warm to room temperature), then irradiated with a 26 W fluorescent lamp (at approximately 2 cm away from the light source). After 20 h, the reaction mixture was diluted with water, extracted with EtOAc (3 x 5 mL), combined organic layers were washed with brine, dried (Na_2SO_4), and concentrated *in vacuo*. Purification by flash chromatography on SiO_2 (15-30% EtOAc in hexanes) provided the desired product **49**.

3-(Hydroxydiphenylmethyl)cyclohexan-1-one (49a)

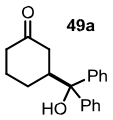

The product was isolated as a colorless oil (170.0 mg, 81%) and as an inseparable equilibrium mixture of the title compound and the corresponding hemiacetal in *ca.* 9:1 ratio:

[136] W. C. Still, M. Kahn, A. J. Mitra. Rapid chromatographic technique for preparative separations with moderate resolution. *J. Org. Chem.* **1978**, *43*, 2923.

IR (film) 3475, 3949, 1701, 1448 cm^{-1};

^{1}H NMR (500 MHz, CDCl3) δ 7.54 (dd, 0.33 H, *J* = 8.4, 1.3 Hz), 7.50–7.46 (m, 0.34 H), 7.42–7.36 (m, 2 H), 7.36–7.31 (m, 2 H), 7.26 (dd, 2 H, *J* = 8.5, 7.1 Hz), 7.24–7.20 (m, 2 H), 7.17–7.09 (m, 2 H), 2.85 (ddt, 1 H, *J* = 11.7, 4.8, 3.2 Hz), 2.32 (ddt, 1 H, *J* = 14.6, 4.1, 2.3 Hz), 2.28–2.14 (m, 3 H), 2.07–1.96 (m, 1 H), 1.74 (ddt, 1 H, *J* = 11.9, 3.5, 1.8 Hz), 1.61 (ddq, 1 H, *J* = 13.3, 5.2, 3.0 Hz), 1.42 (ddt, 1 H, *J* = 13.0, 11.5, 3.6 Hz); 13C NMR (125 MHz, CDCl3) δ 212.3, 145.6, 144.7, 128.4 (2 C), 126.9 (2 C), 125.6, 125.4, 79.7, 46.2, 42.8, 41.2, 25.8, 24.8;

HRMS (ESI) *m/z* calcd for $C_{19}H_{20}O_2Na$ [$(M+Na)^+$] 303.1361, found 303.1350.

5-Methoxy-2,7,7-triphenyl-6-oxabicyclo[3.2.1]octane (49b')

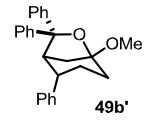

49b'

According to general procedure, the crude product was subjected to the next step without previous purification and characterization. The crude material was dissolved in MeOH (10.0 mL), treated with *p*-TsOH•H_2O (10.0 mg, 0.0526 mmol), and stirred at room temperature for 12 h. The reaction mixture was then diluted with water and extracted with EtOAc. The combined organic layers were washed with brine, dried (Na_2SO_4), and concentrated *in vacuo*. Purification by chromatography on SiO_2 (5-10% EtOAc in hexanes) gave the desired methyl acetal (180.0 mg, 65% over two steps) as a colorless oil:

IR (film) 2959, 2926, 1727, 1449 cm^{-1};

^{1}H NMR (500 MHz, CDCl3) δ 7.67 (d, 2 H, *J* = 7.8 Hz), 7.60 (dd, 2 H, *J* = 8.2, 1.4 Hz), 7.38–7.30 (m, 5 H), 7.30–7.25 (m, 3 H), 7.25–7.11 (m, 3 H), 3.53–3.46 (m, 1 H), 3.24 (s, 3 H), 3.13–3.02 (m, 1 H), 2.25–2.13 (m, 1 H), 2.09–1.89 (m, 3 H), 1.84–1.75 (m, 1 H), 1.54 (d, 1 H, *J* = 11.6 Hz); ^{13}C NMR (125 MHz, CDCl3) δ 147.8, 145.6, 144.2, 128.4 (2 C), 128.1, 127.6, 126.4, 126.3, 125.9, 125.5, 125.1, 110.3, 88.6, 50.7, 50.0, 38.9, 35.3, 30.9, 22.4;

HRMS (ESI) *m/z* calcd for $C_{26}H_{26}O_2Na$ [$(M+Na)^+$] 393.1830, found 393.1831. **5-(Hydroxydiphenylmethyl)-3,3-dimethylcyclohexan-1-one (49c)**

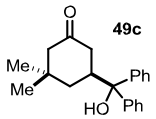

49c

The desired product (98.7 mg, 43%) as a colorless oil:

IR (film) 3480, 2955, 1701, 1448 cm^{-1};

^{1}H NMR (500 MHz, CDCl3) δ 7.51–7.46 (m, 2 H), 7.44–7.39 (m, 2 H), 7.35 (dd, 2 H, *J* = 8.5, 7.1 Hz), 7.31–7.26 (m, 2 H), 7.26–7.21 (m, 1 H), 7.21–7.15 (m, 1 H), 3.10 (ddt, 1 H, *J* = 12.7, 11.0, 4.2 Hz), 2.33 (s, 1 H), 2.29–2.21 (m, 1 H), 2.19 (d, 1 H, *J* = 13.6), 2.16–2.08 (m, 2 H), 1.55–1.52 (m, 1 H), 1.03 (s, 3 H), 1.00 (s, 3 H); ^{13}C NMR (125 MHz, CDCl3) δ 212.4, 145.6, 144.9, 128.5, 128.4, 126.9, 126.8, 125.5, 125.3, 79.5, 54.4, 41.8 (2 C), 38.9, 34.5, 32.1, 25.7; HRMS (ESI) *m/z* calcd for $C_{21}H_{24}O_2Na$ [$(M+Na)^+$] 331.1674, found 331.1668.

(3R*,4R*)-3-(hydroxydiphenylmethyl)-4-methylcyclohexan-1-one (49d)

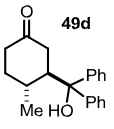

The product was isolated as a white solid (175 mg, 79%) and as an inseparable equilibrium mixture of the title compound and the corresponding hemiacetal in ca. 2:1 ratio:

IR (film) 3413, 2956, 1700, 1448 cm^{-1};

^{1}H NMR (500 MHz, CDCl3) δ 7.56–7.54 (m, 2 H), 7.48 (d, 2 H, *J* = 10.0 Hz), 7.37–7.31 (m, 2 H), 7.25–7.17 (m, 6 H), 7.13–7.10 (m, 1 H), 7.08–7.04 (m, 2 H), 2.99 (dd, 1 H, *J* = 5.0 Hz), 2.89 (dt, 0.5 H, *J* = 10.0, 5.0 Hz), 2.55 (s, 1 H), 2.42 (dd, 0.5 H, *J* = 15.0, 5.0 Hz), 2.35 (dd, *J* = 0.5 H, *J* = 15.0, 5.0 Hz), 2.30–2.22 (m, 1 H), 2.16–2.08 (m, 1 H), 1.93 (dt, 1 H, *J* = 10.0, 5.0 Hz), 1.89 (d, 1 H, *J* = 10.0 Hz), 1.84–1.79 (m, 1 H), 1.78–1.70 (m, 3 H), 1.61–1.53 (m, 1 H), 1.52–1.45 (m, 1 H), 1.01–0.97 (m, 1 H), 0.95 (d, 3 H, *J* = 10.0 Hz), 0.86 (d, 1.5 H, 5.0 Hz); ^{13}C NMR (125 MHz, CDCl3) δ 214.1, 148.9, 146.2, 145.8, 143.8, 128.7, 128.3, 128.2, 127.9, 127.0, 126.5, 126.3, 126.1, 125.6, 125.5, 125.4, 124.7, 106.7, 89.6, 81.9, 50.5, 48.7, 39.5, 37.0, 36.6, 34.2, 29.4, 28.0, 27.3, 25.5, 21.5, 19.4; HRMS (ESI) *m/z* calcd for $C_{20}H_{22}O_2Na$ [(M+Na)$^+$] 317.1517, found 317.1509.

The relative stereochemistry was confirmed by a single-crystal X-ray analysis (see section 5.8.4).

(1S*,2S*,5S*)-5-Methoxy-2-methyl-7,7-diphenyl-6-oxabicyclo[3.2.1]octane (49d')

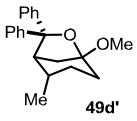

3- (Hydroxydiphenylmethyl)-4-methylcyclohexan-1-one **49d** (22.5 mg, 0.0760 mmol) was dissolved in MeOH (0.3 mL), treated with *p*-TsOH•H2O (1.1 mg, 5.8 µmol), and stirred at room temperature for 12 h. The reaction mixture was then diluted with water and extracted with EtOAc. The combined organic layers were washed with brine, dried (Na_2SO_4), and concentrated *in vacuo*. Purification by chromatography on SiO_2 (5-10% EtOAc in hexanes) gave the desired methyl acetal (22.0 mg, 93%) as a colorless oil:

IR (film) 2958, 1599, 1448, 1136 cm^{-1};

^{1}H NMR (500 MHz, CDCl3) δ 7.59–7.57 (m, 2 H), 7.55–7.53 (m, 2 H), 7.29–7.24 (m, 4 H), 7.14 (tt, 2 H, *J* = 7.4, 1.2 Hz), 3.25 (s, 3 H), 3.18 (t, 1 H, *J* = 3.7 Hz), 2.10 (dt, 1 H, *J* = 11.5, 2.7 Hz), 2.13–2.06 (m, 1 H), 1.90 (ddt, 2 H, *J* = 9.3, 5.1, 1.4 Hz), 1.75–1.64 (m, 3 H), 1.03 (d, 3 H, *J* = 5.0 Hz); 13C NMR (125 MHz, CDCl3) δ 148.2, 144.2, 128.3, 127.8, 126.2, 125.9, 125.6, 125.0, 110.2, 89.1, 50.0, 49.0, 33.0, 30.7, 27.8, 25.3, 19.5;

HRMS (ESI) *m/z* calcd for C21H24O2Na [(M+Na)$^+$] 331.1674, found 331.1668.

3-(Hydroxydiphenylmethyl)-5-methylcyclohexan-1-one (49e)

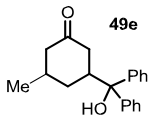

49e

The desired product was isolated (164.8 mg, 75%) as a mixture of two diastereomers in ca. 1:1 ratio.

Diastereomer 1 (R_f = 0.21 (30% EtOAc in hexanes), mixture of the *trans*diastereoisomer and the corresponding hemiacetal in 2:1 ratio, respectively): IR (film) 2958, 1599, 1448, 1136 cm^{-1};

^{1}H NMR (500 MHz, CDCl3) δ 7.63–7.58 (m, 1 H), 7.56–7.51 (m, 1 H), 7.50–7.44 (m, 2 H), 7.44– 7.39 (m, 2 H), 7.33 (t, 2 H, *J* = 7.7 Hz), 7.32–7.10 (m, 7 H), 3.26 (q, 0.5 H *J* = 3.5 Hz), 3.20 (tt, 1 H, *J* = 1 H), 2.53–2.42 (m, 2 H), 2.35 (dd, 1 H, *J* = 14.2, 11.1 Hz), 2.23 (s, 1 H), 2.23–2.19 (m, 1 H), 2.17–2.09 (m, 1 H), 2.09–1.97 (m, 1 H), 1.92 (ddd, 1 H, *J* = 15.5, 5.4, 2.4 Hz), 1.78–1.63 (m, 2 H), 1.63–1.54 (m, 2 H), 1.02 (d, 3 H, *J* = 6.8 Hz), 0.75 (d, 1.5 H, *J* = 6.6 Hz); ^{13}C NMR (125 MHz, CDCl3) δ 212.3, 148.8, 145.7, 145.1, 144.2, 128.5, 128.4, 128.2, 127.9, 126.9, 126.8, 126.2, 125.5, 125.4, 124.7, 106.5, 89.4, 80.1, 47.9, 46.1, 44.3, 42.4, 42.3, 40.8, 35.5, 32.0, 29.2, 26.1, 21.6, 19.8; HRMS (ESI) *m/z* calcd for $C_{20}H_{22}O_2Na$ [(M+Na)$^+$] 317.1517, found 317.1512.

Diastereomer 2 (R_f = 0.1 (30% EtOAc in hexanes), *cis*-diastereoisomer):

IR (film) 3493, 2957, 1704, 1492, 1448, 1267 cm^{-1};

^{1}H NMR (500 MHz, CDCl3) 7.50–7.45 (m, 2 H), 7.43–7.38 (m, 2 H), 7.34 (dd, 2 H, *J* = 8.5, 7.0 Hz), 7.29 (dd, 2 H, *J* = 8.5, 7.0 Hz), 7.26–7.21 (m, 1 H), 7.21–7.16 (m, 1 H), 2.94 (tdd, 1 H, *J* = 11.9, 5.1, 2.9 Hz), 2.38 (ddt, 1 H, *J* = 13.4, 3.2, 1.7 Hz), 2.30–2.18 (m, 3 H), 2.01–1.85 (m, 2 H), 1.79 (dt, 1 H, *J* = 13.4, 2.0 Hz), 1.31–1.19 (m, 2 H), 1.00 (d, 3 H, *J* = 6.0 Hz); ^{13}C NMR (125 MHz, CDCl3) δ 212.0, 145.5, 144.7, 128.4 (2 C), 126.9, 126.8, 125.6, 125.4, 79.5, 49.6, 45.1, 42.0, 34.5, 32.5, 22.5; HRMS (ESI) *m/z* calcd for $C_{21}H_{24}O_2Na$ [(M+Na)$^+$] 317.1517, found 317.1517.

The relative stereochemistry was confirmed by a single crystal X-ray analysis (see section 5.8.4).

(1R*,3R*,5S*)-5-Methoxy-3-methyl-7,7-diphenyl-6-oxabicyclo[3.2.1]octane (49e')

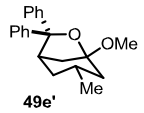

49e'

3-(Hydroxydiphenylmethyl)-5-methylcyclohexan-1-one **49e** (18.2 mg, 0.0762 mmol) was dissolved in MeOH (0.3 mL), treated with *p*-TsOH•H_2O (1.1 mg, 5.8 µmol), and stirred at room temperature for 12 h. The reaction mixture was then diluted with water and extracted with EtOAc. The combined organic layers were washed with brine, dried (Na_2SO_4), and concentrated *in vacuo*. Purification by chromatography on SiO_2 (5-10% EtOAc in hexanes) gave the desired methyl acetal (18.9 mg, 99%) as a white solid:

IR (film) 2953, 1598, 1460, 1330 cm^{-1};

1H NMR (500 MHz, CDCl3) δ 7.54–7.47 (m, 2 H), 7.45 (d, 2 H, J = 7.8 Hz), 7.23–7.13 (m, 4 H), 7.04 (dt, 2 H, J = 7.2, 3.4 Hz), 3.30 (q, 1 H, J = 3.6 Hz), 3.21 (s, 3 H), 2.20 (ddt, 1 H, J = 10.6, 4.8, 2.4 Hz), 2.07 (ddd, 1 H, *J* = 12.9, 6.4, 2.8 Hz), 1.79–1.77 (m, 1 H), 1.67 (ddt, 1 H, *J* = 18.0, 12.2, 5.6 Hz),

1.32 (d, 1 H, *J* = 10.9 Hz), 1.20 (dd, 1 H, *J* = 13.0, 11.0 Hz), 1.07 (ddd, 1 H, *J* = 13.8, 11.5, 2.8 Hz), 0.66 (d, 3 H, *J* = 6.5 Hz); 13C NMR (125 MHz, CDCl3) δ 148.3, 144.6, 128.2, 127.8, 126.2, 126.0, 125.4, 124.9, 109.9, 88.9, 50.1, 44.7, 42.9, 36.9, 36.1, 25.9, 21.8;

HRMS (ESI) *m/z* calcd for $C_{21}H_{24}O_2Na$ [(M+Na)$^+$] 331.1674, found 331.1671.

3-(Hydroxydiphenylmethyl)cyclopentan-1-one (49f)

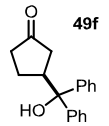

The desired product was isolated (129.3 mg, 65%) as a colorless oil:

IR (film) 3466, 2924, 1731, 1172 cm^{-1};

^{1}H NMR (500 MHz, CDCl3) δ 7.42–7.37 (m, 2 H), 7.37–7.33 (m, 2 H), 7.25 (ddd, 4 H, *J* = 13.2, 8.5, 7.0 Hz), 7.19–7.12 (m, 2 H), 3.31 (tt, 1 H, *J* = 9.5, 7.6 Hz), 2.33–2.07 (m, 5 H), 1.87–1.73 (m, 2 H); ^{13}C NMR (125 MHz, CDCl3) δ 218.9, 146.1, 145.7, 128.4, 128.3, 127.1, 127.0, 125.7, 125.6, 78.8, 45.1, 40.6, 38.5, 24.0;

HRMS (ESI) *m/z* calcd for $C_{18}H_{18}O_2Na$ [(M+Na)$^+$] 289.1204, found 289.1197.

3-(Hydroxydiphenylmethyl)cycloheptan-1-one (49g)

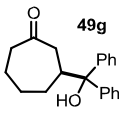

The desired product was isolated (24.0 mg, 11%) as a colorless oil and as an inseparable mixture of the title compound and the corresponding hemiacetal in *ca.* 6:1 ratio:

IR (film) 3429, 2932, 1695, 1449, 1008 cm^{-1};

^{1}H NMR (500 MHz, CDCl3) δ 7.66– 7.58 (m, 2 H), 7.42–7.38 (m, 2 H), 7.25–7.21 (m, 2 H), 7.20–7.13 (m, 2 H), 7.10–7.03 (m, 2 H), 3.30 (dt, 1 H, *J* = 6.5, 3.6 Hz), 2.47–2.33 (m, 1 H), 2.26 (d, 1 H, *J* = 10.0 Hz), 2.07– 1.96 (m, 1 H), 1.93 (ddt, 1 H, *J* = 13.6, 6.5, 1.6 Hz), 1.79 (ddd, *J* = 13.6, 5.6, 3.0 Hz), 1.72–1.60 (m, 1 H), 1.47–1.39 (m, 2 H), 1.28–1.18 (3 H); ^{13}C NMR (125 MHz, CDCl3) δ 214.6, 148.5, 143.6, 128.6, 127.9, 126.7, 125.9, 125.5, 124.9, 108.5, 89.6, 43.7, 41.8, 38.4, 30.0, 23.9, 23.1;

HRMS (ESI) m/z calcd for $C_{20}H_{21}ONa$ [(M–H_2O+Na)$^+$] 277.1592, found 277.1589.

3-((4-Chlorophenyl)(hydroxy)(phenyl)methyl)cyclohexan-1-one (49h)

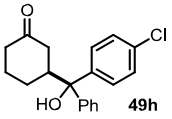

The desired product was isolated (191.0 mg, 81%) as an inseparable mixture of two diastereomeric alcohols (1:1 ratio), and the corresponding hemiacetals (20% with respect to the open form):

IR (film) 3466, 2950, 1701, 1490, 1094 cm^{-1};

^{1}H NMR (500 MHz, CDCl3) δ 7.59–7.57 (m, 0.4 H), 7.57–7.54 (m, 0.4 H), 7.53-7.51 (m, 0.4 H), 7.51- 7.48 (m, 0.4 H), 7.45 (dd, 2 H, *J* = 7.6, 1.7 Hz), 7.42–7.38 (m, 3.9 H), 7.36–7.31 (m, 4.2 H), 7.31–7.14 (m, 9.8 H), 2.88 (dddd, 2 H, *J* = 13.3, 10.5, 5.4, 2.8 Hz), 2.40 (ddt, 2 H, *J* = 14.7, 5.1, 2.3),

2.35–2.14 (m, 7.8 H), 2.10 (ddt, 2 H, *J* = 13.2, 6.3, 3.1 Hz), 2.03–1.61 (m, 6.3 H), 1.54–1.33 (m, 3.4 H); ^{13}C NMR (125 MHz, CDCl3) major peaks (mixture of diastereomeric alcohols): δ 212.0 (2 C), 145.2, 144.4, 144.2, 143.3, 128.7, 128.6, 128.5 (2 C), 127.2 (3 C), 127.0, 125.6 (2 C), 125.4 (2 C), 79.6, 79.5, 46.1 (2 C), 42.8, 42.7, 41.2 (2 C), 25.8, 25.7, 24.8 (2 C); minor peaks (mixture of hemiacetals): δ 148.2, 147.4, 143.7, 142.8, 132.7 (2 C), 128.4 (2 C), 128.1, 128.0, 126.9, 126.5, 126.4, 126.3, 125.3, 124.6, 106.8 (2 C), 69.0 (2 C), 44.6, 44.5, 42.6, 42.4, 37.4, 37.2, 26.4, 26.3, 19.2 (2 C);

HRMS (ESI) m/z calcd for $C_{19}H_{19}ClO_2Na$ [(M+Na)$^+$] 337.0971, found 337.0965.

3-(Hydroxy(4-methoxyphenyl)(phenyl)methyl)cyclohexan-1-one (49i)

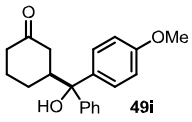

49i

The desired product was isolated (130.5 mg, 56%) as an inseparable mixture of two diastereomeric alcohols (1:1 ratio) with *ca.* 15% of the corresponding hemiacetals:

IR (film) 3481, 2949, 1702, 1510 cm^{-1};

^{1}H NMR (500 MHz, CDCl3) δ 7.47–7.44 (m, 2.3 H), 7.42–7.36 (4.4 H), 7.36–7.26 (m, 8.5 H), 7.26–7.18 (m, 2.8 H), 6.91–6.82 (m, 4.5 H), 3.80 (s, 3 H), 3.78 (s, 3 H), 3.77 (s, 0.4 H), 3.76 (s, 0.4 H), 2.90 (dt, 1 H, *J* = 4.8, 3.1 Hz), 2.89 (dt, 1 H, *J* = 4.8, 3.1 Hz), 2.42–2.38 (m, 2 H), 2.33–2.23 (7 H), 2.16–2.08 (m, 2 H), 1.91–1.76 (m, 3 H), 1.76–1.63 (m, 3 H), 1.53–1.45 (m, 3 H); ^{13}C NMR (125 MHz, CDCl3) 212.4 (2 C), 158.3 (2 C), 145.8, 144.9, 137.7, 136.7, 128.3 (2 C), 126.9 (2 C), 126.8 (2 C), 125.6, 125.4, 113.7 (2 C), 79.5 (2 C), 55.2 (2 C), 46.3 (2 C), 42.9 (2 C), 41.2 (2 C), 25.9, 25.8, 24.9, 24.8;

HRMS (ESI) *m/z* calcd for $C_{20}H_{22}O_3Na$ [(M+Na)$^+$] 333.1467, found 333.1467.

3-(9-Hydroxy-9*H*-xanthen-9-yl)cyclohexan-1-one (49j)

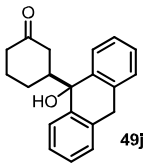

49j

The desired product was isolated (155.1 mg, 70%) as a white solid:

IR (film) 3395, 2927, 1604, 1476, 1450 cm^{-1};

^{1}H NMR (500 MHz, CDCl3) δ 7.68 (dd, 1 H, *J* = 7.8, 1.6 Hz), 7.61 (dd, 1 H, *J* = 7.8, 1.6 Hz), 7.40–7.31 (m, 2 H), 7.20 (dq, 2 H, *J* = 7.2, 1.2 Hz), 7.15 (d, 2 H, *J* = 8.2 Hz), 2.36 (ddt, 1 H, *J* = 13.8, 3.7, 2.2 Hz), 2.23–2.19 (m, 1 H), 2.13 (tt , 1 H, *J* = 12.2, 3.2 Hz), 2.07–1.98 (m, 1 H), 1.97–1.91 (m, 1 H), 1.88 (d, 1 H, *J* = 13.7 Hz), 1.86–1.79 (m, 1 H), 1.66 (s, 1 H), 1.43 (qt, 1 H, *J* = 13.5, 3.9 Hz), 1.10 (dq, 1 H, *J* = 12.9, 3.6 Hz); ^{13}C NMR (125 MHz, CDCl3) 211.6, 151.0 (2 C), 129.2, 129.2, 126.7, 126.6, 126.0, 125.8, 123.4 (2 C), 116.2, 116.1, 71.0, 52.4, 42.5, 41.1, 25.2, 24.6;

HRMS (ESI) *m/z* calcd for $C_{19}H_{18}O_3Na$ [(M+Na)$^+$] 317.1154, found 317.1140.

5.7.3 General Procedure for β-Aldol Reaction of Aryl-Alkyl Ketones

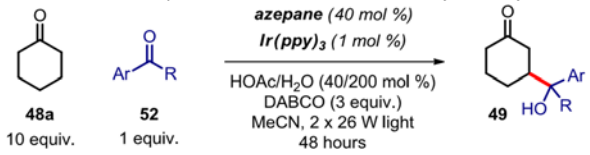

A solution of Ir(*p*-MeO-ppy)$_3$ (5.7 mg, 7.5 µmol, 0.010 equiv.), DABCO (252.0 mg, 2.250 mmol, 3.000 equiv.), methyl aryl ketone **52** (0.75 mmol, 1.00 equiv.), azepane (36.0 µL, 0.300 mmol, 0.400 equiv.), cyclohexanone **48** (0.78 mL, 7.5 mmol, 10.0 equiv.), acetic acid (18.0 µL, 0.300 mmol, 0.400 equiv.) and water (27 µL, 1.5 mmol, 2.0 equiv.) in CH_3CN (4.5 mL) was degassed by bubbling Ar stream for 10 min, and then irradiated with two 26 W fluorescent lamps (at approximately 2 cm away from the light source; temperature at 40 °C). After 48 h, the reaction mixture was concentrated *in vacuo*. Purification by flash chromatography on SiO_2 (15-30% EtOAc in hexanes) provided the desired product **49**.

3-(1-Hydroxy-1-phenylethyl)cyclohexan-1-one (49k)

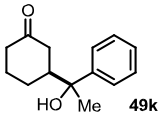

The desired product was isolated (126.3 mg, 77%) as an inseparable mixture of two diastereomers (1:1 ratio):

IR (film) 3456, 2946, 1702, 1447 cm^{-1};

^{1}H NMR (500 MHz, CDCl3) δ 7.41–7.33 (m, 8 H), 7.29–7.25 (m, 2 H), 2.56 (ddt, 1 H, *J* = 13.9, 4.2, 2.2 Hz), 2.35–2.30 (m, 2 H), 2.28–1.96 (m, 10 H), 1.65–1.27 (m, 7 H), 1.62 (s, 3 H), 1.56 (s, 3 H); ^{13}C NMR (125 MHz, CDCl3) 212.5, 212.4, 146.7, 146.2, 128.2 (2 C), 126.9, 126.8, 125.0 (2 C), 75.9, 75.7, 49.4, 49.3, 42.9, 42.8, 41.2, 41.1, 27.8, 27.6, 25.7, 25.3, 24.9 (2 C); HRMS (ESI) *m/z* calcd for $C_{14}H_{18}O_2Na$ [(M+Na)$^+$] 241.1204, found 241.1193.

3-(1-(4-Fluorophenyl)-1-hydroxyethyl)cyclohexan-1-one (49l)

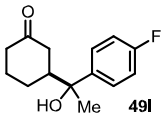

The desired product was isolated (114.7 mg, 65%) as an inseparable mixture of two diastereomers (1:1 ratio):

IR (film) 3447, 2942, 2868, 1704, 1508, 1224 cm^{-1};

^{1}H NMR (500 MHz, CDCl3) δ 7.30–7.25 (m, 4 H), 7.00–6.91 (m, 4 H), 2.44 (dddd, 1 H, *J* = 13.9, 4.0, 2.1 Hz), 2.29–2.24 (m, 2 H), 2.21–1.89 (m, 10 H), 1.53 (s, 3 H), 1.48 (s, 3 H), 1.57–1.29 (m, 7 H); ^{13}C NMR (125 MHz, CDCl3) 212.2 (2 C), 162.6 (d, *J* = 2.5 Hz), 160.7 (d, *J* = 2.5 Hz), 142.4 (d, *J* = 3.75 Hz), 142.0 (d, *J* = 2.5 Hz), 126.8 (d, *J* = 5.0 Hz), 126.7 (d, *J* = 5.0 Hz), 115.0 (d, *J* = 1.25 Hz), 114.8 (d, *J* = 1.25 Hz), 75.6, 75.4, 49.5 (2 C), 42.9, 42.8, 41.2, 41.1, 27.9, 27.7, 25.7, 25.3, 24.9 (2 C);

HRMS (ESI) *m/z* calcd for $C_{14}H_{17}FO_2Na$ [(M+Na)$^+$] 259.1110, found 259.1109. **3-(1-(Benzofuran-2-yl)-1-hydroxyethyl)cyclohexan-1-one (49m)**

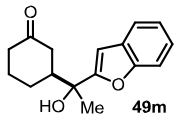

49m

The desired product was isolated (108.6 mg, 56%) as an inseparable mixture of two diastereomers (1:1 ratio):

IR (film) 2937, 1706, 1454, 753 cm^{-1};

^{1}H NMR (500 MHz, CDCl3) δ 7.55 (t, 1 H, *J* = 1.9 Hz), 7.54 (t, 1 H, *J* = 1.9 Hz), 7.46 (dd, 1 H, *J* = 3.4, 1.1 Hz), 7.44 (dd, 1 H, *J* = 3.4, 1.1 Hz), 7.30–7.22 (m, 4 H), 6.64 (d, 1 H, *J* = 0.9 Hz), 6.63 (d, 1 H, *J* = 0.9 Hz), 2.50–2.44 (m, 1 H), 2.44–2.04 (m, 14 H), 2.01–1.95 (m, 1 H), 1.91–1.83 (m, 1 H), 1.65 (s, 3 H), 1.62 (s, 3 H), 1.56–1.46 (m, 3 H); ^{13}C NMR (125 MHz, CDCl3) δ 211.8, 211.6, 161.2, 161.0, 154.6 (2 C), 128.0 (2 C), 124.1, 124.0, 122.9 (2 C), 120.9 (2 C), 111.2 (2 C), 102.4, 102.3;

HRMS (ESI) *m/z* calcd for $C_{16}H_{18}O_3Na$ [(M+Na)$^+$] 281.1154, found 281.1149.

3-(1-(4-Chlorophenyl)-1-hydroxyethyl)cyclohexan-1-one (49n)

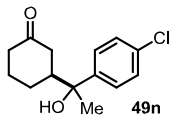

49n

The desired product was isolated (116.1 mg, 65%) as an inseparable mixture of two diastereomers (1:1 ratio):

IR (film) 3449, 2949, 1701, 1490, 1094 cm^{-1};

^{1}H NMR (500 MHz, CDCl3) δ 7.33-7.31 (m, 8 H), 2.53 (ddt, 1 H, *J* = 14.1, 4.1, 2.1 Hz), 2.38–2.30 (m, 2 H), 2.28–2.17 (m, 4 H), 2.16–1.96 (m, 7 H), 1.62–1.30 (m, 9 H), 1.60 (s, 3 H), 1.54 (s, 3 H); ^{13}C NMR (125 MHz, CDCl3) δ 212.2, 212.1, 145.2, 144.8, 132.7, 132.6, 128.3, 128.2, 126.6, 126.5, 75.6, 75.4, 49.3 (2 C), 42.8, 42.7, 41.1 (2 C), 27.8, 27.7, 25.6, 25.2, 24.8 (2 C); HRMS (ESI) m/z calcd for $C_{14}H_{17}ClO_2Na$ [(M+Na)$^+$] 275.0815, found 275.0813.

3-(1-Hydroxy-1-(*p*-tolyl)ethyl)cyclohexan-1-one (49o)

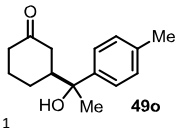

49o

The desired product was isolated (137.4 mg, 79%) as an inseparable mixture of two diastereomers (1:1 ratio):

IR (film) 3452, 2938, 2867, 1699, 1512, 818 cm^{-1};

^{1}H NMR (500 MHz, CDCl3) δ 7.34–7.25 (m, 4 H), 7.18 (t, 4 H, *J* = 8.5 Hz), 2.55 (ddt, 1 H, *J* = 14.1, 4.2, 2.1 Hz), 2.38 (s, 3 H), 2.37 (s, 3 H), 2.41–1.99 (m, 11 H), 1.79 (m, 2 H), 1.76–1.63 (m, 2 H), 1.62 (s, 3 H), 1.57 (s, 3 H), 1.63–1.26 (m, 4 H); ^{13}C NMR (125 MHz, CDCl3) δ 212.6 (2 C), 143.7, 143.2, 136.4 (2 C), 128.8 (2 C), 124.9 (2 C), 75.7, 75.6, 49.5, 49.4, 43.0, 42.9, 41.2, 41.1, 27.7, 27.5, 25.7, 25.4, 25.0 (2 C), 20.9 (2 C);

HRMS (ESI) *m/z* calcd for $C_{15}H_{20}O_2Na$ [(M+Na)$^+$] 255.1361, found 255.1357.

3-(1-Hydroxy-1-(3-methoxyphenyl)ethyl)cyclohexan-1-one (49p)

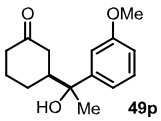

49p

The desired product was isolated (135.2 mg, 73%) as an inseparable mixture of two diastereomers (1:1 ratio):

IR (film) 3450, 1701, 1583, 1254, 1043 cm^{-1};

^{1}H NMR (500 MHz, CDCl3) δ 7.31–7.27 (m, 2 H), 7.00–6.95 (m, 2 H), 6.95–6.89 (m, 2 H), 6.83– 6.77 (m, 2 H), 3.83 (s, 3 H), 3.82 (3 H), 2.57–2.50 (m, 1 H), 2.38–2.28 (m, 3 H), 2.28–1.97 (m, 9 H), 1.70 (d, 2 H *J* = 4.4 Hz), 1.67–1.61 (m, 2 H), 1.60 (s, 3 H), 1.54 (s, 3 H), 1.56–1.32 (m, 3 H); [1373]C NMR (125 MHz, CDCl3) δ 212.5, 212.4, 159.5 (2 C), 148.6, 148.1, 129.2 (2 C), 117.4, 117.3, 111.6, 111.5, 111.4, 111.3, 75.8, 75.7, 55.2 (2 C), 49.3, 49.2, 42.9, 42.8, 41.2, 41.1, 27.8, 27.6, 25.7, 25.3, 24.9 (2 C);

HRMS (ESI) *m/z* calcd for $C_{15}H_{20}O_3Na$ [$(M+Na)^+$] 271.1310, found 271.1300.

3-(1-(Furan-2-yl)-1-hydroxyethyl)cyclohexan-1-one (49q)

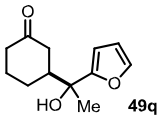

49q

The desired product was isolated (108.1 mg, 69%) as an inseparable mixture of two diastereomers (1:1 ratio):

IR (film) 3441, 2939, 1706, 1450 cm^{-1};

^{1}H NMR (500 MHz, CDCl3) δ 7.36 (dt, 2 H, *J* = 1.7, 0.9 Hz), 6.33 (dd, 2 H, *J* = 3.2, 1.8 Hz), 6.22 (ddd, 2 H, *J* = 3.1, 2.1, 0.9 Hz), 2.44–2.32 (m, 4 H), 2.28–2.13 (m, 6 H), 2.13– 2.06 (m, 3 H), 1.90–1.86 (m, 2 H), 1.64–1.55 (m, 2 H), 1.54 (s, 3 H), 1.53 (s, 3 H), 1.44–1.39 (m, 3 H); ^{13}C NMR (125 MHz, CDCl3) δ 212.0, 211.9, 158.3, 158.2, 141.7 (2 C), 110.2 (2 C), 105.6 (2 C), 73.4, 73.3, 48.1, 47.9, 42.9 (2 C), 41.3, 41.2, 23.7 (2 C), 25.0, 24.9, 24.2, 23.9; HRMS

(ESI) *m/z* calcd for $C_{15}H_{20}O_3Na$ [$(M+Na)^+$] 271.1310, found 271.1300.

3-(1-hydroxy-3-oxo-1-phenylbutyl)cyclohexan-1-one (49r)

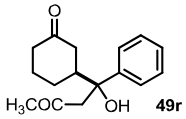

49r

The desired product was isolated (123.5 mg, 54%) as a mixture of two diastereomers (1.1:1 ratio).

Diastereomer 1: IR (film) 3466, 2942, 1706, 1667, 1448, 1218 cm^{-1};

^{1}H NMR (500 MHz, CDCl3) δ 7.83–7.77 (m, 2 H), 7.58–7.52 (m, 1 H), 7.41 (t, *J* = 7.8 Hz, 2 H), 7.38–7.34 (m, 2 H), 7.18–7.12 (m, 1 H), 5.01 (s, 1 H), 3.95 (d, *J* = 16.9 Hz, 1 H),

---

[137] H NMR (500 MHz, CDCl3) δ 7.85 (d, *J* = 8.2 Hz, 2 H), 7.61–7.54 (m, 1 H), 7.48–7.41 (m, 2 H), 7.35 (d, *J* = 7.3 Hz, 2 H), 7.30–7.23 (m, 3 H), 7.22–7.08 (m, 1 H), 5.08 (s, 1 H), 4.03 (d, *J* = 16.9 Hz, 1 H), 3.27 (d, *J* = 16.9 Hz, 1 H), 2.48–1.94 (m, 9 H); 13C NMR (125 MHz, CDCl3) δ 212.2, 201.8, 144.0, 136.8, 133.8, 128.7, 128.2, 128.0, 126.9, 125.2, 49.3, 44.9, 42.3, 41.1, 25.4, 24.9;

HRMS (ESI) *m/z* calcd for $C_{21}H_{22}O_3Na$ [$(M+Na)^+$] 345.1467, found 347.1461.

3.16 (d, *J* = 16.9 Hz, 1 H), 2.66–2.57 (m, 1 H), 2.55–2.44 (m, 1 H), 2.32 (ddq, *J* = 14.4, 4.2, 1.8 Hz), 2.28–2.19 (m, 1 H), 2.15–2.05 (m, 1 H), 1.98 (ddd, *J* = 12.9, 6.1, 3.0 Hz), 1.56–1.38 (m, 1 H); ^{13}C NMR (125 MHz, CDCl3) δ 212.4, 202.0, 144.8, 136.8, 133.9, 128.7, 128.2, 128.0, 126.8, 125.3, 49.4, 44.7, 43.0, 41.3, 25.1, 25.0;

HRMS (ESI) *m/z* calcd for $C_{21}H_{22}O_3Na$ [(M+Na)$^+$] 345.1467, found 347.1458.

Diastereomer 2: IR (film) 3463, 2943, 1704, 1666, 1448, 1219 cm^{-1}; **3-(2-(benzyloxy)-1-hydroxy-1-phenylethyl)cyclohexan-1-one (49s)**

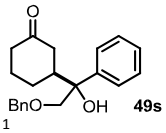

49s

The desired product was isolated (131.2 mg, 54%) as an inseparable mixture of two diastereomers (1:1 ratio):

IR (film) 2933, 1706, 1450, 1100 cm^{-1};

H NMR (500 MHz, CDCl3) δ 7.40–7.26 (m, 16 H), 7.20 (dt, *J* = 8.3, 7.6, 6.1 Hz, 4 H), 4.60–4.44 (m, 4 H), 3.83–3.69 (m, 4 H), 3.02 (s, 1 H), 2.96 (s, 1 H), 2.30 (ddq, *J* =12.3, 4.1, 2.2 Hz, 2 H), 2.27–2.03 (m, 9 H), 1.97 (ddt, *J* = 12.5, 6.2, 3.1 Hz), 1.60–1.30 (m, 6 H); ^{13}C NMR (125 MHz, CDCl3) δ 213.0, 212.0, 142.8, 142.3, 128.4 (2 C), 128.1, 128.0 (2 C), 127.9, 127.7 (2 C), 127.1, 127.0, 125.5, 74.8, 74.7, 73.5 (2 C), 46.5, 46.4, 42.9, 42.8, 41.2 (2 C), 25.6, 25.3, 25.0 (2 C); HRMS (ESI) *m/z* calcd for $C_{21}H_{24}O_3Na$ [(M+Na)$^+$] 347.1623, found 347.1614.

5.7.4 X-Ray Crystal Structures of Compounds 49d and 49e

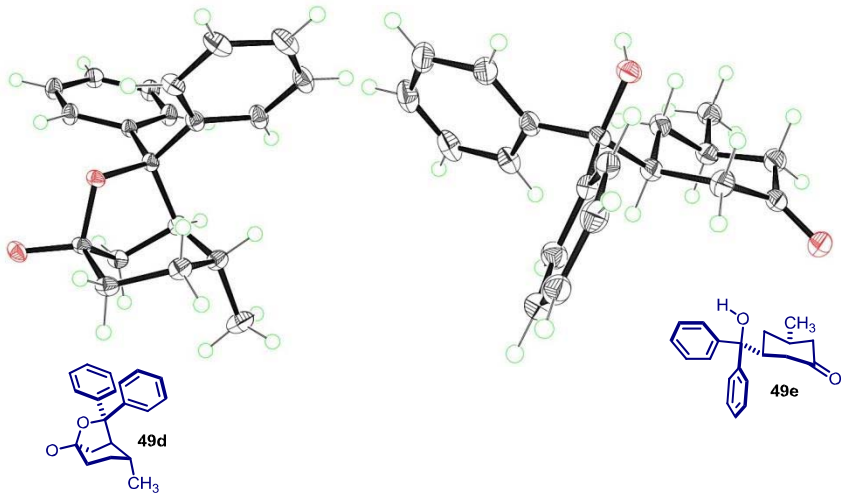

5.7.5 Emission Quenching Experiments (Stern–Volmer Studies)

Emission intensities were recorded using a Perkin Elmer LS50 luminescence spectrophotometer. All $Ir(ppy)_3$ solutions were excited at 320 nm and the emission intensity was collected at 518 nm. In a typical experiment, to a $1.2 \bullet 10^{-5}$ M solution of $Ir(ppy)_3$ in DMPU was added the appropriate

amount of quencher in a screw-top quartz cuvette. After degassing the sample with a stream of argon for 10 minutes, the emission of the sample was collected. All Ir(*p*-MeO-ppy)$_3$ solutions were excited at 350 nm and the emission intensity was collected at 500 nm. In a typical experiment, to a $2.0 \bullet 10^{-6}$ M solution of Ir(*p*-MeO-ppy)$_3$ in acetonitrile was added the appropriate amount of quencher in a screw-top quartz cuvette. After degassing the sample with a stream of argon for 10 minutes, the emission of the sample was collected.

UNIVERSITAT ROVIRA I VIRGILI
NOVEL AMINOCATALYTIC AND PHOTOCHEMICAL REACTIONS
Manuel Nappi

Chapter VI Metal-Free Photochemical Aromatic Perfluoroalkylation of α-Cyano Arylacetates via Electron Donor-Acceptor Complexes

Target

Photochemical perfluoroalkylation of aromatic compounds without the use of photocatalysts or photoinitiators.

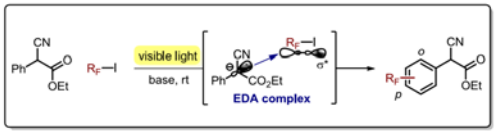

Tool

Ability of electron donor-acceptor (EDA) complexes to absorb visible light and generate openshell species under mild reaction conditions.[138]

The previous chapter has discussed how the use of metal-based photoactive complexes and their combination with other types of catalysis (i.e. aminocatalysis)[2] has allowed the development of unprecedent synthetic transformations. The ability of ruthenium- and iridiumbased polypyridyl complexes to absorb *visible light* and undergo single electron transfer processes was the key to form open-shell species in the reaction media. The modern field of photoredox catalysis has great potential toward a more sustainable way to conduct synthetic reactions. A further step toward a more environmentally benign organic synthesis would be to avoid the use of expensive metal-based photoactive complexes. Recently, our research group initiated a campaign aimed at using electron donor-acceptor (EDA) complexes to produce radical species under mild reaction conditions with the only use of *visible light*. Since EDA complex activation lies at the heart of the chemistry discussed in this chapter, some basic principle are detailed in the next section.

6.1 Principles of Electron Donor-Acceptor (EDA) Complexes

Electron donor-acceptor complex activation relies on the interaction between a donor (D), a molecule with a low ionization potential (IP), and an acceptor (A), a substrate with a high electron affinity (EA).

[138] The work discussed in this chapter has been published. see: M. Nappi, G. Bergonzini, P. Melchiorre. Metal-Free Photochemical Aromatic Perfluoroalkylation of α-Cyano Arylacetates. *Angew. Chem. Int. Ed.* **2014**, *53*, 4921–4925. G. Bergonzini discovered the unexpected reactivity and participated in the initial part of the optimization studies. This chemistry has been highlighted as a *Synstory* in *Synform* **2014**, (9) A116. [2] M. N. Hopkinson, B. Sahoo, J.-L. Li, F. Glorius. Dual Catalysis Sees the Light: Combining Photoredox with Organo-, Acid, and Transition-Metal Catalysis. *Chem. Eur. J.* **2014**, *20*, 3874.

The association is diffusion-controlled and generally forms a 1:1 intermolecular complex (Equation 1).[139]

$$D + A \overset{K_{EDA}}{\rightleftharpoons} [D,A] \qquad \text{(Eq. 1)}$$

For electrically charged species, such as anion/cation pairs, the association results in contact ion pairs (CIP) (Equation 2).[140]

$$D^- + A^+ \overset{K_{CIP}}{\rightleftharpoons} [D^-,A^+] \qquad \text{(Eq. 2)}$$

In each case, the intermolecular (ionic) complexation or association result in the highly oriented organization of the donor/acceptor pair (independently of whether they bear positive, negative or no charge) that is sometime sufficient to afford crystalline complexes amenable to direct Xray structure elucidation.[141]

The resulting molecular association is characterized by a new absorption band that is generally included in the visible range of the light, making the complexes colored.[142] Because one partner is intrinsically a good electron donor (low ionization potential) while the other is a good acceptor (high electron affinity), the excited state will have a large contribution from states such as $[D^{+}\cdot A^{-}]$ that involves an electron transfer, a configuration that is not possible for either isolated molecules. This preferentially stabilizes the excited state, leading to low energy (longer wavelength) absorption. As such, the photoexcitation of the charge-transfer absorption band of the electrically neutral EDA complex generates the ion-radical pair (Equation 3) and the contact ion pair generates the geminate radical pair (Equation 4) via photoinduced electron transfer (PET).[143]

$$[D,A]_{EDA} \overset{k_{PET}}{\rightleftharpoons} [D^{\bullet+},A^{\bullet-}] \qquad \text{(Eq. 3)}$$

$$[D^-,A^+]_{CIP} \overset{k_{PET}}{\rightleftharpoons} [D^{\bullet},A^{\bullet}] \qquad \text{(Eq. 4)}$$

Since the intensity of the charge-transfer (CT) absorption is directly related to the concentration of the EDA complex or contact ion pair in Equations (3) and (4), respectively, it can be used as an analytical tool to quantify complex formation in Equations (1) and (2). In the commonly utilized

---

[139] R. Foster. *Organic Charge-Transfer Complexes*. Academic Press, New York, 1969.
[140] T .M. Bockman, J. K. Kochi. Organometallic Ions and Ion Pairs. *Adv. Organometal. Chem.* **1991**, *33*, 51.
[141] C. K. Prout, B. Kamenar. In *Molecular Complexes,* Vol. 1, (ed. R. Foster) Russak, Crane, New York, 1973.
[142] a) R. S. Mulliken. Molecular compounds and their spectra II. *J. Am. Chem. Soc.* **1952**, *74*, 811–824; b) R. Foster. Electron donor–acceptor complexes. *J. Phys. Chem.* **1980**, *84*, 2135–2141.
[143] a) T. M. Bockman, J. K. Kochi. Photoinduced Electron Transfer in Contact Ion Pairs. *J. Am. Chem. Soc.* **1988**, *110*, 1294. For the behavior of geminate radical pairs, see b) J. K. Kochi. *Free Radicals,* Vols 1 and 2. Wiley, New York, 1973.

Benesi-Hildebrand equation,[144] the formation constants (K_{EDA}) are quantitatively evaluated from the graphical plot of the CT absorbance change (ΔA_{CT}) as the donor is progressively added to a solution of the acceptor (or vice versa, Equation 5).

$$\frac{[A]}{\Delta A_{CT}} = \frac{1}{K_{EDA}\varepsilon_{CT}}\frac{1}{[D]} + \frac{1}{\varepsilon_{CT}} \qquad \text{(Eq. 5)}$$

In Eq. 5, K_{EDA} is the EDA association constant and ε_{CT} is the molar extinction coefficient. If the K_{EDA} is higher than 10 M^{-1}, the EDA organization is considered relatively strong; intermediate values, *i.e.* $1 < K_{EDA} < 10$ M^{-1}, indicate a relatively weak association,[145] while values much lower than 1 M^{-1} define the contact charge-transfer complexes (lifetimes in the same order as molecular collisions).[146] This association favors the electronic coupling of the individual frontier molecular orbitals, which are the HOMO of the donor and LUMO of the acceptor, independently of the EDA complex strength. The new molecular orbitals created upon association define the energy of the electronic transition responsible for the CT absorption band observed experimentally (Scheme 1).

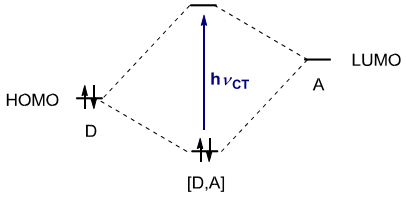

Scheme 1. Electronic coupling of the individual frontier molecular orbitals; HOMO of the donor (D) and LUMO of the acceptor (A).

After the photoinduced electron transfer, two open-shell species are formed. The donor/acceptor association in Equations 1 and 2 together with the photoinduced electron transfer (Equations 3 and 4) act in combination as a coupled set of equilibria (Equation 6).[147]

$$D + A \overset{K_{EDA}}{\rightleftharpoons} [D,A] \overset{k_{PET}}{\rightleftharpoons} [D^{\bullet+},A^{\bullet-}] \qquad \text{(Eq. 6)}$$

In order for EDA complexes to be synthetically useful, the two open-shell intermediates should undergo an irreversible chemical rearrangement or transformation at a rate faster than the back electron transfer (BET, return to the ground state of the EDA complex). In this case, products P would be generated in a rate described by the constant k_P (characteristic of highly reactive radical anion and radical cation, Equation 7).

---

[144] H. A. Benesi, J. H. Hildebrand. A Spectrophotometric Investigation of the Interaction of Iodine with Aromatic Hydrocarbons. *J. Am. Chem. Soc.* **1949**, *71*, 2703.
[145] R. Foster. In *Molecular Complexes,* Vol. 2. (ed. R. Foster), Russak, Crane, New York, 1974.
[146] M. Tamres, R. L. Strong. In *Molecular Association,* Vol. 2. (ed. R. F. Foster), Academic Press, New York, 1979.
[147] R. Rathore, J. K. Kochi. Donor/Acceptor Organizations and the Electron-Transfer Paradigm for Organic Reactivity. *Adv. Phys. Org. Chem.* **2000**, *53*, 193.

$$D + A \rightleftharpoons [D,A] \underset{k_{BET}}{\overset{k_{PET}}{\rightleftharpoons}} [D^{\bullet+},A^{\bullet-}] \xrightarrow{k_P} P \qquad \text{(Eq. 7)}$$

Despite the possibility for the EDA complex formation has been recognized in the 50's of the last century by Mulliken,[148] this type of activation has found very limited applications in organic chemistry. This is mainly because of the fast unproductive back electron transfer (BET) processes.[11] Open-shell species are in fact high-energy intermediates and, after the first photoinduced electron transfer (PET), they usually return to the initial status. The fact that the BET is generally very fast with comparison to all the other physical and chemical processes, has greatly limited the use of EDA activation in synthetic photochemistry.

6.2 Recent Advances in EDA Complex Activation

In 2013, our group successfully applied the electron donor-acceptor (EDA) complex theory to develop a photochemical enantioselective α-alkylation of aldehydes (Scheme 2).[149]

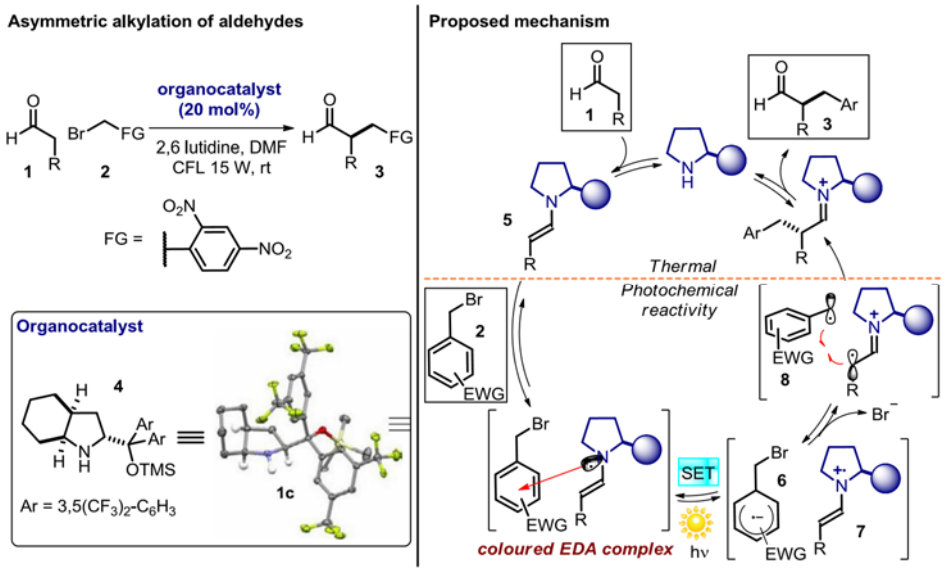

Scheme 2. Asymmetric alkylation of aldehydes *via* EDA complex activation.

The success of this asymmetric, metal-free process relied upon the formation of photonabsorbing EDA complexes, which arose from the ground-state association of a transiently generated chiral electron-rich enamine **5** (low ionization potential) with alkyl bromides **2** (high electron affinity).[150]

---

[148] R. S. Mulliken. Molecular Compounds and their Spectra. III. The Interaction of Electron Donors and Acceptors. *J. Phys. Chem.* **1952**, *56*, 801.

[149] As highlighted in Section 5.2, the first asymmetric organocatalytic photoredox alkylation of aldehydes was reported by MacMillan and Nicewicz, see *Science* **2008**, *322*, 77.

[150] E. Arceo, I. D. Jurberg, A. Alvarez-Fernandez, P. Melchiorre. Photochemical Activity of a Key Donor–Acceptor Complex Can Drive Stereoselective Catalytic α-Alkylation of Aldehydes. *Nat. Chem.* **2013**, *5*, 751.

Specifically, the condensation of an aldehyde **1** with a chiral secondary amine (the prolinol silyl ether derivative **4**) provides the expected enamine **5**. The electron-rich species **5** forms a yellow-orange colored EDA complex with the electron-deficient benzyl bromide **2**. Irradiation with visible light promotes the single electron transfer (SET) from enamine **5** to the bromo-compound **2**, affording the radical anion **6** and the enamine radical cation **7**. The radical anion **6** undergoes a very fast fragmentation (mesolysis) of the carbon-halogen bond yielding bromide and the benzyl radical **8**, which subsequently reacts with the chiral enamine radical cation intermediate **7** in the solvent cage to afford the desired α-alkylated aldehyde **3**. Alternative pathways are feasible, where the photo-excitation of the EDA complex acts only as initiation of a radical chain mechanism proceeding via a Kornblum-Russell $S_{RN}1$-type alkylation pathway.[15] In this case, the process would proceed through a traditional enamine catalysis pathway, with the radical **8** being trapped by the chiral enamine **5**.

6.3 Target of the Research Project and Initial Results

Motivated by this precedent, we wondered if the EDA activation could be used to achieve other synthetically useful photochemical transformations. In particular, we envisioned the possibility of using electron donor substrates other than enamine **5** to form a photoactive EDA complex. Given the electronic similarities to **5**, *in situ* generated enolates **9** were considered as suitable donors (Scheme 3).[151]

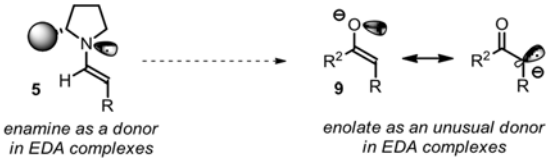

Scheme 3. Initial idea: using enolates as electron donors for EDA complex formation.

Perfluoroalkyl iodides **10** were selected as electron-accepting substrates, since a few literature precedents[152] qualified them as potential acceptors for the formation of EDA complexes. We envisioned that a facile-enolizable compound, such as ester **11**, can be easily deprotonated by an appropriate base to yield the key donor intermediate, the enolate **15** (Scheme 4). Anion **15** could then form a colored charge-transfer complex with perfluoroalkyl iodide **10**, which would

[15] G. A. Russell, & K. Wang. Electron Transfer Processes. 53. Homolytic Alkylation of Enamines by Electrophilic Radicals. *J. Org. Chem.* **1991**, *56*, 3475.

[151] a) For precedents describing the participation of enolates in the formation of EDA complexes, see: a) M. A. Fox, J. Younathan, G. E. Fryxell. Photoinitiation of the $S_{RN}1$ Reaction by Excitation of Charge-Transfer Complexes *J. Org. Chem.* **1983**, *48*, 3109; b) J. E. Argüello, A. B. Peñeñory, R. A. Rossi. Quantum Yields of the Initiation Step and Chain Propagation Turnovers in $S_{RN}1$ Reactions: Photostimulated Reaction of 1Iodo-2-methyl-2-phenyl Propane with Carbanions in DMSO. *J. Org. Chem.* **2000**, *65*, 7175.

[152] a) D. Cantacuzene, C. Wakeselman, R. Dorme. Condensation of perfluoroalkyl iodides with unsaturated nitrogen compounds. *J. Chem. Soc. Perkin Trans. 1* **1977**, 1365. b) P. V. Pham, D. A. Nagib, D. W. C. MacMillan. Photoredox Catalysis: A Mild, Operationally Simple Approach to the Synthesis of αTrifluoromethyl Carbonyl Compounds. *Angew. Chem. Int. Ed.* **2011**, *50*, 6119.

potentially undergo a photoinduced electron transfer (PET) driven by visible light. In particular, enolate **15** would donate an electron to the perfluoroalkyl iodide **10**, forming the α-radical **12** and the radical anion **16**, which would generate perfluorinated radical **13** and iodide through mesolysis. In analogy with the key C-C bond formation within the previous aldehyde α-alkylation strategy (Scheme 2), radical-radical coupling in the solvent cage would be the final step to afford the quaternarized α-perfluoroalkylated product **14**. In this manner, a metal-free photochemical α-perfluoroalkylation of carbonyl compounds could be obtained.

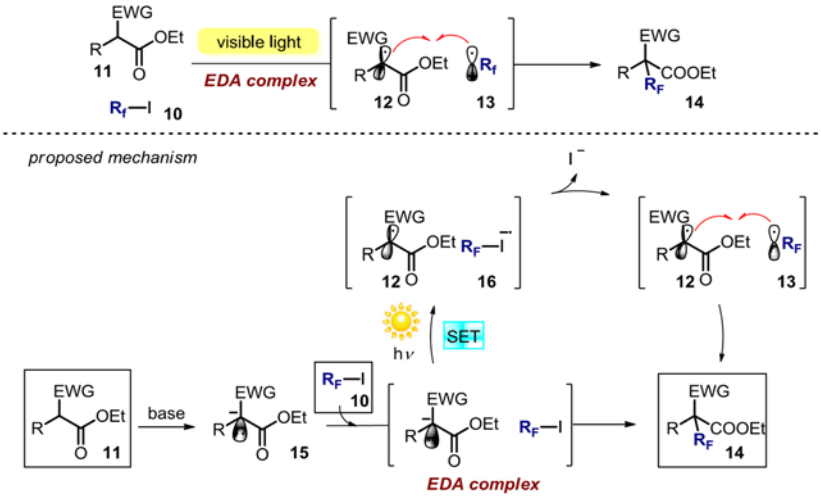

Scheme 4. Design plan for photochemical perfluoroalkylation via EDA complex activation. EWG = electron-withdrawing group.

The feasibility of our plan was tested by reacting the easy-enolizable ethyl α-cyano phenyl acetate **11a** with perfluorohexyl iodide **10a** under irradiation of 23W CFL bulb (Scheme 5). The reaction was conducted in acetonitrile and in the presence of potassium carbonate as the base to favor the deprotonation of **11a** and the formation of the corresponding enolate **15**. Immediately after mixing with the iodide **10a**, the solution developed a marked yellow-orange color; we considered this as the first visual indication that the desired EDA complex was generated in the media (all the starting materials and enolates are colorless, see the mechanistic investigation - Section 6.6.1).

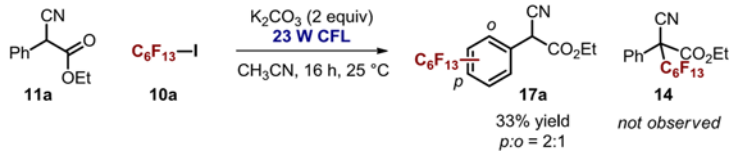

Scheme 5. The initial experiment and the discovery of an unexpected reactivity.

After 16 hours, the expected product **14** was not formed; however, the perfluoroalkylation of the aromatic moiety was observed instead, with the the *para* and *ortho* regioisomers (ratio 2:1) of product **17a** formed in 33% total yield.

Excited by this unexpected reactivity, we contextualized our photochemical perfluoroalkylation of aromatic compounds with respect to the previously reported transformations. We recognized that our methodology requires very mild conditions, since it occurs in the presence of a simple base, at room temperature and under visible light irradiation.

6.4 State-Of-The-Art of Aromatic Perfluoroalkylation

The increasing demand of more potent and efficient drugs requires the chemical community to come up with new synthetic strategies. Installation of particular moieties on potential biologically active compounds is recognized as one of the most powerful methodologies to enhance their efficiency. Among various chemical functional groups, fluorinated substituents are broadly used because of their ability to influence the physicochemical and conformational properties of possible drugs, such as bioavailability and lipophilicity. Moreover, fluorine atoms, due to their strong electronegativity, can establish non covalent interaction within the active sites of enzymes, increasing the binding affinity of the compounds.[153] During the last five decades chemists have developed new methodologies to install fluorine atoms, trifluoromethyl groups and perfluoroalkyl substituents into aromatic moieties. Typically, cross-coupling reactions promoted by transition metals served to accomplish this purpose, though the stoichiometric use of metal salts and organometallic complexes is necessary to obtain reasonable yields.[154][155] Recently, in 2009, Amii and colleagues developed the first example of copper-catalyzed trifluoromethylation of arenes (Scheme 6).[20]

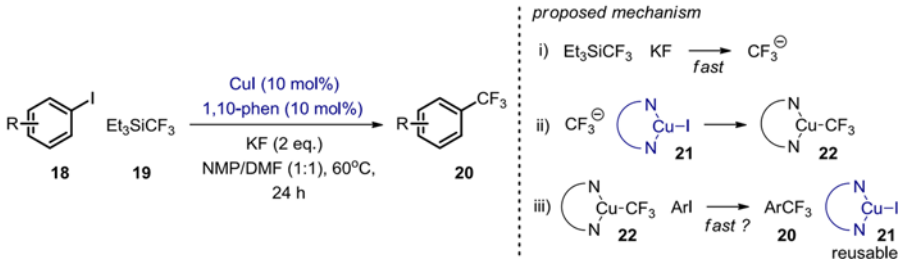

Scheme 6. The first copper-catalyzed trifluoromethylation of arenes.

Trifluoromethyl arenes **20** were synthesized starting from aryl iodides **18** and triethyl(trifluoromethyl)silane **19** using only 10 mol% of copper iodide and 1,10-phenanotroline (phen) as the ligand. Complex **22**, formed from the ligand exchange between the copper(I)

---

[153] For reviews in fluorine medicinal chemistry, see: a) S. Purser, P. R. Moore, S. Swallow, V. Gouverneur. Fluorine in Medicinal Chemistry. *Chem. Soc. Rev.* **2008**, *37*, 320. b) C. Isanbor, D. O'Hagan. Fluorine in Medicinal Chemistry: A Review of Anti-Cancer Agents. *J. Fluor. Chem.* **2006**, 127, 303.

[154] O. A. Tomashenko, V. V. Grushin. Aromatic Trifluoromethylation with Metal Complexes. *Chem. Rev.* **2011**, *111*, 4475.

[155] M. Oishi, H. Kondo, H. Amii. Aromatic Trifluoromethylation Catalytic in Copper. *Chem. Commun.* **2009**, 1909.

complex **21** and the CF_3 anion, is the key intermediate of this chemistry (Scheme 6; i, ii and iii). Complex **22** enhances the nucleophilicity and stability of the trifluoromethyl group, thus increasing the rate of the reductive elimination and the reformation of complex **21**.

In 2010, Buchwald reported the first example of palladium-catalyzed trifluoromethylation of arenes (Scheme 7).[156]

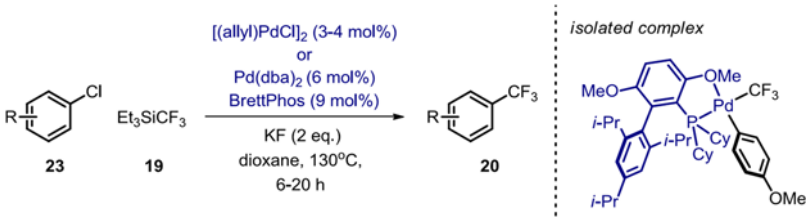

Scheme 7. The first palladium-catalyzed trifluoromethylation of arenes.

This challenging transformation was successfully realized using 3-6 mol% of $[(allyl)PdCl]_2$ or $Pd(dba)_2$ and the bulky phosphine ligand BrettPhos. In analogy with the approach of Amii, the trifluoromethyl anions were generated from the combination of $TESCF_3$ and KF (Scheme 6). High temperatures were required to speed up the reductive elimination step and obtain catalytic turnover. The authors proposed the classical Pd(0)-Pd(II) cycle as the mechanism of this trifluoromethylation reaction of arenes.

A large proportion of direct arene perfluoroalkylation methods were developed capitalizing upon the electrophilicity of the perfluoroalkyl radicals,[157] which typically react with arenes *via* the classical homolytic aromatic substitution (HAS) pathway.[23] The generation of such radicals generally requires harsh reaction conditions, including high reaction temperatures,[158] the use of stoichiometric radical initiators and/or metals,[159] and potentially explosive oxidants.[160] Recently, Baran developed an "innate" C-H trifluoromethylation of heterocycles using a well-known reagent, the Langlois' salt **24** (Scheme 8).[161]

---

[156] E. J. Cho, T. D. Senecal, T. Kinzel, Y. Zhang, D. A. Watson, S. L. Buchwald. The Palladium-Catalyzed Trifluoromethylation of Aryl Chlorides. *Science* **2010**, *328*, 1679.
[157] W. R. Dolbier, Jr.. Structure, Reactivity, and Chemistry of Fluoroalkyl Radicals. *Chem. Rev.* **1996**, *96*, 1557. [23] A. Studer. A " enaissance" in adical Trifluoromethylation. *Angew. Chem. Int. Ed.* **2012**, *51*, 8950.
[158] a) G. V. D. Tiers. Perfluoroalkylation of Aromatic Compounds. *J. Am. Chem. Soc.* **1960**, *82*, 5513; b) A. B. Cowell, C. Tamborski. Fluoroalkylation of Aromatic Compounds. *J. Fluorine Chem.* **1981**, *17*, 345;
[159] Y. Tanabe, N. Matsuo, N. Ohno. Direct Perfluoroalkylation Including Trifluoromethylation of Aromatics with Perfluoro-Carboxylic Acids Mediated by Xenon Difluoride. *J. Org. Chem.* **1988**, *53*, 4582
[160] a) H. Sawada, M. Nakayama, M. Yoshida, T. Yoshida, N. Kamigata. Trifluoromethylation of Aromatic Compounds with Bis(trifluoroacetyl) peroxide. *J. Fluorine Chem.* **1990**, *46*, 423; b) B. R. Langlois, E. Laurent, N. Roidot. Trifluoromethylation of Aromatic Compounds with Sodium Trifluoromethanesulfinate under Oxidative Conditions. *Tetrahedron Lett.* **1991**, *32*, 7525.
[161] Y. Ji, T. Brueckl, R. D. Baxter, Y. Fujiwara, I. B. Seiple, S. Su, D. G. Blackmond, P. S. Baran. Innate C-H Trifluoromethylation of Heterocycles. *Proc. Natl. Acad. Sci. USA* **2011**, *108*, 14411.

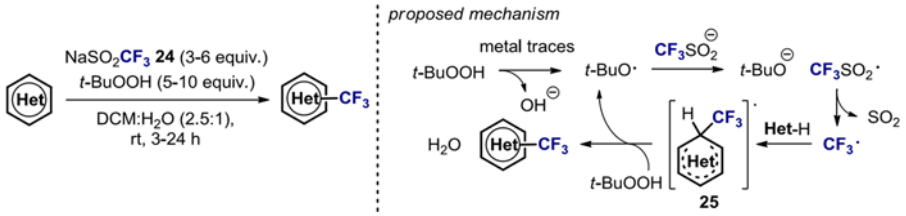

Scheme 8. Innate C-H trifluoromethylation of heterocycles.

The reaction proceedes at ambient temperature, in aqueous conditions and in air, though 5-10 equivalents of *tert*-butyl peroxide were needed. The authors proposed a mechanism where metal traces were responsible of the initial reduction of the peroxide (Scheme 8). The resulting *tert*-butoxy radical was then formed, which could oxidize the trifluormethanesulfinate ($CF_3SO_2^-$) to the corresponding trifluormethanesulfinyl radical ($CF_3SO_2\cdot$). Consequent loss of sulfur dioxide furnished the trifluoromethyl radical ($CF_3\cdot$), which undergoes a classical HAS chain pathway. Another molecule of *tert*-butyl peroxide was reduced by the cyclohexadienyl radical **25** of the heteroarene product (generated by the attack of the trifluoromethyl radical on the neutral heteroarene, Het-H) to obtain the final trifluoromethylated heteroarene and another trifluormethanesulfinyl radical ($CF_3SO_2\cdot$).

A different approach for the trifluoromethylation of arenes was described by MacMillan. Metalbased photoredox catalysis driven by visible light was a suitable method for generating perfluoroalkyl radical intermediates under very mild reaction conditions.[162] In particular, 1 mol% of ruthenium-based photocatalyst **26** ($Ru(phen)_3^{2+}$) generated trifluoromethyl radical from trifluoromethansulfonyl chloride **27** under irradiation from a normal compact fluorescence lamp (CFL) of 26 W (Scheme 9).

[162] D. A. Nagib, D. W. C. MacMillan. Trifluoromethylation of Arenes and Heteroarenes by Means of Photoredox Catalysis. *Nature* **2011**, *480*, 224.

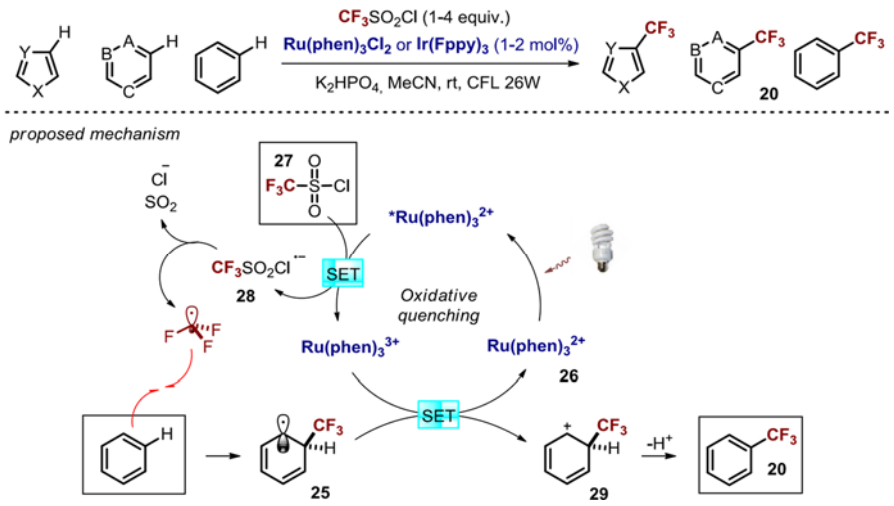

Scheme 9. Trifluoromethylation of arenes and heteroarenes by means of photoredox catalysis.

Irradiation of $Ru(phen)_3^{2+}$ **26** provided the excited state of the photocatalyst ($E_{1/2}^{III/II*}$ = -0.90 V) that could readily reduce trifluoromethansulfonyl chloride **27** ($E_{1/2}$ = -0.18 V). Trifluoromethansulfonyl radical anion **28** was then formed, which underwent an irreversible fragmentation to generate the reactive trifluoromethyl radical along with sulfur dioxide and chloride. Consequent radical-arene coupling afforded the cyclohexadienyl radical **25** ($E_{1/2}$ = -0.1 V), which could be easily oxidized by $Ru(phen)^{3+}$ ($E_{1/2}^{III/II}$ = +1.31 V). This SET returned the ground state of the photocatalyst **26** (closing the photocatalytic cycle), along with the cyclohexadienyl cation **29**. Deprotonation of the positive charged intermediate **29** finally furnished the trifluoromethylated arenes and heteroarenes **20**.

In 2013, Itoh and colleagues reported a direct C-H perfluoroalkylation of arenes and heteroarenes using a photoredox organocatalyst as the promoter of the perfluoroalkyl radical species.[163] In this case, an organic molecule such as anthraquinone-2-carboxylic acid **30** was used as photocatalyst, generating open-shell species from Langlois' salts (Scheme 10).

[163] L. Cui, Y. Matusaki, N. Tada, T. Miura, B. Uno, A. Itoh. Metal-Free Direct C-H Perfluoroalkylation of Arenes and Heteroarenes Using a Photoredox Organocatalyst. *Adv. Synth. Catal.* **2013**, *355*, 2203.

Metal-Free Photochemical Aromatic Perfluoroalkylation of α

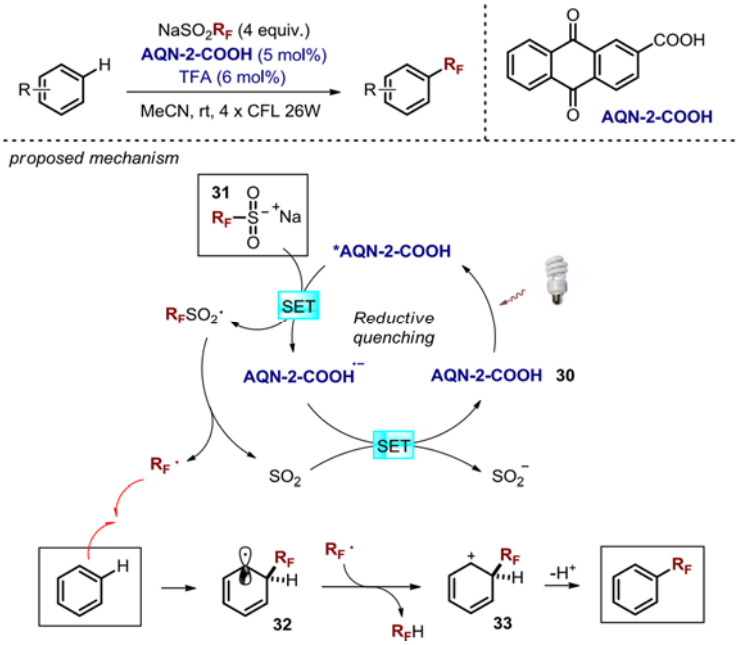

Scheme 10. Direct C-H perfluoroalkylation of arenes using a photoredox organocatalyst.

According to the proposed mechanism, the excited state of antraquinone **30** ($E_{1/2}^{0*/-1}$ = >1.5 V) was able to oxidize the perfluoroalkylsulfinate **31** to the corresponding perfluoroalkylsulfinyl radical ($R_FSO_2\cdot$) ($E_{1/2}$ = 0.6 V). Perfluoroalkyl radical $R_F\cdot$ was generated along with sulfur dioxide ($E_{1/2}$ = -1.1 V), which readily oxidized the radical anion of the antraquinone to the ground state of the organocatalyst ($E_{1/2}^{0/-1}$ = -1.3 V), closing the photoredox cycle. Meanwhile, the perfluoroalkyl radical could react with the neutral arene to afford the cyclohexadienyl radical **32**, which was oxidized to the corresponding cyclohexadienyl cation **33** by another perfluoroalkyl radical. Further deprotonation provided the desired perfluoroalkylated aromatic compounds.

The methodologies recently developed for the trifluoromethylation and the perfluoroalkylation of arenes relies upon strong oxidants or metal- or organic-based photoredox catalysts. We recognised the importance of a methodology that allows the construction of perfluoroalkylated arenes without the use of photocatalyst, while requiring mild reaction conditions.

6.5 Results and Discussion

We initially tested different inorganic and organic bases in order to improve the reactivity of our unanticipated perfluoroalkylation of arenes (Table 1). The base is crucial to form the key enolate intermediate from the α-cyano arylacetate **11a**. The best results were obtained when using cesium carbonate, which afforded the product **17a** in 70% total yield. The product percent distribution was: 60% of the *para* regioisomer (*p*-**17a**), 33% of the *ortho* regioisomer (*o*-**17a**) and 7% of the bifuctionalized compound in both *ortho* and *para* positions (*o,p*-**17a**, entry 3).

Table 1. Bases screening and initial control experiments.

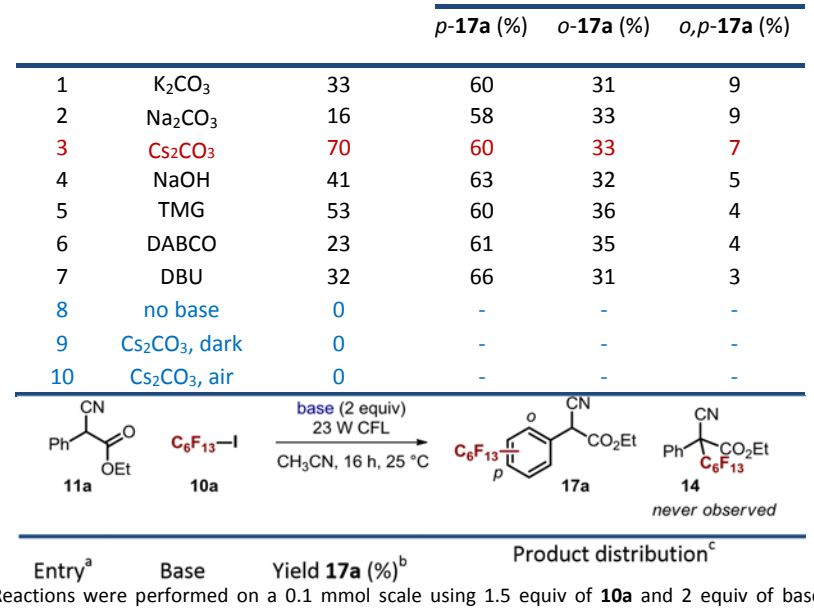

Entry[a]	Base	Yield **17a** (%)[b]	Product distribution[c]		
			p-**17a** (%)	*o*-**17a** (%)	*o,p*-**17a** (%)
1	K_2CO_3	33	60	31	9
2	Na_2CO_3	16	58	33	9
3	Cs_2CO_3	70	60	33	7
4	NaOH	41	63	32	5
5	TMG	53	60	36	4
6	DABCO	23	61	35	4
7	DBU	32	66	31	3
8	no base	0	-	-	-
9	Cs_2CO_3, dark	0	-	-	-
10	Cs_2CO_3, air	0	-	-	-

[a] Reactions were performed on a 0.1 mmol scale using 1.5 equiv of **10a** and 2 equiv of base, [**11a**]$_0$=0.5 M, and a 23 W CFL bulb to illuminate the reaction vessel. [b] Total yield determined by ^{1}H and ^{19}F NMR analysis using 1-fluoro-2-nitrobenzene as the internal standard. [c] Percent distribution of the *para*- (*p*-**17a**), *ortho*- (*o*-**17a**), and *ortho,para*-functionalized (*o,p*-**17a**) products determined by ^{1}H and ^{19}F NMR analysis of the crude mixture.

We next performed control experiments to confirm the necessity of the light and the base. Both of the components were required to have reactivity (entries 8 and 9); moreover, the presence of oxygen completely inhibited the reactivity (entry 10). It is worth noting that the site selectivity remained unaltered under the different conditions screened in Table 1. Further screening of the solvents identified acetonitrile as the appropriate medium for the photochemical aromatic perfluoroalkylation reaction (Table 2). Notably, less polar solvents completely suppressed the reactivity (entries 4 and 5).

Table 2. Solvent screening.

Metal-Free Photochemical Aromatic Perfluoroalkylation of α

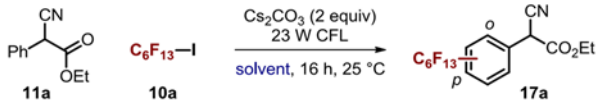

Entry[a]	Solvent	Yield **17a** (%)[b]	Product distribution[c]		
			p-**17a** (%)	*o*-**17a** (%)	*o,p*-**17a** (%)
1	CH_3CN	70	60	33	7
2	DMF	45	65	32	3
3	AcOEt	22	66	31	3
4	DCM 0	-	-	-	
5	Toluene	0	-	-	-

[a] Reactions were performed on a 0.1 mmol scale using 1.5 equiv of **10a** and 2 equiv of base, [**11a**]$_0$=0.5 M, and a 23 W CFL bulb to illuminate the reaction vessel. [b] Total yield determined by ^{1}H and ^{19}F NMR analysis using 1-fluoro-2-nitrobenzene as the internal standard. [c] Percent distribution of the *para*- (*p*-**17a**), *ortho*- (*o*-**17a**), and *ortho,para*-functionalized (*o,p*-**17a**) products determined by ^{1}H and ^{19}F NMR analysis of the crude mixture.

Variation of the standard reaction parameters, such as the temperature, the concentration and the stoichiometry, did not afford any improvement on the reaction yield. We noticed that the starting ethyl α-cyano phenyl acetate **11a** could be recovered (24%) even after prolonged irradiation. The inability of the reaction to progress till completion was rationalized on the basis of control experiments, which showed how the product **17a** inhibited the process. Specifically, when the *para* (*p*-**17a**) and *ortho* (*o*-1**7a**) regioisomers of the product were added in separate reactions, both of them decreased the reactivity of the system, furnishing half conversion in the products **17a** compared to the blank reaction (carried out in absence of product **17a**, Scheme 11).

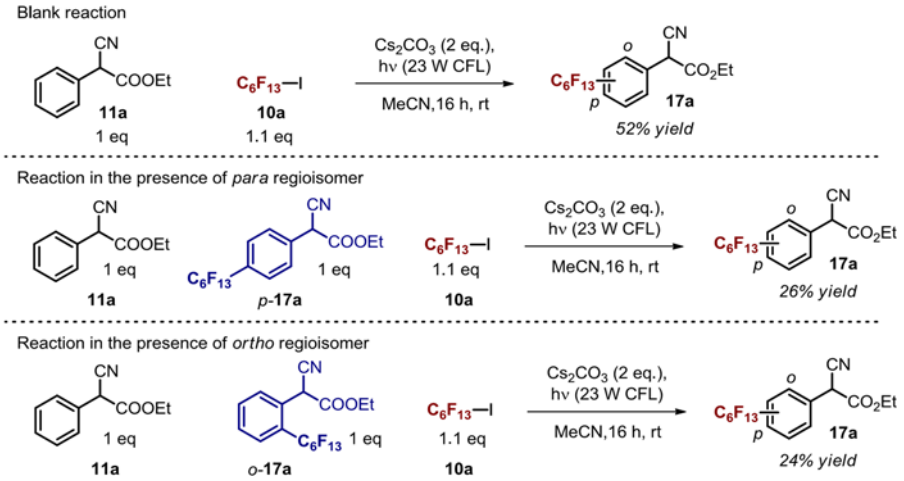

Scheme 11. Control experiments for product inhibition.

The reason for the product inhibition is probably ascribable to the strong visible light absorption showed by the enolates of the *para* and *ortho* regioisomers of the product **17a** (more details within the mechanistic investigation - Section 6.6.2). To address this issue, we added a perfluorinated solvent to the reaction mixture to partition the generated perfluorinated products **17a** in a different phase. Perfluorinated molecules have a strong affinity to remain in a perfluorinated phase rather than aqueous or organic phases; moreover, perfluorinated solvents are immiscible with most of the traditional organic solvents.[164] We evaluated the effect of perfluorinated solvents in combination with *N,N,N',N'*-tetramethylguanidine (TMG) and cesium carbonate as the bases (Table 3). TMG and perfluorohexane provided the best combination for the new biphasic system (entries 1-3), but offered reduced reactivity in comparison to the previous optimal reaction conditions (40% of yield, entry 2, *vs* 70% yield, entry 1, Table 2). We reasoned that, in the biphasic system, also the perfluorohexyl iodide **10a** would be preferentially solubilized in the perfluorinated phase along with the products **17a**, though the EDA association would happen in the organic phase exclusively (at the beginning of the reaction, the yelloworange color was only observed in the organic phase). Thus, the amount of perfluorohexyl iodide and the amount of perfluorohexane was presumed to affect the reactivity.

Table 3. Evaluation of perfluorinated solvents.

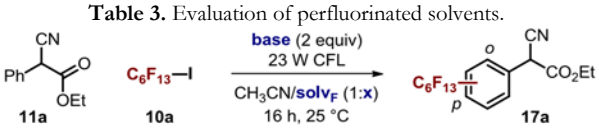

Entry[a]	Base	Solvent$_F$ (x)	**10a** (eq)	**17a** (%)[b]	Product distribution[c]		
					p-**17a** (%)	*o*-**17a** (%)	*o,p*-**17a** (%)
1	Cs_2CO_3	Hex_F (1)	1.5	30	68	32	traces
2	TMG	Hex_F (1)	1.5	40	65	35	traces
3	TMG	$MeCy_F$ (1)	1.5	34	65	35	traces
4	TMG	Hex_F (1)	2	45	65	35	traces
5	TMG	Hex_F (1)	3	66	62	35	3
6	TMG	Hex_F (1)	5	82	50	35	15
7	TMG	Hex_F (0.5)	1.5	46	62	35	3
8	TMG	Hex_F (0.33)	1.5	49	62	35	3
9	TMG	Hex_F (0.2)	1.5	54	62	35	3
10	TMG	Hex_F (0.2)	3	86	49	36	15

[a] Reactions were performed on a 0.1 mmol scale using 2 equiv of base, [**11a**]$_0$=0.5 M, and a 23 W CFL bulb to illuminate the reaction vessel. [b] Total yield determined by ^{1}H and ^{19}F NMR analysis using 1-fluoro-2-nitrobenzene as the internal standard. [c] Percent distribution of the *para*- (*p***17a**), *ortho*- (*o*-**17a**), and *ortho,para*-functionalized (*o,p*-**17a**) products, determined by ^{1}H and ^{19}F NMR analysis. $MeCy_F$ = perflurometylcyclohexane, Hex_F = perfluorohexane.

The fine tuning of these parameters led us to the best reaction conditions: as detailed in entry

[164] D. P. Curran. Strategy-Level Separations in Organic Synthesis: From Planning to Practice. *Angew. Chem. Int. Ed.* **1998**, *37*, 1174.

10, the desired perfluoroalkylated products **17a** where obtained in high yield (86%) using 3 equiv. of perfluorohexyl iodide, 2 equiv. of TMG and 20% of perfluorohexane respect to the amount of acetonitrile.

However, the site selectivity of the reaction was lower (*para*/*ortho*/*ortho,para* 5:3.5:1.5) with respect to the results obtained using acetonitrile as the only solvent (*para*/*ortho*/*ortho,para* 6:3.3:<1, entry 1, Table 2). We noticed that the percent distribution of *o*-**17a** remained consistently unaltered under the different conditions evaluated, indicating that the variation in the product distribution affected only *p*-**17a** and the *o,p*-**17a**. These results imply that the second perfluoroalkylation to give the bifuctionalized product (*o,p*-**17a**) occurred exclusively on the *para* regioisomer (*p*-**17a**). We then realized that the concentration of the perfluoroalkyl agent correlated with the amount of *o,p*-**17a** formed. Thus, we investigated the variation of both the yield and the product distribution during the time, hoping the rate of the second perfluoroalkylation (giving *o,p*-**17a**) to be much slower than the first one. We found that, performing the reaction over 5 hours instead of 16, product **17a** was obtained in 82% yield with a better site selectivity (*para*/*ortho*/*ortho,para* 5.8/3.2/1 entry 3, Table 4). It is of note that this reflects the orginal selectivity obtained in pure acetonitrile. 2.5 equiv. of TMG, 3 equiv. of **10a**, 20% of perfluorohexane respect to acetonitrile and a reaction time of 5 hours under the irradiation from a 23 W CFL were selected as the conditions to investigate the scope of the reaction.

Table 4. Evaluation of the yield and the product distribution during the time.

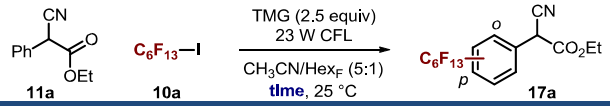

Entry[a]	Time (h)	**17a** (%)[b]	(%) **17a** (%)	Product distribution[c] *o*-**17a** (%)	*p*-**17a** *o,p*-
1	2	65	60	33	7
2	3.5	74	58	33	9
3	5	82	58	32	10
4	6.5	83	58	32	10
5	8	83	56	33	11
6	16	86	49	36	15
7	5 (no Hex_F)	64	60	33	7

[a] Reactions were performed on a 0.1 mmol scale, [**11a**]$_0$=0.5 M, and a 23 W CFL bulb to illuminate the reaction vessel. [b] Total yield determined by ^{1}H and ^{19}F NMR analysis using 1fluoro-2-nitrobenzene as the internal standard. [c] Percent distribution of the *para*- (*p*-**17a**), *ortho*- (*o*-**17a**), and *ortho,para*-functionalized (*o,p*-**17a**) products, determined by ^{1}H and ^{19}F NMR analysis of the crude mixture. Hex_F = perfluorohexane.

To confirm the benefit of the perfluorinated phase, we performed a control experiment in pure acetonitrile. The products **17a** were formed in lower yield of 64%, confirming the necessity of the perfluorinated solvent to obtain a higher level of efficiency (entry 7).

After the optimization process, we evaluated the synthetic potential of the photochemical perfluoroalkylation strategy by reacting differently substituted α-cyano arylacetates with perfluorohexyl iodide **10a**. A variety of electron donating groups were well tolerated, independently of their position on the aromatic ring (Figure 3b). *Para* substituted ethyl α-cyano arylacetates were functionalized selectively only at the *ortho* position, providing high chemical yields (products **17b-d**). Electro-withdrawing groups greatly reduced the efficiency of our photochemical perfluoroalkylation protocol (product **17e**).

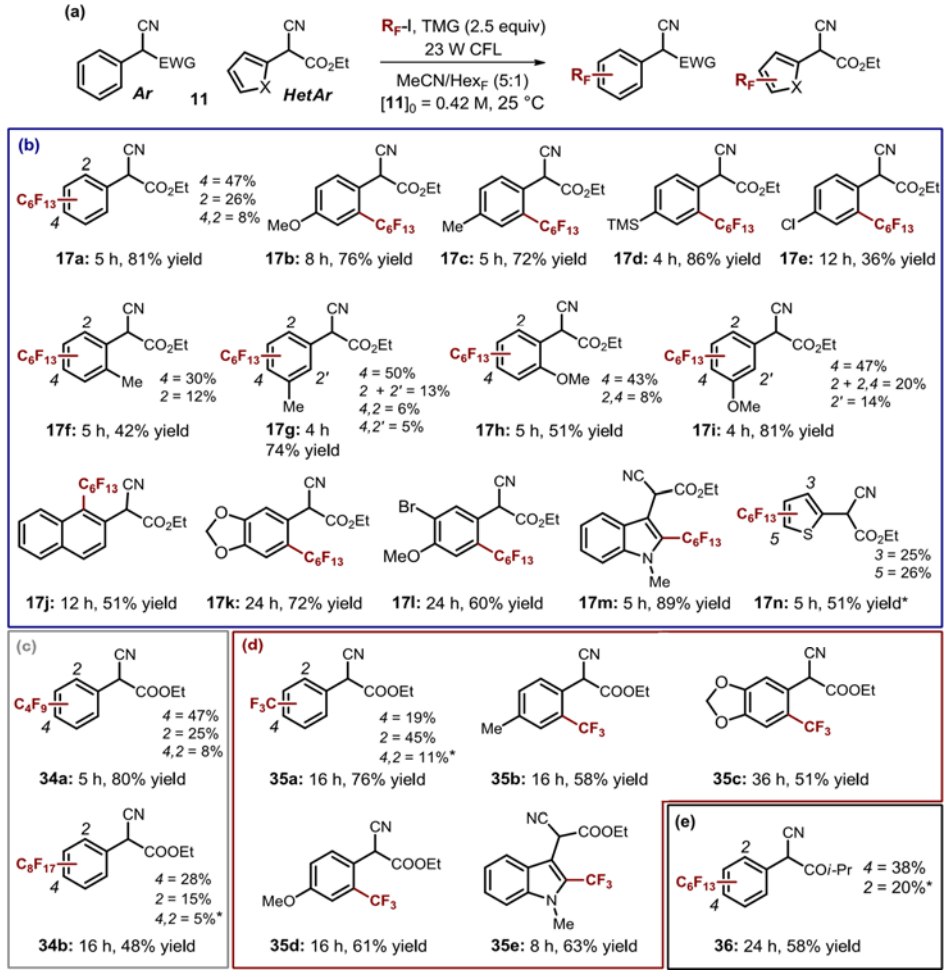

Figure 1. Metal-free photochemical aromatic perfluoroalkylation of α-cyano arylacetates. The overall yields refer to the sum of the yields of isolated regioisomeric compounds; as most of the regioisomers could be isolated by chromatography, individual yields for the isomers are also given. * Yields determined by ^{19}F

NMR spectroscopy. a) General conditions: reactions performed on a 0.2 mmol scale using 3 equiv of perfluoroalkyl iodides **10**, 2.5 equiv of TMG, 0.4 mL of MeCN, 0 μL of perfluorohexane, and a 23 W C L bulb; an acidic work-up (HCl 1 M) is required to isolate the products. b) Scope of the perfluoroalkylation with **10a**. c) Scope of the perfluoroalkylating agents. d) Trifluoromethylation of α-cyano arylacetates. e) Extending the reactivity to α-cyano phenylketone.

Ortho- and *meta*-substituted aromatic compounds afforded the *para* regioisomers as the major perfluoroalkylated adducts (**17f-i**). Remarkably, the different regioisomers could be easily isolated by flash chromatography on silica gel, increasing the synthetic utility of this approach. Surprisingly, the 2-naphthyl derivative was perfluoroalkylated only at the α position (product **17j**). High regioselectivity was also obtained with disubstituted aromatic compound (adducts **17k** and **17l**). In particular, a *meta*-electron-withdrawing substituent, such as bromine, was well tolerated furnishing product **17l** in good yield. Hetero-aromatic molecules could also be perfluoroalkylated, including indole and thiophene derivatives (**17m** and **17n**). In consonance with the poor reactivity observed when using electro-withdrawing substituents, electron-poor heteroarenes, like pyridines, did not react at all (results not shown in Figure 1).

After the evaluation of the aromatic partner, we explored different perfluoroalkylating agents (Figure 1c). A shorter perfluorobutyl chain could be installed in a fairly good yield (product **34a** same efficiency observed in **17a**); while a longer chain (octyl derivative) resulted in less reactivity than observed in the model reaction, even at a longer reaction time (product **34b**). Remarkably, the trifluoromethylation of ethyl α-cyano arylacetate was also achieved starting from CF_3I (Figure 1d). The *ortho*-regioisomer of product **35a** was favored *versus* the *para* adduct, in sharp contrast to the perfluoroalkylation with **10a**. This regiochemical divergence likely arose from the different steric impediments of the two radical fragments. Mono- (adducts **35b** and **35d**) and disubstituted (product **35c**) aromatic compounds, as well as hetero-aromatic counterpart (adduct **35e**), underwent trifluoromethylation with a high chemical yield.

We then investigated the importance of the two electron-withdrawing groups (cyano and ester) at the benzylic position on the model substrate **11a**. Replacement of the cyano group with other substituents, including nitro ($-NO_2$), ester (CO_2Et), or a keto moiety (-COR), resulted in the complete loss of reactivity (Scheme 12a). However, when the ester group was replaced by the *iso*-propyl ketone moiety, the corresponding product **36** could be obtained in a good yield (see Figure 1e).

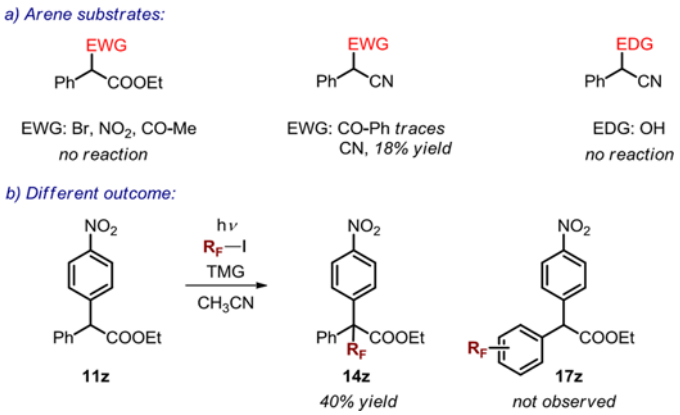

Scheme 12. Effects of the groups at the benzylic position of **11** on the reactivity.

It is worth to note that, when the cyano group was replaced with a *p*-nitrophenyl substituent (**11z**, Scheme 12b), product **14z** was obtained (40% yield) instead of the aromatic perfluoroalkylated product **17z**.[165]

6.6 Mechanistic Investigations

6.6.1 Evidence for EDA Activation

The first evidence that demonstrates the existence of an electron donor-acceptor (EDA) complex is the color formation when the two partners are mixed in acetonitrile. We immediately observed the formation of a yellow-orange color when ethyl α-cyano arylacetate **11a** was mixed with *N-N-N'-N'*-tetramethylguanidine (TMG) and perfluorohexyl iodide **10a**. Further measurement of the absorption spectrum confirmed the EDA association; a new band was generated in the visible range of the light (blue line, Figure 2).

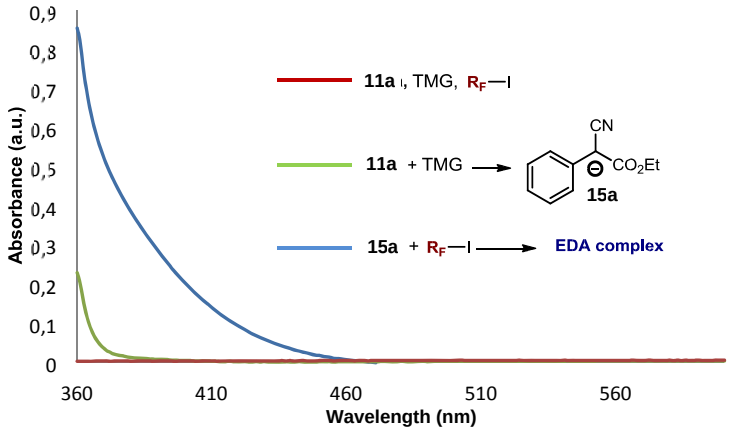

[165] Theoretical mechanistic studies are ongoing in collaboration with Professor F. Maseras (ICIQ) to explain this alternative reactivity.

Figure 2. Optical absorption spectra recorded in MeCN in quartz cuvettes (1 cm path) using a Shimadzu 2401PC UV-visible spectrophotometer. [**11a**] = 0.01 M, [**10a**] = 0.03 M; [TMG] = 0.02 M.

All the starting reagents (**11a**, **10a** and TMG) do not absorb in the visible region, as well as most the combinations between them (red line). The only compound that slightly absorbed over 360 nm is the corresponding enolate **15a**, generated by mixing **11a** with a base such as TMG (green line in Figure 2). In order to verify if the EDA complex activation was responsible for the reactivity (the main activation pathway to produce the open-shell species), we performed a control experiment using a 300 W xenon lamp, equipped with a cut-off filter at 385 nm, where the enolate **15a** cannot absorb (Scheme 13). The desired perfluoroalkylated products were formed in 61% yield after 2 hours, a reactivity comparable with the one observed using the normal 23 W CFL (65% yield, entry 1, Table 4).

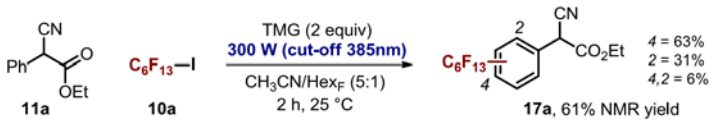

Scheme 13. Control experiment using 300 W Xenon lamp equipped with a cut-off filter at 385 nm.

Under these conditions (λ > 385 nm), the EDA complex (blue line in Figure 2) is the only species that can absorb light, as the enolate **15a** formed by deprotonation of **11a** has an absorption residue at around 360 nm. This leaves the visible-light-induced photoactivity of the EDA complex as the only plausible means to access radical reactivity, as homolytic cleavage of the C-I bond and exciplex formation between excited enolate **15a** and perfluorohexyl iodide **10a** are not feasible at wavelength > 385 nm.

6.6.2 Possible Explanation for the Observed Product Inhibition

The control experiments described in Scheme 11 indicated a product inhibition effect on the reaction rate. Therefore, we measured the absorption spectra of the products **17a** in combination with TMG and perfluorohexyl iodide **10a** (Figure 3 for the *para*-product and Figure 4 for the *ortho*-product). The UV-Vis spectra indicated that the molar extinction coefficients of **17a** enolates (both *ortho* and *para*, red lines) are considerably higher than the coefficient of the productive EDA complex of **15a** and **10a** (black dashed line). Moreover, only *p*-**17a** enolate seems to form a new EDA complex with perfluorohexyl iodide **10a** (yellow line, Figure 3), reinforcing the hypothesis that the bifuctionalized product *o,p*-**17a** came from the *para* regioisomer of the product *p*-**17a**.

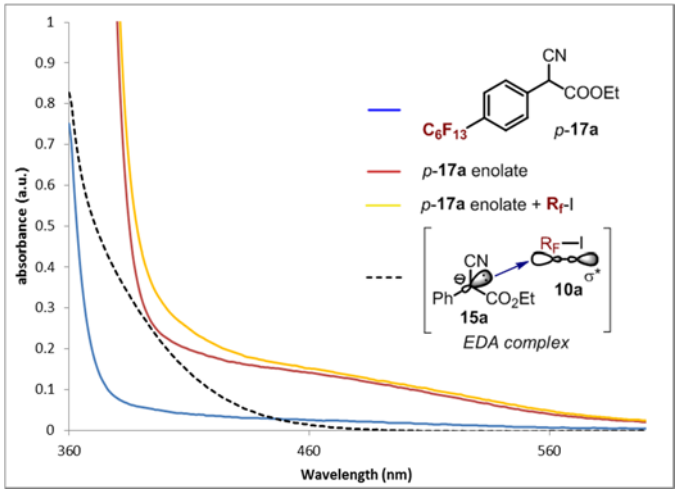

Figure 3. Optical absorption spectra recorded in MeCN in quartz cuvettes (1 cm path) using a Shimadzu 2401PC UV-visible spectrophotometer. [*p*-**17a**] = 0.01 M, [**10a**] = 0.03 M; [TMG] = 0.02 M.

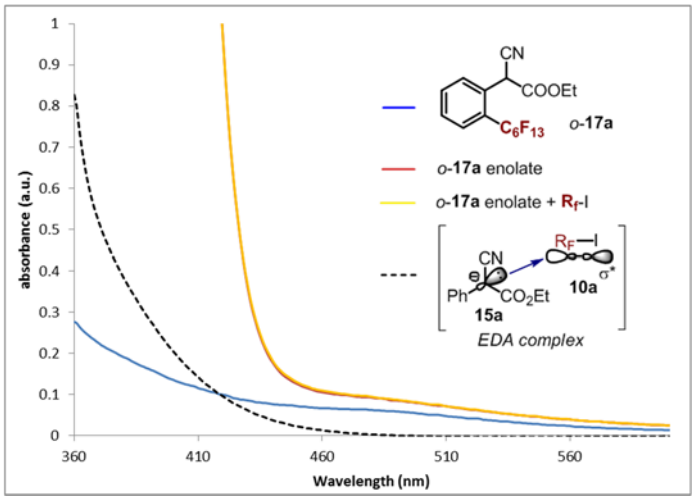

Figure 4. Optical absorption spectra recorded in MeCN in quartz cuvettes (1 cm path) using a Shimadzu 2401PC UV-visible spectrophotometer. [*o*-**17a**] = 0.01 M, [**10a**] = 0.03 M; [TMG] = 0.02 M.

The higher absorption in the region of visible light showed by the enolate of the products **17a** could explain the observed product inhibition effect, since the light will be absorb only by the enalotes of **17a** when a significant amount of the product **17a** is formed during the process.

6.6.3 Reaction Mechanism Investigations

In analogy with the previously reported photochemical α-alkylation of aldehydes *via* EDA complexes (Scheme 2), we firstly hypothesized that the key C-C bond formation of the perfluoroalkylation would occur in a solvent cage by means of a radical-radical combination (Scheme 14).

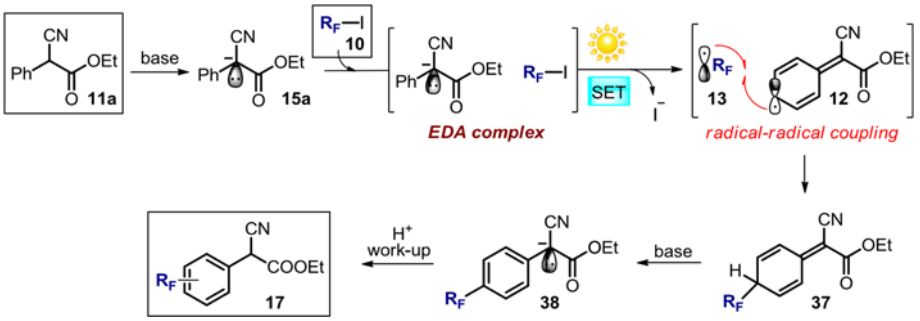

Scheme 14. Initial mechanistic proposal for the unexpected aromatic perfluoroalkylation.

In particular, the perfluoroalkyl radical **13**, generated after the photoinduced electron transfer (PET) within the EDA complex and C-I fragmentation, would react with the delocalized radical **12** inside the solvent cage to form the perfluoroalkylated intermediate **37**. Deprotonation of **37** by a second equivalent of base would restore the aromaticity leading to the product enolate **38**.

The determination of the quantum yield is one of the most useful experiments to understand the mechanism of a photochemical reaction. The quantum yield of a photochemical reaction defines the amount (moles) of product formed per amount (moles) of photon absorbed by the system (Equation 8).[166]

$$\Phi_{(\lambda)} = \frac{\text{Moles of product formed}}{\text{Moles of photon absorbed}} \qquad \text{(Eq. 8)}$$

This number considers all the photophysical and photochemical processes that occur from the primary absorption of photons to the generation of the desired product. For a process where one photon produces only one molecule of the product, the quantum yield can be maximum 1, while for a *chain* process where one photon can form *n* molecules of product, the quantum yield is expected to be >> 1. In the first case, a quantum yield equal to one indicates a 100% efficiency of all the processes: one electron promoted by each photon serves to generate one radical that led to one chemical product. This ideal situation is rare, since other parallel photophysical and photochemical processes can be involved. The mechanism proposed in Scheme 14 should provide a quantum yield less than or equal to 1 (in case of 100% of efficiency), since, for each photoinduced electron transfer (PET), one molecule of product would be generated.

However, when we performed the quantum yield experiments, we obtained a value of 2.03 (ferrioxalate actinometer, which measures the decomposition of ferric ions to ferrous ions, was used as the standard reference, see experimental section 6.8 for details). This value, higher than 1, indicates a radical chain mechanism as the main reaction pathway. This prompted us to

[166] S. E. Braslavsky. Glossary of terms used in photochemistry, 3rd edition (IUPAC Recommendations 2006) *Pure and Apply Chemistry* **2007**, *79*, 293 (on page 406).

propose a different mechanism (detailed in Scheme 15), where a homolytic aromatic substitution (HAS) chain mechanism is operative in our photochemical perfluoroalkylation. After the photoinduced electron transfer and mesolysis processes, the two radical intermediates **12** and **13** are formed, which can escape from the solvent cage. The perfluoroalkyl radical **13** (electrophilic radical) then reacts with the enolate **15** (electron-rich system) to form the radical anion **39** (corresponding to the cyclohexandienyl radical **40** in a normal HAS pathway, see Scheme 16).[167] At this stage, another molecule of perfluoroalkyl iodide **10** can be reduced by the radical anion **39**, thus propagating the chain by creating another perfluoroalkyl radical (after fast mesolysis of the C-I bond) along with intermediate **37**. Species **37** undergoes deprotonation and re-aromatization to generate the desired perfluoroalkylated products **17**.

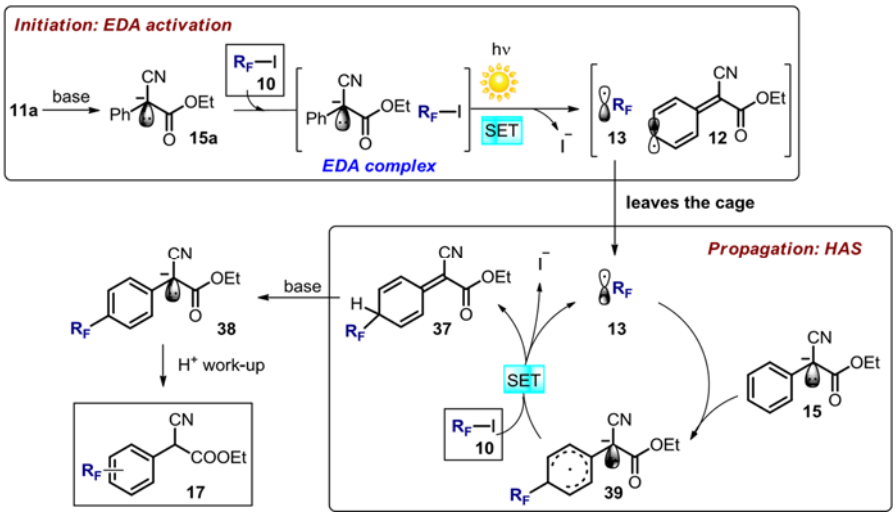

Scheme 15. Homolityc aromatic substitution (HAS) proposed chain mechanism.

Performing the trifluoromethylation with equivalent amounts of **11a** and [D_5]-**11a** showed a kinetic isotope effect (KIE) of 0.97±0.01 after 41% conversion, which excludes the aromatization being the rate-limiting event. The reactivity of the key system, as discussed in Figure 1, is in agreement with the classic HAS reactivity (Scheme 16): electron-withdrawing groups on α-cyano arylacetates **11** greatly reduced the efficiency of the reaction because of the reduced electron density on the arene. In particular, this effect i) decreases the reactivity of the arene toward electron-poor radicals and ii) generates a weaker reductant intermediate **39**, which is unable to

[167] A. Studer, D. P. Curran. Organocatalysis and C-H Activation Meet Radical- and Electron-Transfer Reactions. *Angew. Chem. Int. Ed.* **2011**, *50*, 5018.

efficiently reduce the perfluorinated agent **10** for propagating the chain reaction and form the perfluoroalkylated product.[168]

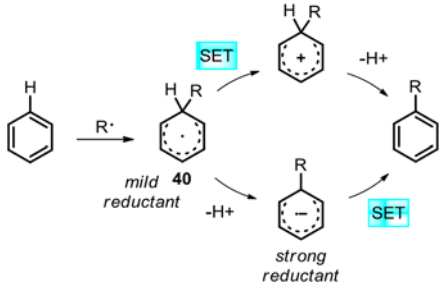

Scheme 16. Classical homolytic aromatic substitution (HAS) pathway.

To corroborate our mechanistic proposal, we conducted the model reaction under exclusion of light in order to completely suppress a mechanism initiated by the excitation of an EDA complex. We added instead Et_3B and O_2 to generate the perfluoroalkyl radical from iodine **10a**. The formation of the desired perfluoroalkylated product **17a** (11% yield, Scheme 17) was indicative that the key step of the radical chain mechanism, *i.e.* the trapping of the radical from the substrate, can occur.

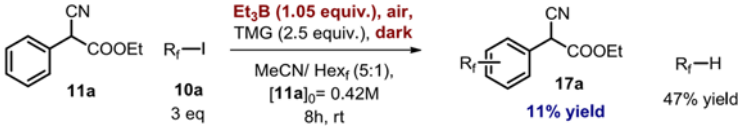

Scheme 17. Experimental evidence for the chain mechanism.

Notably, the same experiment, when conducted in the absence of TMG as the base, did not provide the product **17a**, thus indicating that the enolate **15a**, and not the neutral α-cyano arylacetate **11a**, is the active species of the HAS pathway.

During our studies, we could not detect the formation of the *meta*-substituted adducts. This result is in contrast with the very low regioselectivity generally observed in the HAS of substituted arenes with perfluoroalkyl radicals.[23] It seems that, under our reaction conditions, the reactivity is mainly governed by the mesomeric effects of the anionic benzylic substituent (enolate **15**), which directs the reaction exclusively toward the *para* and *ortho* alkylation pathways. Moreover, the results in Figure 1 indicate that the electronic properties of the EWGs at the benzylic position of α-cyano arylacetate **11** play a crucial role: their polar effect should be strong enough to allow the easy formation of the enolate under basic conditions, but without affecting the ensuing C-C bond formation by depleting the electro density on the aromatic ring. To corroborate our

[168] A. Bravo, H.-R. Bjørsvik, F. Fontana, L. Liguori, A. Mele, F. Minisci. New Methods of Free-Radical Perfluoroalkylation of Aromatics and Alkenes. Absolute Rate Constants and Partial Rate Factors for the Homolytic Aromatic Substitution by n-Perfluorobutyl Radical. *J. Org. Chem.* **1997**, *62*, 7128.

interpretation that the enolate **15a** derived from **11a** acts as a powerful electron-releasing group, we measured the Taft resonance parameter. In 1963 Taft and colleagues introduced a simple and practical method to evaluate the pure resonance effect of a substituent onto an aromatic ring using ^{19}F NMR spectroscopy.[169] Using this approach, we determined a reactivity resonance parameter (σ_R) for the enolate **15** of -0.40, a considerable value that confirms the electron-releasing ability of the anionic group (for comparison, an *N*,*N*dimethyl amino substituent, a strong EDG, has a σ_R = -0.56;[35] for experimental details and calculation see the Experimental Section 6.7). To further verify our interpretation, we ran the model reaction in the presence of 5 equivalents of anisole, an electron-rich arene. This competitive experiment provided adducts **17a** exclusively and only traces of the perfluoroalkylated anisole derivative (Table 5, entry 1)

Table 5. Experimental evidence for proposed HAS mechanism.

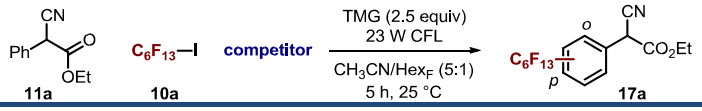

Entry	Competitor	Amount	**17a** (%)[b]	Others[b]
1	Anisole	1 equiv.	69	Traces of perfluoroalkylated anisole
2	TEMPO	2 equiv	0	5% of C_6F_{13}-TEMPO
3	1,4-dinitrobenzene	20 mol%	22	-

[a] Reactions were performed on a 0.1 mmol scale, [**11a**]$_0$=0.5 M, and a 23 W CFL bulb to illuminate the reaction vessel. [b] Total yield determined by ^1H and ^{19}F NMR analysis using 1fluoro-2-nitrobenzene as the internal standard.

Additionally, when 2,2,6,6-tetramethylpiperidine-1-oxyl (TEMPO) was added in the reaction condition, no products **17a** were observed, indicating that a radical mechanism is operative (entry 2). 20 mol% of 1,4-dinitrobenzene greatly decreased the reaction efficiency to 22% (entry 3), confirming that single electron transfers are occurring in the reaction conditions (1,4dinitrobenzene is a good electron acceptor with a strong electron affinity).

During our mechanistic studies, we envisioned another possible pathway based on the involvement of radical **12**. It is known that the dimer **41** is a good radical initiator for "living" polymerization due to the weak C-C bond between the two monomers (50 °C is enough to start the polymerization by promoting a thermally-induced homolytic cleavage of **41**,[170] Scheme 18).

---

[169] a) R.W. Taft, E. Price, I. R. Fox, I. C. Lewis, K. K. Andersen, G. T. Davis. Fluorine Nuclear Magnetic Resonance Shielding in p-Substituted Fluorobenzenes. The Influence of Structure and Solvent on Resonance Effects. *J. Am. Chem. Soc.* **1963**, *85*, 3146; b) C. Hansch, A. Leo, R.W. Taft. A Survey of Hammett Substituent Constants and Resonance and Field Parameters. *Chem. Rev.* **1991**, *91*, 165.

[170] S.-H. Qin, K.-Y. Qiu, G. Swift, D.-G. Westmoreland, S. Wu. "Living" adical Polymerization of Methyl Methacrylate with Diethyl 2,3-Dicyano-2,3-Diphenylsuccinate as a Thermal Iniferter. *J Polym Sci Polym Chem* **1999**, *37*, 4610.

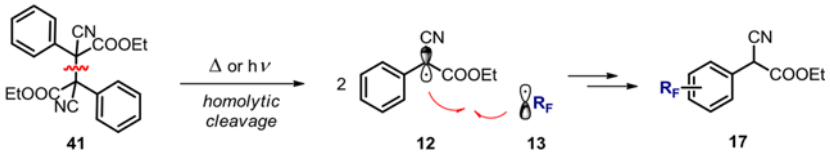

Scheme 18. Dimer **41** as a possible source of radicals **12** in the photochemical perfluoroalkylation reaction.

The observation of traces of dimer **41** under the reaction conditions led us to consider that, under our photochemical reaction conditions, a homolytic cleavage of dimer **41** could occur, generating radicals **12** that could undergo radical-radical coupling with the perfluoroalkyl radical **13** to form the product (Scheme 18). Dimers **41** (*meso* and *racemic* forms) were synthesized in order to investigate this mechanistic alternative. We conducted the model reaction under careful exclusion of light in order to completely suppress a mechanism initiated by the photochemical activity of the EDA complex. We added the synthesized dimers **41** while heating the reaction up to 50-70°C. Only traces of perfluorinated product **17a** were detected after 5 hours. A control experiment conducted at the same temperature but in the absence of the dimers **41** also provided traces of **17a**, suggesting that a minimal thermal activation is operative under these reaction conditions (Scheme 19).

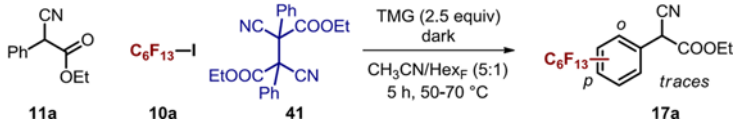

Scheme 19. Experimental evidence against the involvement of the dimer **41** in the perfluoroalkylation chemistry.

On this basis, we excluded the participation of the dimer **41** in the perfluoroalkylation mechanism. This leaves the homolytic aromatic substitution chain pathway (Scheme 15) as the most possible mechanism of the photochemical perfluoroalkylation of arenes.

6.7 Conclusions

We have reported an operationally simple protocol for the direct aromatic perfluoroalkylation and trifluoromethylation of α-cyano arylacetates. This metal-free approach, which occurs at ambient temperature and under visible-light irradiation, is driven by the photochemical activity of electron donor–acceptor (EDA) complexes, formed *in situ* by the interaction of transiently generated enolates and perfluoroalkyl iodides. Preliminary mechanistic studies and a quantum yield of 2.03 suggested a homolytic aromatic substitution radical chain mechanism as the operative reaction pathway.

6.8 Experimental Section

6.8.1 General Information

The ^{1}H and ^{13}C NMR spectra were recorded at 400 MHz or 500 MHz for ^{1}H and at 100 MHz or 125 MHz for ^{13}C, respectively. The chemical shifts (δ) for ^{1}H and ^{13}C are given in ppm relative to residual signals of the solvents (CHCl3 @ 7.26 ppm ^{1}H NMR, 77.0 ppm ^{13}C NMR). Coupling constants are given in Hz. When necessary, ^{1}H and ^{13}C signals were assigned by means of g-COSY 2D-NMR sequence. The following abbreviations are used to indicate the multiplicity: s, singlet; d, doublet; t, triplet; q, quartet; qn, quintet; m, multiplet; bs, broad signal.

Mass spectra (high and low resolution) were obtained from the ICIQ High Resolution Mass Spectrometry Unit on a Bruker Maxis Impact (QTOF) or Waters Micromass LCT-Premier (TOF) in Electrospray Ionization (ESI) by direct infusion.

The ^{1}H and ^{13}C NMR spectra are available in the literature[1] and are not reported in the present thesis.

General Procedures. All reactions were set up under an argon atmosphere in oven-dried glassware using standard Schlenk techniques, unless otherwise stated. Synthesis grade solvents were used as purchased and the reaction mixtures were deoxygenated by three cycles of freezepump-thaw. Chromatographic purification of products was accomplished using force-flow chromatography (FC) on silica gel (35-70 mesh). For thin layer chromatography (TLC) analysis throughout this work, Merck precoated TLC plates (silica gel 60 GF254, 0.25 mm) were employed, using UV light as the visualizing agent and an acidic mixture of para-anisaldehyde or basic aqueous potassium permangante ($KMnO_4$) stain solutions, and heat as developing agents. Organic solutions were concentrated under reduced pressure on a Büchi rotatory evaporator.

Materials. Reagents were purchased at the highest commercial quality and used without further purification, unless otherwise stated. Esters **11b**-**11n** were synthesized from the commercially available acetonitriles.[171] Ester **11d** (p-TMS aryl substituted) was synthetized following a twosteps procedure from (4-iodophenyl)trimethylsilane and ethyl cyanoacetate.[172] Ketone **11o** was prepared from commercially available ethyl ester and benzyl cyanide.[173] d_5-Ethyl cyanophenylacetate (**d_5 - 11a**) was synthetized according to the literature procedure reported

---

[171] Y. Takeuchi, H. Fujisawa, R. Noyori. A Very Reliable Method for Determination of Absolute Configuration of Chiral Secondary Alcohols by 1H NMR Spectroscopy. *Org. Lett.* **2004**, *6*, 4607.
[172] H.-J. Cristau, P. P. Cellier, J.-F. Spindler, M. Taillefer. Highly Efficient and Mild Copper-Catalyzed N- and C-Arylations with Aryl Bromides and Iodides *Chem. Eur. J.* **2004**, *10*, 5607.
[173] Y. Ji, W. C. Trenkle, J. V. Vowles. A High-Yielding Preparation of β-Ketonitriles. *Org. Lett.* **2006**, *8*, 1161.
[40] Q. Wang, D. Deredas, C. Huynh, M. Schlosser. Sequestered Alkyllithiums: Why Phenyllithium Alone is Suitable for Betaine-Ylide Generation *Chem. Eur. J.* **2003**, *9*, 570.

in.[40,174]

6.8.2 Synthesis of Starting Materials

General Procedure for α-Cyano Arylacetates (11)[37]

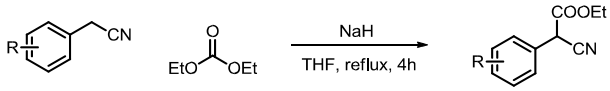

To a solution of the appropriate commercially available benzyl cyanide (10.0 mmol) in dry THF (0.5 M), NaH (60 % dispersion in mineral oil, 20.0 mmol, 2 equiv.) was added carefully at 0 °C. Diethylcarbonate (1.94 mL, 20.0 mmol, 2 equiv.) was then added at ambient temperature. The reaction mixture was stirred for 4 h under reflux. After quenching with H_2O (30 mL), most of the THF was removed under vacuum. 6 M HCl (10 mL) was the added to the reaction mixture, and the aqueous solution vigorously extracted with EtOAc (3 × 20 mL). The organic layer was dried over anhydrous Na_2SO_4 and filtered. The solvent was evaporated under reduced pressure and the crude product was purified by flash chromatography (silica; hex /EtOAc) to give the desired α-cyano arylacetates **11** (isolated yields ranging from 71% to 98%).

Ethyl 2-cyano-2-(4-methoxyphenyl)acetate (**11b**). ^{1}H NMR (400 MHz, $CDCl_3$) δ 7.43 – 7.30 (m, 2H), 6.99 – 6.84 (m, 2H), 4.65 (s, 1H), 4.31 – 4.17 (m, 2H), 3.82 (s, 3H), 1.28 (td, J = 7.1, 0.6 Hz, 3H) ppm.

Ethyl 2-cyano-2-(p-tolyl)acetate (**11c**). ^{1}H NMR (400 MHz, $CDCl_3$) δ 7.38 – 7.30 (m, 2H), 7.25 – 7.17 (m, 2H), 4.67 (s, 1H), 4.24 (qd, J = 7.1, 1.1 Hz, 2H), 2.36 (s, 3H), 1.28 (t, J = 7.1 Hz, 3H) ppm.

Ethyl 2-(4-chlorophenyl)-2-cyanoacetate (**11e**). ^{1}H NMR (400 MHz, $CDCl_3$) δ 7.43 (s, 4H), 4.72 (s, 1H), 4.28 (qd, J = 7.2, 1.6 Hz, 2H), 1.31 (t, J = 7.2 Hz, 3H) ppm.

Ethyl 2-cyano-2-(o-tolyl)acetate (**11f**). ^{1}H NMR (400 MHz, $CDCl_3$) δ 7.49 (dd, J = 7.3, 1.8 Hz, 1H), 7.35 – 7.24 (m, 3H), 4.91 (s, 1H), 4.32 – 4.23 (m, 2H), 2.43 (s, 3H), 1.31 (t, J = 7.1 Hz, 3H) ppm.

Ethyl 2-cyano-2-(m-tolyl)acetate (**11g**). ^{1}H NMR (400 MHz, $CDCl_3$) δ 7.35 – 7.20 (m, 4H), 4.69 (s, 1H), 4.27 (qd, J = 7.1, 1.9 Hz, 2H), 2.40 (d, J = 0.8 Hz, 3H), 1.31 (t, J = 7.1 Hz, 3H) ppm.

Ethyl 2-cyano-2-(2-methoxyphenyl)acetate (**11h**). ^{1}H-NMR (400 MHz, $CDCl_3$) δ: 7.46 – 7.36 (m, 2H), 7.04 (td, J = 7.6, 1.1 Hz, 1H), 6.98 – 6.93 (m, 1H), 5.05 (s, 1H), 4.29 (q, J = 7.1, 1.6 Hz, 2H), 3.89 (s, 3H), 1.32 (t, J = 7.1 Hz, 3H) ppm.

Ethyl 2-cyano-2-(3-methoxyphenyl)acetate (**11i**). ^{1}H NMR (400 MHz, $CDCl_3$) δ 7.39 – 7.31 (m, 1H), 7.09 – 7.04 (m, 1H), 7.01 (dd, J = 2.5, 1.8 Hz, 1H), 6.95 (ddd, J = 8.3, 2.5, 0.9 Hz, 1H), 4.70 (s, 1H), 4.27 (qd, J = 7.1, 1.8 Hz, 2H), 3.85 (d, J = 0.7 Hz, 3H), 1.31 (td, J = 7.1, 0.7 Hz, 3H) ppm.

---

[174] J. M. Atkins, S. A.; Moteki, S. G. DiMagno, J. M. Takacs. Single Enantiomer, Chiral Donor-Acceptor Metal Complexes from Bisoxazoline Pseudoracemates. *Org. Lett.* **2006**, *8*, 2759.

Ethyl 2-cyano-2-(naphthalen-2-yl)acetate (**11j**). ^{1}H NMR (400 MHz, $CDCl_3$) δ 8.05 – 7.96 (m, 1H), 7.96 – 7.84 (m, 3H), 7.65 – 7.47 (m, 3H), 4.91 (s, 1H), 4.28 (qd, J = 7.1, 1.6 Hz, 2H), 1.31 (t, J = 7.1 Hz, 3H) ppm.

Ethyl 2-(benzo[d][1,3]dioxol-5-yl)-2-cyanoacetate (**11k**). ^{1}H NMR (400 MHz, $CDCl_3$) δ 6.99 – 6.89 (m, 2H), 6.84 (dd, J = 7.7, 0.7 Hz, 1H), 6.03 (s, 2H), 4.63 (s, 1H), 4.27 (qd, J = 7.1, 2.1 Hz, 2H), 1.31 (t, J = 7.1 Hz, 3H) ppm.

Ethyl 2-(3-bromo-4-methoxyphenyl)-2-cyanoacetate (**11l**). ^{1}H NMR (400 MHz, $CDCl_3$) δ 7.66 (d, J = 2.4 Hz, 1H), 7.41 (dd, J = 8.5, 2.4 Hz, 1H), 6.95 (d, J = 8.5 Hz, 1H), 4.66 (s, 1H), 4.28 (qd, J = 7.1, 2.3 Hz, 2H), 3.94 (s, 3H), 1.32 (t, J = 7.1 Hz, 3H) ppm.

Ethyl 2-cyano-2-(1-methyl-1H-indol-3-yl)acetate (**11m**). ^{1}H NMR (400 MHz, $CDCl_3$) δ 7.73 (dt, J = 8.0, 1.0 Hz, 1H), 7.37 (dt, J = 8.3, 1.0 Hz, 1H), 7.32 (ddd, J = 8.3, 6.9, 1.2 Hz, 1H), 7.28 – 7.25 (m, 1H), 7.22 (ddd, J = 8.0, 6.9, 1.2 Hz, 1H), 5.00 (d, J = 0.7 Hz, 1H), 4.36 – 4.17 (m, 2H), 3.83 (s, 3H), 1.31 (t, J = 7.1 Hz, 3H) ppm.

Ethyl 2-cyano-2-(thiophen-2-yl)acetate (**11n**). ^{1}H NMR (400 MHz, CDCl3) δ 7.38 (dd, J = 5.2, 1.3 Hz, 1H), 7.24 (dt, J = 3.6, 1.3 Hz, 1H), 7.05 (dd, J = 5.2, 3.6 Hz, 1H), 5.00 (d, J = 1.3 Hz, 1H), 4.38 – 4.26 (m, 2H), 1.35 (t, J = 7.2 Hz, 3H) ppm.

Ethyl 2-cyano-2-(4-fluorophenyl)acetate (**11p**). ^{1}H NMR (400 MHz, CDCl3) δ 7.52 – 7.42 (m, 2H), 7.19 – 7.08 (m, 2H), 4.72 (s, 1H), 4.28 (qd, J = 7.1, 1.2 Hz, 2H), 1.31 (t, J = 7.1 Hz, 3H) ppm.

Ethyl 2-cyano-2-(3-fluorophenyl)acetate (**11q**). ^{1}H NMR (400 MHz, CDCl3) δ 7.43 (m, 1H), 7.28 (m, 1H), 7.22 (m, 1H), 7.13 (m, 1H), 4.74 (s, 1H), 4.29 (m, 2H), 1.32 (t, J = 7.2 Hz, 3H) ppm.

Preparation of ethyl 2-cyano-2-(4-(trimethylsilyl)phenyl)acetate (11d)

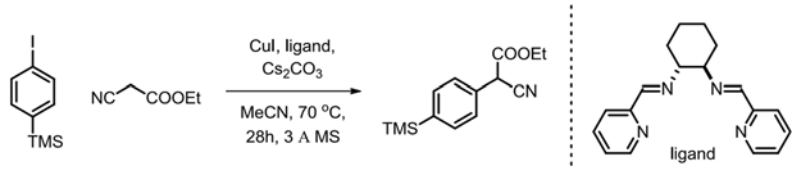

After standard cycles of evacuation and back-fill with dry and pure nitrogen, an oven-dried Schlenk tube equipped with a magnetic stir bar was charged with CuI (19 mg, 0.1 mmol, 10 mol%), ligand (59 mg, 0.2 mmol, 20 mol%), Cs_2CO_3 (489 mg, 1.5 mmol, 1.5 equiv.) and 3 Å MS powdered (300 mg). The tube was evacuated, back-filled with nitrogen and capped with a rubber septum. Ethyl cyanoacetate (0.214 mL, 2 mmol, 2 equiv.) and (4-iodophenyl)trimethylsilane (276 mg, 1 mmol) were added at room temperature under a stream of nitrogen by syringe, followed by anhydrous and degassed acetonitrile (0.6 mL). The septum was removed; the tube was sealed under a positive pressure of nitrogen and stirred in an oil bath (preheated to the required temperature), for 28 hours. The reaction mixture was neutralized with aqueous hydrochloric acid (3 mL, 1 N) before being filtered through a plug of celite, extracted

with CH_2Cl_2 (10 mL) and concentrated in vacuum. The crude residue was directly purified by flash chromatography on silica gel (gradient hexane/diethyl ether 12:1 – 5:1) to provide 201 mg (77% yield) of the desired product as a colorless oil.[38]

^{1}H NMR (500 MHz, CDCl3) δ 7.61 – 7.54 (m, 2H), 7.49 – 7.40 (m, 2H), 4.70 (s, 1H), 4.25 (qq, *J* = 7.0, 3.7 Hz, 2H), 1.29 (t, *J* = 7.0 Hz, 3H), 0.27 (s, 9H) ppm. **General**

Procedure for the preparation of α-cyano arylketones[39]

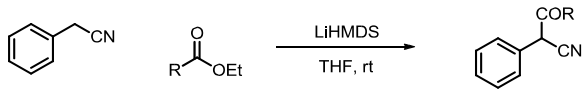

Lithium bis(trimethylsilyl)amide (6 mL 1M in THF, 6 mmol, 3 equiv.) was added dropwise to a solution of phenylacetonitrile (0.231 mL, 2 mmol) in anhydrous THF (6 ml) at 0 °C, followed by the addition of the appropriate ester (8 mmol, 4 equiv.). The mixture was stirred at room temperature for 1 hour, then diluted with a 1N HCl solution (25 mL), H_2O (75 mL) and ethyl acetate (100 mL). The organic layer was separated, washed with brine (50 ml X 2), dried (Na_2SO_4) and concentrated to afford yellow oil. The crude product was purified by flash chromatography (silica; hex /EtOAc) to give the corresponding α-cyano arylketones **11o**.

4-methyl-3-oxo-2-phenylpentanenitrile (**11o**). ^{1}H NMR (400 MHz, $CDCl_3$) δ 7.53 – 7.36 (m, 5H), 4.82 (s, 1H), 2.95 (hept, J = 6.9 Hz, 1H), 1.11 (dd, J = 7.7, 6.9 Hz, 6H) ppm.

Preparation of d_5 - ethyl α-cyano phenylacetate (d_5 - 11a)

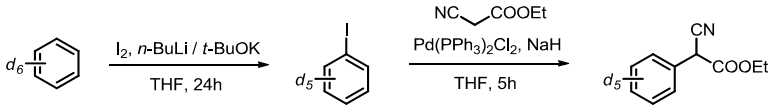

Synthesis of d_5 – iodobenzene.[40]

d_6 - benzene (8.8 mL, 0.1 mol; 99% isotopically pure), potassium *tert*-butoxide (freshly sublimated, 11 g, 0.1 mol) and 20 mL of anhydrous hexane were introduced into a 3 necks round bottom flask under an argon atmosphere. *n*-Butyl lithium (10M, 10 mL, 0.1 mol) was then carefully added dropwise to the solution at -78 °C. The resulting mixture was vigorously stirred for 20 h at 0 °C. After lowering the temperature to -78 °C, precooled tetrahydrofuran (20 mL) was added. After 15 min of continuous stirring at -78 °C, a homogeneous solution was obtained. Keeping a temperature of -78 °C, a solution of iodine (25.6 g, 0.1 mol) in tetrahydrofuran (60 mL) was added dropwise over the course of 30 min. The solvent and the unconsumed benzene were then removed by distillation. The residue was dissolved in diethyl ether (50 mL) and thoroughly washed with a saturated aqueous solution of sodium thiosulfate (3 x 50 mL) and with brine (2 x 25 mL). The organic layer was dried and evaporated. Distillation afforded a colorless liquid; 3.7 g (18%); b.p. 90 ± 92 °C/ 30 mbar.

Synthesis of d_5 - ethyl cyanophenylacetate.[41]

NaH (60 % dispersion in mineral oil, 15 mmol, 3 equiv.) was added carefully at 0 °C to a solution of ethyl cyanoacetate (1.07 mL, 10 mmol, 2 equiv.) in dry THF (30 mL, 0.5 M). $Pd(PPh_3)_2Cl_2$ (105 mg, 0.15 mmol, 3 mol%) and *d_5* - iodobenzene (0.559 mL, 5 mmol) were then added at ambient temperature. The resulting mixture was stirred at reflux for 5 hours. Afterwards, the mixture was cooled to room temperature, carefully quenched by the addition of water and concentrated under reduced pressure. HCl 1M aqueous solution was then added until an acidic pH (around 2) was obtained. Following an extractive workup with ethyl acetate, the organic layer was dried (anhydrous Na_2SO_4), filtered, and concentrated. The *d_5* - ethyl cyanophenylacetate was purified by flash column chromatography on silica (hexane/AcOEt 5:1 – 2:1). Isolated yield: 40%.

^{1}H NMR (400 MHz, $CDCl_3$) δ 4.74 (s, 1H), 4.27 (qd, J = 7.1, 1.4 Hz, 2H), 1.30 (t, J = 7.1 Hz, 3H) ppm.

^{13}C NMR (101 MHz, CDCl3) δ 164.98, 129.80, 128.82 (t), 128.71 (t), 127.48 (t), 115.65, 63.31, 43.68, 13.89 ppm.

6.8.3 General Procedure for the Light-driven Perfluoroalkylation of α-Cyano Arylacetates

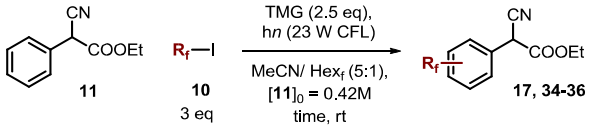

A 10 mL Schlenk tube was charged with the appropriate α-cyano arylacetate **11** (0.2 mmol), acetonitrile (0.4 mL, 0.5 M referring to **11**), perfluorohexane (0.08 mL), perfluoroalkyl iodide (0.130 mL, 0.6 mmol, 3 equiv) and *N,N,N′,N′*-tetramethylguanidine (0.063 mL, 0.5 mmol, 2.5 equiv.). The reaction mixture was degassed via freeze pump thaw (x 3 cycles), and the vessel refilled with nitrogen. After the reaction mixture was thoroughly degassed, the vial was sealed and positioned approximately 5 cm away from a household full spectrum 23 W compact fluorescent light (CFL). After stirring for the indicated time, the reaction was diluted with DCM, quenched with aqueous HCl 1M solution and extracted 3 times with DCM. The organic phase was then dried and the solvent removed under reduced pressure. The residue was purified by flash column chromatography to afford the title compounds **17**, **34-36**. **ethyl 2-cyano-2-(4-(perfluorohexyl)phenyl)acetate (*p*-17a), ethyl 2-cyano-2-(2(perfluorohexyl)phenyl)acetate (*o*-17a) and ethyl 2-(2,4-bis(perfluorohexyl)phenyl)-2cyanoacetate (*p,o*-17a).**

Prepared according to the general procedure using ethyl cyanophenylacetate (0.2 mmol, 0.035 mL) and perfluorohexyl iodide. Time of irradiation: 5 h. Purification by flash column chromatography (gradient eluent hexane/diethyl ether 12:1 – 3:1).

p-**17a**. The title compound was isolated (R_f = 0.2 hexane/diethyl ether 4:1) in 47% yield (48 mg) as a white solid.

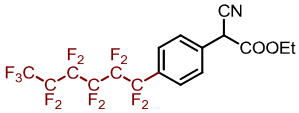

HRMS calculated for $C_{17}H_9F_{13}NO_2$ (M-H): 506.0431, found: 506.0427.

^{1}H NMR (400 MHz, $CDCl_3$) δ 7.72 – 7.59 (m, 4H), 4.81 (s, 1H), 4.27 (qd, J = 7.1, 0.6 Hz, 2H), 1.29 (t, J = 7.1 Hz, 3H) ppm. ^{19}F NMR decoupled ^{1}H (376 MHz, $CDCl_3$) δ -81.01 (td, J = 10.0, 2.8 Hz, 3F), 111.12 (t, J = 14.8 Hz, 2F), -121.59 (m, 2F), -121.88 (m, 2F), -122.96 (m, 2F), -126.31 (m, 2F) ppm. ^{13}C NMR (101 MHz, $CDCl_3$) δ 164.31, 134.17, 130.24 (t, *J* = 24.6 Hz), 128.53, 128.08 (t, *J* = 6.5 Hz), 115.03, 63.91, 43.62, 13.95 ppm.

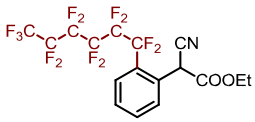

o-**17a**. The title compound was isolated (R_f = 0.4 hexane/diethyl ether 4:1) in 26% yield (26 mg) as a colorless oil.

HRMS calculated for $C_{17}H_{10}F_{13}NNaO_2$ (M+Na): 530.0396, found: 530.0373.

^{1}H NMR (400 MHz, $CDCl_3$) δ 7.80 (d, J = 8.2 Hz, 1H), 7.70 (t, J = 8.2 Hz, 1H), 7.66 (d, J = 8.2 Hz, 1H), 7.58 (t, J = 8.2 Hz, 1H), 5.11 (d, J = 0.9 Hz, 1H), 4.28 (qd, J = 7.1, 3.2 Hz, 2H), 1.29 (t, J = 7.1 Hz, 3H) ppm. ^{19}F NMR decoupled ^{1}H (376 MHz, $CDCl_3$) δ -80.90 (m, 3F), -104.65 (m, 2F), -120.85 (m, 2F), -121.65 (m, 2F), -122.79 (m, 2F), -126.19 (m, 2F) ppm. ^{13}C NMR (101 MHz, CDCl3) δ 164.36, 133.11, 131.20, 130.06 (t, *J* = 2.1 Hz), 129.57, 129.31 (t, *J* = 9.0 Hz), 126.64 (t, *J* = 22.8 Hz), 115.46, 63.68, 40.16, 13.76 ppm.

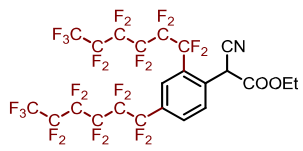

o,p-**17a**. The title compound was isolated (R_f = 0.5 hexane/diethyl ether 4:1) in 8% yield (13 mg) as yellowish oil.

HRMS calculated for $C_{23}H_8F_{26}NO_2$ (M-H): 824.0145, found: 824.0181.

^{1}H NMR (400 MHz, $CDCl_3$) δ 8.02 (d, J = 8.3 Hz, 1H), 7.96 (dd, J = 8.3, 1.7 Hz, 1H), 7.88 (d, J = 1.7 Hz, 1H), 5.19 (s, 1H), 4.34 (qd, J = 7.1, 2.3 Hz, 2H), 1.33 (t, J = 7.1 Hz, 3H) ppm. ^{19}F NMR decoupled ^{1}H (376 MHz, $CDCl_3$) δ -80.81 (m, 6F), -105.02 (m, 2F), -111.50 (m, 2F), -120.83 (m, 2F), -121.36 (m, 4F), -121.75 (m, 2F), -122.74 (m, 4F), -126.13 (m, 4F) ppm. ^{13}C NMR (126 MHz, CDCl3) δ 163.69, 134.35, 132.35, 131.60 (m), 131.05 (t, *J* = 25.2 Hz), 127.91 (m), 114.84, 64.36, 40.23, 13.92 ppm.

ethyl 2-cyano-2-(4-methoxy-2-(perfluorohexyl)phenyl)acetate (17b).

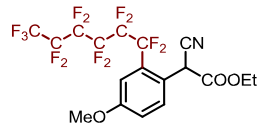

Prepared according to the general procedure using ethyl 2-cyano-2(4-methoxyphenyl)acetate **11b** (0.2 mmol, 44 mg) and perfluorohexyl iodide **10a**. Time of irradiation: 8 h. Purification by flash column chromatography (gradient eluent hexane/diethyl ether 10:1 – 4:1). The title compound was isolated (R_f = 0.3 hexane/diethyl ether 4:1) in 76% yield (81 mg) as a colorless oil.

HRMS calculated for $C_{18}H_{12}F_{13}NNaO_3$ (M+Na): 560.0502, found: 560.0508.

^{1}H NMR (500 MHz, CDCl3) δ 7.71 (d, J = 8.7 Hz, 1H), 7.21 (dd, J = 8.7, 2.8 Hz, 1H), 7.15 (d, J = 2.8 Hz, 1H), 5.05 (s, 1H), 4.29 (qd, J = 7.1, 4.5 Hz, 2H), 3.90 (s, 3H), 1.31 (t, J = 7.1 Hz, 3H) ppm. ^{19}F NMR decoupled ^{1}H (376 MHz, $CDCl_3$) δ -80.80 (t, J = 10.2 Hz, 3F), -104.93 (t, J = 16.0 Hz, 2F), 120.66 (m, 2F), -121.46 (m, 2F), -122.70 (m, 2F), -126.10 (m, 2F) ppm. ^{13}C NMR (126 MHz, CDCl3) δ 164.87, 160.15, 132.73, 127.98 (t, J = 23.0 Hz), 121.65, 118.25, 115.86, 115.31 (t, *J* = 9.2 Hz), 63.70, 55.85, 39.64, 13.94 ppm.

ethyl 2-cyano-2-(4-methyl-2-(perfluorohexyl)phenyl)acetate (17c).

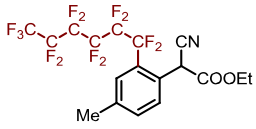

Prepared according to the general procedure using ethyl 2-cyano-2(4-methylphenyl)acetate **11c** (0.2 mmol, 41 mg) and perfluorohexyl iodide **10a**. Time of irradiation: 5 h. Purification by flash column chromatography (gradient eluent hexane/diethyl ether 12:1 – 8:1). The title compound was isolated (R_f = 0.5 hexane/diethyl ether 4:1) in 72% yield (75 mg) as a colorless oil.

HRMS calculated for $C_{18}H_{12}F_{13}NNaO_2$ (M+Na): 544.0553, found: 544.0558.

^{1}H NMR (400 MHz, CDCl3) δ 7.68 (d, J = 8.0 Hz, 1H), 7.51 (dt, J = 8.0, 1.2 Hz, 1H), 7.49 – 7.43 (m, 1H), 5.09 (s, 1H), 4.29 (qq, J = 7.1, 3.6 Hz, 2H), 2.47 (s, 3H), 1.31 (t, J = 7.1 Hz, 3H) ppm. ^{19}F NMR decoupled ^{1}H (376 MHz, CDCl3) δ -80.91 (t, J = 9.9 Hz, 3F), -104.71 (m, 2F), -120.77 (m, 2F), 121.57 (m, 2F), -122.81 (m, 2F), -126.20 (m, 2F) ppm. ^{13}C NMR (100 MHz, CDCl3) δ 164.73, 140.18, 133.96, 131.21, 129.88 (t, J = 8.8 Hz), 127.17, 126.53 (t, J = 22.8 Hz), 115.77, 63.74, 40.02, 21.23, 13.92 ppm.

ethyl 2-cyano-2-(4-methyl-2-(perfluorohexyl)phenyl)acetate (17d).

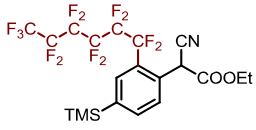

Prepared according to the general procedure using ethyl 2-cyano-2(4-(trimethylsilyl)phenyl)acetate **11d** (0.2 mmol, 52 mg) and perfluorohexyl iodide **10a**. Time of irradiation: 5 h. Purification by flash column chromatography (gradient eluent hexane/diethyl ether

12:1 – 6:1). The title compound was isolated (R_f = 0.5 hexane/diethyl ether 4:1) in 86% yield (100 mg) as a colorless oil.

HRMS calculated for $C_{20}H_{17}F_{13}NO_2Si$ (M-H): 578.0826, found: 578.0855.

^{1}H NMR (400 MHz, CDCl3) δ 7.84 (dd, J = 7.8, 1.2 Hz 1H), 7.77 (d, J = 7.8 Hz, 1H), 7.74 (d, J = 1.2 Hz, 1H), 5.12 (s, 1H), 4.39 – 4.22 (m, 2H), 1.32 (t, J = 7.1 Hz, 3H), 0.34 (s, 9H) ppm. ^{19}F NMR decoupled ^{1}H (376 MHz, CDCl3) δ -80.88 (m, 3F), -104.60 (m, 2F), -120.88 (m, 2F), -121.48 (m, 2F), -122.77 (m, 2F), -126.20 (m, 2F) ppm. ^{13}C NMR (100 MHz, CDCl3) 164.43, 143.39, 137.97, 133.73 (m), 130.23, 130.14, 125.67 (t, *J* = 22.2 Hz), 115.48, 63.65, 40.16, 13.78, -1.52 ppm.

ethyl 2-(4-chloro-2-(perfluorohexyl)phenyl)-2-cyanoacetate (17e).

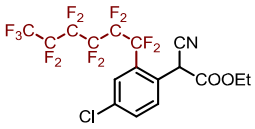

Prepared according to the general procedure using ethyl 2-(4chlorophenyl)-2-cyanoacetate **11e** (0.2 mmol, 45 mg) and perfluorohexyl iodide **10a**. Time of irradiation: 12 h. Purification by flash column chromatography (gradient eluent hexane/diethyl ether 12:1 – 8:1). The title compound was isolated (R_f = 0.4 hexane/diethyl ether 4:1) in 36% yield (39 mg) as a colorless oil.

HRMS calculated for $C_{17}H_8ClF_{13}NO_2$ (M-H): 540.0041, found: 540.0047.

^{1}H NMR (400 MHz, CDCl3) δ 7.77 (d, J = 8.5 Hz, 1H), 7.70 (dd, J = 8.5, 2.2 Hz, 1H), 7.66 (d, J = 2.2 Hz, 1H), 5.09 (s, 1H), 4.31 (qd, J = 7.1, 3.0 Hz, 2H), 1.32 (t, J = 7.1 Hz, 3H) ppm. ^{19}F NMR decoupled ^{1}H (376 MHz, CDCl3) δ -80.85 (m, 3F), -105.11 (m, 2F), -120.66 (m, 2F), -121.49 (m, 2F), -122.71 (m, 2F), -126.16 (m, 2F) ppm. ^{13}C NMR (100 MHz, CDCl3) δ 164.11, 136.36, 133.46, 132.84, 129.57 (t, J = 9.3 Hz), 128.67, 128.42 (t, J = 23.2 Hz), 115.19, 64.10, 39.92, 13.94 ppm.

ethyl 2-cyano-2-(2-methyl-4-(perfluorohexyl)phenyl)acetate (*p*-17f) and ethyl 2-cyano-2-(2methyl-6-(perfluorohexyl)phenyl)acetate (*o*-17f).

Prepared according to the general procedure using ethyl 2-cyano-2-(o-tolyl)acetate **11f** (0.2 mmol, 41 mg) and perfluorohexyl iodide **10a**. Time of irradiation: 5 h. Purification by flash column chromatography (gradient eluent hexane/diethyl ether 12:1 – 3:1).

p-**17f**. The title compound was isolated (R_f = 0.3 hexane/diethyl ether 4:1) in 30% yield (31 mg) as an off-white solid.

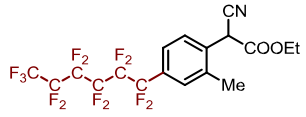

HRMS calculated for $C_{18}H_{11}F_{13}NO_2$ (M-H): 520.0588, found: 520.0590.

^{1}H NMR (400 MHz, $CDCl_3$) δ 7.64 (d, J = 8.1 Hz, 1H), 7.51 (dd, J = 8.1, 1.4 Hz, 1H), 7.47 (d, J = 1.4 Hz, 1H), 4.93 (s, 1H), 4.29 (qd, J = 7.2, 2.6 Hz, 2H), 2.49 (s, 3H), 1.30 (t, J = 7.2 Hz, 3H) ppm. ^{19}F NMR decoupled ^{1}H (376 MHz, $CDCl_3$) δ -80.89 (m, 3F), -111.06 (m, 2F), -121.54 (m, 2F), -121.76 (m, 2F), -122.89 (m, 2F), -126.22 (m, 2F) ppm. ^{13}C NMR (101 MHz, $CDCl_3$) δ 164.30, 137.36, 133.12,

130.19 (t, J = 24.4 Hz), 129.68 (t, J = 6.6 Hz), 129.28, 125.69 (t, J = 6.9 Hz), 115.25, 63.83, 41.11, 19.72, 14.03 ppm.

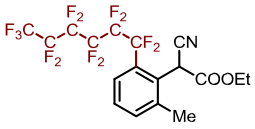

o-**17f**. The title compound was isolated (R_f = 0.4 hexane/diethyl ether 4:1) in 12% yield (13 mg) as colorless oil.

HRMS calculated for $C_{18}H_{11}F_{13}NO_2$ (M-H): 520.0588, found: 520.0598.

^{1}H NMR (400 MHz, $CDCl_3$) δ 7.59 – 7.55 (m, 1H), 7.55 – 7.48 (m, 2H), 5.34 (t, J = 4.3 Hz, 1H), 4.42 – 4.27 (m, 2H), 2.51 (s, 3H), 1.34 (t, J = 7.1 Hz, 3H) ppm.^{19}F NMR decoupled ^{1}H (376 MHz, $CDCl_3$) δ -80.84 (m, 3F), -102.93 (m, 2F), -120.54 (m, 2F), -121.45 (m, 2F), -122.72 (m, 2F), -126.16 (m, 2F) ppm.^{13}C NMR (101 MHz, CDCl3) δ 164.55, 140.40, 136.19, 129.40, 128.21 (d, J = 21.8 Hz), 128.12, 127.47 (d, J = 9.7 Hz), 114.67, 63.78, 38.61, 20.36, 14.02 ppm.

ethyl 2-cyano-2-(3-methyl-4-(perfluorohexyl)phenyl)acetate (*p*-17g), ethyl 2-cyano-2-(5methyl-2-(perfluorohexyl)phenyl)acetate (*o*-17g), ethyl 2-cyano-2-(3-methyl-2(perfluorohexyl)phenyl)acetate (*o'*-17g), ethyl 2-cyano-2-(5-methyl-2,4bis(perfluorohexyl)phenyl)acetate (*o,p*-17g) and ethyl 2-cyano-2-(3-methyl-2,4bis(perfluorohexyl)phenyl)acetate (*o',p*-17g).

Prepared according to the general procedure using ethyl 2-cyano-2-(m-tolyl)acetate **11g** (0.2 mmol, 41 mg) and perfluorohexyl iodide. Time of irradiation: 4 h. Purification by flash column chromatography (gradient eluent hexane/diethyl ether 15:1 – 8:1).

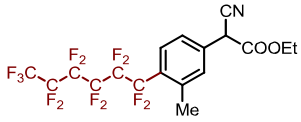

p-**17g**. The title compound was isolated (R_f = 0.3 hexane/diethyl ether 4:1) in 50% yield (52 mg) as a white solid.

HRMS calculated for $C_{18}H_{12}F_{13}NNaO_2$ (M+Na): 544.0553, found: 544.0541.

^{1}H NMR (400 MHz, $CDCl_3$) δ 7.60 (d, J = 8.2 Hz, 1H), 7.45 (m, 2H), 4.77 (d, J = 1.3 Hz, 1H), 4.30 (qd, J = 7.1, 1.2 Hz, 2H), 2.55 (t, J = 3.1 Hz, 3H), 1.33 (td, J = 7.1, 0.6 Hz, 3H) ppm.^{19}F NMR decoupled ^{1}H (376 MHz, $CDCl_3$) δ -80.93 (m, 3F), -106.61 (m, 2F), -120.91 (m, 2F), -121.77 (m, 2F), -122.86 (m, 2F), -126.24 (m, 2F) ppm.^{13}C NMR (101 MHz, $CDCl_3$) δ 164.25, 139.72, 133.55, 131.96, 129.62 (t, J = 9.0 Hz), 128.14 (t, J = 22.8 Hz), 125.54, 114.94, 63.70, 43.27, 20.50, 13.84 ppm.

o-**17g** and *o'*-**17g** were isolated as a mixture (R_f = 0.5 hexane/diethyl ether 4:1) in 14% yield (26 mg) as yellowish oil.

HRMS calculated for $C_{18}H_{12}F_{13}NNaO_2$ (M+Na): 544.0553, found: 544.0544.

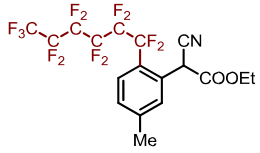

o-**17g**. ^{1}H NMR (400 MHz, $CDCl_3$) δ 7.59 (d, J = 1.6 Hz, 1H), 7.55 (d, J = 8.2 Hz, 1H), 7.43 – 7.36 (m, 1H), 5.10 (d, J = 1.1 Hz, 1H), 4.38 – 4.24 (m, 2H), 2.50 (s, 3H), 1.32 (t, J = 7.1 Hz, 3H) ppm. ^{19}F NMR decoupled ^{1}H (376 MHz, $CDCl_3$) δ -80.85 (m, 3F), -104.40 (m, 2F),

120.88 (m, 2F), -121.52 (m, 2F), -122.76 (m, 2F), -126.16 (m, 2F) ppm. ^{13}C NMR (101 MHz, CDCl3) δ 164.51, 144.00, 131.67, 130.33, 129.73, 129.23 (t, J = 8.8 Hz), 123.72 (t, J = 23.1 Hz), 115.60, 63.62, 40.04, 21.31, 13.79 ppm.

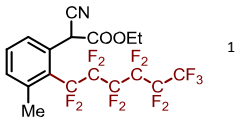

1

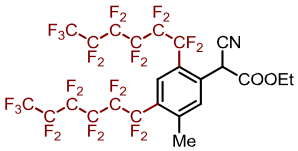

13

1

o'-**17g**. Characteristic signals:

H NMR (400 MHz, $CDCl_3$) δ 5.14 (s, 1H), 2.57 (t, *J* = 4.9 Hz, 3H) ppm. ^{19}F NMR decoupled ^{1}H (376 MHz, $CDCl_3$) δ -120.25 (m, 2F), -121.75 (m, 2F) ppm. C NMR (126 MHz, CDCl3) δ 164.79, 132.32, 129.48 ppm.

o,p-**17g**. The title compound was isolated (Rf = 0.6 hexane/diethyl ether 4:1) in 6% yield (10 mg) as yellowish oil.

HRMS calculated for $C_{24}H_{11}F_{26}NNaO_2$ (M+Na): 862.0267, found: 862.0249.

H NMR (400 MHz, $CDCl_3$) δ 7.78 (s, 1H), 7.75 (s, 1H), 5.14 (s, 1H), 4.41 – 4.27 (m, 2H), 2.65 (m, 3H), 1.38 – 1.26 (m, 3H) ppm. ^{19}F NMR decoupled ^{1}H (376 MHz, $CDCl_3$) δ -80.85 (m, 6F), -105.11 (m, 2F), -107-13 (m, 2F), -120.99 (m, 4F), -121.45 (m, 4F), -122.79 (m, 4F), -126.19 (m, 4F) ppm.

13

C NMR (126 MHz, CDCl3) δ 163.68, 144.26, 135.59, 133.34, 129.75, 128.93, 124.81, 114.81, 64.12, 39.85, 22.65, 13.79 ppm.

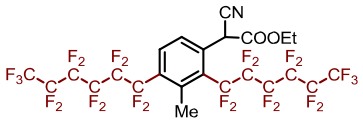

o',p-**17g**. The title compound was isolated (R_f = 0.7 hexane/diethyl ether 4:1) in 5% yield (8 mg) as yellowish oil.

HRMS calculated for $C_{24}H_{10}F_{26}NO_2$ (M-H): 838.0302, found: 838.0310.

1

H NMR (400 MHz, $CDCl_3$) δ 7.89 (d, J = 8.6 Hz, 1H), 7.83 (d, J = 8.6 Hz, 1H), 5.19 (s, 1H), 4.34 (qd, J = 7.1, 2.5 Hz, 3H), 2.61 (m, 3H), 1.35 (t, J = 7.1 Hz, 4H) ppm. ^{19}F NMR decoupled ^{1}H (376 MHz, $CDCl_3$) δ -80.84 (m, 6F), -119.00 (m, 2F), -119.74 (m, 2F), -121.71 (m, 4F), -122.73 (m, 4F), -126.16 (m, 4F) ppm. ^{13}C NMR (126 MHz, $CDCl_3$) δ 164.00, 142.02, 135.90, 132.94, 129.78, 115.25, 64.04, 41.57, 22.65, 13.81 ppm.

ethyl 2-cyano-2-(2-methyl-4-(perfluorohexyl)phenyl)acetate (*p*-17h) and ethyl 2-cyano-2-(2methyl-6-(perfluorohexyl)phenyl)acetate (o,*p*,-17h).

Prepared according to the general procedure using ethyl ethyl 2-cyano-2-(2-methoxyphenyl)acetate **11h** (0.2 mmol, 44 mg) and perfluorohexyl iodide. Time of irradiation: 5

h. Purification by flash column chromatography (gradient eluent hexane/diethyl ether 10:1 – 3:1). Compounds *p*-**17h** and *p,o*-**17h** were isolated as a mixture (R_f = 0.3 hexane/diethyl ether 4:1) in 51% yield (58 mg) as an yellowish oil.

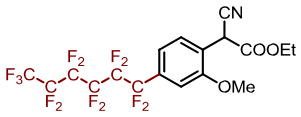

p-**17h.** HRMS calculated for $C_{18}H_{12}F_{13}NNaO_3$ (M+Na): 560.0502, found: 560.0505.

^{1}H NMR (400 MHz, $CDCl_3$) δ 7.59 (d, J = 8.0 Hz, 1H), 7.30 (d, J = 8.0 Hz, 1H), 7.12 (m, 1H), 5.09 (s, 1H), 4.31 (qd, J = 7.1, 1.3 Hz, 2H), 3.95 (s, 3H), 1.33 (td, J = 7.1, 1.5 Hz, 3H) ppm. ^{19}F NMR decoupled ^{1}H (376 MHz, $CDCl_3$) δ 80.91 (m, 3F), -110.85 (m, 2F), -121.56 (m, 2F), -121.75 (m, 2F), -122.89 (m, 2F), -126.23 (m, 2F) ppm.^{13}C NMR (101 MHz, $CDCl_3$) δ 164.28, 156.59, 131.42 (t, J = 24.4 Hz), 129.85, 123.22, 119.76 (t, J = 6.7 Hz), 115.08, 109.40 (t, J = 6.7 Hz), 63.35, 56.12, 38.03, 13.91 ppm.

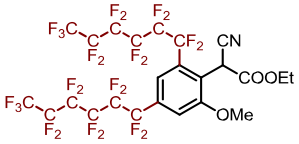

o,p-**17h**. HRMS calculated for $C_{24}H_{11}F_{26}NNaO_3$ (M+Na): 878.0216, found: 878.0210.

Characteristic signals:

^{1}H NMR (400 MHz, $CDCl_3$) 7.51 (d, J = 1.6 Hz, 1H), 7.39 (d, J = 1.6 Hz, 1H), 5.14 (t, J = 2.9 Hz, 1H), 4.05 (s, 3H) ppm.^{19}F NMR decoupled ^{1}H (471 MHz, $CDCl_3$) δ 104.75 (m, 2F), -111.46 (m, 2F), -120.97 (m, 2F) ppm.^{13}C NMR (126 MHz, CDCl3) δ 163.78, 158.64, 56.90 ppm.

ethyl 2-cyano-2-(3-methoxy-4-(perfluorohexyl)phenyl)acetate (*p*-17i), ethyl 2-cyano-2-(5methoxy-2-(perfluorohexyl)phenyl)acetate (*o*-17i), ethyl 2-cyano-2-(5-methoxy-2,4bis(perfluorohexyl)phenyl) acetate (*o,p*-17i) and ethyl 2-cyano-2-(3- methoxy-2(perfluorohexyl)phenyl)acetate (*o'*-17i).

Prepared according to the general procedure using ethyl 2-cyano-2-(m-tolyl)acetate **11i** (0.2 mmol, 41 mg) and perfluorohexyl iodide. Time of irradiation: 4 h. Purification by flash column chromatography (gradient eluent hexane/diethyl ether 12:1 – 3:1).

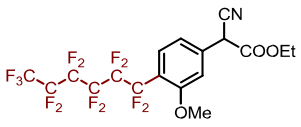

p-**17i**. The title compound was isolated (R_f = 0.3 hexane/diethyl ether 4:1) in 47% yield (50 mg) as a yellowish oil.

HRMS calculated for $C_{18}H_{12}F_{13}NNaO_3$ (M+Na): 560.0502, found: 560.0497.

^{1}H NMR (400 MHz, $CDCl_3$) δ 7.57 (d, J = 8.1 Hz, 1H), 7.20 – 7.12 (m, 2H), 4.78 (s, 1H), 4.31 (m, 2H), 3.94 (d, J = 1.2 Hz, 3H), 1.33 (t, J = 7.1, 3H) ppm. ^{19}F NMR decoupled ^{1}H (376 MHz, $CDCl_3$) δ 80.96 (m, 3F), -108.17 (m, 2F), -121.25 (m, 2F), -122.01 (m, 2F), -122.85 (m, 2F), -126.27 (m, 2F) ppm. ^{13}C NMR (101 MHz, $CDCl_3$) δ 164.31, 159.18, 135.63, 130.41 (t, J = 8.9 Hz), 119.93, 118.31 (t, J = 23.1 Hz), 115.06, 112.06, 63.90, 56.34, 43.80, 14.00 ppm.

o-**17i** and *o,p*-**17i** were isolated as a mixture (R_f = 0.4 hexane/diethyl ether 4:1) in 20% yield (25 mg) as yellowish oil.

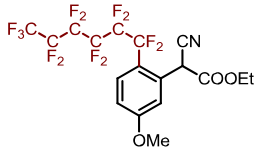

o-**17i**. HRMS calculated for $C_{18}H_{12}F_{13}NNaO_3$ (M+Na): 560.0502, found: 560.0503.

^{1}H NMR (400 MHz, $CDCl_3$) δ 7.59 (d, J = 8.0 Hz, 1H), 7.33 – 7.27 (m, 1H), 7.13 (s, 1H), 5.09 (s, 1H), 4.31 (qd, J = 7.1, 1.3 Hz, 2H), 3.95 (s, 3H), 1.33 (td, J = 7.1, 1.5 Hz, 3H) ppm. ^{19}F NMR decoupled ^{1}H (376 MHz, $CDCl_3$) δ -80.87 (m, 3F), 103.74 (m, 2F), -121.03 (m, 2F), -121.53 (m, 2F), -122.80 (m, 2F), -126.19 (m, 2F) ppm. ^{13}C NMR (101 MHz, CDCl3) δ 164.33, 162.71, 131.64, 130.99 (t, J = 9.0 Hz), 118.48 (m), 116.64, 115.45, 114.84, 63.66, 55.73, 40.18, 13.79 ppm.

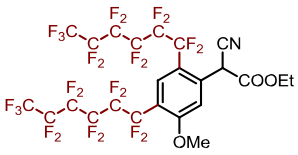

o,p-**17i**. HRMS calculated for $C_{24}H_{11}F_{26}NNaO_3$ (M+Na): 878.0216, found: 878.0210.

Characteristic signals:

^{1}H NMR (400 MHz, $CDCl_3$) δ 7.51 (s, 1H), 7.39 (s,1H), 5.14 (t, J = 2.9 Hz, 1H) ppm. ^{19}F NMR decoupled ^{1}H (376 MHz, $CDCl_3$) δ -104.31 (m, 2F), -108.83 (m, 2F), 121.95 (m, 2F) ppm. ^{13}C NMR (126 MHz, CDCl3) δ 163.63, 161.21, 115.02, 64.15, 56.68 ppm.

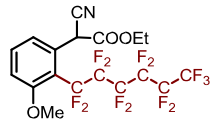

o'-**17i**. The title compound was isolated (R_f = 0.5 hexane/diethyl ether 4:1) in 14% yield (15 mg) as yellowish oil.

HRMS calculated for $C_{18}H_{12}F_{13}NNaO_3$ (M+Na): 560.0502, found: 560.0523.

^{1}H NMR (400 MHz, $CDCl_3$) δ 7.63 (t, J = 7.9 Hz, 1H), 7.37 (d, J = 7.9 Hz, 1H), 7.14 (d, J = 7.9 Hz, 1H), 5.16 (s, 1H), 4.31 (qd, J = 7.1, 3.7 Hz, 2H), 3.91 (s, 3H), 1.2 (t, J = 7.1 Hz, 3H) ppm. ^{19}F NMR decoupled ^{1}H (376 MHz, $CDCl_3$) δ -80.85 (m, 3F), -99.81 (m, 2F), -120.66 (m, 2F), -122.02 (m, 2F), -122.68 (m, 2F), -126.17 (m, 2F) ppm. ^{13}C NMR (126 MHz, CDCl3) δ 164.59, 160.21, 133.83, 132.05, 123.25, 115.74, 114.02, 63.56, 56.64, 29.70, 13.81 ppm. **ethyl 2-cyano-2-(1-(perfluorohexyl)naphthalen-2-yl)acetate (17j).**

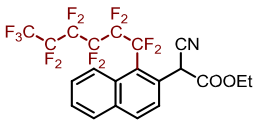

Prepared according to the general procedure using ethyl 2-cyano-2(naphthalen-2-yl)acetate **11j** (0.2 mmol, 48 mg) and perfluorohexyl iodide **10a**. Time of irradiation: 12 h. Purification by flash column chromatography (gradient eluent hexane/diethyl ether 12:1 – 8:1). The title compound was isolated (R_f = 0.4 hexane/diethyl ether 4:1) in 51% yield (57 mg) as a yellow-brown oil.

HRMS calculated for $C_{21}H_{12}F_{13}NNaO_2$ (M+Na): 580.0553, found: 580.0543.

^{1}H NMR (400 MHz, CDCl3) δ 8.31 – 8.22 (m, 1H), 8.16 (d, J = 8.7 Hz, 1H), 7.99 – 7.92 (m, 1H), 7.79 (d, J = 8.7 Hz, 1H), 7.66 (m, 2H), 5.38 (s, 1H), 4.41 – 4.25 (m, 2H), 1.32 (t, J = 7.1 Hz, 3H) ppm. ^{19}F NMR decoupled ^{1}H (376 MHz, CDCl3) δ -80.80 (m, 3F), -94.92 (bs, 2F), -119.40 (bs, 2F), -121.57 (m, 2F), -122.60 (m, 2F), -126.08 (m, 2F) ppm. ^{13}C NMR (100 MHz, CDCl3) δ 164.57, 134.43, 134.03, 131.27, 130.96, 129.04, 128.56, 127.47, 126.55, 125.80 (m), 123.51 (m), 115.68, 63.74, 41.76, 13.83 ppm.

ethyl 2-cyano-2-(6-(perfluorohexyl)benzo[d][1,3]dioxol-5-yl)acetate (17k).

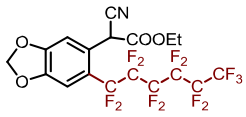

Prepared according to the general procedure using ethyl 2(benzo[d][1,3]dioxol-5-yl)-2-cyanoacetate **11k** (0.2 mmol, 47 mg) and perfluorohexyl iodide **10a**. Time of irradiation: 24 h. Purification by flash column chromatography (gradient eluent hexane/diethyl ether 12:1 – 8:1). The title compound was isolated (R_f = 0.4 hexane/diethyl ether 4:1) in 72% yield (79 mg) as a yellowish oil.

HRMS calculated for $C_{18}H_{10}F_{13}NNaO_4$ (M+Na): 574.0294, found: 574.0299.

^{1}H NMR (400 MHz, CDCl3) δ 7.19 (s, 1H), 7.05 (s, 1H), 6.15 (q, J = 1.3 Hz, 2H), 5.05 (s, 1H), 4.39 – 4.22 (m, 2H), 1.32 (t, J = 7.1 Hz, 3H) ppm. ^{19}F NMR decoupled ^{1}H (376 MHz, CDCl3) δ -80.92 (m, 3F), -103.41 (m, 2F), -120.88 (m, 2F), -121.59 (m, 2F), -122.82 (m, 2F), -126.23 (m, 2F) ppm. ^{13}C NMR (100 MHz, CDCl3) δ 164.59, 151.59, 149.03, 125.02, 120.47 (t, J = 23.6 Hz), 115.63, 110.77, 108.79 (t, J = 9.9 Hz), 103.16, 63.85, 39.99, 13.93 ppm.

ethyl 2-(5-bromo-4-methoxy-2-(perfluorohexyl)phenyl)-2-cyanoacetate (17l).

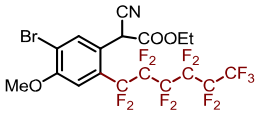

Prepared according to the general procedure using ethyl 2-(3bromo-4-methoxyphenyl)-2-cyanoacetate **11l** (0.2 mmol, 50 mg) and perfluorohexyl iodide **10a**. Time of irradiation: 24 h. Purification by flash column chromatography (gradient eluent hexane/diethyl ether 12:1 – 10:1). The title compound was isolated (R_f = 0.6 hexane/diethyl ether 4:1) in 60% yield (74 mg) as a yellowish oil.

HRMS calculated for $C_{18}H_{11}BrF_{13}NNaO_3$ (M+Na): 637.9607, found: 637.9600.

^{1}H NMR (400 MHz, CDCl3) δ 7.95 (s, 1H), 7.05 (s, 1H), 5.02 (s, Hz, 1H), 4.32 (qd, J = 7.1, 4.6 Hz, 2H), 3.99 (s, 3H), 1.33 (t, J = 7.1 Hz, 3H) ppm. ^{19}F NMR decoupled ^{1}H (376 MHz, CDCl3) δ -80.86 (m, 3F), -104.97 (m, 2F), -120.75 (m, 2F), -121.49 (m, 2F), -122.75 (m, 2F), -126.17 (m, 2F) ppm.

^{13}C NMR (100 MHz, CDCl3) δ 164.17, 156.73, 135.86, 126.84 (t, J = 23.1 Hz), 122.89, 117.48, 115.16, 111.54 (t, J = 9.4 Hz), 63.85, 56.67, 39.20, 13.79 ppm.

ethyl 2-cyano-2-(1-methyl-2-(perfluorohexyl)-1H-indol-3-yl)acetate (17m).

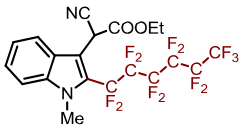

Prepared according to the general procedure using ethyl 2-cyano-2-(1-methyl-1H-indol-3-yl)acetate **11m** (0.2 mmol, 48 mg) and perfluorohexyl iodide **10a**. Time of irradiation: 5 h. Purification by flash column chromatography (gradient eluent hexane/diethyl ether 12:1 – 6:1). The title compound was isolated (R_f = 0.3 hexane/diethyl ether 4:1) in 89% yield (100 mg) as an orange-red oil.

HRMS calculated for $C_{20}H_{13}F_{13}N_2NaO_2$ (M+Na): 583.0662, found: 583.0668.

^{1}H NMR (400 MHz, CDCl3) δ 7.93 (d, J = 8.2, 1H), 7.53 – 7.43 (m, 2H), 7.32 (m, 1H), 5.27 (t, J = 1.5 Hz, 1H), 4.39 – 4.18 (m, 2H), 3.90 (s, 3H), 1.29 (t, J = 7.1 Hz, 3H) ppm. ^{19}F NMR decoupled ^{1}H (376 MHz, CDCl3) δ -80.86 (m, 3F), -103.32 (m, 2F), -120.93 (m, 2F), -121.75 (m, 2F), -122.71 (m, 2F), 126.17 (m, 2F) ppm. ^{13}C NMR (100 MHz, CDCl3) δ 164.42, 138.56, 125.81, 124.62, 122.24 (m), 121.97, 120.57, 114.81, 110.47, 109.19 (m), 63.45, 34.71, 32.15, 13.82 ppm.

ethyl 2-cyano-2-(4-(perfluorobutyl)phenyl)acetate (*p*-34a), ethyl 2-cyano-2-(2-(perfluorobutyl)phenyl)acetate (*o*-34a) and ethyl 2-(2,4-bis(perfluorobutyl)phenyl)-2cyanoacetate (*o,p*-34a).

Prepared according to the general procedure using ethyl cyanophenylacetate (0.2 mmol, 0.035 mL) and nonafluorobutyl iodide (0.6 mmol, 0.103 mL). Time of irradiation: 5 h. Purification by flash column chromatography (gradient eluent hexane/diethyl ether 12:1 – 3:1).

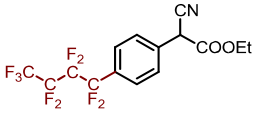

p-**34a**. The title compound was isolated (R_f = 0.2 hexane/diethyl ether 4:1) in 47% yield (38 mg) as a white solid.

HRMS calculated for $C_{15}H_9F_9NO_2$ (M-H): 406.0495, found: 406.0509.

^{1}H NMR (400 MHz, $CDCl_3$) δ 7.73 – 7.62 (m, 4H), 4.83 (s, 1H), 4.30 (qd, J = 7.1, 0.6 Hz, 2H), 1.32 (t, J = 7.1 Hz, 3H) ppm. ^{19}F NMR decoupled ^{1}H (376 MHz, $CDCl_3$) δ -81.14 (m, 3F), -111.31 (m, 2F), 122.75 (m, 2F), -125.67 (m, 2F) ppm. ^{13}C NMR (101 MHz, $CDCl_3$) δ 164.14, 133.99, 130.01 (t, J = 24.6 Hz), 128.37, 127.93 (t, J = 6.6 Hz), 114.85, 63.77, 43.47, 13.84 ppm.

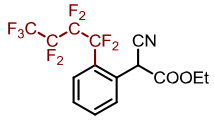

o-**34a**. The title compound was isolated (R_f = 0.4 hexane/diethyl ether 4:1) in 25% yield (20 mg) as colorless oil.

HRMS calculated for $C_{15}H_{10}F_9NNaO_2$ (M+Na): 430.0460, found: 430.0468.

^{1}H NMR (400 MHz, $CDCl_3$) δ 7.81 (d, J = 7.9 Hz, 1H), 7.71 (m, 2H), 7.60 (m, 1H), 5.13 (s, 1H), 4.31 (qd, J = 7.1, 2.9 Hz, 2H), 1.31 (t, J = 7.1 Hz, 3H) ppm. ^{19}F NMR decoupled ^{1}H (376 MHz, $CDCl_3$) δ -80.99 (m, 3F), -104.85 (m, 2F), -121.86 (m, 2F), -125.66 (m, 2F) ppm. ^{13}C NMR (101 MHz, CDCl3) δ

164.36, 133.12, 131.20, 130.05, 129.57, 129.29 (t, J = 8.9 Hz), 126.57 (t, J = 22.9 Hz), 115.47, 63.70, 40.18, 13.79 ppm.

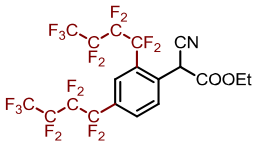

o,p-**34a**. The title compound was isolated (R_f = 0.5 hexane/diethyl ether 4:1) in 8% yield (10 mg) as yellowish oil.

^{1}H NMR (400 MHz, $CDCl_3$) δ 8.02 (d, J = 8.2 Hz, 1H), 7.96 (d, J = 8.2 Hz, 1H), 7.88 (s, 1H), 5.19 (s, 1H), 4.34 (qd, J = 7.1, 2.2 Hz, 2H), 1.34 (t, J = 7.1 Hz, 3H) ppm. ^{19}F NMR decoupled ^{1}H (376 MHz, $CDCl_3$) δ -80.93 (m, 6F), -105.37 (m, 2F), -111.81 (m, 2F), -121.67 (m, 2F), -122.67 (m, 2F), -125.60 (m, 4F) ppm. ^{13}C NMR (126 MHz, CDCl3) δ 163.52, 134.20, 132.18, 131.46 (m), 130.80, 127.95 (m), 127.66, 114.69, 64.21, 40.09, 13.78 ppm.

ethyl 2-cyano-2-(4-(perfluorooctyl)phenyl)acetate (*p*-34b), ethyl 2-cyano-2-(2-(perfluorooctyl)phenyl)acetate (*o*-34b).

Prepared according to the general procedure using ethyl cyanophenylacetate (0.2 mmol, 0.035 mL) and perfluorooctyl iodide. Time of irradiation (2 lamps): 16 h. Purification by flash column chromatography (gradient eluent hexane/diethyl ether 12:1 – 3:1).

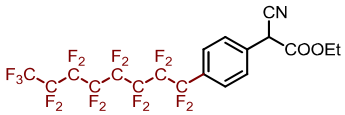

p-**34b**. The title compound was isolated (R_f = 0.2 hexane/diethyl ether 4:1) in 28% yield (34 mg) as a white solid.

HRMS calculated for $C_{19}H_9F_{17}NO_2$ (M-H): 606.0367, found: 606.0365.

^{1}H NMR (400 MHz, $CDCl_3$) δ 7.68 (m, 4H), 4.83 (s, 1H), 4.30 (qd, J = 7.2, 0.8 Hz, 2H), 1.32 (t, J = 7.2 Hz, 3H) ppm. ^{19}F NMR decoupled ^{1}H (376 MHz, $CDCl_3$) δ -80.79 (m, 3F), -110.95 (m, 2F), -121.21 (m, 2F), -121.72 (m, 2F), -121.89 (m, 4F), -122.71 (m, 2F), -126.12 (m, 2F) ppm. ^{13}C NMR (101 MHz, $CDCl_3$) δ 164.13, 133.97, 130.10 (m), 128.36, 127.94 (t, J = 6.4 Hz), 114.84, 63.76, 43.46, 13.83 ppm.

o-**34b**. The title compound was isolated (R_f = 0.4 hexane/diethyl ether 4:1) in 15% yield (18 mg) as yellowish oil.

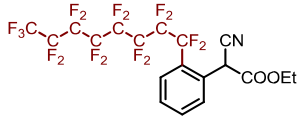

HRMS calculated for $C_{19}H_9F_{17}NO_2$ (M-H): 606.0367, found: 606.0377.

^{1}H NMR (400 MHz, $CDCl_3$) 7.82 (d, J = 8.1 Hz, 1H), 7.72 (t, J = 8.1 Hz, 1H), 7.68 (d, J = 8.1 Hz, 1H), 7.61 (t, J = 8.1 Hz, 1H), 5.14 (s, 1H), 4.31 (qd, J = 7.1, 4.4 Hz, 2H), 1.32 (t, J = 7.1 Hz, 3H) ppm. ^{19}F NMR decoupled ^{1}H (376 MHz, $CDCl_3$) δ -80.74 (m, 3F), -104.52 (m, 2F), -120.74 (m, 2F), -121.19 (m, 2F), -121.67 (m, 2F), -121.84 (m, 2F), -122.66 (m, 2F), -126.07 (m, 2F) ppm. ^{13}C NMR (101 MHz, CDCl3) δ 164.36, 133.11, 131.20, 130.04, 129.57, 129.31 (m), 126.66 (m), 115.46, 63.69, 40.15, 13.78 ppm.

ethyl 2-cyano-2-(4-(trifluoromethyl)phenyl)acetate (*p*-35a), ethyl 2-cyano-2-(2(trifluoromethyl)phenyl)acetate (*o*-35a)

Prepared according to the general procedure using ethyl cyanophenylacetate (0.2 mmol, 0.035 mL) and trifluoroiodomethane (0.6 mmol, 15 mL, gas). The latter was added after the 3 cycles of freeze pump thaw via gas syringe at -196 °C (nitrogen bath). Time of irradiation (2 lamps): 16 h. Purification by flash column chromatography (gradient eluent hexane/diethyl ether 12:1 – 4:1).

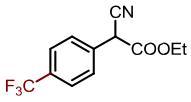

p-**35a**. The title compound was isolated (R_f = 0.3 hexane/diethyl ether 4:1) in 19% yield (10 mg) as a colorless oil.

HRMS calculated for $C_{12}H_9F_3NO_2$ (M-H): 256.0591, found: 256.0603.

^{1}H NMR (400 MHz, $CDCl_3$) δ 7.72 (d, J = 8.2 Hz, 2H), 7.60 (d, J = 8.2 Hz, 2H), 4.81 (s, 1H), 4.29 (qd, J = 7.1, 1.0 Hz, 2H), 1.32 (t, J = 7.1 Hz, 3H) ppm. ^{19}F NMR decoupled ^{1}H (376 MHz, $CDCl_3$) δ -63.02 (s, 3F) ppm. ^{13}C NMR (101 MHz, $CDCl_3$) δ 164.34, 133.86, 131.79 (q, J = 33.0 Hz), 128.62, 126.49 (m), 123.75 (d, J = 272.4 Hz), 115.04, 63.89, 43.61, 14.01 ppm.

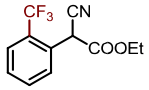

o-**35a**. The title compound was isolated (R_f = 0.5 hexane/diethyl ether 4:1) in 45% yield (23 mg) as colorless oil.

HRMS calculated for $C_{12}H_9F_3NO_2$ (M-H): 256.0591, found: 256.0603.

^{1}H NMR (400 MHz, $CDCl_3$) δ 7.79 (d, J = 7.9 Hz, 1H), 7.76 (d, J = 7.9 Hz, 1H), 7.70 (t, J = 7.9, 1H), 7.57 (t, J = 7.9, 1H), 5.15 (s, 1H), 4.31 (qd, J = 7.1, 1.9 Hz, 2H), 1.32 (t, J = 7.1 Hz, 3H) ppm. ^{19}F NMR decoupled ^{1}H (376 MHz, $CDCl_3$) δ -59.02 (s, 3F) ppm. ^{13}C NMR (101 MHz, CDCl3) δ 164.16, 132.92, 130.69, 129.54, 128.51, 128.46 (q, J = 34.0 Hz), 126.68 (q, J = 5.5 Hz), 123.66 (d, J = 273.8 Hz), 115.24, 63.71, 39.78, 13.81 ppm.

ethyl 2-cyano-2-(4-methyl-2-(trifluoromethyl)phenyl)acetate (35b).

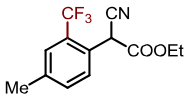

Prepared according to the general procedure using ethyl 2-cyano-2-(4methylphenyl)acetate **11c** (0.2 mmol, 41 mg) and trifluoroiodomethane (0.6 mmol, 15 mL, gas). The latter was added after the 3 cycles of freeze pump thaw via gas syringe at -196 °C (nitrogen bath). Time of irradiation: 16 h. Purification by flash column chromatography (gradient eluent hexane/diethyl ether 12:1 – 8:1). The title compound was isolated (R_f = 0.5 hexane/diethyl ether 4:1) as mixture with the *para* functionalized (dearomatized) adduct (10% by NMR) in 64% yield (35 mg) as a colorless oil.

HRMS calculated for $C_{13}H_{11}F_3NO_2$ (M-H): 270.0747, found: 270.0751.

^{1}H NMR (400 MHz, CDCl3) δ 7.66 (d, J = 8.0 Hz, 1H), 7.55 (s, 1H), 7.48 (d, J = 8.0 Hz, 1H), 5.10 (s, 1H), 4.38 – 4.24 (m, 2H), 2.46 (s, 3H), 1.31 (t, J = 7.1 Hz, 3H) ppm. ^{19}F NMR decoupled ^{1}H (376 MHz, CDCl3) δ -59.04 ppm. ^{13}C NMR (100 MHz, CDCl3) δ 164.38, 140.01, 133.47, 130.57, 128.22 (q, J = 33.0 Hz), 127.25 (q, J = 5.4 Hz), 125.43 (q, J = 1.6 Hz), 123.54 (d, J = 234.6 Hz), 115.41,

63.60, 39.48, 21.11, 13.82 ppm.

ethyl 2-cyano-2-(6-(trifluoromethyl)benzo[d][1,3]dioxol-5-yl)acetate (35c).

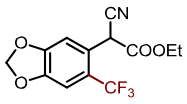

Prepared according to the general procedure using ethyl 2(benzo[d][1,3]dioxol-5-yl)-2-cyanoacetate **11k** (0.2 mmol, 47 mg) and trifluoroiodomethane (0.6 mmol, 15 mL, gas). The latter was added after the 3 cycles of freeze pump thaw via gas syringe at -196 °C (nitrogen bath). Time of irradiation: 36 h. Purification by flash column chromatography (gradient eluent hexane/diethyl ether 12:1 – 8:1). The title compound was isolated (R_f = 0.4 hexane/diethyl ether 4:1) in 51% yield (31 mg) as a yellowish oil.

HRMS calculated for $C_{13}H_{10}F_3NNaO_4$ (M+Na): 324.0454, found: 324.0461.

^{1}H NMR (400 MHz, CDCl3) 7.19 (s, 1H), 7.15 (s, 1H), 6.17 – 6.11 (m, 2H), 5.06 (s, 1H), 4.31 (qd, J = 7.1, 3.2 Hz, 2H), 1.33 (t, J = 7.1 Hz, 3H) ppm. ^{19}F NMR decoupled ^{1}H (376 MHz, CDCl3) δ -57.72 (s, 3F) ppm. ^{13}C NMR (100 MHz, CDCl3) δ 164.24, 151.04, 148.55, 123.54 (d, J = 264.6 Hz), 123.18 (q, J = 1.8 Hz), 122.55 (q, J = 34.0 Hz), 115.27, 110.37, 106.75 (q, J = 5.9 Hz), 102.84, 63.72, 39.44, 13.84 ppm.

ethyl 2-cyano-2-(4-methoxy-2-(trifluoromethyl)phenyl)acetate (35d).

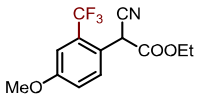

Prepared according to the general procedure using ethyl 2-cyano-2-(4methoxyphenyl)acetate **11b** (0.2 mmol, 44 mg) and trifluoroiodomethane

(0.6 mmol, 15 mL, gas). The latter was added after the 3 cycles of freeze pump thaw via gas syringe at -196 °C (nitrogen bath). Time of irradiation: 16 h. Purification by flash column chromatography (gradient eluent hexane/diethyl ether 10:1 – 4:1). The title compound was isolated (R_f = 0.4 hexane/diethyl ether 4:1) in 61% yield (35 mg) as a yellowish oil.

HRMS calculated for $C_{13}H_{11}F_3NO_3$ (M-H): 286.0697, found: 286.0686.

^{1}H NMR (500 MHz, CDCl3) δ 7.68 (d, J = 8.7 Hz, 1H), 7.24 (d, J = 2.7 Hz, 1H), 7.17 (dd, J = 8.7, 2.7 Hz, 1H), 5.06 (s, 1H), 4.29 (qd, J = 7.1, 2.1 Hz, 2H), 3.89 (s, 3H), 1.31 (t, J = 7.1 Hz, 3H) ppm. ^{19}F NMR decoupled ^{1}H (376 MHz, $CDCl_3$) δ -59.40 (s, 3F) ppm. ^{13}C NMR (126 MHz, CDCl3) δ 164.52, 160.03, 132.13, 129.66 (q, J = 30.9 Hz), 123.42 (d, J = 274.1 Hz), 119.88, 117.65, 115.50, 112.81 (q, J = 5.7 Hz), 63.56, 55.70, 39.14, 13.83 ppm.

ethyl 2-cyano-2-(1-methyl-2-(trifluoromethyl)-1H-indol-3-yl)acetate (35e).

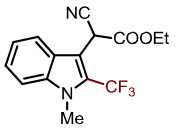

Prepared according to the general procedure using ethyl 2-cyano-2-(1methyl-1H-indol-3-yl)acetate **11m** (0.2 mmol, 48 mg) and trifluoroiodomethane (0.6 mmol, 15 mL, gas). The latter was added after the 3 cycles of freeze pump thaw via gas syringe at -196 °C (nitrogen bath). Time of irradiation: 8 h. Purification by flash column chromatography (gradient eluent hexane/diethyl ether 12:1 – 6:1). The title compound was isolated (Rf = 0.3 hexane/diethyl ether 4:1) in 63% yield (39 mg) as an orange-red oil.

HRMS calculated for $C_{15}H_{12}F_3N_2O_2$ (M-H): 309.0856, found: 309.0856.

^{1}H NMR (400 MHz, CDCl3) δ 7.92 (d, J = 8.2, 1H), 7.49 – 7.43 (m, 2H), 7.31 (m, 1H), 5.40 (s, 1H), 4.36 – 4.22 (m, 2H), 3.91 (s, 3H), 1.30 (t, J = 7.1 Hz, 3H) ppm. ^{19}F NMR decoupled ^{1}H (376 MHz, CDCl3) δ -56.36 (s, 3F) ppm. ^{13}C NMR (100 MHz, CDCl3) δ 164.61, 137.79, 125.77, 124.39, 124.23 (q, J = 32.2 Hz), 121.95, 121.71 (d, J = 251.2 Hz), 120.53, 115.11, 110.42, 106.04, 63.62, 34.40, 31.46, 14.02 ppm.

ethyl 2-cyano-2-(4-(perfluorohexyl)phenyl)acetate (*p*-36) and ethyl 2-cyano-2-(2(perfluorohexyl)phenyl)acetate (*o*-36).

Prepared according to the general procedure using 4-methyl-3-oxo-2-phenylpentanenitrile **11o** (0.2 mmol, 38 mg) and perfluorohexyl iodide **10a**. Time of irradiation: 24 h. Purification by flash column chromatography (gradient eluent hexane/diethyl ether 12:1 – 3:1).

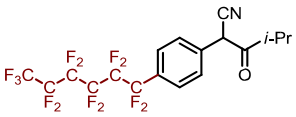

p-**36**. The title compound was isolated (R_f = 0.3 hexane/diethyl ether 4:1) in 38% yield (38 mg) as a colorless oil.
HRMS calculated for $C_{18}H_{11}F_{13}NO$ (M-H): 504.0639, found: 504.0640.

^{1}H NMR (400 MHz, $CDCl_3$) 7.69 (d, J = 8.3 Hz, 2H), 7.58 (d, J = 8.3 Hz, 2H), 4.89 (s, 1H), 3.02 (hept, J = 6.8 Hz, 1H), 1.17 (d, J = 6.8 Hz, 3H), 1.15 (d, J = 6.8 Hz, 3H) ppm. ^{19}F NMR decoupled ^{1}H (376 MHz, $CDCl_3$) δ -80.91 (m, 3F), -111.08 (m, 2F), -121.54 (m, 2F), -121.89 (m, 2F), -122.92 (m, 2F), 126.23 (m, 2F) ppm. ^{13}C NMR (101 MHz, $CDCl_3$) δ 201.72, 134.12, 130.14 (t, J = 24.6 Hz), 128.73, 128.21 (t, J = 6.5 Hz), 115.85, 48.71, 39.43, 18.83, 18.65 ppm.

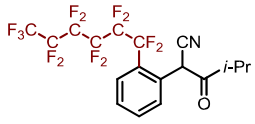

o-**36**. The title compound was isolated (R_f = 0.4 hexane/diethyl ether 4:1) as a mixture with the starting ketone. Additional purification by flash column chromatography (gradient eluent hexane/DCM 2:1 – 1:1) provided the title compound with 20% of unknown impurity.

HRMS calculated for $C_{18}H_{11}F_{13}NO$ (M-H): 504.0639, found: 504.0657.

^{1}H NMR (400 MHz, $CDCl_3$) δ 7.79 – 7.54 (m, 4H), 5.29 (s, 1H), 2.99 (hept, J = 6.8 Hz, 1H), 1.25 (d, J

= 6.8 Hz, 3H), 1.16 (d, J = 6.8 Hz, 3H) ppm. ^{19}F NMR decoupled ^{1}H (376 MHz, $CDCl_3$) δ -80.84 (m, 3F), -104.60 (m, 2F), -120.76 (m, 2F), -121.54 (m, 2F), -122.76 (m, 2F), -126.15 (m, 2F) ppm. ^{13}C NMR (101 MHz, CDCl3) δ 201.57, 134.48, 133.21, 131.76, 129.58 (m), 126.77 (t, J = 22.7 Hz), 116.09, 45.11, 39.50, 18.81, 18.72 ppm.

6.8.4 Quantum Yield Measurement

A ferrioxalate actinometry solution was prepared by following the Hammond variation of the Hatchard and Parker procedure outlined in *Handbook of Photochemistry*. [175] Ferrioxalate actinometer solution measures the decomposition of ferric ions to ferrous ions, which are complexed by 1,10-phenanthroline and monitored by UV/Vis absorbance at 510 nm. The moles of iron-phenanthroline complex formed are related to moles of photons absorbed.

The solutions were prepared and stored in the dark (red light):

1. Potassium ferrioxalate solution: 589.5 mg of potassium ferrioxalate (commercially available from Alfa Aesar) and 278 µL of sulfuric acid (96%) were added to a 100 mL volumetric flask, and filled to the mark with water (HPLC grade).
2. Phenantroline solution: 0.2% by weight of 1,10-phenanthroline in water (200 mg in 100 mL volumetric flask).
3. Buffer solution: to a 100 mL volumetric flask 4.94 g of NaOAc and 1 mL of sulfuric acid (96%) were added and filled to the mark with water (HPLC grade).
4. Model reaction solution: ethyl phenylcyanoacetate **11a** (2.5 mmol, 442 µL), 1.620 mL of perfluorohexyl iodide **10a** (7.5 mmol, 3 equiv.) and 790 µL *N,N,N,N*tetramethylguanidine (TMG, 6.25 mmol, 2.5 equiv.) were added to a 5 mL volumetric flask and filled to the mark with acetonitrile (HPLC grade).

The actinometry measurements were done as follows:

1. 1 mL of the actinometer solution was added to a quartz cuvette (l = 10 mm). The cuvette was placed along with a sample solution (1 mL in a similar cuvette) whose quantum yield has to be measured (our model reaction). The sample and actinometry solutions (placed 10 cm away from the lamp) were irradiated with 300 W Xenon Lamp (25% of light intensity, 400 ± 5 nm bandpass filter high transmittance) *for specified time intervals* (5, 7.5, 10, 12.5) min.
2. After irradiation all the actinometer solution was removed and placed in a 10 mL volumetric flask. 0.5mL of 1,10-phenanthroline solution and 2 mL of buffer solution was added to this flask and filled to the mark with water (HPLC grade).

[175] S. L. Murov, *Handbook of Photochemistry*, Marcel Dekker, New York, 1973.

3. The UV-Vis spectra of actinometry samples were recorded for each time interval. The absorbance of the actinometry solution was monitored at 510 nm.

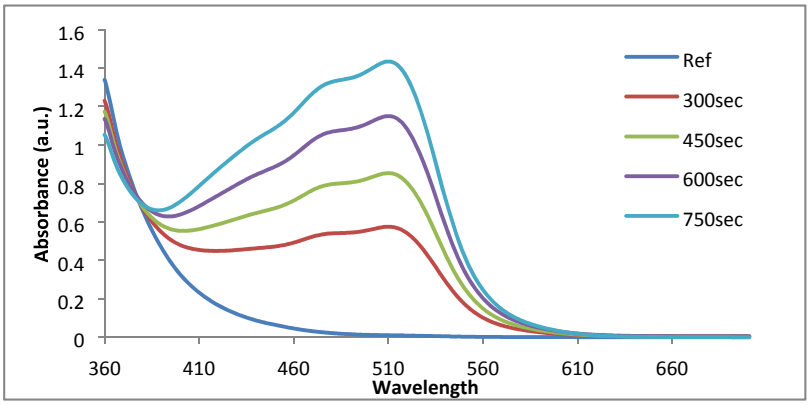

4. The moles of Fe^{2+} formed for each sample is determined using Beers' Law:

$$\text{Moles } Fe^{2+} = \frac{V_1\, V_3\, \Delta A_{(510nm)}}{10^3\, V_2\, l\, \varepsilon_{(510nm)}}$$

where V_1 is the irradiated volume (1 mL), V_2 is the aliquot of the irradiated solution taken for the determination of the ferrous ions (1 mL), V_3 is the final volume after complexation with phenanthroline (10 mL), l is the optical path-length of the irradiation cell (1 cm), ΔA(510 nm) the optical difference in absorbance between the irradiated solution and that taken in the dark, ε(510 nm) is that of the complex $Fe(phen)_3^{2+}$ (11100 L mol^{-1} cm^1).

5. The moles of Fe^{2+} formed (N) are plotted as a function of time (t). The slope is a product of the photon flux (F) and the quantum yield for Fe^{2+} (ϕ_{Fe2+} = 1.13) at 400 nm as, F = N/Φ_{Fe2+} t. The F was determined to be 1.50 10^{-9} einstein s^{-1}.

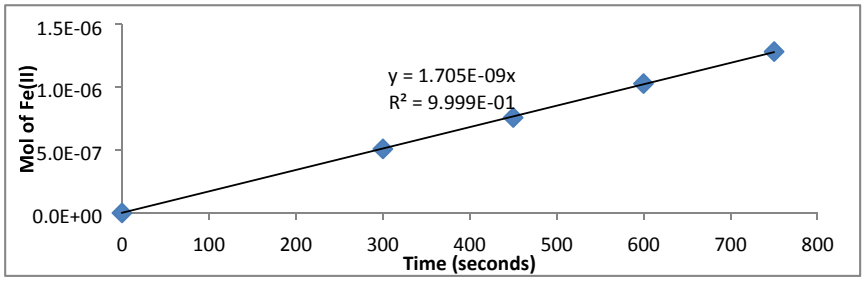

6. The moles of products formed for the reaction of interest (done by irradiating the sample alongside the actinometer solution) are described above. The moles of products

formed were determined by GC measurement (FID detector) using 2-nitro-1fluorobenzene as reference standard. The number of moles of product per unit time is related to the number of photons absorbed. The slope yields the quantum yield (Φ) of the photoreaction, **3.81**.

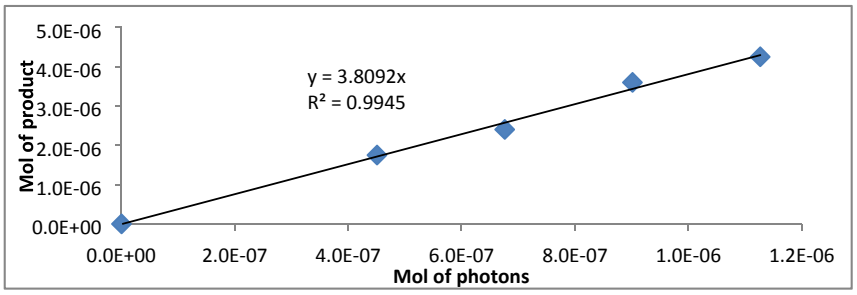

The procedure was repeated a second time to provide a similar value, a quantum yield (Φ) of **3.78**.

Since the ferrioxalate actinometer absorbance at 400 nm is 0.33 and inferior to 2 (if is major then 2 at the wavelength used, it can be assumed that the entire incident light is absorbed), a correction factor (C) based on the fraction of light absorbed by the actinometer has to be considered to calculate the photon flux and the final quantum yield of the reaction (note that is also needed if the absorbance of the reaction under study at the optimized concentration is inferior to 2 at the wavelength used). Thus, according to the definition of quantum yield,[32]

$$\Phi_{Fe2+} = \frac{(d_{moles\text{-}Fe2+}/d_{time})}{F\, C_{Fe2+}} \rightarrow F = \frac{(d_{moles\text{-}Fe2+}/d_{time})}{\Phi_{Fe2+}\, C_{Fe2+}} \qquad C_{Fe2+} = [1\text{-}10^{-A(\lambda)}]$$

the photo flux (F) previously found has to be divided by the appropriate correction factor C (0.532, calculated with $A_{(400nm)}$ = 0.33 for the actinometer solution). The new photo flux was determined to be 2.82 10^{-9} einstein s^{-1}. Thus, the number of moles of product per unit time is related to the number of photons absorbed as shown above and the slope yields the new quantum yield (Φ) of the photoreaction, **2.03**.

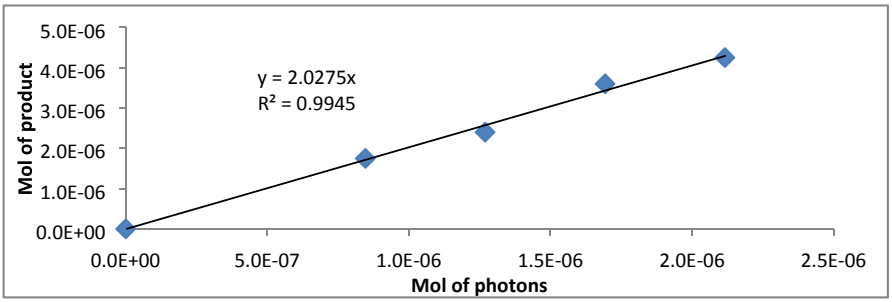

Due to the previous definition of the quantum yield, also the new value found should be divided by the correction factor calculates for the reaction at 400 nm.

$$\Phi_{react} = \frac{(d_{moles\text{-}prod}/d_{time})}{F\,C_{react}} \rightarrow \Phi_{react} = \frac{(d_{moles\text{-}prod}/d_{moles\text{-}photons})}{C_{react}} \qquad C_{react} = [1\text{-}10^{-A(\lambda)}]$$

In this case, the reaction absorbance at 400 nm at the optimized concentration (0.5 M) is higher than 2, so the C_{react} is 1 and the final quantum yield remains **2.03**.

6.8.5 Triethylborane Experiments

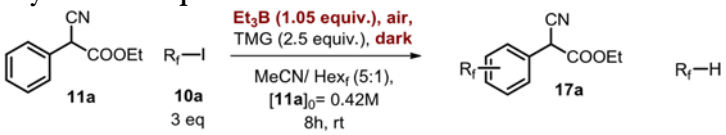

A 5 mL vial was charged with ethyl cyanophenylacetate **11a** (0.035 mL, 0.2 mmol), acetonitrile (0.4 mL, 0.5 M referring to **11a**, perfluorohexane (0.08 mL), perfluoroalkyl iodide **10a** (0.130 mL, 0.6 mmol, 3 equiv), *N,N,N',N'*-tetramethylguanidine (0.063 mL, 0.5 mmol, 2.5 equiv.) and triethylborane (1M in hexanes, 0.210 mL, 0.21 mmol, 1.05 equiv.). The reaction mixture was stirred for 8 hours and directly quenched with a solution in acetonitrile of trichloroacetic acid (130 mg, 0.8 mmol, 4 equiv.). 1-Fluoro-2-nitrobenzene (internal standard, 0.021 mL, 0.2 mmol) was added and the resulting mixture was analyzed by 1H and 19F NMR to showed 11% of perfluorinated products **17a**, 47% of protonated perflurohexyl compound (R_f-H) and 87% of starting **11a**.

The same experiment was repeat in absence of base (TMG) showing no perfluorinated product **17a** and 43% of protonated perflurohexyl compound R_f-H.

6.8.6 Reactivity Resonance Effect Parameter Measurement

Ethyl 2-cyano-2-(4-fluorophenyl)acetate **11p** (21 mg, 0.1 mmol), acetonitrile (0.530 mL, 5% w/w), *N,N,N',N'* tetramethylguanidine (0.013 mL, 0.1 mmol) and fluorobenzene (0.002 mL, 20%, internal standard, identified in the following discussion as **X**) were placed in a vial (3 mL) and stirred for 2 minutes. The reaction mixture was then directly analyzed by ^{19}F NMR (deuterated acetone was placed in an NMR insert and used to lock the field).

The same procedure was used for ethyl 2-cyano-2-(3-fluorophenyl)acetate **11q**.

- ^{19}F chemical shift of fluorobenzene, -113.15 ppm.
- ^{19}F chemical shift of 2-cyano-2-(4-fluorophenyl)acetate, *para* isomer, -126.80 ppm.
- ^{19}F chemical shift of 2-cyano-2-(3-fluorophenyl)acetate, *meta* isomer, -114.99 ppm.

According to Taft and co-workers,[35] the reactivity resonance effect parameter (σ_R) could be calculated using the ^{19}F NMR shifts by the following equation:

$$\sigma_R = -0.0359\ (\pm 0.004)\ (-\delta^{19}F\ NMR_{p,m}) + 0.02\ (\pm 0.02)$$

where -Δ^{19}F $NMR_{p,m}$ is the negative difference between the Δ^{19}F $NMR_{p,X}$ (^{19}F NMR shift to the fluorobenzene for *para* isomer) and Δ^{19}F $NMR_{m,X}$ (^{19}F NMR shift to the fluorobenzene for *meta* isomer).

$$\Delta^{19}F\ NMR_{p,X} = -13.65$$

$$\Delta^{19}F\ NMR_{m,X} = -1.84$$

$$-\Delta^{19}F\ NMR_{p,m} = 11.81$$

$$\Delta_R = -0.40$$

6.8.7 Kinetic Isotope Effect Measurement

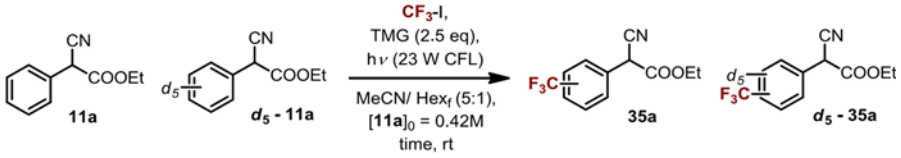

A 10 mL Schlenk tube was charged with ethyl cyanophenylacetate **11a** (19 mg, 0.1 mmol), d_5 -ethyl cyanophenylacetate ***d*$_5$-11a** (19 mg, 0.1 mmol), acetonitrile (0.4 mL, 0.25 M referring to **11a**), perfluorohexane (0.08 mL) and *N,N,N',N'*-tetramethylguanidine (0.063 mL, 0.5 mmol, 5 equiv.). The reaction mixture was degassed via freeze pump thaw (x 3 cycles), and the vessel refilled with nitrogen. Trifluoroiodomethane (0.6 mmol, 15 mL, gas, 6 equiv.) was then added after the 3 cycles of freeze pump thaw via gas syringe at -196 °C (nitrogen bath). After the reaction mixture was thoroughly degassed, the vial was sealed and positioned approximately 5 cm away from household full spectrum 23 W compact fluorescent light (CFL). After stirring for 5 hours, the reaction was diluted with DCM, quenched with aqueous HCl 1M solution and extracted 3 times with DCM. The organic phase was then dried and the solvent removed under reduced pressure. 1-Fluoro-2-nitrobenzene (internal standard) was added and the reaction mixture was analyzed by ^{19}F NMR and Mass to determine the amounts and relative ratios of products resulting from trifluoromethylation of **35a** and ***d*$_5$ - 35a** (41% ± 5% conversion).

^{19}F chemical shift of protiated 2-cyano-2-(2-(trifluoromethyl)phenyl)acetate (*ortho*), -59.01 ppm.

^{19}F chemical shift of deuterated 2-cyano-2-(2-(trifluoromethyl)phenyl)acetate (*ortho*), -59.02 ppm.

^{19}F chemical shift of protiated 2-cyano-2-(4-(trifluoromethyl)phenyl)acetate (*para*), -63.00 ppm.

^{19}F chemical shift of deuterated 2-cyano-2-(4-(trifluoromethyl)phenyl)acetate (*para*), -62.99 ppm.

Parent ion peak for protiated *ortho* and *para* products, m/z = 256.0

Parent ion peak for deuterated *ortho* and *para* products, m/z = 260.0

Unfortunately, signals in ^{19}F NMR of the protiated and deuterated products partially overlapped so that it was not possible to determine a precise ratio between them. However, it was clear that the KIE was not primary (ratio around 1). The relative rates for the trifluoromethylation of **35a** and d_5 **- 35a** was instead well determined to be **0.97 ± 0.01** by Mass analysis, indicating an expected negative secondary isotope effect.